Comparative Pathogenesis of Influenza in Ferrets

Thesis

Kathryn Ann Ryan

The Comparative Pathogenesis of Influenza in Ferrets

Doctor of Philosophy

School of Life, Health and Chemical Sciences

Public Health England
Porton Down

October 2019

The Comparative Pathogenesis of Influenza in Ferrets

Abstract

Influenza is an enveloped, segmented, single-stranded, negative sense RNA virus that causes annual seasonal epidemics and occasional pandemics. Influenza causes roughly 200,000 to 500,000 deaths per year globally and affects up to 15% of the world's population annually. Influenza is a major public health concern. Influenza presents a spectrum of clinical signs including: fever, sneezing, lethargy and can range from a mild to a severe disease. It also leads to death in high-risk individuals such as pregnant women, the elderly and very young, the immunocompromised and those with underlying medical conditions. Seasonal influenza viruses continuously evolve antigenically meaning individuals can become infected on numerous occasions throughout their lives. Due to the rapid evolution of these viruses, the influenza vaccine composition needs to be updated regularly to protect against current circulating strains.

The ferret is the gold standard model for influenza infections in the laboratory. The model produces similar clinical readouts to humans; sneezing, nasal discharge, fever and malaise. Human isolates can be used to infect ferrets with no prior need for adaptation. This PhD investigates the pathogenesis of H3N2 A/Perth/16/2009 and its ability to cause disease in the ferret using three different models of infection; intranasal, nose-only aerosol and non-contact transmission. Scrutiny of these models using a range of virological and immunological techniques showed while there are some small differences between routes of infection, using the same influenza virus strain results in similar disease in ferrets. Further analysis of the intranasal route of inoculation and comparison with H1N1 A/California/04/2009, showed distinctions in pathogenesis between viruses despite identical routes of infection, highlighting the differences in the viral kinetics and cellular immune response between H3N2 and H1N1 in the ferret model. This work enhances and improves the versatility of the ferret model for studying the pathogenesis of influenza.

Acknowledgements

I would like to express my sincere gratitude to my PhD Supervisors – Dr Anthony Marriott, Dr Catherine Whittaker, Professor Nigel Silman and Professor Miles Carroll. The extent of their knowledge has contributed greatly to this research and their guidance has been valued throughout. I want to extend additional thanks to my line manager, Dr Catherine Whittaker. I have been lucky to receive such a constant source of support throughout my studies. I am extremely grateful for her continued encouragement.

During my PhD I have been very fortunate to have contact with people so willing to share their time and expertise. I am indebted to the staff in the Biological Investigations Group at Porton Down. Without them the high standard of ferret work within this thesis would not have been able to be completed.

I would like to give special thanks to my colleague Dr Karen Gooch for her supervision, support and direction throughout this PhD, especially regarding the immunology and animal modelling. I would also like to acknowledge my laboratory colleagues who have offered help, managed laboratories and other resources that were used during this project. Special mention goes to Dr Gillian Slack and Jennifer Logue for their practical assistance during this project.

I am grateful to members of the Biosafety Group at Porton Down; Simon Parks for designing and building the ferret transmission cages, and Dr Katy-Ann Thompson for her advice and support regarding air sampling. I would also like to thank Simon Bate and Graham Hatch for their expertise and assistance in designing and implementing the nose-only aerosol model.

I would like to acknowledge my friends; Dr Debs Roebuck, who, since our time at university has been an invaluable source of support. Thank you for sacrificing your time to review this thesis. And Dr Kimberly Steeds and Steve Thomas for their personal support during this PhD. The past year and a half has been a struggle, and without their insistence on regular coffee breaks I would have been lost.

To my husband Wilty, I could never thank you enough for your patience whilst I moaned about my PhD. To my father John and my brother Andrew, thank you for support and always inspiring me to work my hardest. And finally, to Mummy. Thank you for always encouraging and believing in me, especially when I didn't believe in myself. I'm so sorry that I didn't finish my thesis in time for you to see, but I hope wherever you are that you are proud of me.

Contents

Abbreviations

α	alpha
γ	gamma
µ	mu
µg	microgram
µl	microlitre
°C	Degrees Celsius
%	Percentage
ACK	Ammonium-Chloride-Potassium
ADCC	Antibody-dependent cellular cytotoxicity
BAL	Bronchealveolar Lavage
BSA	Bovine serum albumin
CDC	Centre for Disease Control and Prevention
cDNA	Complementary DNA
CL	Containment Level
CPE	Cytopathic effect
CTL	Cytotoxic T lymphocyte
DC	Dendritic Cell
DEAE	Diethylaminoethyl
DMEM	Dulbecco's Modified Eagle Medium
dpi	Days post infection
DNA	Deoxyribonucleic Acid
ECACC	European Collection of Authenticated Cell Cultures
EDTA	Ethylenediaminetetraacetic acid
EID_{50}	50% egg infectious dose
ELISA	Enzyme linked immunosorbent assay

ELISpot	Enzyme linked immunospot
Fab	Fragment antigen binding
FBS	Foetal bovine serum
Fc	Fragment crystallisable
FcR	Fc Receptor
FCS	Foetal calf serum
HA	Haemagglutinin
HAI	Haemagglutinin Inhibition
HEPES	4-(2-hydroxyethyl)-1-piperazineethanesulfonic acid
HPAI	Highly pathogenic avian influenza
IAV	Influenza A virus
IBV	Influenza B virus
ICV	Influenza C virus
IDV	Influenza D virus
IFN	Interferon
Ig	Immunoglobulin
IL	Interleukin
kDa	Kilo Dalton
LPAI	Low pathogenic avian influenza
mAb	Monoclonal antibody
MEM	Minimum essential media
MDCK	Mandin-Darby Canine Kidney
MHC	Major histocompatibility complex
ml	millilitre
MNC	Mononuclear cell
MOI	Multiplicity of infection
mRNA	Messenger RNA

NA	Neuraminidase
NAI	Neuraminidase inhibitor
NHP	Non-human primate
NK	Natural Killer
NP	Nucleoprotein
NT	Nasal Turbinate
PBMC	Peripheral blood mononuclear cell
PCR	Polymerase chain reaction
PFU	Plaque forming unit
qRT-PCR	Quantitative reverse transcriptase – polymerase chain reaction
RBC	Red blood cell
RNA	Ribonucleic acid
RNP	Ribonucleoprotein
Rpm	Revolutions per minute
TAE	Tris base, acetic acid and EDTA
$TCID_{50}$	50% tissue culture infectious dose
TCR	T cell receptor
TNF	Tumour necrosis factor
TPCK	N-toysyl-L-phenylalanine choromethyl ketone
UK	United Kingdom
USA	United States of America
vRNA	Viral RNA
WHO	World Health Organisation

1 Introduction

1.1 Influenza Overview

Influenza is a multi-segmented, negative sense, single stranded (ss) RNA virus and a member of the *Orthomyxoviridae* virus family. It presents two distinct challenges to public health. The first is from influenza viruses circulating endemically in the human population that seasonally cause a low severity respiratory illness with symptoms such as fever, headache, myalgia, malaise and cough. It has a high attack rate and results in annual epidemics. Although seasonal influenza is preventable, annual vaccinations are required due to the plasticity of the virus' RNA genome and the high error rate of the viral polymerase. This allows the virus to continually evolve, causing antigenic drift. The second challenge is the emergence of a novel influenza A virus from a diverse animal reservoir (WHO, 2014) or genetic reassortment between several viruses in an animal host (CDC, 2009, Smith *et al.*, 2009), known as antigenic shift creating novel viruses that the human population have not been exposed to. These viruses cross the species barrier sporadically, going on to cause human illness and could potentially lead to global pandemics with high fatality rates. Currently, there are four recognised types of influenza virus (summarised in **Table 1.1.1**).

1.1.1 **Influenza A**

Influenza A virus (IAV) is endemic in the world's wild bird population. It has spilt over into the domestic bird population and subsequently been able to infect other domesticated mammals and humans (**Fig. 1.1**). The introduction and adaptation of IAVs to the human population has been the cause of several global pandemics which has resulted in the IAVs continued circulation in the human population as endemic seasonal viruses (Petrova and Russell, 2017). IAV's have been able to continually evolve due to their RNA genome, host immune pressures and their broad host range. Influenza A subtypes are categorised by their two surface glycoproteins; haemagglutinin (HA) and neuraminidase (NA). There are numerous subtypes (potentially 144) (Spackman, 2008) circulating within the wild bird population and there are two current IAV subtypes circulating in the human population; H1N1 and H3N2, causing seasonal epidemics.

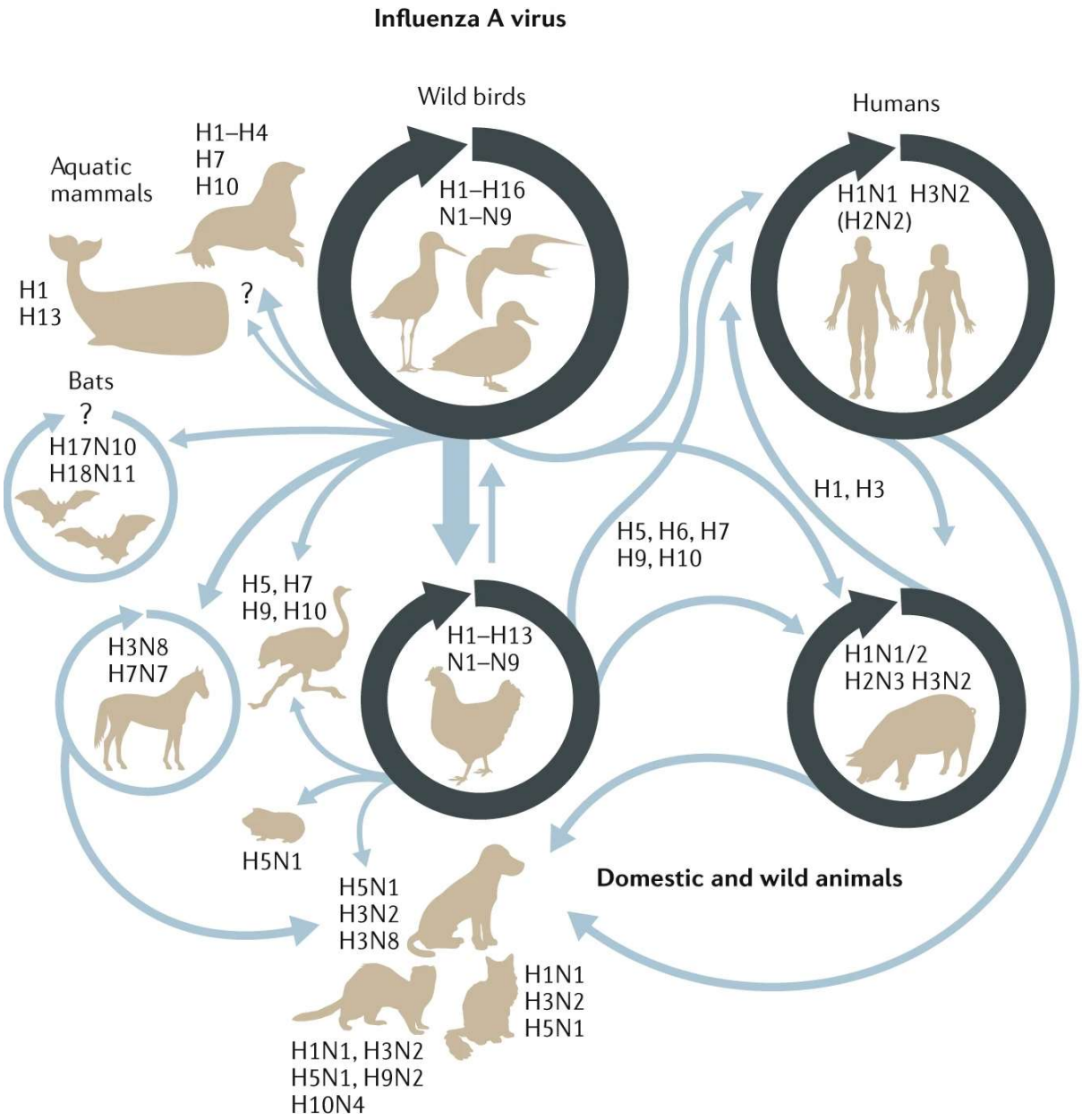

Figure 1.1 Ecology of Influenza A Viruses (Long *et al.*, 2019) Influenza A viruses (haemagglutinin (HA) subtypes 1-16) circulate in the wild bird reservoir. The light blue arrows denote subtypes that cross into different species either through intermediate hosts or via adaptive mutations. The dark blue circles denote subtypes that predominately circulate within species. HA subtypes H17 and H18 currently only circulate in bats (Tong *et al.*, 2012). Many species have been experimentally infected with influenza viruses including ferrets, mice, guinea pig and NHPs (Bouvier, 2015, Bouvier and Lowen, 2010, Maher and DeStefano, 2004, Lowen *et al.*, 2006) .

1.1.2 **Influenza B**

Influenza B virus (IBV) was first identified in 1940 (Francis, 1940) and has no known animal reservoir. Two antigenically and genetically distinct lineages of influenza B, B/Victoria/2/87-like (Victoria lineage) and B/Yamagata/16/88-like (Yamagata lineage), emerged in 1983 and sequence analysis of the hemagglutinin (HA) genes of several isolates indicated that the HA1 domains of the two virus lineages isolated differed by 27 amino acids (Rota *et al.*, 1990). Historically, new strains of IBV have emerged much less frequently compared to IAV due to its limited host range. Between 1985 and 2000 one of the two lineages of IBV has dominated the other during the influenza season; however, since 2001 both lineages of IBV have been co-circulating globally. IBV is less of a disease burden in humans than IAV and unlike IAV is not known to cause severe pandemics. More research is focussed on IAV and limited global media coverage of IBV compared to that of IAV reinforces the perception that IBV does not pose a serious public health risk.

1.1.3 **Influenza C**

Influenza C virus (ICV) has a seven-segmented genome which codes for nine proteins and can infect humans and pigs. In humans, influenza C has been associated with milder symptoms than types A and B and has been found to cause infections mostly during childhood. Unlike IAV, ICV has very little genetic diversity and therefore evolves at a comparatively slower pace. In contrast to IAV, ICVs consist of a single subtype in humans with a novel strain identified in swine with no cross reaction observed between human and swine strains (Hause *et al.*, 2013).

1.1.4 **Influenza D**

Influenza D viruses (IDV) are known to infect cattle, sheep and goats (Quast *et al.*, 2015) but do not infect humans. IDV is a single-strand, negative-sense RNA virus with seven genomic segments encoding nine proteins. IDV shares less than 50% of its protein sequence identity with ICV, its genetically closest member of the influenza virus family (Hause *et al.*, 2013). Studies have shown that IDV has the ability to infect swine and ferrets (Hause *et al.*, 2013) however, it's been shown that transmission of IDV from infected cattle to ferrets via fomites does not occur (Ferguson *et al.*, 2016). Studies have shown that there are two lineages of IDV that share a common ancestor of approximately 44.6 years ago, suggesting that these lineages emerged recently (Su *et al.*, 2017).

The body of work described in this thesis will focus on the currently circulating seasonal influenza A virus subtype H3N2.

Table 1.1.1 Comparison of Current Influenza Types

	IAV	IBV	ICV	IDV
Genome	-ssRNA 8 segments	-ssRNA 8 segments	-ssRNA 7 segments	-ssRNA 7 segments
Subtypes	Up to 144	Two lineages; Yamagata & Victoria	One	Two
Spread in humans	Pandemic Epidemic	Epidemic	Sporadic	None observed
Antigenic changes	Shift Drift	Slow Drift	V. Slow Drift	V. Slow Drift
Severity of illness in humans	+++	++	+	N/A
Vaccine	Yes; seasonal & pandemic	Yes; seasonal	No	No
Animal reservoir	Yes; wild birds	No	No	Cattle, sheep, goats

1.1.5 **History of Influenza**

Influenza pandemics have occurred at irregular intervals since at least the 9th century AD (Saunders-Hastings and Krewski, 2016). Influenza was first recognised as an infectious disease in the 17th Century, with recurrent epidemics of disease recorded as occurring every 1 to 3 years over the past 400 years (Treanor, 2015). Influenza was first experimentally administered to ferrets in 1933 contributing significantly to the modern understanding of the virus (Smith *et al.*, 1933). Major developments then followed with the discovery that the virus could be propagated in fertilised hens eggs (Burnet, 1936) and the ability of the virus to cause the haemagglutination of red blood cells (Hirst, 1942). Both discoveries allowed for extensive studies of the properties of influenza.

One of the worst recorded IAV pandemics in history was the 1918 Spanish Flu outbreak, which killed an estimated 50-100 million people worldwide. In March of 1918 severe cases of influenza were reported in the United States marking the first wave of Spanish Flu (Taubenberger J K, 2001, Watanabe and Kawaoka, 2011). Following the deployment of US military troops to Europe the virus began to spread throughout the US, Europe and Asia. As Spain was neutral during the First World War they did not have a censored media and were able to report on the spread of the disease, hence the name “Spanish Flu”. The first wave of Spanish Flu killed relatively few people. However, by the second and third waves in the autumn and winter of 1918 the virus, having had several passages through humans, became lethal. It is estimated that 30% of the world’s 1.7 billion individuals became clinically infected (Taubenberger J K, 2001, Watanabe and Kawaoka, 2011). Due to the scarcity of antibiotics, secondary bacterial pneumonia is thought to have caused most of deaths. However, the virus also killed quickly with either acute pulmonary haemorrhage or pulmonary oedema with the disease course often less than 5 days.

A further two milder pandemics occurred in 1957 and 1968, caused by IAV H2N2 and H3N2 respectively. The 1957 pandemic, also known as the Asian Pandemic, first occurred in localised outbreaks in continental China during February and March of 1957 with the virus quickly reaching Hong Kong and other parts of Asia in the following weeks (Chowell, 2017, Influenza Other Respir Viruses). The pandemic reached Europe in June 1957 and had spread to the rest of the world by August 1957. Phylogenic studies show that the H2N2 strain that caused the 1957 pandemic was a genetic reassortant. A genetic reassortant is a virus that has resulted from the mixing of the genetic material from two or more strains. In 1957 this occurred between a previously circulating human H1N1 virus and an avian virus, with novel H2, N2 and PB1 (a subunit of the RNA polymerase) genes derived from an avian Eurasian virus (Kilbourne 2006). This highlights the key role antigenic shift plays in pandemic influenza outbreaks.

In 1968 a novel strain of H3N2 IAV emerged in Hong Kong (Alymova *et al.*, 2016) resulting from a reassortment of the HA and PB1 genes from an avian H3N2 with the NA from the 1957 pandemic subtype. The new strain possessed the ability to infect and transmit between humans effectively (Westgeest *et al.*, 2014) and the emergence of novel H3N2 led to a global pandemic associated with more than one million deaths worldwide. Since 1968, H3N2 IAVs have circulated seasonally in the human population resulting in frequent, significant morbidity and mortality (Allen and Ross, 2018). The H3N2 IAV subtype has now been circulating in the human population for 51 years causing annual seasonal outbreaks (**Fig. 1.1.5.1**).

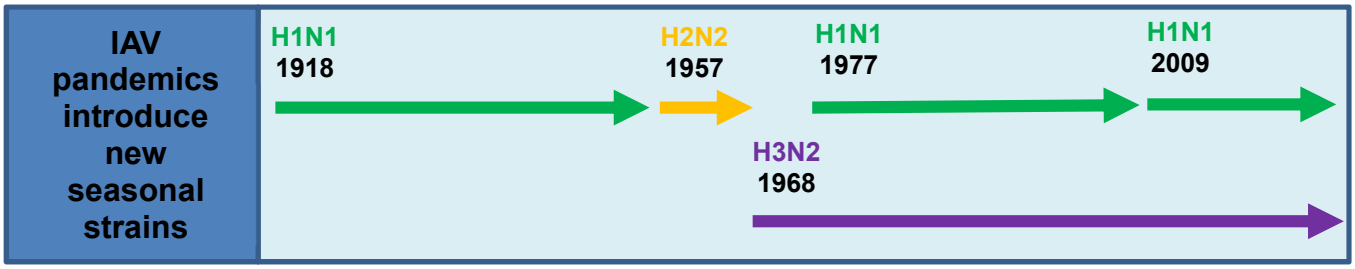

Figure 1.1.5.1 Introduction of Seasonal Subtypes (Hutchinson, 2018) Timeline briefly summarising the history of the introduction of seasonal influenza strains into global circulation. The 1918 H1N1, 1957 H2N2, 1968 H3N2 and the 2009 H1N1 all began circulating seasonally following pandemics caused by these subtypes.

The Global Influenza Surveillance and Response System (GISRS) was introduced by the WHO in 1952 to support the worldwide detection and characterisation of influenza viruses. It was formerly known as the Global Influenza Surveillance Network (GISN) and the new name came into effect after adoption of the Pandemic Influenza Preparedness (PIP) framework in 2011. (The PIP framework brings together Member States, industry, stakeholders and the WHO to implement a global approach to pandemic influenza preparedness and response). GISRS performs two main functions:

1) Monitoring the evolution of influenza viruses and providing recommendations in areas including laboratory diagnostics, vaccines, antiviral susceptibility and risk assessment (WHO, 2017a).

2) Serving as a global alert mechanism for the emergence of influenza viruses with pandemic potential (WHO, 2017a).

Globally, 143 influenza centres perform polymerase chain reaction (PCR) testing of clinical samples, characterising the influenza virus type and subtype, and isolate the viruses in culture. These centres submit samples to one of six international reference laboratories (located in Melbourne, Beijing, Tokyo, London, Atlanta, & Memphis) where samples undergo further characterisations as well a whole genome sequencing (Jernigan and Cox, 2013). This increased surveillance coupled with greater movement of people and livestock has resulted in an increase in the recognition of novel IAVs with the ability to infect the human population. There are several key strains that have been identified in the past years that have remained under surveillance by GISRS due to their pandemic potential.

In 1996 a high pathogenicity avian influenza (HPAI) A(H5N1) was first identified (WHO, 2014). It has now spread throughout South East Asia and beyond, with migratory birds being the main reservoir for the virus. The first human cases were confirmed in Hong Kong in 1997 (WHO, 2014). Ongoing surveillance has shown that globally from January 2003 to June 2019 there were 861 cases of human infection with HPAI A(H5N1) reported across 17 countries. Of these 861 cases, 455 were fatal (WHO, 2019a). HPAI A(H5N1) causes severe disease characterised by a high viral load and intense inflammatory responses that progresses to severe pneumonia, acute respiratory distress syndrome and death; with a fatality rate of 53% (de Jong *et al.*, 2006). The majority of HPAI A(H5N1) cases have occurred following exposure to infected poultry, and the virus is yet to sustain successful transmission from human to human. However, despite the relatively low number of human infections annually, compared to seasonal influenzas, the high case fatality associated with HPAI A(H5N1) infection and the potential for the virus to acquire a transmissible phenotype and cause a pandemic means that this virus is an ongoing public health threat.

Swine-origin influenza A(H1N1) emerged in the Americas in 2009 (Smith *et al.*, 2009). It was the first influenza pandemic of the 21st century and was the first to emerge following major global investment in pandemic preparedness (Leung and Nicoll, 2010). The virus was identified in May 2009 (Team, 2009) as a reassortment of a triple reassortant virus with a Eurasian avian-like swine virus (**Fig. 1.1.5.2**) containing three classical swine genes (H1, NP and NS), one human gene (H3N2 PB1), two North American avian genes (PB2 and PA), and two Eurasian avian-like swine genes (N1 and M). While previous pandemics had been marked by an antigenic shift to a different subtype the 2009 pandemic involved an antigenic change from a human H1N1 to a swine H1N1 subtype.

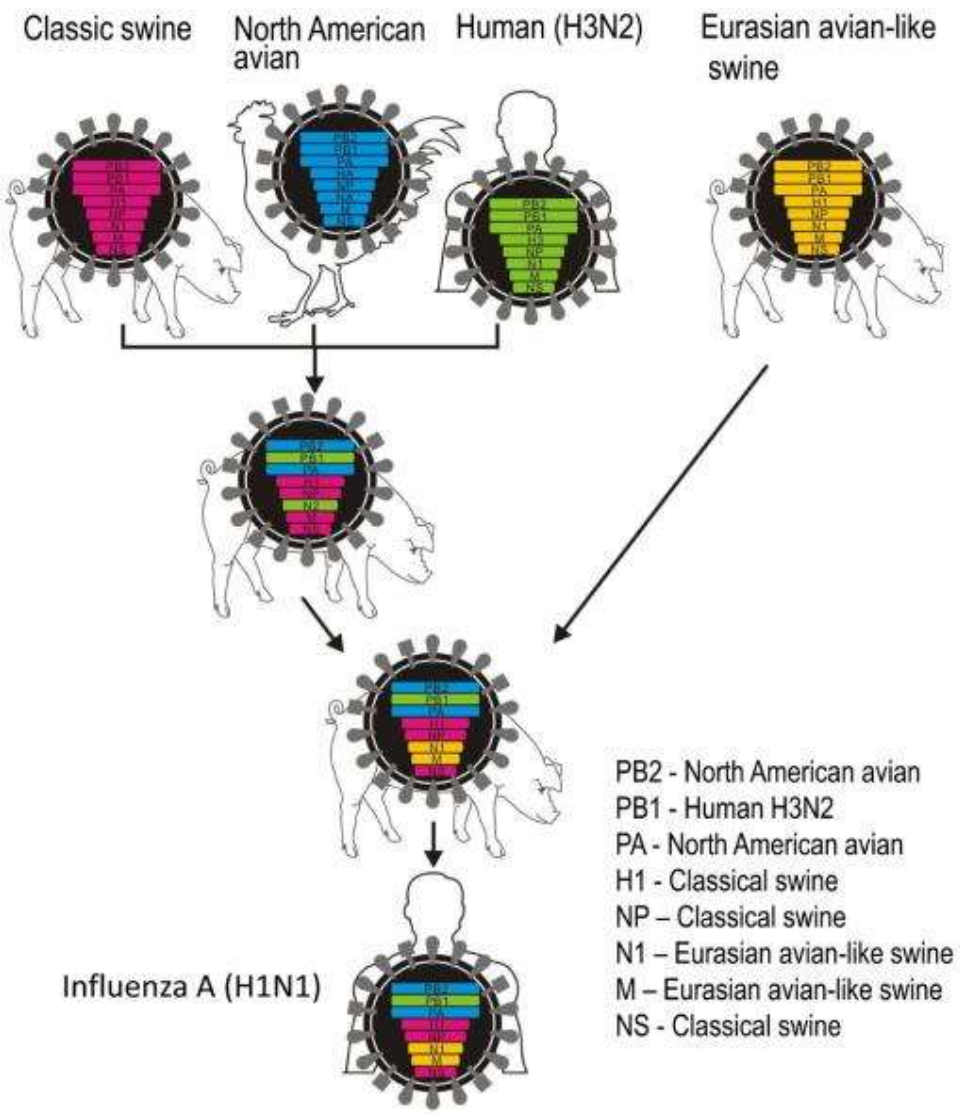

Figure 1.1.5.2 Genesis of swine-origin H1N1 influenza viruses (Neumann *et al.*, 2009) The diagram shows the origin of the 2009 pandemic H1N1. In the late 1990s, reassortment between human H3N2, North American avian, and classical swine viruses resulted in triple reassortant H3N2 and H1N2 swine viruses that have since circulated in North American pig populations. A triple reassortant swine virus reassorted with a Eurasian avian-like swine virus, resulting in the swine-origin influenza virus that began circulating in humans in 2009.

Around 60% of the reported cases of swine-origin influenza A(H1N1) were reported to have occurred in individuals under 18 years of age (Team, 2009). The clinical characteristics of swine-origin influenza A(H1N1) was like those of seasonal influenza; fever, headache, myalgia, malaise and cough. Additionally, it was noted that patients infected with this strain were more likely to have gastrointestinal symptoms such as nausea, vomiting and diarrhoea. An estimated 1 in 10 infected patients were admitted to hospital. In 2010 the WHO declared the pandemic over. The H1N1 strain in now a circulating seasonal strain (**Fig. 1.5.1.1**) and is included in the annual influenza vaccine.

In March 2013 the first human infections with a low-pathogenicity avian influenza (LPAI) A(H7N9) virus were reported in China (Chowell *et al.*, 2013). Subsequently the virus spread rapidly throughout the country, with 1567 laboratory confirmed cases and 612 deaths recorded as of January 2019 (PHE, 2019). In December 2016, the first human infection caused by a A(H7N9) virus strain with a poly-basic cleavage site at the HA cleavage site was recorded. This cleavage site is often associated with HPAI strains of avian influenza, this particular isolate did not appear to cause disease that differed from previous infections with LPAI A(H7N9) and clinical and virological evidence suggested that systemic dissemination did not occur (Ke *et al.*, 2017). However, the number of human infections with A(H7N9) and the geographical range of human cases in the previous wave of infection (fifth, originated 1st October 2016) were greater than any other previous and subsequent waves (WHO, 2017b) highlighting the need for continued surveillance.

1.1.6 **Clinical Manifestation**

There are several characteristic symptoms of influenza infection, including; fever, headache, myalgia, malaise and anorexia, these are usually accompanied by respiratory symptoms such as non-productive coughing, nasal discharge, and sore throat. Cough and malaise can occasionally persist for up to two weeks after resolution of fever (Paules and Subbarao, 2017, WHO, 2018). These are known as influenza like-illness (ILI) and are often applied to a wide range of infectious diseases. Otitis media and vomiting is often reported in children infected with influenza. Influenza can also cause primary viral pneumonia; exacerbate underlying conditions (such as cardiac or pulmonary disease); and lead to secondary bacterial pneumonia, sinusitis, or otitis media; or contribute to coinfections with other viral or bacterial infections (CDC, 2018).

The typical incubation period for influenza is approximately 1-4 days. Healthy adults usually begin to infect others 1 day before symptoms develop and can remain infectious up to 5 to 7 days after symptoms manifest. Some groups of people, especially young children and immunocompromised may remain infectious for a longer period (CDC, 2018). Many individuals will recover from the fever and other symptoms within a week without requiring medical attention, however influenza infection can cause severe illness and even death, especially in people at high risk. Hospitalisation and deaths occur in mainly high-risk groups. Annual epidemics are estimated to result in approximately 3-5 million severe cases of illness and around 290,000 to 650,000 respiratory deaths (WHO, 2018). Yearly epidemics can result in high levels of worker and school absenteeism as well as productivity loss. In addition, clinics and hospitals can often be overwhelmed during peak illness periods.

Organisations, such as the WHO, release yearly campaigns (**Fig. 1.1.6.1**) to help the public recognise the signs of influenza infection and encourage those who are most vulnerable to infection to get vaccinated.

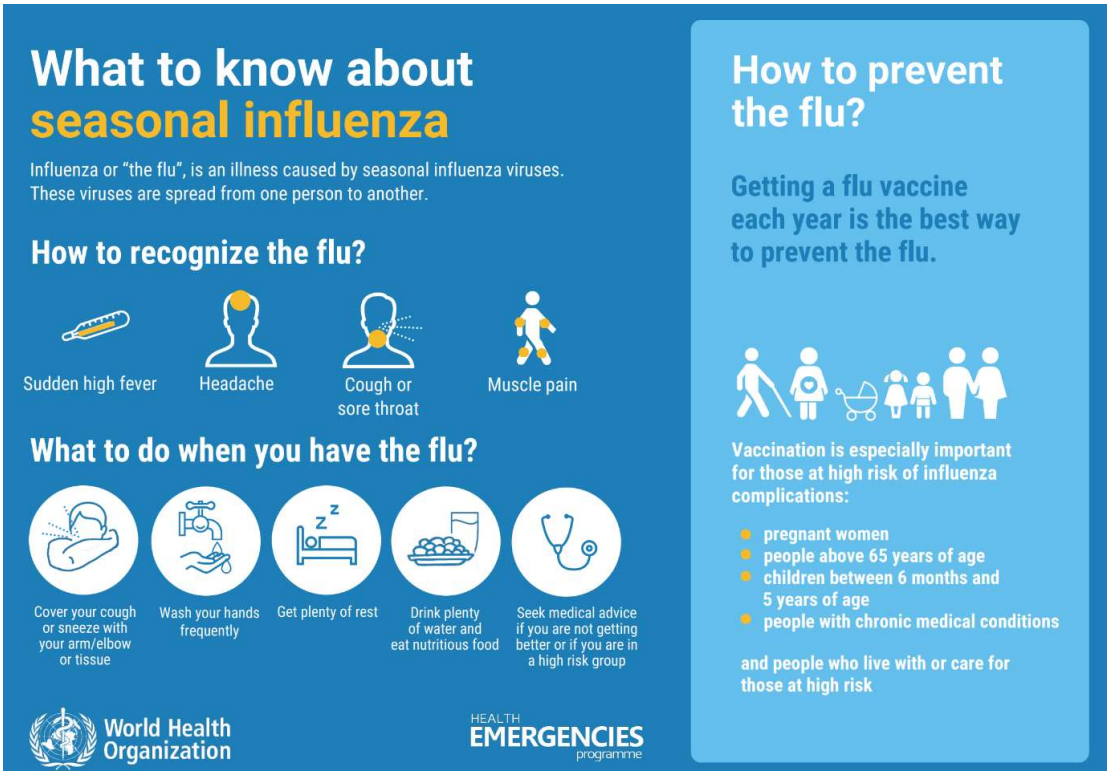

Figure 1.1.6.1. World Health Organisation Infographic (WHO, 2019b). These infographics help present ideas on how influenza affects health to the public concisely.

1.2 Virology

1.2.1 **Genome**

Influenza A viruses have a single stranded, segmented, negative-sense RNA genome of approximately 13.5Kb (**Fig. 1.2.1.1**). IAVs have eight gene segments, which code 17 proteins. To date there are 18 types of HA and 11 types of NA, with the combination of HA and NA subtypes providing the basis for IAV classification (Deng *et al.*, 2015).

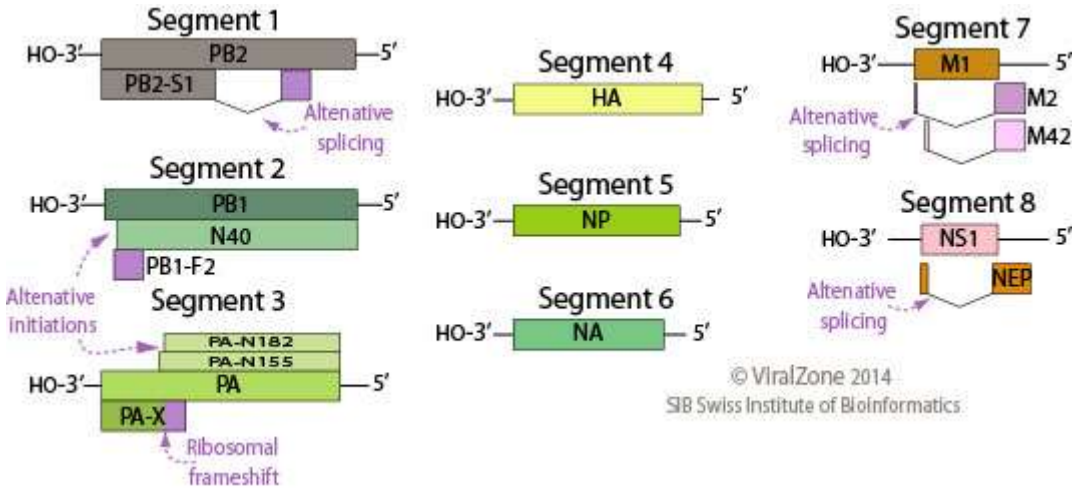

Figure 1.2.1.1 Influenza Genome (ViralZone, 2014) Segmented ssRNA(-) linear genome. Contains 8 segments coding for 17 proteins depending on strains. Segments size range from 890 to 2,341nt. Genome total size is 13.5Kb.

The majority of IAV subtypes are found in avian, and some in swine, human and other species such as bats. For IAVs to be capable of infecting multiple host species they require adaptations to allow replication in different host cells, increasing their fitness and permitting sustainable replication and transmition of the virus. For example, it is well recognised that avian IAV HAs have a binding preference for α-2,3 sialic acid residues, commonly found on the surface of avian cells. To gain entry to human cells, with α-2,6 sialic acid residues,

modifications to the HA binding site may be required to allow this interaction (Horman *et al.*, 2018).

Currently H1N1 and H3N2 are the subtypes of IAV circulating endemically in the human population; with sporadic cases of human infection with other IAV subtypes such as H5N1 and H7N9 in recent years. The influenza RNA genome has a high mutation rate because the viral RNA polymerase does not have the ability to proofread, unlike DNA polymerase, and therefore more errors are introduced into the genome.

The plasticity of influenza's RNA genome means that it can undergo two processes, antigenic drift and antigenic shift (**Fig. 1.2.1.2**). Antigenic drift occurs due to gradual changes in the surface antigens of the virus, the HA and NA. These two proteins continuously evolve due to host immune pressures from previous influenza infections. This causes seasonal epidemics. In contrast to this, the six internal genes of the virus are relatively conserved. Antigenic shift occurs less frequently and is caused by the sporadic genetic reassortment between different IAV subtypes from avian and swine species, and less frequently from humans. Such a reassortment took place to produce the 2009 swine flu pandemic virus (Smith *et al.*, 2009), where genes from several influenza swine origins reasserted (Garten *et al.*, 2009). Antigenic shift can lead to pandemic influenza outbreaks.

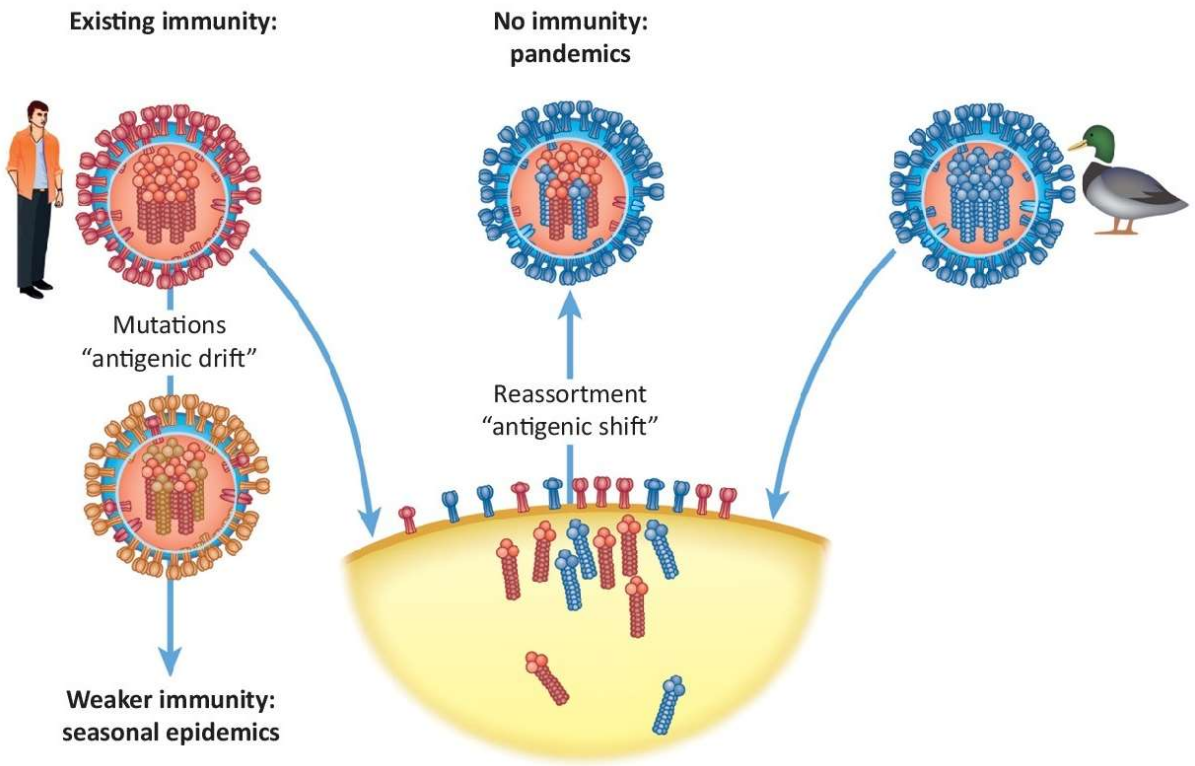

Figure 1.2.1.2. Antigenic Drift and Antigenic Shift (Hutchinson, 2018) An illustration of the mechanisms of antigenic drift and antigenic shift.

The IAV genome (**Fig. 1.2.1.3**) is made up of eight viral ribonucleoproteins. These encode the proteins described below. The surface of the virion is coated in the haemagglutinin (HA) and neuraminidase (NA) glycoproteins. The virus surface protein (M2) acts as an ion channel and the nuclear export protein (NEP) mediates the export of vRNP complexes from the nucleus.

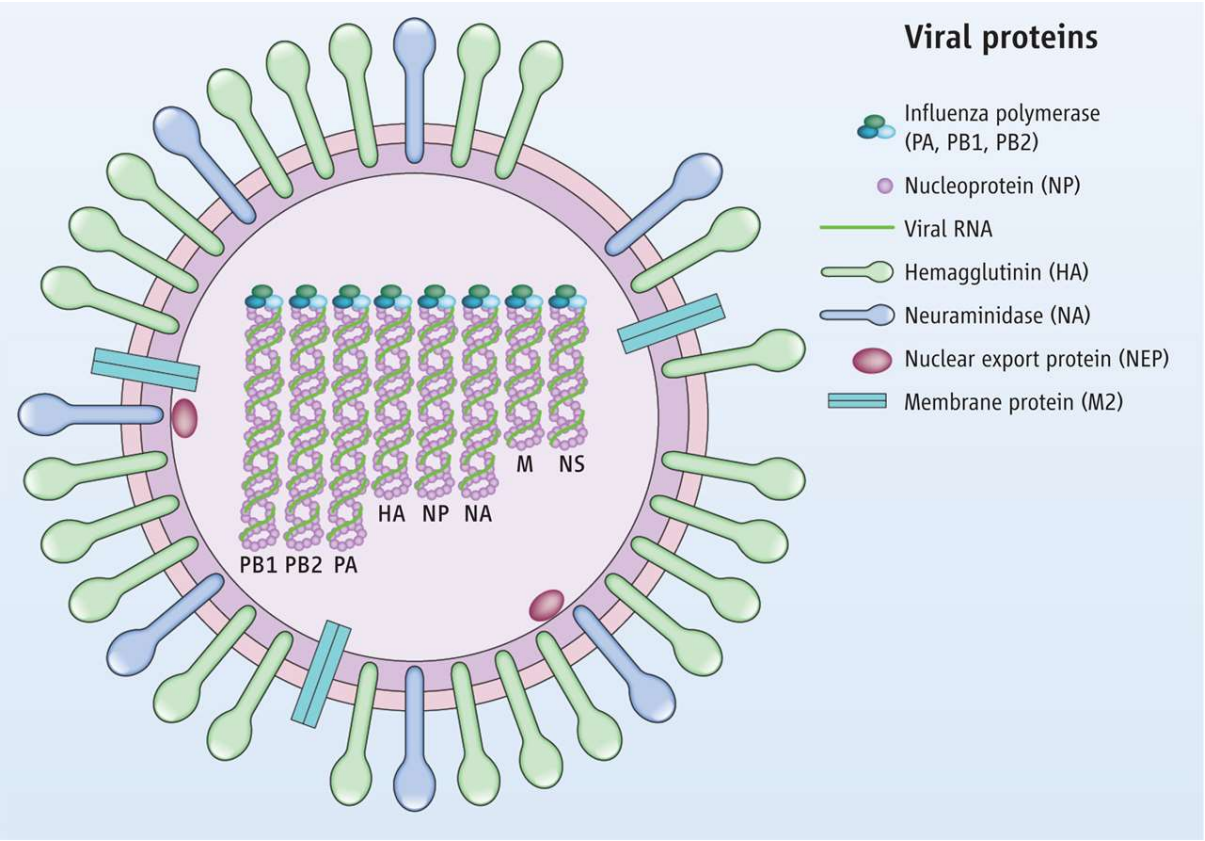

Figure 1.2.1.3 Influenza A Virion (Tao and Zheng, 2012) The IAV genome is composed of eight viral ribonucleoproteins (vRNP) complexes.

Table 1.2.1.1 contains a summary of the eight segments of the influenza genome, the protein name and a brief function

Table 1.2.1.1 Summary of Influenza A Virus Genome

Segment	Protein	Function(s)
1	PB2	Cap-binding subunit of the viral RdRp;cap-binding
2	PB1	Central location of the polymerase domain of the viral RdRp
3	PA	Cap-snatching endonuclease subunit of the viral RdRp
4	HA	Surface glycoprotein; receptor binding, membrane fusion
5	NP	Nucleoprotein; encapsidation of viral genomic and anti-genomic RNA
6	NA	Surface glycoprotein; receptor destroying neuraminidase activity enabling virus release
7	M1	Matrix protein
	M2	Ion channel activity
8	NS1	Regulation of viral RdRp activity; Interferon antagonist; Enhancer of viral mRNA translation.
	NEP	Nuclear export factor

1.2.1.1 **Haemagglutinin (HA)**

The haemagglutinin (HA) gene encodes the major viral surface antigen that is responsible for sialic acid binding and membrane fusion protein during virus entry into cells. The HA consists of two domains; a globular head (HA1) and stalk domain (HA2), linked by a single disulphide bond following cleavage from a single polypeptide precursor (HA0) (Skehel and Wiley, 2000). Cleavage of precursor HA0 by host proteases is a prerequisite for virus infectivity (Hashem,

2015) as well as a determinant of virulence and tissue tropism (Bertram *et al.*, 2010). The receptor binding and antigenic sites are located at the immune-dominant globular head which continuously undergoes antigenic drift. The HA is highly variable and is classified into 18 subtypes, which cluster into two major phylogenetic groups (Medina and García-Sastre, 2011). Antibodies that are directed against the stalk tend to be less effective but are broadly neutralising against seasonal and pandemic strains.

During viral replication the HA glycoprotein binds to specific sialic acid receptors on the surface of susceptible cells. Human IAVs target α 2, 6- linked sialic acid receptors which are found in abundance in the upper respiratory tract of humans while avian influenza viruses target α 2, 3- linked sialic acid receptors distributed in the intestinal tract of birds and lower respiratory tract of humans. Following binding of the HA to the sialic acid receptors the virus enters the cell via receptor mediated endocytosis. Following this a drop in the pH in the endosome leads to a conformational change of the HA which then mediates fusion of the viral membrane with the endosomal membrane and the viral ribonucleoproteins are released into the cell. It is thought that the HA stalk could be a promising target for a future universal vaccine, however some have suggested this may not be the case as the stalk is also susceptible to immune pressures (Anderson *et al.*, 2017).

1.2.1.2 **Neuraminidase (NA)**

Neuraminidase (NA) enables the virus to be released from the host cell and is not required for viral entry. Neuraminidases are receptor destroying enzymes that function as sialidases by cleaving sialic acid groups from glycoproteins. They are required for influenza virus release preventing HA mediated aggregation of nascent virus particles at the surface of the viral cell and allowing for viral release (Krammer *et al.*, 2014).

NA is a homotetrameric protein (made up of four identical subunits), with each subunit composed of a stalk domain which supports a head domain. NA is classified into 11 subtypes, N1 to N11. Much like HA, NA sequences can be phylogenetically classified into two groups; Group 1 including N1, N4, N5 and N8 and Group 2 including N2, N3, N6, N7 and N9. The more recently discovered novel NA subtypes isolated in bats (N10 and N11) appear to be quite distantly related to existing subtypes and do not display any sialidase activity (Tong *et al.*, 2013). In the absence of NA activity the virus is able to infect the cell and carry out one replication cycle, but virus particles are unable to be cleaved from the host cell surface and fail to spread to uninfected cells (Palese *et al.*, 1974).

1.2.1.3 **Matrix (M)**

The Matrix (M) gene encodes the matrix – 1(M1) and matrix – 2 (M2) proteins. The M1 protein is a membrane/RNA-binding protein with two functions. It mediates the encapsidation of RNA-nucleoprotein cores into the membrane envelope. It also mediates the transport of newly synthesised viral nucleoproteins from the nucleus to the cytoplasm. The M2 protein is a proton-selective ion-channel protein, integral in the viral envelope. The ion channels are responsible for the acidification of the virion and neutralisation of pH in the endosomes and Golgi network, early and late in the virus replication. The M1 and M2 proteins have been found to be highly conserved among different sub-types of influenza (Kreijtz *et al.*, 2011).

1.2.1.4 **Polymerase Basic Protein 1 (PB1), Polymerase Basic Protein 2 (PB2) and Polymerase Acidic Protein (PA)**

Polymerase basic protein 1 (PB1), polymerase basic protein 2 (PB2) and polymerase acidic protein (PA) working together make up the IAV viral polymerase. Following release of viral ribonucleoproteins into the cell, viral proteins are trafficked to the cell's nucleus where the viral RNA-dependent RNA polymerase complex transcribes and replicates the viral nucleoproteins.

1.2.1.5 **Nucleocapsid Protein (NP)**

The Nucleocapsid Protein (NP) plays a central role in viral replication by encapsidating the virus genome for the purposes of RNA transcription, replication and packaging (Eisfeld *et al.*, 2015) . The NP is a structural protein with no intrinsic enzymatic activity (Compans *et al.*, 1972) and is an important target for protective T cells. Following virus replication genetic material is packaged and released from infected cells. Each of the eight genome segments are associated with multiple NP molecules and a single, trimeric polymerase comprising of the PB2, PB1 and PA proteins. This complex of vRNA-NP-polymerase is referred to as the viral ribonucleoprotein (vRNP) (Eisfeld *et al.*, 2015).

1.2.1.6 **Non- Structural (NS)**

The non-structual (NS) gene encodes non-structual protein 1 (NS1) and the nuclear export protein (NEP). NS1 is multifuctional with the ability to regulate viral RNA-dependent RNA polymerase activity, enhance viral mRNA translation and act to circumvent antiviral repsonses

of the host. NEP acts to mediate the export of the virus ribonucleoprotein complexes from the nucleus alongside M1.

1.2.1.7 **Accessory Proteins**

In addition to the eight major viral proteins encoded by the IAV segmented genome, various accessory proteins have been identified that have been shown to modulate influenza infection both *in vitro* and *in vivo*.

PB1-F2

The translation of PB1-F2 occurs in a second open reading frame of the PB1 gene segment via a leaky ribosomal scanning mechanism (Chen *et al.*, 2001). PB1-F2 has been implicated in regulation of polymerase activity, immunopathology, susceptibility to secondary bacterial infection, and induction of apoptosis (Buehler *et al.*, 2013). Leaky ribosomal scanning combined with re-initiation of PB1 mRNA is also responsible for the translation of a third protein known as N-40 (Wise *et al.*, 2011).

PB2-S1

PB2-S1 is translated from spliced mRNA transcribed from the PB2 segment and appears to be conserved among pre-2009 human pandemic H1N1 viruses. This protein is able to bind to PB1, localise to mitochondria, and inhibit the RIG-I-dependent signalling pathway (Yamayoshi *et al.*, 2016).

PA-X

When IAV enters the cells it relies of the molecular machinery of the host to help it replicate, relying on the ribosomes of the host cell to translate viral messenger RNA (mRNA) into polypeptides. "Host shut-off" occurs when IAV impairs the translation of cellular mRNA to prevent the production of anti-viral, host defence proteins. PA-X is a novel protein expressed by ribosomal frameshifting has been found to play a major role in influenza virus-induced host shut-off (Hayashi *et al.*, 2016).

PA-N155 & PA-N182

Expression of PA-N155 and PA-N182 is universal among most IAVs and also occurs due to leaky ribosomal scanning (Gong *et al.*, 2014).

1.3 Transmission of Influenza

Transmission of an infectious disease is the process by which an infectious organism moves from one host to another and causes disease. There are many factors that contribute to and influence this process and to appreciate them one must first understand the basic pathophysiology of the underlying disease process (Killingley and Nguyen-Van-Tam, 2013).

The multiple mechanisms affecting influenza transmission are still not fully understood and this influences infection prevention and mitigation strategies during outbreaks. There are several key factors that can affect the effective transmission of IAV.

1.3.1 **Host Specificity of Influenza**

The human respiratory tract expresses α2-6-linked sialic acids more abundantly in the upper respiratory tract when compared to the lower respiratory tract (**Fig. 1.3.1.1**). In the nasopharynx of humans SA receptors are detected on both ciliated and mucus producing cells. In contrast, in the bronchus, these receptors are distributed in the epithelium with no obvious distinction between ciliated and non-ciliated cells (de Graaf and Fouchier, 2014). It has been noted that the bronchial epithelium of the human respiratory tract contains a higher percentage of α2-3-linked SAs compared to α2-6-linked SAs (Nicholls *et al.*, 2007).

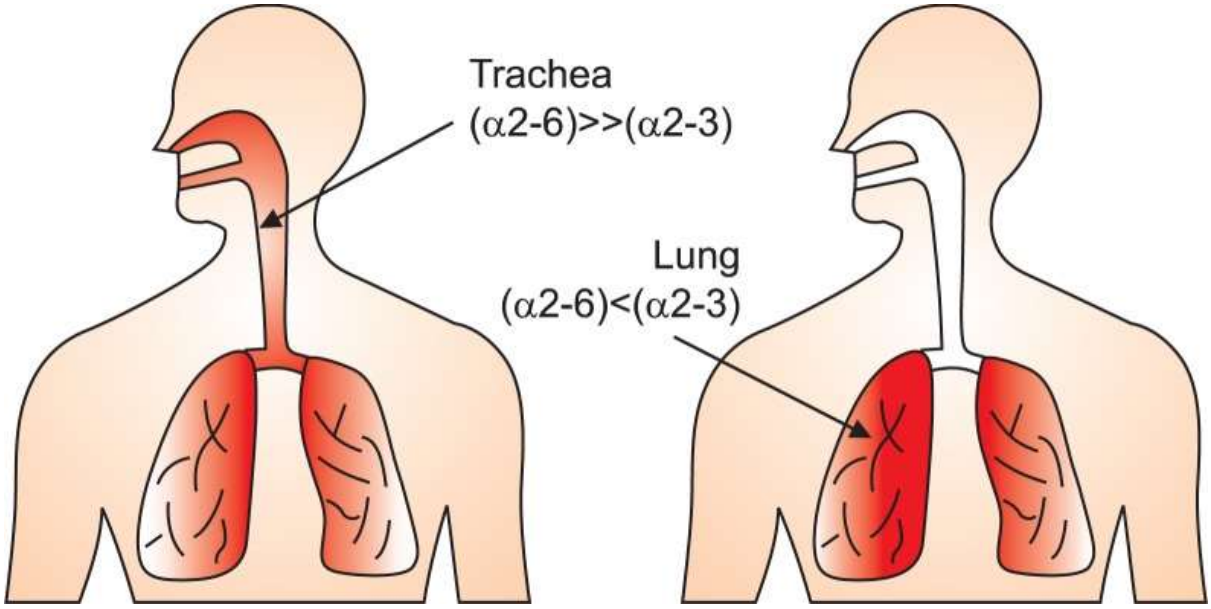

Figure 1.3.1.1 Distribution of sialyl (α2-3) and/or (α2-6) linkages containing oligosaccharides in human respiratory tracts (Yoo, 2014). The human lungs and lower respiratory tract have mainly sialyl (α2-3)-linked receptors for avian viruses, such as H5N1. The human bronchus and upper respiratory contain mixtures of (α2-3)- and (α2-6)-linked sialic acid, which are receptors for human-adapted viruses, such as H3N2 and H1N1. The bronchus contains more (α2-3)-linked sialic acid than does the upper respiratory tract.

Birds have both α2-3-linked SAs and α2-6-linked SAs in their respiratory and intestinal tract, with the abundance of these receptors varying amongst species. Pigs also express both α2-3-linked SAs and α2-6-linked SAs in their respiratory tract (de Graaf and Fouchier, 2014). Ferrets are used as the 'gold standard' experimental animal model because they have a similar α2-3-linked SA and α2-6-linked SA distribution throughout their respiratory tract as humans (Kirkeby *et al.*, 2009). Much like humans, α2-6-linked SAs are found in abundance in the trachea and bronchus on ciliated cells and submucosal glands. With alveoli expressing both α2-6-linked SA and α2-3-linked SA, with the former being far more abundant (Jayaraman *et al.*, 2012).

Sialic acid moiety is fundamental to species specificity of IAVs. The majority of mammalian and avian species present two main types of sialic acid on the terminal positions of the glycan of their glycoproteins or glycolipids. The receptor binding site on the HAs of avian IAVs bind to the thin, straight *trans* confirmation α2-3-linked SAs (**Fig. 1.3.1.2A**), whereas human-adapted IAVs HAs bind to a bulkier *cis* conformation α2-6-linked SA (**Fig. 1.3.1.2B**). Human IAVs have adapted mutations in the receptor binding site of their HAs allowing them to bind to this bulkier *cis* conformation. Receptor specificity of IAV strains has consequences for HPAI such as H5N1 infecting humans. H5N1 undergoes limited replication in the human respiratory tract due to the limited number of α2-3-linked SAs. However, efficient human to human transmission of these viruses requires that avian influenzas recognise α2-6-linked SAs. For example, isolates from the 1918, 1957 and 1968 pandemics suggest that these viruses preferentially recognise α2-6-linked SAs.

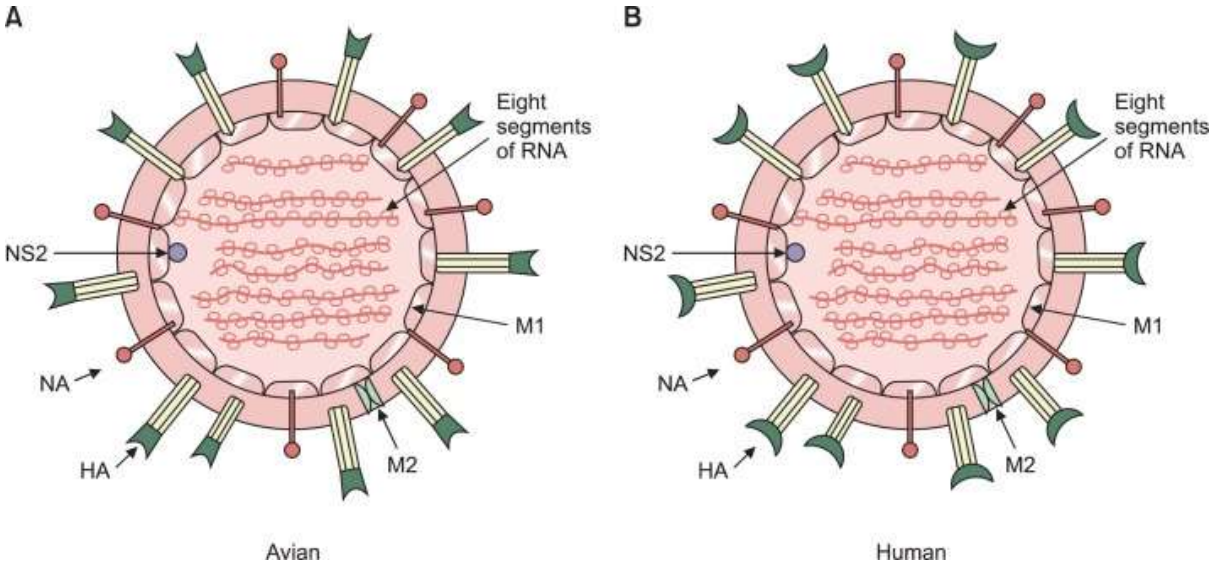

Figure 1.3.1.2 (Yoo, 2014) IAV HAs bind to sialic acids (SAs) on the cell surface. SAs are terminal sugars lined to larger glycans of glycoproteins and glycolipids on vertebrate cells. Differences in the structure of the SAs can determine species specific susceptibility to IAV infection (**A** & **B**).

Human infection with avian or swine IAVs occur sporadically and do not usually result in the establishment of a new lineage. The viral HA protein and its ability to bind to specific SA receptors has been identified as a major host restriction factor that can limit interspecies transmission.

1.3.2 **Physical Transmission of Influenza**

There are three routes of human influenza infection transmission that are widely accepted:

- Droplet (>5μm): Large droplets that deposit in the upper respiratory tract such as the mouth and the nose.
- Droplet nuclei (<5μm): Small aerosol particles that can be deposited along the respiratory tract and can reach the lower respiratory tract.
- Contact transmission: Particles are transferred to mucous membranes of the upper respiratory tract either directly or via contaminated object or person (Killingley and Nguyen-Van-Tam, 2013).

Currently, evidence on influenza transmission supports a potential role for all the above routes. Transmission can likely occur through multiple routes during the same 'event' and therefore is a dynamic and opportunistic process.

Respiratory droplets can be expelled by talking, coughing, sneezing and normal tidal breathing. There is evidence that humans generate infectious particles in both respiratory droplets and aerosols (Lindsley *et al.*, 2010) and this is enhanced during influenza infection (Lindsley *et al.*, 2012). Data from ferret studies also shows that when the animals are infected

with highly transmissible human influenza viruses (H3N2 & H1N1) they exhale and sneeze out more respiratory particles overall than those infected with poorly transmissible avian influenzas (H5N1) (Gustin *et al.*, 2013). Experimental data has also confirmed the association between influenza transmissibility in ferrets and the amount of viral RNA found in exhaled aerosols (Lakdawala *et al.*, 2011). However, the longer the time between the inoculation of the donor and the exposure of the naïve ferret, the less efficient the transmission despite viral RNA level remaining constant over the monitored timeframe (5 days) (Koster *et al.*, 2012).

Transmission via fomites (inanimate objects that can transfer disease when contaminated with an infectious agent) can occur when infectious particles are deposited onto hand-touch surfaces. These surface act as a vector for the transfer of viral particles to mucus membranes of susceptible individuals. The detection of infectious virus from surfaces is relatively limited and often constrained by low collection efficiencies associated with swab sampling and high detection limits of influenza enumeration assays (Killingley *et al.*, 2010). However, it has been shown that viability of influenza viruses can be maintained for a considerable period if the initial viral titres are high enough (Thompson and Bennett, 2017).

1.3.3 **Environmental factors affecting transmissibility**

Studies have reported that variations in humidity and temperature are important in IAV survival and therefore ability for the virus to be transmitted. For example, at constant humidity avian IAVs have been shown to remain viable in aerosols for longer periods of time that human IAVs (Mitchell *et al.*, 1968). Influenza transmission has also been shown to have increased efficiency at lower relative and absolute humidities (Lowen *et al.*, 2007) which correlates with findings that show the biological decay of IAVs increases as relative humidity is increased

(Richard and Fouchier, 2016). Higher temperatures (of around 30ºC) have also been shown to be detrimental to transmission of IAVs (Lowen *et al.*, 2008). These findings suggest that cool dry conditions enhance influenza survival and transmissibility and could be one explanation for the seasonality of influenza.

1.3.4 **Zoonotic Transmission of Influenza**

Researchers are yet to have a complete picture of the factors and mechanisms that are required for influenza virus transmission within species and between species. (**Fig. 1.3.4.1**) Zoonotic transmission of IAVs from wildfowl to humans is rarely reported, most likely due to the frequency of human exposure to large, wild bird populations. Far more common is the zoonotic transmission of IAVs through an intermediate host such as poultry or swine to humans. This is thought to be due to more frequent exposure to these animals through agricultural practices. Most of these transmission events do not include human to human transfer and result from close contact with animals either at markets or on farms.

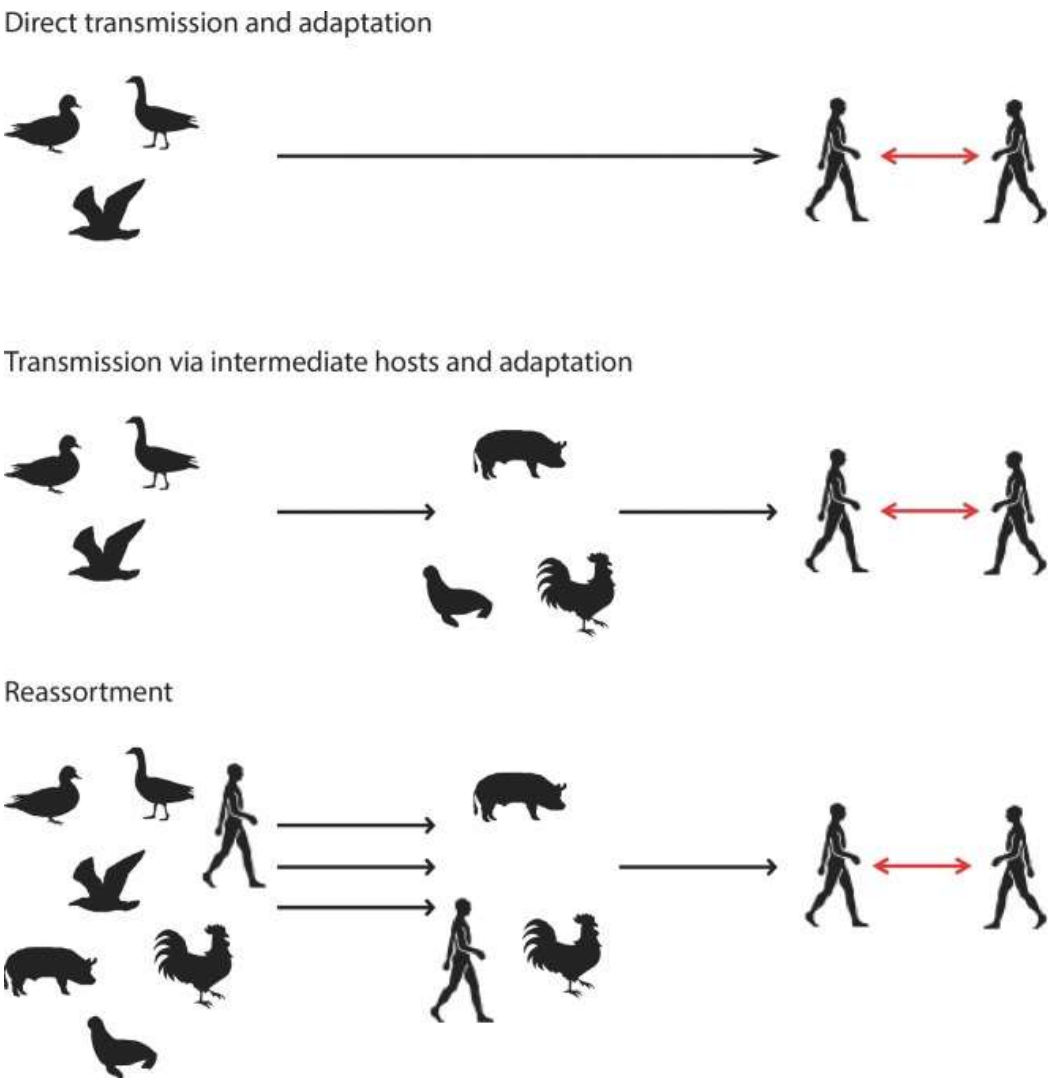

Figure 1.3.4.1 Zoonotic transmission of Influenza (Richard and Fouchier, 2016) Potential routes of transmission and adaptation of influenza viruses. Many scenarios could support the transmission of influenza viruses from their original reservoir to humans and subsequent adaption to transmit via the airborne route: (i) direct transmission from waterfowl to humans and subsequent adaptation in humans; (ii) transmission from waterfowl to intermediate hosts, adaptation in these hosts and subsequent transmission to humans; and (iii) reassortment in intermediate hosts of influenza viruses originating from diverse animals species and transmission to humans.

1.3.5 **Cell Entry, Replication, Assembly and Movement**

1.3.5.1 **Attachment**

IAVs use the HA molecules on their envelope surface to initiate the infection process (**Fig. 1.3.5.1.1**). The HA receptor-binding site attaches the virus surface to terminal sialic acid residues (Hamilton *et al.*, 2012, Gamblin and Skehel, 2010) and the HA-mediated binding to the receptor triggers endocytosis of the virion. Endocytosis occurs either by macrophagocytosis (de Vries *et al.*, 2011, De Conto *et al.*, 2011), or in a clathrin-dependent manner (Lakadamyali *et al.*, 2004). Once the virus has successfully entered the cell it is trafficked to the endosome where the low pH activates the M2 ion channel on the viral envelope causing a conformational change in the HA exposing the fusion peptide. The opening of the M2 ion channel allows the inside of the virus to become acidified causing the release of the packaged vRNPs to the host cell cytoplasm. Fusion of the viral-endosomal membranes occurs through several steps and requires the cleavage of the HA into two subunits, HA1 and HA2, by host cell proteases.

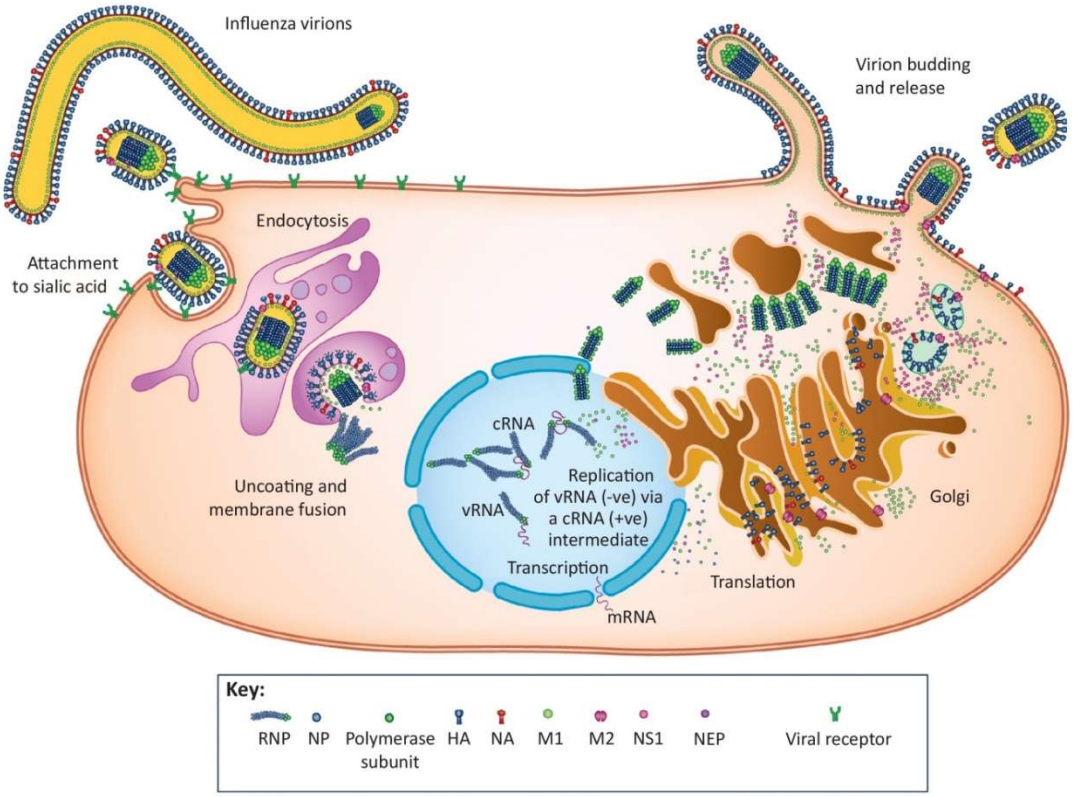

Figure 1.3.5.1.1 Influenza replication cycle (Hutchinson, 2018) A brief summary of the replication cycle of influenza virus. Influenza viruses infect the respiratory epithelium. The haemagglutinin (HA) proteins of IAV bind sialic acid, causing endocytosis. The viral genome replicates in the nucleus. New viruses assemble at the cell surface and are released by the receptor-cleaving neuraminidase (NA) proteins of IAV.

1.3.5.2 **Replication & Transcription**

Once inside the nucleus the viral RNA-dependent RNA polymerase functions to carry out the transcription and replication of vRNA (Pflug *et al.*, 2017). Replication occurs in two steps: transcription of complimentary RNA (cRNA) and transcription of new vRNA using the cRNA as templates (Matsuoka *et al.*, 2013).

1.3.5.3 **Translation**

IAV viral mRNAs are translated by the host cell translation machinery. Following synthesis in the cytoplasm, the viral polymerase subunit proteins and NP are imported into the nucleus via their nuclear localisation signals to catalyse the replication and translation of vRNA (Matsuoka *et al.*, 2013). M1 and NEP/NS2 are imported into the nucleus as part of their role in vRNP nuclear export. Meanwhile NS1 is also imported into the nucleus for its role in the processing and export in cellular and viral mRNAs (Schneider and Wolff, 2009).

1.3.5.4 **Assembly and Budding**

Viral NEP/NS2 and M1 help export newly synthesised vRNP from the nucleus. Following synthesis by cellular machinery HA, NA and M2 proteins enter the endoplasmic reticulum (Klenk *et al.*, 2001). These proteins are then transported to the plasma membrane of the cell where HA and NA associate with distinct membrane regions rich in sphingolipids and cholesterol (lipid rafts) (Gerl *et al.*, 2012) (Lingwood and Simons, 2010, Dou *et al.*, 2018). Virion assembly and incorporation of the eight vRNPs occurs following specific signals from the viral RNAs. The M2 protein appears to mediate membrane scission and particle release (Rossman *et al.*, 2010). The virus is then released from the cellular membrane by the enzyme activity of viral NA protein.

1.4 The Immune Response to Influenza

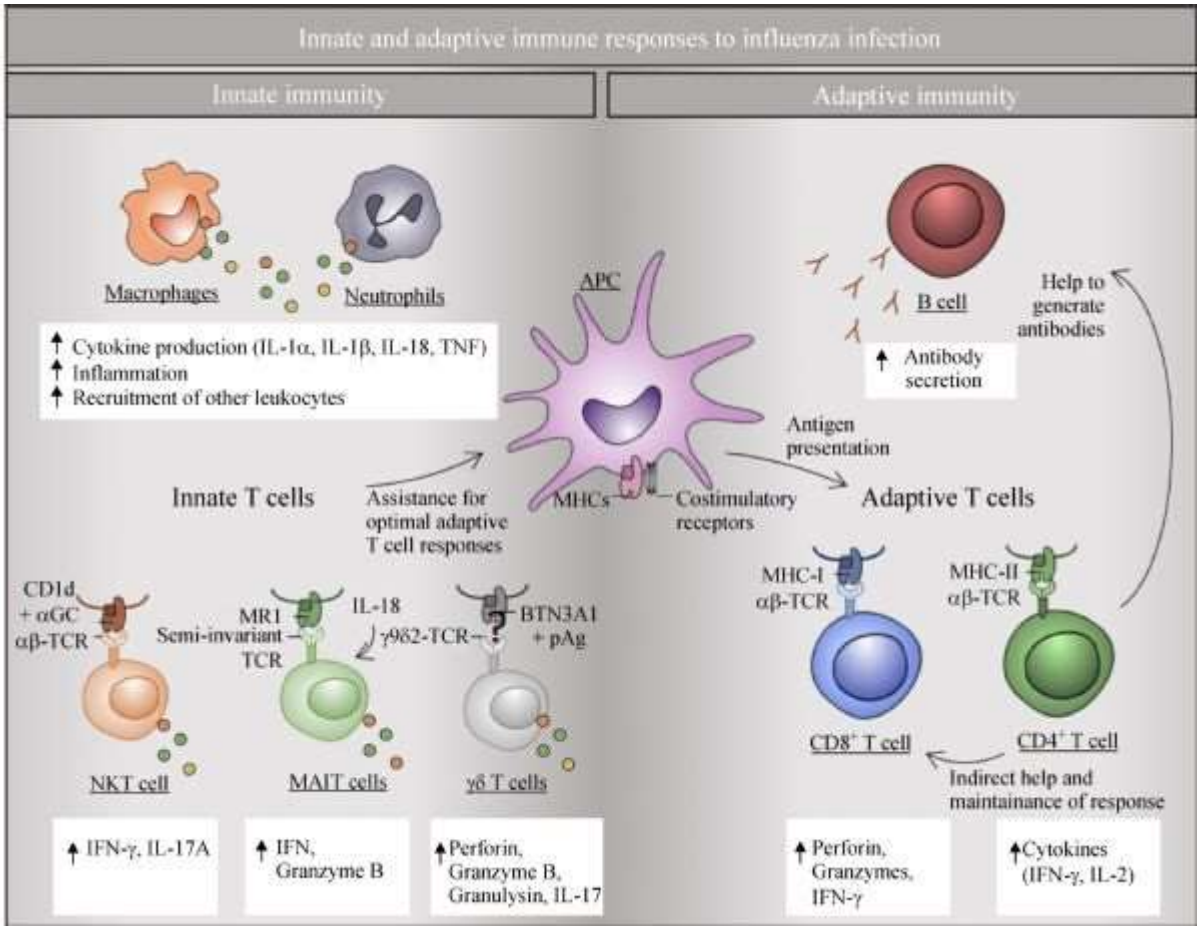

Figure 1.4.1 Innate and adaptive immune responses to influenza (Nüssing *et al.*, 2018) IAV infection leads to activation of innate cells, such as macrophages and neutrophils, to secrete pro-inflammatory cytokines resulting in the recruitment of other leukocytes. Innate T cells play an important role in reducing the effects of influenza infection by the secretion of cytokines and cytotoxic molecules. Innate T cells provide important signal molecules to enhance antigen presenting cell activity, which present influenza antigens to CD8+ T cells and CD4+ T cells for effective viral clearance.

1.4.1 **The Innate Immune Response**

The first line of defence against influenza is chiefly controlled by the innate immune response. The mucosal barrier produces a sialic acid rich layer of mucus which is able to bind viral HA protein and trap some of the influenza virus particles that have infected the host (Matrosovich and Klenk, 2003). This mechanism effectively acts to reduce the infectious dose to the host (Cohen *et al.*, 2013) by preventing the infection of epithelial cells. Following successful infection pattern recognition receptors (PRRs) can recognise viral RNA, the major pathogen-associated marker pattern (PAMP) of IAV. The PRRs consist of host cell toll-like receptors (TLRs), retinoic acid inducible gene-I (RIG-I) and the NOD- like receptor family pyrin domain containing 3 (NLRP3) protein (Pang and Iwasaki, 2011). Following signalling via these receptors type I interferons and pro-inflammatory cytokines are produced. The expression of interferon alpha (IFN-α) and interferon beta (IFN-β) is stimulated, both of which possess antiviral activity by inhibiting protein synthesis in host cells therefore limiting viral replication (Kreijtz *et al.*, 2011). Interferon stimulated genes are also induced by type 1 interferons via the JAK/STAT signalling pathway. One of these genes is the myxovirus gene that encodes the MxA protein which has been shown to have strong antiviral activity that inhibits influenza replication (Haller and Kochs, 2002).

Type I interferons also stimulate dendritic cells (DCs) which act as antigen-presenting cells (APCs) during influenza infection. This stimulation results in enhanced antigen presentation to CD4+ and CD8+ T cells (lymphocytes that mature in the thymus and express a T cell receptor (TCR)). DCs are usually situated underneath the airway epithelium barrier and are able to monitor the airway lumen, detecting and opsonising virions and apoptotic bodies from infected cells (Kreijtz *et al.*, 2011). They can also be infected themselves, and upon infection migrate to the draining lymph node presenting the influenza virus-derived antigens to T cells

and activating them (Hintzen *et al.*, 2006) therefore contributing to the adaptive immune response. DCs degrade the viral proteins and present the immune-peptides by major histocompatibility complex (MHC) class I or class II molecules. MHC class I presentation occurs when IAV derived peptides are released in the cytosol and transported to the endoplasmic reticulum where they associate with MHC class I molecules. These are then trafficked to the cell membrane where they are recognised by specific CD8+ cytotoxic T cells. MHC class II presentation occurs when IAV proteins are degraded in endosomes or lysosomes giving rise to peptides which associate with MHC class II molecules. Again, these molecules are trafficked to the cell membrane, and recognised by CD4+ T helper cells (Kreijtz *et al.*, 2011).

Alveolar macrophages become activated and phagocytose influenza infected cells upon infection of the alveoli. This action can limit viral spread (Tumpey *et al.*, 2005, Kim *et al.*, 2008). Conversely, following activation, alveolar macrophages produce tumour necrosis factor alpha (TNF-α) nitric oxide synthase 2 (NOS2) which contribute towards the virus induced pathology found in the lung (Jayasekera *et al.*, 2006, Lin *et al.*, 2008). These two contrasting functions of alveolar macrophages highlight the careful balancing act of responses during IAV infection. Highly pathogenic avian influenza viruses such as H5N1 have been shown to infect both blood-derived and alveolar macrophages due to their ability to cause systemic infection, and are therefore more prone to causing immunopathology (Peiris *et al.*, 2010).

Natural killer (NK) cells are important effector cells of the innate immune response. They perform antibody-dependent cell cytotoxicity by recognising antibody-bound IAV infected cells and lysing them. NK cells recognise IAV infected cells via two cytotoxicity receptors, NKp44

and NKp46. Once bound to the IAV haemagglutinin the receptor triggers the NK cell to lyse the infected cell (Arnon *et al.*, 2001, Mandelboim *et al.*, 2001).

1.4.2 **The Adaptive Immune Response**

The adaptive immune response is responsible for eliminating pathogens from infected hosts, preventing pathogen replication and spread, and generating immunological memory (Bonilla and Oettgen, 2010). It comprises of humoral and cellular immunity mediated by IAV specific antibodies produced by B cells (lymphocytes that mature in bone marrow) and T cells.

B cells are activated and differentiate into antibody-secreting plasma cells or memory B cells following binding of antigen to membrane bound surface cell receptors. Antibodies are 'Y' shaped glycoproteins that consist of two identical heavy (H) polypeptide chains and two identical light (L) polypeptide chains linked by di-sulphide bonds. Different parts of the antibody molecule are responsible for specific functions. Antibody specificity is mediated by the binding of fragment antigen binding (Fab) domains of antibodies to the antigenic target. On the other end of the antibody is a constant region known as the fragment crystallisable (Fc) domain which binds to cell surface receptors providing a link between the antibody recognition of the infected cell and the effector cell. Antibodies function by binding to and coating pathogens or cells, allowing them to be targeted for destruction by phagocytosis, death or, in the case of viral infection, degranulation of the pathogen infected cell which induces lysis or apoptosis of the target cell. This process is known as antibody dependent cellular cytotoxicity (ADCC). In humans NK cells are the primary effector for ADCC, but ADCC of influenza-infected cells has been demonstrated in neutrophils, monocytes, lymphocytes and core blood cells (Jegaskanda *et al.*, 2016).

There are two main classes of T cell, defined by the co-receptor they express; CD4+ or CD8+. Upon activation CD8+ T cells differentiate into cytotoxic T lymphocytes (CTLs), which kill infected cells or tumour cells by inducing apoptosis. CD4+ cells differentiate into T helper (Th) cells which release cytokines that can stimulate further T cell function, macrophage activation or B cell antibody production. Th cells can further be divided into Th1, Th2, Th17 and regulatory T (Treg) cells based on cytokine secretion profiles and functions (Bonilla and Oettgen, 2010). Th1 cells are associated with the regulation of intracellular pathogens and produce cytokines such as interferon gamma (IFN-γ) and IL-12. Th2 cells are involved in the protection of the body against extracellular pathogens and helminths producing cytokines such as IL-4, IL-5 and IL-13. Th17 cells are characterised by the production of IL-17 and are important in the defence against extracellular pathogens, and have also been linked to autoimmunity (Bettelli *et al.*, 2008).

1.4.2.1 **Humoral Immune Response**

IAV infection induces a viral-specific antibody response (Mancini *et al.*, 2011), with the most significant antibodies produced against the HA and NA (Gerhard, 2001). HA specific antibodies can neutralise the virus as the action of binding to the trimeric globular head of HA inhibits viral attachment and entry into the host cell. Antibodies against the HA are a well-established correlate of protection providing they match the virus causing infection (de Jong *et al.*, 2000). Antibodies to NA have been shown to have protective potential. NA antibodies do not directly neutralise the virus, but they have been shown to inhibit enzymatic activity limiting the spread of the virus. NA specific antibodies also facilitate ADCC and may also contribute to the clearance of virus-infected cells (Mozdzanowska *et al.*, 1999). Antibodies against the matrix (M2) protein do exist, however the protein is in such low concentrations in

infected cells that they are only raised to a limited extent (Kreijtz *et al.*, 2011). Nucleoprotein (NP) antibodies may also contribute to protection against influenza (Carragher *et al.*, 2008).

The main antibody isotypes in the influenza-specific humoral immune response are immunoglobulin A (IgA), IgM and IgG. Secretory IgA or mucosal antibodies locate to the site of infection affording protection by trans epithelial transport by using the mucus of the respiratory tract. These antibodies are also able to neutralise intracellular virus (Mazanec *et al.*, 1995). Serum IgA antibodies are usually produced following IAV infection and the presence of these antibodies is a marker for recent IAV infection (Rothbarth *et al.*, 1999), while serum IgG antibodies move via transudate into the respiratory tract and provide long-lived protection (Murphy *et al.*, 1982). Finally, IgM antibodies are known to initiate complement mediated neutralisation of IAV and are a characteristic of primary infection (Jayasekera *et al.*, 2007).

ADCC against influenza can be mediated by multiple cell types and can arise following infection or vaccination. It's thought that ADCC is primarily directed against HA, however other antigens to ADCC cannot be ruled out. As stated previously, antibodies directed against the globular head of HA lack breadth of recognition across strains, while antibodies directed against the more conserved HA stem can recognise multiple strains and subtypes of HA (Air, 2015). Antibodies with neutralisation and haemagglutination inhibition activity tend to be directed against the HA head domain.

ADCC mediating antibodies also target other proteins on the virus surface. NA antibody titres have been shown to correlate with protection against influenza (Murphy *et al.*, 1972, Couch *et al.*, 2013, Memoli *et al.*, 2016), however NA responses are not as well documented as HA responses. NA is present in most vaccines originating from influenza virions, however unlike

HA it is not quantified for the vaccine and therefore its contribution towards protection in not well understood. The highly conserved M2 antigen has also been shown to have antibodies to M2 mediated ADCC and shown protection in mouse studies (Von Holle and Moody, 2019). Additionally, the influenza nucleoprotein (NP) has been shown to mediate ADCC *in vitro* and humans vaccinated with the seasonal vaccine have demonstrated H7N9 cross-reactive ADCC activity that correlated with binding to NP (Jegaskanda *et al.*, 2016).

1.4.2.2 **Cell-mediated Immune Response**

The cellular immune response to IAV involves the activation of phagocytes, antigen-specific cytotoxic T-lymphocytes (CTLs), and the release of various cytokines in response to antigen. CD8+ and CD4+ T cells have distinct but significant roles in the control and clearance of influenza (Doherty and Christensen, 2000).

Influenza-specific CD8+ T cells play a key role in broadly cross-reactive immunity to influenza viruses because they recognise small peptide fragments (8-11 amino acids) derived from highly conserved internal viral proteins presented as MHC class I molecules. Influenza-specific CD8+ T-mediated cross-protection against different influenza subtypes has been supported by several animal studies (Altenburg *et al.*, 2015). CD8+ T cells recognise the more conserved internal proteins of IAV allowing them to be broadly cross protective (**Fig. 1.4.2.2.1**). Therefore, pre-existing CD8+ T cell immunity cannot prevent IAV infection but are important in controlling an mediating recovery from infection (Wang *et al.*, 2015). Upon infection CD8+ T cells differentiate into CTLs which go on to release cytokines and effector molecules to restrict viral replication and kill virus-infected cells (Chen *et al.*, 2018).

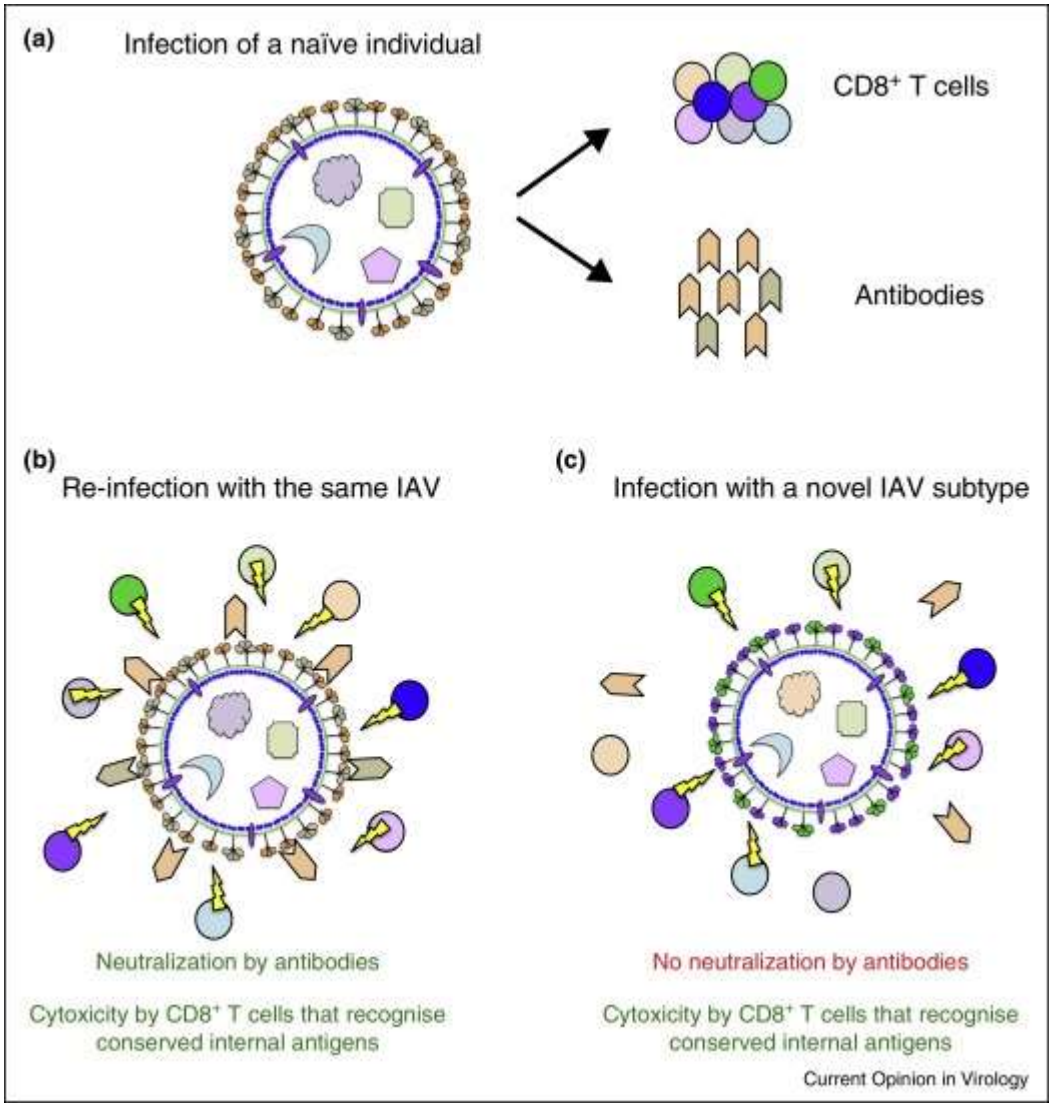

Figure 1.4.2.2.1. CD8+ T cells providing protection (Grant *et al.*, 2016) (a) Infection of a naïve individual will elicit humoral and cellular mediated immunity. **(b)** Re-infection with the same IAV strain reactivates immune memory and antibodies neutralise the virus with CD8+ T cells **(c)** During infection with a novel IAV strain neutralising antibodies will not bind, however CD8+ T cells that recognise conserved internal proteins will mediate immunity, still providing protection.

Naïve CD8+ T cells are activated by dendritic cells that have migrated from the lungs to the T-cell zone of the draining lymph nodes, this leads to T cell proliferation and differentiation into CTLs (Ho *et al.*, 2011). CTLs then migrate from lymph nodes to the lungs where they can kill influenza infected cells. CTLs can release cytotoxic granules, such as perforin and granzymes,

that are able to destroy virus infect cells. Following infection, virus-specific memory CTLs circulate in blood, lymphoid organs and the site of infection. Therefore they are able to respond to secondary influenza infection by recognising conserved influenza epitopes such as M1 and NP (Grant *et al.*, 2016). The CTL response is heterosubtypic in nature. Heterosubtypic immunity can be defined as cross-protection to infection with an IAV virus strain other than the one used for primary infection.

A longitudinal study in China has shown that recovery from severe H7N9 infection in humans was associated with robust early CD8+ T cell responses, in contrast, patients who succumbed to infection had delayed and/or minimal cytotoxic CD8+ T cell responses (Wang *et al.*, 2015). Influenza-specific CD8+ T cells have been found to be stable in the peripheral blood of healthy adults over a period of 13 years, demonstrating that CD8+ T cells are long lived (van de Sandt *et al.*, 2015b). There have been a variety of studies demonstrating that human CD8+ T cells specific for seasonal IAVs are cross-reactive across avian IAVs; H7N9 (Quiñones-Parra *et al.*, 2014, van de Sandt *et al.*, 2014), H5N1 (Kreijtz *et al.*, 2008, Lee *et al.*, 2008), and the two-lineages of IBV (van de Sandt *et al.*, 2015a).

CD4+ T cells recognise viral peptide fragments presented on MHC II molecules and perform an important part of promoting optimal CD8+ T cell and B cell responses during influenza infection. Naïve CD4+ T cells are activated in the draining lymph node following IAV infection much like CD8+ T cells. They go on to differentiate into Th1 cells following infection. Th1 effector CD4+ T cells produce cytokines such as IFN-γ, TNF and IL-2, and migrate to the lung activating alveolar macrophages (Liu *et al.*, 2012).

CD4+ T cells also differentiate into Th2, Th17 and Treg, follicular helper T cells and killer cells (Zhu *et al.*, 2010). Th2 cells have been shown to bind to virus-derived MHC class II-

associated peptides by APCs and produce several cytokines to promote B cell responses. Th17 and Treg cells have been shown to be involved in regulating cellular immunity again influenza (Mukherjee *et al.*, 2011) and memory CD4+ T cells can regulate early innate responses upon influenza infection independent of PAMP recognition (Strutt *et al.*, 2010).

T cell soluble mediators

CTLs and Th cells produce a wide variety of cytokines and chemokines (**Fig 1.4.2.2.2**). The T cell receptor (TCR) mediated production of soluble mediators is important for viral clearance and to minimise inflammation.

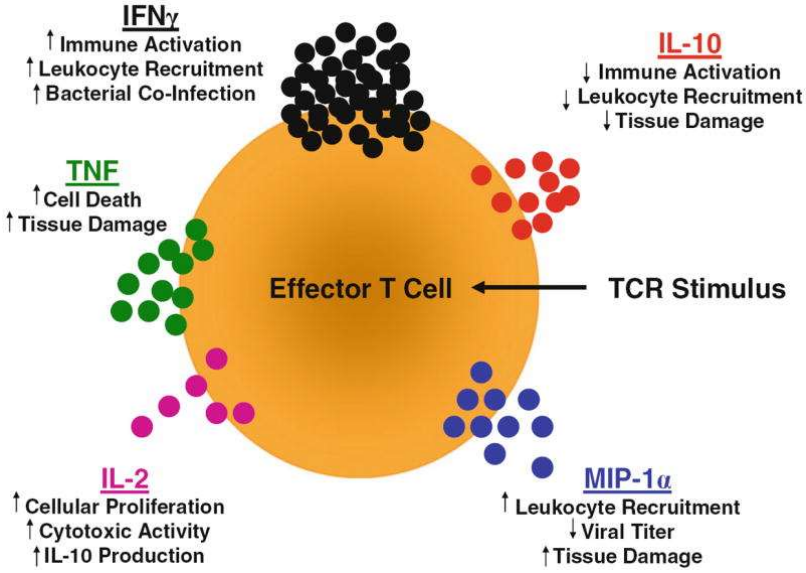

Figure 1.4.2.2.2 T cell soluble mediators the major types of soluble T cell mediator produced by effector T cells during IAV infection.

IFN-γ

The most well-known cytokine produced by influenza-specific Th cells and CTLs upon infection is interferon gamma (IFN-γ). Peak IFN-γ production has been shown to coincide with the arrival of influenza-specific Th cells and CTLs into the respiratory tract (Hufford *et al.*, 2011).

IFN-γ activates immune cells (macrophages), upregulates immunomodulating molecules (MHC), and modulates antibody isotype switching (the change of a B cell's immunoglobulin from one type to another). IFN-γ most likely contributes to viral clearance but isn't essential due to other antiviral mechanisms. It's been demonstrated that despite its activity, IFN-γ deficiency was not shown to have an impact on influenza clearance (Graham *et al.*, 1993). The absence of IFN-γ has also been linked to reduced tissue damage, most likely due to recruitment of leukocytes (Wiley *et al.*, 2001). It's also thought that IFN-γ may contribute to a patient's susceptibility to secondary bacterial infections often seen in severe influenza infections (Sun and Metzger, 2008).

TNF

Tumour necrosis factor (TNF) is a pleotropic cytokine, with its functions dependent on target cell type as well as inflammatory environment (Parameswaran and Patial, 2010). TNF is commonly produced in conjunction with IFN-γ by both influenza-specific Th cells and CTLs during infection. Unlike other soluble mediators (IFN-γ) TNF release isn't directed towards specific target cells and therefore allows for potent non-specific effects (Huse *et al.*, 2006). TNF has also been noted to have significant impact on immune-mediated tissue damage during influenza infection with no discernible impact on viral clearance (Belisle *et al.*, 2010). Because of the general complexity of TNF signalling, TNF may promote anti-inflammatory

(diminish cytokine production, inhibit phagocytosis, trigger apoptosis) or pro-inflammatory (stimulate cytokine production, augment cellular proliferation, trigger cellular necrosis) outcomes (Hufford *et al.*, 2011).

IL-10

Interleukin-10 (IL-10) is a regulatory cytokine which down regulates MHC and co-stimulatory molecule expression, modulates inflammatory cytokine expression and can inhibit cell proliferation. Sources of IL-10 during infection are CTLs, Th cells and regulatory T cells; however, studies in mice have shown lung CTLs are the main source of IL-10, producing it in large amounts during infection (Sun *et al.*, 2009). These CTLs also have been shown to have the capacity to produce inflammatory cytokines such as IFN-γ, therefore associated IL-10 production is more likely to limit inflammation than completely inhibit it (Hufford *et al.*, 2011).

MIP-1α

Macrophage inflammatory protein (MIP) - 1α is produced by both influenza-specific Th cells and CTLs upon activation. Other possible sources are B lymphocytes, NK cells and myeloid cells). MIP-1α is a chemokine which, when bound to its receptors, can exert a potent chemotactic and pro-inflammatory effect. It can enhance lymphocyte cytokine production and is an effective recruiter of monocytes, lymphocytes, immature DCs and activated neutrophils (Menten *et al.*, 2002). Studies have shown that MIP-1α is likely a significant pro-inflammatory soluble mediator necessary for influenza clearance (Hufford *et al.*, 2011).

IL-2

Interleukin-2 (IL-2) is a regulatory cytokine and its main function is to promote the development of T regulatory (Treg) cells. IL-2 has been shown to promote Treg cell responses while inhibiting T follicular helper cells (Botta *et al.*, 2017).

1.5 Treatment and Prevention

1.5.1 **Antivirals**

Antivirals are important in the prevention and management of IAVs.

Neuraminidase Inhibitors

Neuraminidase inhibitors (NAIs) act to block the neuraminidase (NA) enzyme preventing ongoing viral replication by blocking budding from an infected host cell. The NA active site is highly conserved amongst IAV and IBV and NAIs are effective against all currently circulating human influenzas. NAI compounds were designed to mimic natural substrate of the NA enzyme and compete for binding to the active site, with a higher binding affinity (Samson *et al.*, 2013).

There are currently two licensed NAIs; oseltamivir (Tamiflu) and zanamivir (Relenza), and a further NAI that has received approval in Japan and the US; peramivir (Thorlund *et al.*, 2011). Oseltamivir is the most commonly used NAI in response to influenza infection and is often distributed during outbreaks, as was the case during the 2009 H1N1 pandemic. During a pandemic outbreak it is recommended that a full course of oseltamivir is used alongside early detection for effective control of an outbreak.

Influenza resistance to NAIs has been well documented. Resistance to oseltamivir has been found to occur not only during treatment and prophylaxis but also in the absence of NAI pressure. This was found to be the case during the 2009 H1N1 pandemic with the H274Y

variant. The susceptibility of oseltamivir resistance appears to differ between subtypes depending on the structure of their neuraminidase (Li *et al.*, 2015).

Cap-dependent endonuclease inhibitor

Baloxavir marboxil (Xofluza) is a therapeutic which inhibits the cap-dependent endonuclease activity of the influenza polymerase. It inhibits the process known as cap-snatching during the process of viral mRNA biosynthesis (DuBois *et al.*, 2012). Baloxavir marboxil has been approved since 2018 for use in adolescents and adults in the US and Japan, with antiviral activity against both IAV and IBV. Clinical trials have shown that treatment with baloxavir marboxil significantly shortened the duration of symptoms compared with a placebo and also reduced infectious viral titres shed and the duration of shedding more rapidly than oseltamivir in healthy and high risk patients (Fukao *et al.*, 2019).

1.5.2 **Vaccination**

Annual vaccination is currently the most effective way of controlling influenza infection and spread. A wide variety of vaccine platforms have been evaluated against influenza; DNA-based vaccines, viral vectors, virus-like particles, recombinant DNA, novel live attenuated, and adjuvanted vaccines have all been developed to improve vaccine development and immunogenicity (Paules and Subbarao, 2017). A universal vaccine that is broadly cross-protective could potentially replace the need for an annual vaccination as well as provide protection against the emergence of novel strains (Hashem, 2015, Keshavarz *et al.*, 2019). Currently there are only three forms of licensed vaccine used to protect individuals annually; inactivated, live attenuated and recombinant HA vaccines, all of which are focused on

producing antibodies against viral HA. All three of these vaccines are multivalent. This means that the vaccine containing multiple components which can target current globally circulating seasonal influenza A and B viruses. These multicomponent vaccines can either be trivalent or quadrivalent. Trivalent vaccines contain both circulating A subtypes; H1N1 and H3N2, and one B subtype, of either Yamagata or Victoria lineage. Quadrivalent vaccines contain both circulating A subtypes; H1N1 and H3N2, and both circulating B subtypes; Yamagata and Victoria.

Inactivated Influenza Vaccine

The first formulation of the inactivated influenza vaccine (IIV) was a monovalent formulation which contained a subtype of influenza A virus. When influenza B was discovered in 1940 it was found to be antigenically distinct to the A/PR8 strain used in the monovalent inactivated vaccine, however it shared the ability to grow in eggs and therefore it was incorporated into the vaccine creating a bivalent inactivated influenza vaccine. Following this, large scale clinical studies with the first bivalent vaccine containing both type A and B viruses began in December 1942 and provided researches with the first evidence that the vaccines had the capability to provide protection from influenza epidemics (Francis *et al.*, 1945). Safety and efficacy studies were carried out from 1942 to 1945.

The current IIV is produced as a split virion or subunit vaccine which can be administered intramuscularly or intradermally, with 15μg and 9μg of HA protein respectively. There is a higher dose of antigen (60μg) available for those aged 65 years and over. This is designed to elicit an increased immune response to the vaccine (Paules and Subbarao, 2017). The IIVs induced strain specific serum IgG antibody response and are licensed for individuals aged 6 months and older. An adjuvanted inactivated trivalent vaccine, FluAd, is also approved for

use in individuals over the age of 65. The adjuvanted vaccine has been shown to have a higher immunogenicity and effectiveness that non-adjuvented vaccines in this age group.

Live Attenuated Influenza Vaccine

Live attenuated vaccines (LAIVs) are designed to represent a natural transient influenza infection, therefore eliciting a longer lasting and broader immune response in recipients. The first LAIV was developed in the USSR and has subsequently been used in Russia since 1987 to vaccinate children over three years, adults and the elderly. The reassortant viruses for Russian LAIV are prepared by classical reassortment in eggs of chosen wild-type IAV and IBV viruses with one of two cold adapted (*ca*) master donor viruses (MDVs) as a backbone (A/Leningrad/134/17/57 (H2N2) and B/USSR/60/69). Cold adapted viruses can only replicate at lower temperatures found in the human nasal cavity. A/Leningrad/134/17/57 underwent several passages in chicken embryos at 25°C to generate the temperature sensitive phenotype found in LAIV.

MedImmune developed the current licensed LAIV used in the UK for school aged children (2-10) and in the US for healthy individuals between the ages of 2 and 49 (Grohskopf *et al.*, 2014). *ca* A/Ann Arbour/6/60 forms the backbone of the live attenuated quadrivalent vaccine and is sold under the trade name of Fluenz (Europe) and Flumist (United States). Prior to license, during randomised controlled trials, the LAIV was not shown to be any more efficacious than the inactivated vaccine in adults. Vaccination with the LAIV results in the production of strain specific IgG as well as mucosal IgA and T cell responses (Coelingh *et al.*, 2014). The LAIV has also been found to be effective against some seasonally drifted strains. However, it has been hypothesised that an adult may have a previous immune history from influenza infections and therefore possess the cellular immunity to conserved internal viral

proteins that supress local mucosal replication of the LAIV in the nasal cavity well enough to prohibit a robust immune response (Sridhar *et al.*, 2013).

Recombinant Influenza Vaccine

FluBlock is a recombinant HA vaccine. It contains HA that has been expressed in insect cells using baculovirus vectors. It is currently licensed for adults aged 18 to 49 and can be used in individuals with an allergy to eggs (Grohskopf *et al.*, 2014). The manufacturing process has a shorter timeframe to other egg based vaccines which would be advantageous in a pandemic response (Paules and Subbarao, 2017).

1.6 Animal Models of Human IAVs

Animal research and animal models are necessary tools to model the complexity of the human host, where *in vitro* and *in silico* models are unable to adequately simulate immunological and physiological response to disease. Animal models are also essential to evaluate new vaccines, therapeutics and interventions to influenza before proceeding to human clinical trials. Animal research undergoes strict scrutiny in Europe. In 2015 the European Commission underlined that while animal research remains important for improving animal and human health, it is committed to promoting development and validation of non-animal-based approaches, and to enforcing the application of the 3Rs (replacement, reduction and refinement) (EuropeanCommision, 2015).

Animal research is conducted in compliance with strict regulatory provisions which covers the licensing and inspection of the premises, the training and competence of all project personnel and authorisation of every project by a competent Animal Welfare and Ethical Review Body (Barré-Sinoussi and Montagutelli, 2015). The criteria for evaluation are based on the 3Rs. As well as a cost-benefit analysis that evaluates whether potential harm to the animals, which must be reduced to the lowest possible level, is outweighed by significant progress in terms of knowledge to human or animal health.

Several animal models have been used in the past to assess IAV including; mice, cotton rats, Syrian hamsters, ferrets, dogs, cats, domestic swine and non-human primates such as rhesus, pigtailed and cynomolgus macaques, and marmosets (Bouvier and Lowen, 2010, Moncla *et al.*, 2013, Eichelberger and Green, 2011). The most commonly used models are the mouse, guinea pig and ferret models. These are discussed below in further detail.

1.6.1 **Mice**

Mice are the most widely used animal model in influenza research (Bouvier, 2015). Practically, mice have inexpensive purchase and husbandry costs, they are a convenient model in terms of size and there is a wealth of frequently used species-specific reagents accessible to researchers. When carrying out preliminary animal studies mice are the ideal animal model to choose. However, there are some disadvantages to the mouse model that can leave data obtained difficult to interpret and associate with the human situation of influenza infection. The susceptibility of a mouse model to influenza and the clinical signs produced depends upon both the strain of mouse being used and the strain of influenza (Bouvier and Lowen, 2010, Margine and Krammer, 2014). Many human influenza strains must be mouse adapted which requires the virus to be passaged *in vivo* in mouse lungs. This can lead to significant amino acid changes which improve the receptor binding in the mouse respiratory tract allowing for replication and increased virulence. However, this can mean that the adapted virus becomes either antigenically or phenotypically distinct from the initial strain (Margine and Krammer, 2014), potentially producing a disease very different to human flu infection. It has also been noted that transmission between a donor and sentinel mouse can be difficult (Lowen *et al.*, 2006); therefore the mouse model is not suitable for transmission modelling investigations. Nonetheless, the mouse model does provide an opportunity for an in depth investigation of immune responses elicited by infection and vaccination and, due to their inbred nature the mouse model tends to mount a very reproducible response to infection (Margine and Krammer, 2014).

1.6.2 **Guinea Pig**

The most commonly used guinea pig strain for influenza research is the outbred Hartley guinea pig (Bouvier and Lowen, 2010). They are susceptible to human strains of influenza, without need for adaptation and the virus transmits between animals with ease (Lowen *et al.*, 2006). As with mice, guinea pigs are widely available, relatively cheap to acquire and house, and their size means that they are easy to work with. Unlike mice the strain of guinea pig used does not seem to alter the outcome of disease in the animal. Viral growth occurs mainly in the upper respiratory tract and virus usually grows to high titres. Growth in the lungs can be moderate but this is usually short lived (Lowen *et al.*, 2006, Bouvier and Lowen, 2010).

Guinea pigs can be infected with avian and swine strains of influenza without prior adaptation of the virus (Lowen *et al.*, 2006) however; despite inoculation with similar virus titres, the resulting titres reached in the nasal passages by these viruses are not as high as when inoculated with human isolates. Despite the high viral titres reached in the upper respiratory tract IAVs do not cause noticeable clinical disease in guinea pigs. This is most striking when infecting guinea pigs with HPAI H5N1, a virus that is lethal in mice and ferrets, but only a mild disease is obtained following an infectious a dose of 10^6 EID_{50} (50% egg infectious dose) (Kwon *et al.*, 2009) making the guinea pig model unsuitable for assessing clinical severity of viruses. However, it has been demonstrated that un-adapted human influenza viruses which replicate in high titres in the guinea pig respiratory tract are able to be transmitted via aerosol from donor guinea pigs to sentinel guinea pigs (Lowen *et al.*, 2006). This makes guinea pigs a suitable small animal model in which to pilot initial transmission studies (Bouvier and Lowen, 2010).

1.6.3 **Non-human Primates**

The use of non-human primates (NHPs) in the investigation of influenza dates to the 1890s. Researchers attempted to infect NHPs with “bacteria” recovered from influenza patients, this produced a mild illness (Davis *et al.*, 2015). One of the key advantages of NHP models is their close genetic and physiological match to humans when compared to other mammalian models (Moncla *et al.*, 2013). However, it is important to note that there is variability in suitability amongst species. For example it has been found that cynomolgus macaques have 50-73 times higher expression levels of α 2, 6-linked sialic acid receptors in their respiratory tracts compared to rhesus macaques which could cause a difference in the replication of the virus (Mooij *et al.*, 2015). It is thought that NHPs are able to model the human immunological response to IAV infection much more strongly than seen in rodent and ferret models (Mooij *et al.*, 2015). A wide range of NHP species have been shown to be susceptible to influenza A virus infection (Davis *et al.*, 2015), however, they develop varying clinical signs and histopathological changes which are not always characteristic of human H1N1 or H3N2 infection (Bouvier and Lowen, 2010).

Some studies have shown successful infection of NHPs comparable to human infection; marmosets infected with a pandemic H1N1 isolate resulted in virus replication, antibody response, symptom development and transmission which are all typical of human influenza infection (Moncla *et al.*, 2013, Mooij *et al.*, 2015). A comparison study between rhesus and cynomolgus macaques showed that rhesus macaques exhibited the most easily observed clinical symptoms of the two sub-species when infected with a pandemic H1N1 virus.

A review of the literature in this area shows that researchers still need to establish the optimal route of infection to simulate a reproducible human influenza infection in NHPs. Researchers

usually inoculate animals via multiple routes ensuring that infection takes place, this, however does not mirror natural exposure seen in humans (Davis *et al.*, 2015). Introduction of the virus directly into the lower respiratory tract maximises the severity of the disease, consequently this method is less optimal for modelling typical seasonal infections. Investigations have found that the respiratory tract of NHPs differ from that in humans, with a greater affinity for avian influenza viruses compared to human influenza viruses (Davis *et al.*, 2015). The NHP model comes with high costs and complex husbandry needs that only a small number of researchers can accommodate. This coupled with the low availability of NHPs mean that this animal model is less accessible than other animal models used to study IAV.

1.6.4 **Ferret**

Ferrets are small carnivorous mammals from the mustelid family. Due to their small size and comparable physiology, anatomy and metabolism to humans they are considered a more suitable animal model for the study of influenza virus infection when compared to larger animal models such as pigs, dogs and NHPs (Enkirch and von Messling, 2015). The ferret model for IAV was first characterised in 1933 (Smith *et al.*, 1933) following exposure of two ferrets to filtered throat washings from human patients infected with influenza. Since then it has been established that ferrets are susceptible to a wide variety of human influenza isolates without need for prior adaptation of the virus, as well as avian and swine viruses. Consequently, ferrets are widely considered the gold standard for influenza infection and the ferret model has made a remarkable contribution to our current understanding of influenza.

Early experiments with ferrets showed that they produced similar symptomology to humans when infected with influenza; such as sneezing, lethargy, fever, nasal discharge and anorexia. As with humans, ferrets inoculated with influenza present a primarily upper respiratory tract

infection due to humans and ferrets having a similar distribution of sialic acid receptors in their respiratory tracts. In the upper respiratory tract of both species there is an abundance of alpha 2,6- linked sialic acid receptors, while both alpha 2,6- linked and alpha 2,3-linked sialic acid receptors are present in the lower respiratory tract. As in humans, ferrets infected with seasonal H1N1 and H3N2 strains usually produce mild clinical symptoms with widespread infection of the upper respiratory tract due to the viruses high affinity for alpha 2,6- linked sialic acid receptors while tissues in the lower respiratory tract are decreasingly affected (Enkirch and von Messling, 2015). In contrast, both humans and ferrets infected with pandemic strains of influenza experience extensive infection throughout the lung with associated pneumonia due to the highly pathogenic influenza viruses increased affinity (with respect to seasonal strains) for alpha 2,3-linked sialic acid receptors. Because ferrets show symptoms to IAV infection they are often used in studies to look at the efficacy of antiviral agents in preventing disease. In addition, the ferret remains the primary animal model for assessing the efficacy of new antiviral drugs and vaccine strategies (Bodewes *et al.*, 2010).

The initiation of IAV infection in the ferret model, and indeed other animal models as well as humans, is most routinely carried out by instilling virus via the intranasal route. It is the most straightforward procedure compared to other methods of infection. **Figure 1.6.4.1** illustrates other inoculation route commonly used in the ferret influenza model. The choice of which route to use is dependent on the stain of virus used and the question being posed. For example, with avian influenzas such as H5N1 and H7N9 intratracheal instillation is used to allow the virus direct access to the lower respiratory tract inducing a more severe clinical disease. This is with the view to produce a more severe pneumonia which represents the pathogenesis seen in humans infected with these viruses (Bodewes *et al.*, 2011, Kreijtz *et al.*, 2013).

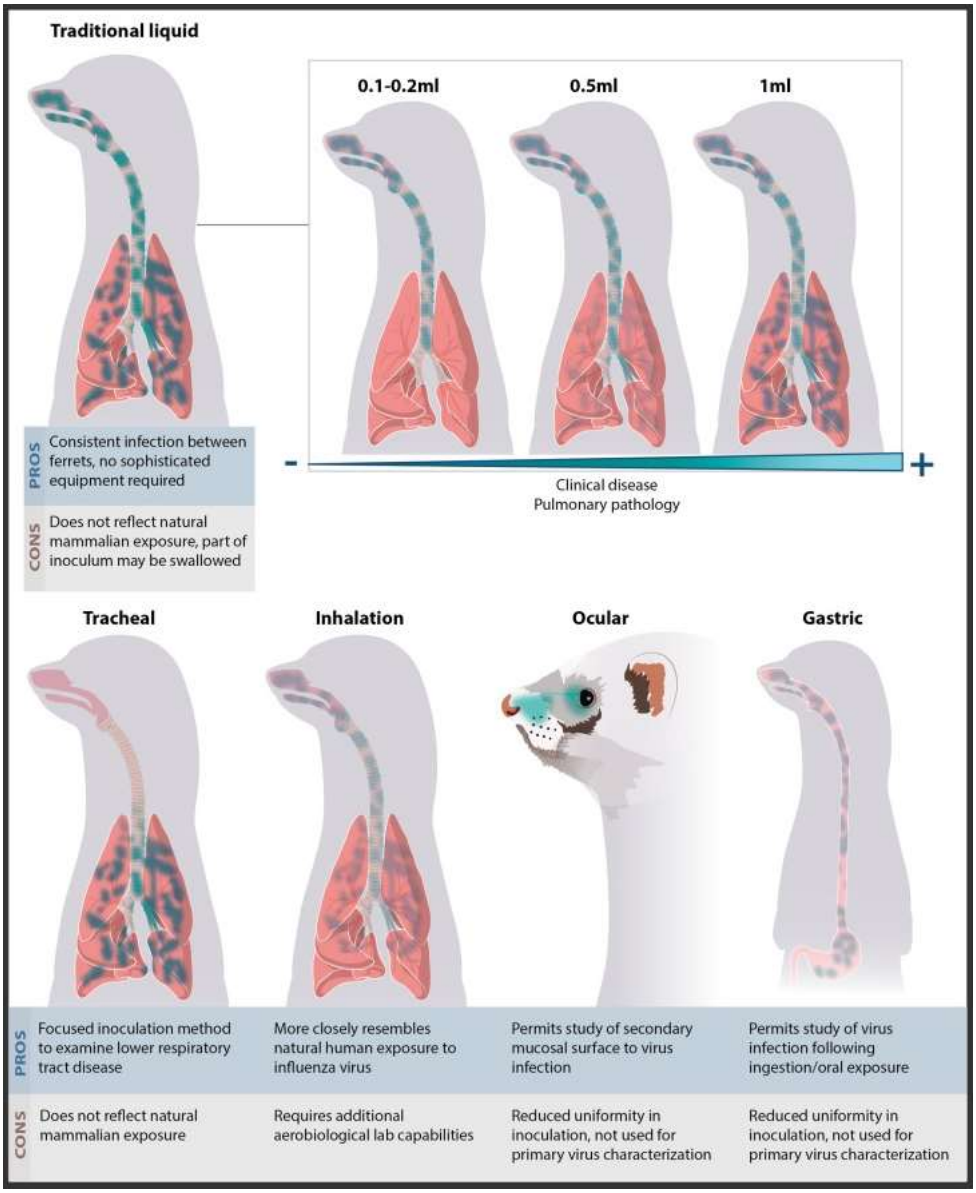

Figure 1.6.4.1 Contribution of inoculation route contributes to ferret pathogenesis (Belser *et al.*, 2016) Contribution of inoculum volume and route of infection to influenza virus virulence in the ferret. This figure illustates the variance in location and viral load between multiple different inoculum routes employed in the ferret. Shading indicates locations with high viral loads. Selected advantages and disadvantages for each inoculum route are highlighted.

Ferrets are commonly infected with seasonal IAVs via the intranasal route. It has been noted that the clinical severity of influenza infection caused by intranasal infection can vary depending on the volume of virus given to the ferret (Moore *et al.*, 2014). It has been shown

(**Fig 1.6.4.1**) that smaller volumes of inoculum (0.2ml and 0.5ml) remained in the upper respiratory tract of the ferret whilst larger volumes of inoculum (1.0ml) resulted in the delivery of the virus to the lower respiratory tract. The larger volume (1.0ml) of incoula also gave the ferrets more severe clinical signs and lung histopathology when compared to ferrets infected with smaller volumes (0.5ml and 0.2ml) (Moore *et al.*, 2014). The Influenza Group at Public Health England routinely infect their ferrets with an inoculum volume of 0.2ml (Marriott *et al.*, 2014) (Ryan *et al.*, 2018) (Gooch *et al.*, 2019).

One criticism of intranasal infection is that it does not represent a 'natural' route of infection. Past investigations into more 'natural' routes of influenza infection in the ferret model have included; contact (Yen *et al.*, 2001, Frise *et al.*, 2016) and non-contact transmission experiments (Koster *et al.*, 2012) (Otte *et al.*, 2016), aerosol exposure of animals using a plethysmography chamber (Gustin *et al.*, 2011), aerosol-ocular exposure (Belser *et al.*, 2012) and nose inhalation exposure system (Lednicky *et al.*, 2010). These 'natural infection' models often provide a more clinically relevant route of transmission. However, none of these studies have made any comparison between all three methods of experimental infection: intranasal, aerosol and transmission cage.

The model is a valuable tool for assessment of the acute phase of infection as there are numerous samples that can be collected from the ferrets without termination of animals (**Fig. 1.6.4.2**). Successful virus infection is largely assessed based on quantification of virus shed from the respiratory tract. Nasal washes can be collected frequently to allow titration of the virus from the upper respiratory tract. Additionally, bronchiolar lavage (BAL) washes have been used to allow for consecutive quantification of influenza virus replication in the lower respiratory tract of living ferrets (Lee *et al.*, 2014). Swabbing at specific sites in the upper respiratory can provide an alternative to nasal washing. Swabbing can also be carried out

rectally to assess the presence of virus in the gastrointestinal tract. These samples can then be titrated for the presence of virus. Collection of peripheral blood samples during the infection and at cull allows observation of viremia and antibody titres throughout infection.

When ferrets are terminated, tissues can be collected for virus quantification, and the extent of virus burden throughout the ferret can be determined. Collection of tissue samples from throughout the upper and lower respiratory tract can provide more specific location of viral replication in the ferret than nasal or BAL washes, which are more likely to be inclusive of most or all the respiratory tract.

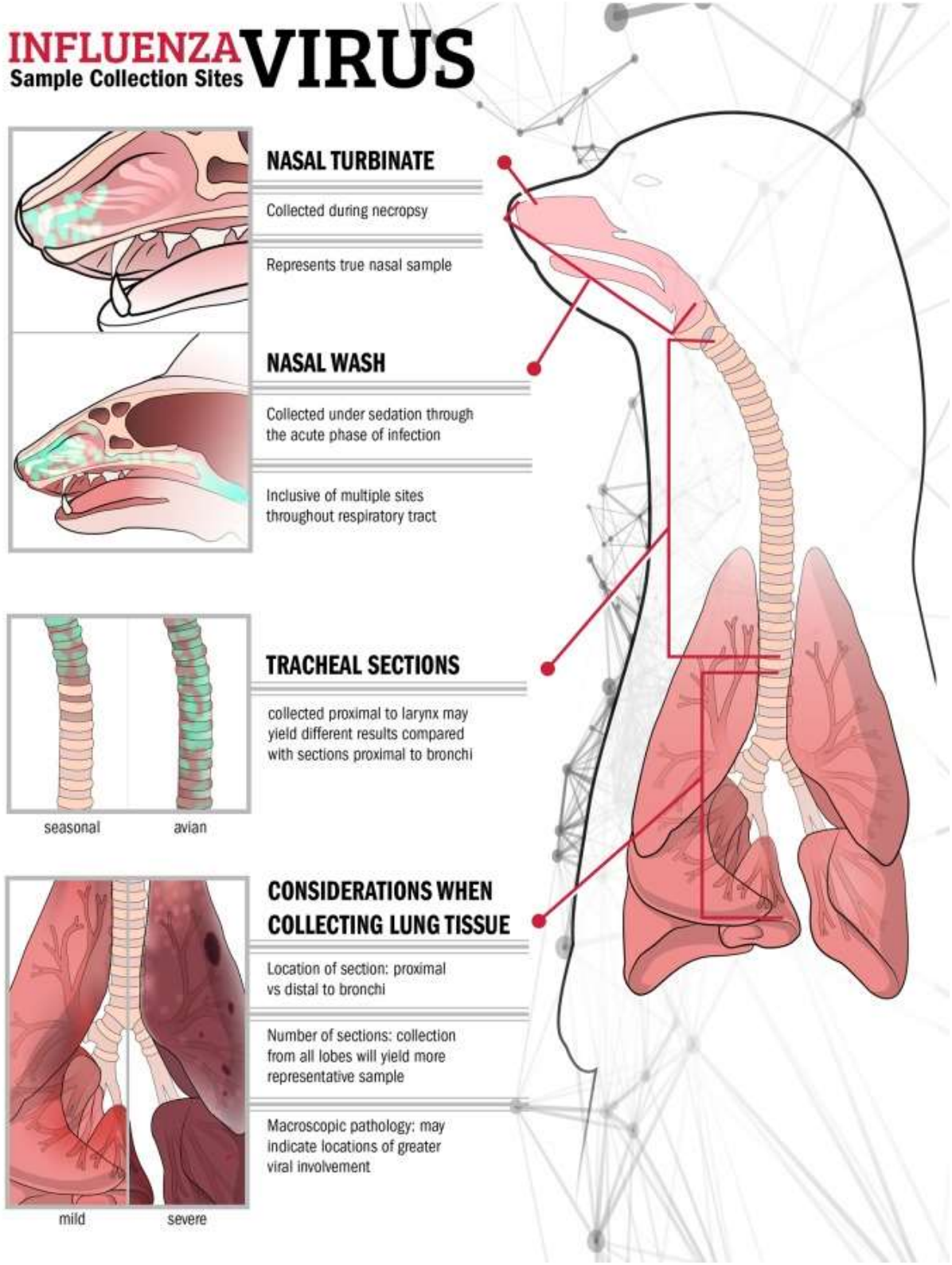

Figure 1.6.4.2 Influenza virus sample collection sites (Belser *et al.*, 2016) Frequently collected samples from the ferret respiratory tract during the acute phase of infection. Examples of variance in location precision and viral load between different sites and types of samples collected during influenza

virus infection in the ferret, and different viral loads and pathology present between mild/seasonal and virulent/avian influenza virus infection, are shown. Green shading indicates locations of high viral loads in nasal and tracheal samples. Sites sampled during nasal wash collection may extend beyond the upper respiratory tract.

Despite criticisms, the majority of ferret influenza studies use intranasal infection and inoculate with high viral titres (10^{4-6} plaque forming units (PFU) per ferret) which allows many infectious particles to infect the upper respiratory tract in a short period of time. Ferrets infected with these titres often experience their highest shedding titres at 1dpi (day post infection) (Marriott *et al.*, 2014). In contrast, ferret infected with lower doses (10^2 PFU) appear to more closely resemble a 'natural infection' where nasal wash viral titres gradually rise, peak and then fall (Marriott *et al.*, 2014), (Oh and Hurt, 2016). Higher viral titres are often used to infect ferrets to guarantee infection and to increase pathogenicity, however this may not be necessary as a low dose intranasal infection has been shown to be reproducible and show comparable disease severity in ferrets (Marriott *et al.*, 2014), (Oh *et al.*, 2015).

The draft of the ferret genome was published in 2014 (Peng *et al.*, 2014) and has provided researchers with the opportunity to improve the sophistication of ferret respiratory disease models, particularly in overcoming the lack of immunological reagents. Analysis of the ferret genome revealed a high protein-sequence similarity and shared tissue expression patterns with humans (Peng *et al.*, 2014), reiterating the ferret's suitability as an effective model for human influenza. Despite the ferret's ability to demonstrate a very similar disease to humans, the model still lacks appropriate reagents required to carry out in depth immunological studies (Thangavel and Bouvier, 2014) and remains inaccessible to some researchers due the cost, size and husbandry requirements of the animals.

1.7 Summary

For this set of studies the ferret has been chosen as the most appropriate animal model for the following reasons:

1. The ferret model for human IAV is widely used in then influenza research field and has several advantages over other animal models such as comparable symptomology, similar receptor distribution in the respiratory tract to humans.

2. The ferret has the ability to be infected with human isolates without the need for prior adaptation unlike other animal models.

3. At PHE Porton Down there is extensive experience of performing studies on ferrets using H1N1 influenza strains. This body of work hopes to build on this experience, by developing a H3N2 ferret model by evaluating routes of transmission, and the viral kinetics and cellular immune response induced by these routes.

It is already known that the seasonal H3N2 virus is able to successfully cause disease in ferrets following infection, however the vast majority of these experimental models have been carried out using high titres of virus. There are several gaps in knowledge surrounding the H3N2 virus in the ferret model, for example, the robustness and reproducibility of a low dose of infection and the effect of a low dose of infection on the viral kinetics in the ferret model and the cellular immune response seen as a result.

The H3N2 strain that was chosen for this piece of work was A/Perth/16/2009. The A/Perth16/2009 strain was initially chosen as this was the most up to date H3N2 strain

available for testing at the start of this piece of work. As the work progressed the question of whether the H3N2 strain should be updated from A/Perth/16/2009 to a more recent strain to make it more relavent and comparable to the current H3N2 circulating strains was posed. It was decided that this was not the best course of action. Many models of influenza use older strains that have been well characterised and updating the strain could potentially cause unforeseen problems with assays that have been used to evaluate results from the pilot studies of the model. It would be difficult to select the most up to date strain of H3N2, as the following year the strain would no doubt change due to antigenic drift. As such, the A/Perth/16/2009 of H3N2 was worked with throughout this piece of work.

These studies are important because they will enhance the ferrets model's applicability when assessing vaccine strategies and therapeutics. For this reason, it is also important to understand the similarities and differences between seasonal H3N2 and H1N1 infection in the ferret as these differences can most likely be translated to human disease.

1.8 Hypothesis

The following hypotheses were investigated:

1. That the pathogenesis of disease following different infection delivery models is similar despite the route of delivery and that pathogenesis is a property of the virus receptor rather than delivery route.

2. That influenza infection results from a combination of both droplet (fomite) and aerosol particles and that both particle types contribute to transfer.

Aims:

a. Developing and comparing intra-nasal, natural transmission and aerosol modes of experimental infection.

b. Investigating the robustness of the three infection models in terms of reproducibility and reliability.

2 Material & Methods

2.1 Cell & Virus Culture

2.1.1 Media

Cell Culture Media for Resuscitation

500ml of DMEM + GlutaMAX™ (Gibco, Loughborough, United Kingdom) supplemented with 100ml of (20% (v/v)) Foetal Calf Serum (FCS) (Sigma- Aldrich, Dorset, United Kingdom) and 5ml of 1x PenStrep (100 U/ml penicillin and 100µg/ml streptomycin) (Gibco, Loughborough, United Kingdom).

Cell Culture Media for Cell Maintenance

500ml of DMEM + GlutaMAX™ (Gibco, Loughborough, United Kingdom) supplemented with 50ml of (10% (v/v)) FCS, (Sigma- Aldrich, Dorset, United Kingdom) and 5ml of 1x PenStrep (100U/ml penicillin and 100 µg/ml streptomycin) (Gibco, Loughborough, United Kingdom).

Influenza Growth Media

500ml of DMEM + GlutaMAX™ (Gibco, Loughborough, United Kingdom), 13ml of BSA Fraction V (Gibco, Loughborough, United Kingdom) and Trypsin TPCK (-1-Tosylamide-2-phenylethyl chloromethyl ketone) (Sigma- Aldrich, Dorset, United Kingdom). The trypsin TPCK value is based on a titrated value and varies from one batch to another therefore exact volumes cannot be supplied.

Plaque Assay Overlay Media

100ml of 10x MEM (Gibco, Loughborough, United Kingdom), 20ml of 7.5 % $NaHCO_3$ (Sigma-Aldrich, Dorset, United Kingdom), 10ml of 1M HEPES (Sigma- Aldrich, Dorset, United Kingdom), 28ml of 7.5% BSA fraction V (Gibco, Loughborough, United Kingdom), 5ml of 1% DEAE (diethylaminoethyl) Dextran (Sigma- Aldrich, Dorset, United Kingdom), 10ml of 100x Anti-Anti (Fisher Scientific UK Ltd, Loughborough, United Kingdom), 10ml of 100x L-Glutamine (Fisher Scientific UK Ltd, Loughborough, United Kingdom) and 517ml of Irrigation H_2O (water) (PamSupplies).

2.1.2 **Cells**

Madin-Darby canine kidney cells (MDCK cells **Fig. 2.1.2.1**) were originally isolated from a cocker Spaniel in 1958. MDCK cells are an adherent cell line and like most epithelial cell lines exhibit strong contact inhibition when grown in cell culture. MDCK cells are permissive and support the growth of influenza virus (Green, 1962), making them suitable for influenza research. MDCK cells were obtained from The European Collection of Authenticated Cell Cultures (ECACC, Porton Down, United Kingdom).

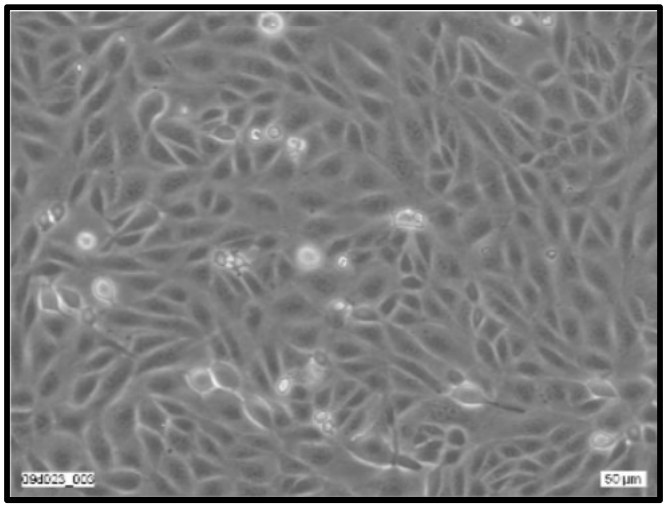

Figure 2.1.2.1 Image of MDCK Cell Line (ECACC) Healthy, normal confluent MDCK cells.

2.1.3 **Cell Resuscitation**

The appropriate number of vials were removed from liquid nitrogen and defrosted in a 37ºC water bath for approximately 1 to 2 minutes until no more than two ice crystals remain. Rapid thawing in this manner was required to minimise the damge to cells. Cells were removed from water bath and transferred to a sterile centrifuge tube containing 12ml of cell culture media. Cells were washed by centrifugation at 200 g for 5 minutes and resuspended in 12ml of fresh cell culture media. The centrifugation step was repeated, and cells were resuspended in 10ml of media and seeded into a 175cm^2 flask with an additional 20ml of cell culture media. Cells were incubated overnight at 37ºC at 5% CO_2 to allow cell attachment. The following day cell debris and dead cells were removed by changing cell culture media and replacing with 30ml of cell culture media.

2.1.4 **Cell Maintenance**

MDCK cells were passaged at approximately 80% confluency. Media was removed, and cells were washed twice with sterile PBS pH 7.4 (Gibco, Loughborough, United Kingdom). After the second wash was discarded 2ml of 1 x Trypsin-EDTA (ethylenediaminetetraacetic acid) (0.05% Trypsin, 0.02% EDTA) was added to evenly cover the cell monolayer. Trypsin is used to detach the cell monolayer from the flask. The flask was placed at 37ºC, 5% CO_2 for 5-10 minutes to aid detachment of the monolayer. Detachment of the monolayer was confirmed as the trypsin solution becomes visibly opaque and cells move upon rocking the flask. Following cell detachment 10 ml of cell culture media was added to stop trypsinisation and to resuspend cells. Long term incubation of cells with a high concentration of trypsin damages cells by stripping cell surface proteins and eventually killing the cells. Vented 175cm^2 flasks were typically seeded with 0.75 -1.5ml of resuspended cells (exact volume depended on cell confluency, **Figure 2.1.4.1**, gives an example, and time to next passage) and 30ml of cell culture media was added.

2.1.5 **Virus**

Passages of IAV A/Perth/16/2009 (H3N2) used during this piece of work were either; propagated in Madin-Darby Canine Kidney (MDCK) cells (**Section 2.1.2**) or propagated in specified pathogen free (SPF) hens eggs (Charles River Ltd, Wisconsin, United States). The passage batch: P+2A of A/Perth/16/2009, propagated in MDCK cells, was used for all animal infections during this piece of work. The identity of passage batch: P+2A was confirmed by sequencing of the HA and NA genes. Passage batches: P+3B and P+3A were propagated in SPF hens' eggs were used for immunological assays.

2.1.6 **Virus Propagation in Cell Culture**

MDCK cells are used to grow influenza virus due to its high susceptibility to infection with various influenza strains. MDCK cells are widely used for influenza virus isolation and vaccine production (Seitz *et al.*, 2010).

MDCK cells were grown to 90 – 100% confluency. Media was removed, and cells were washed twice with sterile PBS pH 7.4 (Gibco, Loughborough, United Kingdom). Virus was removed from storage and diluted appropriately in influenza growth media. Diluted virus was added to cells and incubated for 1 hour at 37ºC, 5% CO_2. Following incubation 25ml of virus growth media was added and flasks were incubated until at least 75% of the cell monolayer displayed cytopathic effect (CPE). Cytopathic effect describes the structural changes that take place in the cell following viral infection. This is usually lysis of the cell or where the cell dies due to an inability to reproduce. Media were harvested and centrifuged at 750g for 5 minutes to remove cell debris. Virus was aliquoted and frozen at -70±10ºC for long term storage.

2.1.7 **Virus Propagation in Eggs**

Eggs are commonly used to grow influenza viruses. Eggs often provide a high yield of influenza virus and allow for large volumes of virus to be produced.

Eggs were set for primary incubation at 37 °C, 40- 80% Relative Humidity (RH) and rocking for 9 – 11 days. Prior to inoculation eggs were candled using a LED (light-emitting diode) lamp to visualise the chicken embryo in the egg and ensure the embryo was alive (**Fig. 2.1.7.1**). A mark was placed on the egg above the air sack, opposite the embryo and avoiding major blood vessels to indicate where the site of inoculation should be. Any unfertilised,

cracked, or dead eggs were not suitable for inoculation and were placed in the fridge overnight prior to discarding.

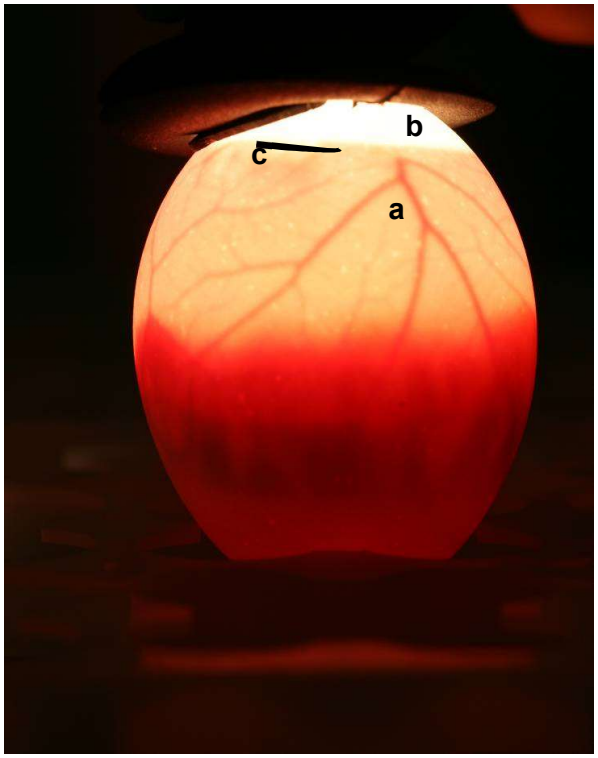

Figure 2.1.7.1 Normal viable egg. (a) Well defined vein structure and **(b)** fixed air sack at the top pole of the eggs. Upon candling the chicken embryo, a mark is placed just above the air sack **(c)** to indicate where the egg should be inoculated.

A lancet was used to create a hole in the egg between 2 and 5mm above the mark made on the egg and another hole approximately 5mm was made above the first hole. Virus was diluted in PBS pH 7.4 (Gibco, Loughborough, United Kingdom) to approximately 10^3 PFU (plaque forming units) per egg. 100µl of virus inoculum was injected into each egg. Eggs were sealed with a glue stick and incubated 37±1°C for 48 h or at 33±1°C for 72 hours.

Following secondary incubation, eggs were chilled at 5 ±3°C for a minimum of 4 hours. Disposable forceps were used to crack the top of the egg and peel back the membrane. Allantoic fluid (AF) was collected with a pipette into a sterile tube. AF was clarified by centrifugation at 1000g for 5 minutes prior to aliquoting and long-term storage at -70±10ºC. The number of PFU/ml was assessed by performing a plaque assay.

2.1.8 **Haemagglutination (HA) Assay**

The HA assay is a method used to titre influenza viruses based on their ability to attached to the sialic acid receptors present on the surface of red blood cells (RBCs) via their HA receptor.

A 0.5% blood suspension chicken RBCs (Envigo, Huntingdon, United Kingdom) was prepared on the day of the HA assay. Virus to be assayed was thawed and serially diluted 1:2 across a 96 v-well plate in triplicate (50µl of stock virus added to 50µl of PBS pH 7.4 (Gibco, Loughborough, United Kingdom)). An appropriate volume (usually 50µl) of 0.5% blood was added and the plate was incubated at room temperature for 45-60 minutes. It was determined whether wells showed no haemagglutination (red blood cells formed a button) or haemagglutination (red blood cells formed a latticework) (**Fig. 2.1.8.1**). The highest dilution of the virus antigen showing complete agglutination was the end point of the titration; containing one HA unit in 50µl. The virus was then diluted appropriately with PBS pH 7.4 (Gibco, Loughborough, United Kingdom) to 4 HA units per 25µl for use in the haemagglutination inhibition (HAI) assay (**Section 2.3.8**). A back titration of the diluted virus was then performed to ensure correct dilution.

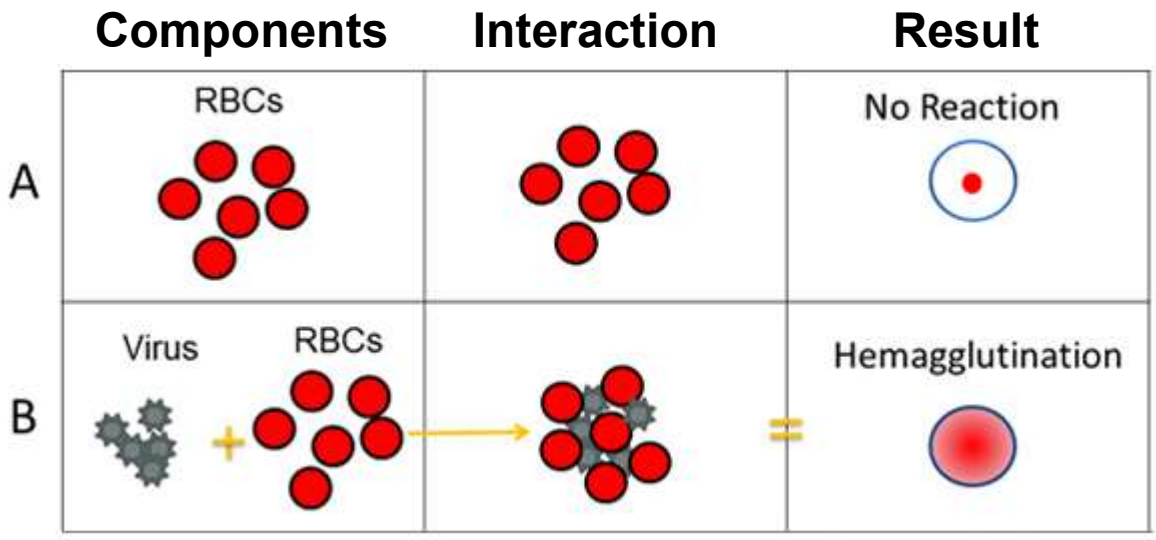

Figure 2.1.8.1 The HA Assay (adapted from (CDC, 2017)) The assay involves the interaction of red blood cells (RBCs) with influenza virus. Row A illustrates in the absence of virus, RBCs in a solution will sink to the bottom of a v-well microtitre plate well and look like a red button. Row B shows that influenza viruses will bind to red blood cells when placed in the same solution. This is called hemagglutination and is represented by the formation of the latticework structure, as shown in "result".

2.1.9 **Plaque Assay**

The plaque assay is a cell culture-based technique and is used to quantify the amount of live virus in a sample.

MDCK cells were seeded into 12 well cell culture plates at a density $4x10^5$ cells/ml and incubated overnight to be used the following day. Samples to be titrated were diluted appropriately with serum free DMEM + GlutaMAX™ (Gibco, Loughborough, United Kingdom). Serum is omitted because it contains inhibitors of trypsin. Many influenza strains are trypsin dependent for replication in cell culture. The trypsin cleaves the HA on the virus, so it becomes fusion competent. Cells were washed with PBS 7.4 (Gibco, Loughborough, United Kingdom), and incubated with 200µl of sample for 1 hour at 37°C, 5% CO_2. Overlay media (21ml) was

used with 2% Agar Overlay (9ml) (melted and maintained at 55°C) (Oxoid, Basingstoke, United Kingdom) and 1.6 mg/ml TPCK Trypsin (Sigma- Aldrich, Dorset, United Kingdom). Plates were incubated for 3 days at 37°C, 5% CO_2. Agar was removed after three days and plates were fixed and stained with Crystal Violet Stain; 40ml 2.5 % Crystal Violet stock (Sigma-Aldrich, Dorset, United Kingdom), 80ml Methanol, 300ml Irrigation H_2O (PamSupplies).

2.2 Molecular Virology

2.2.1 Generation of synthetic standard curve used during qRT-PCR

A synthetic T7 transcript of full length M gene for A/Perth/16/2009 was generated for use as standard curve during quantitative RT-PCR.

2.2.1.1 *Complementary DNA (cDNA) Generation*

Viral RNA was extracted from virus stock P+2A using QiaAmp Kit (Qiagen, Manchester, United Kingdom). cDNA was transcribed using Superscript III RT kit (Invitrogen).

Table 2.2.1.1.1 Primer Sequence

Primer	**Sequence 5'→ 3'**
Uni-12	AGC AAA AGC AGG

For a 32.5µl reaction 25µl viral RNA was mixed with 5µl of primer (**Table 2.2.1.1.1**) and 2.5µl of 10mM dNTP mix (Invitrogen, Fisher Scientific, Loughborough, United Kingdom). The reaction was heated in a water bath to 65ºC for 5 minutes and then snap-cooled on wet ice. To the same reaction tube, 10µl of 5xFS buffer + 2.5µl 0.1M DTT + 2.5µl RnaseOUT (Invitrogen, Fisher Scientific, Loughborough, United Kingdom) + 2.5µl Superscript III enzyme was added. This reaction was incubated at 50ºC for 60 minutes followed by 70ºC for 15 minutes and the held at 4ºC until the cDNA was stored at -20ºC.

2.2.1.2 *PCR*

The GRAM-1Fw and GRAM-1027Rv sequences (**Table 2.2.1.2.1**) amplified all IAV subtypes. PCR was carried out using Phusion High-Fidelity PCR kit (Fisher Scientific, Loughborough, United Kingdom). A master mix (x1) was made as follows: 10 µl 5x Phusion High-Fidelity buffer + 0.4µl 25mM dNTPs + 2.5µl GRAM-1Fw (20 µM) + 2.5µl GRAM-1027RvwT7 (20 µM) + 2µl cDNA + 0.5 µl Phusion DNA Polymerase + 34.6µl RNase-free water. This reaction was incubated in a [3]Prime Thermal Cycler (Techne, Stone, United Kingdom) at 98°C for 30 seconds followed by 35 cycles of 98°C for 10 secs, 63.5°C for 20 secs and 72°C for 55 secs, finishing with 72°C for 8 min, finally being held at 10°C until removal from the PCR machine.

Table 2.2.1.2.1 Primer Sequence

Primers	**Sequence 5'→ 3'**
GRAM-1Fw	AGC AAA AGC AGG TAG ATA TAT TGA
GRAM-1027Rvw/T7[1]	GAA ATT AAT ACG ACT CAC TAT AGG GAG TAG AAA CAA GGT AGT TTT TTA CTC

[1]Reverse primer GRAM-1027vw/T7 has T7 promoter attached

To confirm presence of the correct amplicon gel electrophoresis was performed. Buffer was 1x TAE (from 10x TAE stock) (Invitrogen, Fisher Scientific, Loughborough, United Kingdom). Gel was 1.2 % agarose (Invitrogen, Fisher Scientific, Loughborough, United Kingdom) in 1x TAE containing 3µl per 30ml SYBR Safe (Invitrogen, Fisher Scientific, Loughborough, United Kingdom). 5µl of PCR product with 1µl dye (10x Blue Juice, Invitrogen) was loaded onto gel

alongside 10µl Size Standard from Phusion kit. Gel was electrophoresed at 100V ~1 hr and visualised on Geldoc. Product was a single band of 1027bp. Remaining sample was stored at -20ºC.

2.2.1.3 *Transcription*

Once amplicon product was confirmed transcription with MEGAscript kit (Ambion Fisher Scientific, Loughborough, United Kingdom) was carried out. The MEGAscript Kit is used to generate large amounts of RNA from linearized DNA template.

The following reaction was assembled at room temperature: 5µl PCR product + 3µl water (from kit) + 2µl each of 4 rNTPs (75mM, from kit) + 2µl 10x Megascript buffer + 2µl T7 enzyme mix. Reaction was incubated in an incubator 37°C for approximately 4 hours. Following incubation sample was stored at -20ºC.

2.2.1.4 *RNA Clean Up and Quantitation*

Product was purified using Qiagen RNeasy Kit (Qiagen, Manchester, United Kingdom). The RNA was eluted into RNase-free water and quantified spectrophotometrically using a NanoDrop™ Lite Spectrophotometer (ThermoFisher Scientific, Loughborough, United Kingdom). The number of M segment copies per µl was calculated using the concentration ascertained from the nanodrop as follows:

The rNTP molecular weight (assumed) is 320.5 and the M segment of IAV has 1027 bases.

M.W. of ssRNA = (# nucleotides x 320.5) + 159.0

M.W. = (1027 x 320.5) + 159.0 = 329312.5

(X^{-9}g/µl)/ 329312.5 = (answer) x (6.022 x 10^{23*})

*Avogadro's Number – defines the amount of substance in on mole.

2.2.2 **Quantitative Real-Time Reverse Transcriptase Polymerase Chain Reaction**

qRT-PCR was used to quantify the amount of virus present in a sample. qRT-PCR is unable to differentiate between live and dead virus, it is only able to indicate the presence of a specific part of the virus genome.

The target for this qRT-PCR was the consereved M (matrix) segment found in the influenza virus genome.

Total RNA was extracted from ferret tissues (lung, trachea and nasal turbinate) which had been collected into RNALater (Qiagen, Manchester, United Kingdom) and stored at -20°, using the Qiagen RNeasy Mini kit (lung) or RNeasy Fibrous kit (trachea, nasal turbinates). Lung samples were taken from the upper left lobe in each case. RNA was quantified spectrophotometrically using a NanoDrop™ Lite Spectrophotometer (ThermoFisher Scientific, Loughborough, United Kingdom). RNA quality was assessed using an Agilent 2100 Bioanalyzer. Absolute quantification of influenza virus M segment was determined using a quantified, negative-sense synthetic T7 RNA polymerase transcript, from either a synthetic T7

transcript of A/Perth/16/2009 M segment (**Section 2.2.1.4**) or a full-length plasmid clone of A/California/04/2009 M segment, to construct a standard curve. Reactions used primers (M+24, M-124, M-124Mod) and probe (M+64 with 5'-FAM and 3'-BHQ1) (**Table 2.2.2.1**) with the Superscript III Platinum One-Step qRT-PCR kit (Invitrogen, Fisher Scientific, Loughborough, United Kingdom), and were analysed using the ABI Prism 7900HT and SDS 2.4 software (Applied Biosystems, Fisher Scientific, Loughborough, United Kingdom).

Table 2.2.2.1 Primer Sequences

Primers	Sequence 5'→ 3'
M+64	(6FAM)TCAGGCCCCCTCAAAGCCGA(BHQ1)
M+24	AGATGAGTCTTCTAACCGAGGTCG
M-124mod	TGCAAAGACACTTTCCAGTCTCTG
M-124	TGCAAAAACATCTTCAAGTCTCTG

The master mix (x100) comprised of 546µl water (RNase-free, Ambion AM9937 or AM9906 (DEPC-treated)) + 1ml 2 x Reaction mix + 50µl Enzyme mix + 100µl M+24 primer (6 µM) + 100µl M-124mod (6µM) or M-124 primer (6µM) + 100µl M+64 probe (FAM-BHQ1) (5µM) + 4µl ROX dye. Each reaction used 19µl of master mix and 1µl or RNA. The standard plate layout comprised of 7 serial 10-fold dilutions of standard (10^7-10^1 copies/µl) in triplicate, a no template control (NTC) in triplicate, and up to 36 unknowns in duplicate.

2.3 *In vivo* work

2.3.1 Ferrets

Ferrets (*Mustela putorius furo*) were obtained from Highgate Farm, United Kingdom, and Marshalls Bio Resources, Hull, United Kingdom. All ferrets were confirmed as seronegative for influenza antibodies by haemagglutination-inhibition (HAI) assay (**Section 2.2.7**) prior to study commencement. Identifier chips (Bio-Thermo®, iDENTICHIP®, Cambridge, United Kingdom) were inserted subcutaneously into the dorsal cervical region of each animal. The ferrets were housed in cages or floor pens which were designed in accordance with the requirements of the United Kingdom Home Office Code of Practice for the Housing and Care of Animals Used on Scientific Procedures (1989).

2.3.2 Virus Preparation

Virus was typically diluted in either PBS pH 7.4 (Gibco, Loughborough, United Kingdom) or DMEM with GlutaMAX (Gibco, Loughborough, United Kingdom). For intranasal inoculations a total volume of 200µl challenge material was administered and distributed evenly between both nares. This procedure was performed slowly, ensuring each droplet was absorbed into the nasal cavity of the ferret before releasing another.

2.3.3 Sedation

Animals were sedated by intramuscular injection of ketamine/xylazine (17.9 mg/kg and 3.6 mg/kg bodyweight).

2.3.4 **Clinical Monitoring**

Ferrets were typically monitored for the following signs of disease twice daily (approximately 8 hr apart); appetite loss, sneezing, nasal discharge, diarrhoea and activity level. Information was recorded as yes or no for all metrics excluding activity level, which was scored as **0** for normal, **1** for reduced activity and **2** for inactive. Weight was recorded in grams once daily.

2.3.5 **Nasal Wash**

Nasal washes were obtained (**Fig**. **2.3.5.1**) using 2 ml PBS pH 7.4 (Gibco, Loughborough, United Kingdom).

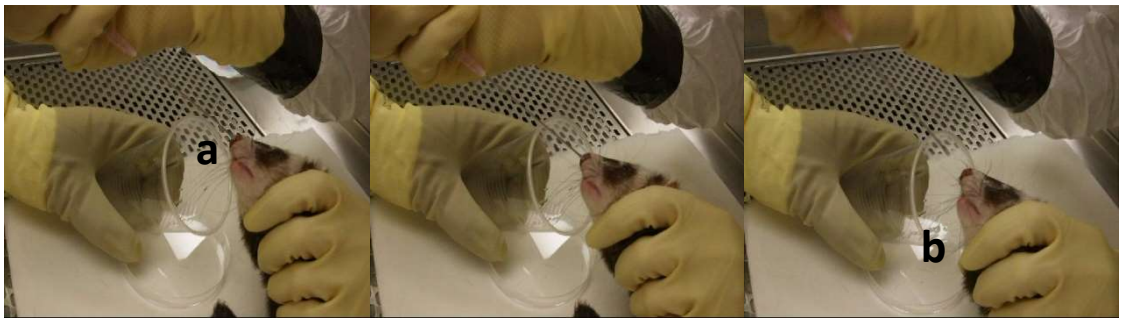

Figure 2.3.5.1 Images of a ferret undergoing nasal washing. Each ferret was anaesthetised prior to nasal washes being carried out. A 20G x 30mm blunt ended needle attached to a 2ml syringed filled with PBS was used to flush the ferrets nose. Ferrets were placed on their backs with nostrils facing down toward a plastic cup and petri dish. The PBS was divided between each nostril equally. The tip of the needle was held just above the nostril **(a)** and the plunger slowly depressed to administer the PBS. The PBS was the allowed to drip into the cup and collection dish **(b)**. Using the same blunt ended syringe, the PBS was drawn back up and dispensed into appropriately labelled tubes.

Nasal washes were stored on ice. A one in 10 dilution of nasal wash to Trypan Blue solution (Sigma- Aldrich, Dorset, United Kingdom) was carried out, mixed and loaded onto a C-Chip™ disposable haemocytometer (NanoEnTek, Seoul, Korea). Trypan Blue solution is a live/dead stain which dead cells dark blue, with live cells staying white. The haemocytometer contained four quadrants with a grid of nine with each quadrant. The live cells were counted in each quadrant and then divided by four to obtain an average. This number was then multiplied by 10^4 (as the total volume of the quadrant is 0.0001ml) to give number of cells per ml. The nasal washes were aliquoted and frozen at -80°C prior to plaque assay analysis. Alternatively, cell counts were carried out using a NucleoCounter® NC-200™ (ChemoMetec, Allerod, Denmark).

2.3.6 **Blood Sampling**

Blood samples were taken from the cranial vena-cava vessel of ferrets using a needle and syringe into either BD Vacutainer® Heparin Blood Collection tubes for whole blood immune-phenotyping, peripheral blood mononucleocyte (PBMC) collection or interferon gamma enzyme linked immunosorbent assay (IFN-γ ELISA) or BD Vacutainer® SST™ tubes for serum collection.

Blood taken for serum in BD Vacutainer® SST™ tubes was left to clot at room temperature for at least 30 minutes. BD Vacutainer® SST™ tubes were then placed into a centrifuge a spun at 1000g for 10 minutes to separate serum. Serum was removed and aliquoted into cryovials (Nunc, Roskilde, Denmark) and stored at -70±10°C for long term storage.

2.3.7 **Ferret Sera Preparation**

Ferret sera were diluted 1:3 with Receptor Destroying Enzyme (RDE, Denka Seiken, Japan) and incubated for 18-20 hours in a 37±1°C incubator. Following incubation, the RDE is inactivated in a 56±1ºC water bath for 45-50 minutes. RDE treated sera was then frozen at -20ºC until use.

2.3.8 **Haemagglutinin Inhibition (HAI) Assay**

The HAI assay is a simple assay used to assess the presence of antibodies to a specific strain of influenza in sera (**Fig. 2.3.8.1**).

A 0.5% blood suspension with appropriate red blood cells was prepared on the day of the HAI assay. RDE treated sera (50µl) to be assayed were placed on a 96 v-well plate (Invitrogen, Paisley, United Kingdom) and serially diluted (1:2) with PBS pH 7.4 (25µl) (Gibco, Loughborough, United Kingdom). Diluted virus (from HA assay 2.1.8) was added to the plate and incubated for 30 minutes at room temperature. Following incubation 0.5% blood (50µl) was added to the plate and incubated for 45-60 minutes. The HAI titre of sera was read by determining which wells showed complete inhibition of haemagglutination (red blood cells formed a teardrop shape) or haemagglutination (red blood cells formed a latticework). The HAI titre was read as the well which showed the last complete inhibition of haemagglutination for each serum sample. Serum from infected animals with known HAI titre were used as positive controls during the HAI assay.

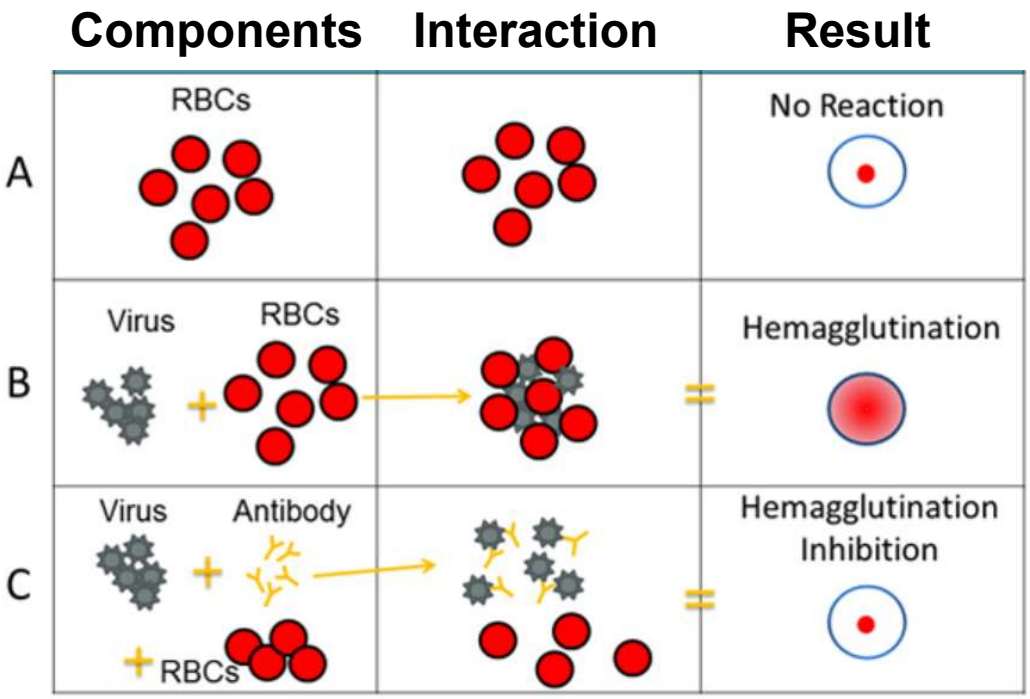

Figure 2.3.8.1 The HAI Assay (CDC, 2017) The HAI assay involves the interaction of red blood cells (RBCs), antibody and influenza virus. Row A illustrates in the absence of virus, RBCs in a solution will sink to the bottom of a v-well microtitre plate well and look like a red button. Row B shows that influenza viruses will bind to red blood cells when placed in the same solution. This is called hemagglutination and is represented by the formation of the latticework structure, as shown in "result". Row C shows how antibodies that are antigenically like a virus being tested will recognise and bind to that influenza virus. This prevents the virus and RBCs from binding, and therefore, haemagglutination does not occur (haemagglutination inhibition occurs instead).

2.3.9 **Terminal Anaesthesia and Necropsy**

Animals were sedated (**Section 2.3.3**). If taking whole blood for immuno-phenotyping and whole blood stimulation this was carried out prior to terminal euthanisation. Ferrets were euthanised by using a lethal dose of sodium pentobarbitone. If required, the remainder of the blood was collected after overdose into BD Vacutainer® Heparin Blood Collection tubes for whole blood and/or BD Vacutainer® SST™ tubes for serum.

2.4 Immune Cell Isolation

2.4.1 **Media**

R10 Medium

500ml of RPMI 1640 medium (Sigma-Aldrich, Dorset, United Kingdom) with the addition of 5ml of L-glutamine (2mM) (Sigma-Aldrich, Dorset, United Kingdom), 0.5ml of 0.05mM 2-mercaptoethanol (Invitrogen, Paisley, United Kingdom), 15ml of 25mM HEPES buffer (Sigma-Aldrich, Dorset, United Kingdom), and 50ml of (10%) heat inactivated foetal bovine serum (Sigma-Aldrich, Dorset, United Kingdom).

R2 Medium

500ml of RPMI 1640 medium (Sigma-Aldrich, Dorset, United Kingdom) with the addition of 5ml of L-glutamine (2mM) (Sigma-Aldrich, Dorset, United Kingdom), 0.5ml of 0.05mM 2-mercaptoethanol (Invitrogen, Paisley, United Kingdom), 15ml of 25mM HEPES buffer (Sigma-Aldrich, Dorset, United Kingdom), and 10 ml of (2%) heat inactivated foetal bovine serum (Sigma-Aldrich, Dorset, United Kingdom).

2.4.2 **Isolation of Peripheral Blood Mononuclear Cells**

Fresh heparin anti-coagulated blood was layered on room temperature Histopaque 1083 (Sigma-Aldrich, Dorset, United Kingdom) in 15ml ACUSPIN^{TM} tubes (Sigma-Aldrich, Dorset, United Kingdom) and a density separation carried out at 800g for 20 minutes. The buffy coat (**Fig. 2.4.2.1**), the fraction of anticoagulated blood containing most of the white blood cells and

platelets following density gradient centrifugation, was collected for each sample and washed with R2 medium cells were pelleted by centrifugation at 400g for 10 minutes.

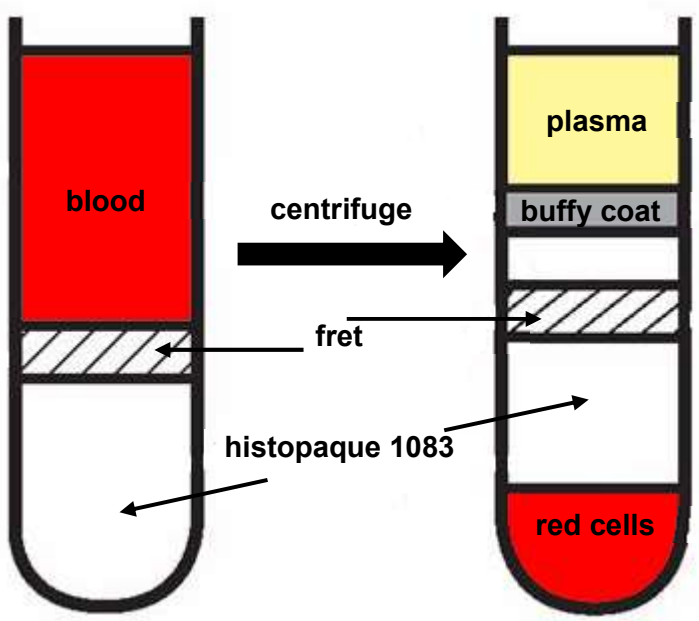

Figure 2.4.2.1 PBMC Isolation. The diagram illustrates where the buffy coat forms following centrifugation on the Histopaque 1083 gradient. The buffy coat is located in the same place during splenocyte and BAL isolation.

2.4.3 **Isolation of Splenocytes**

Spleens were removed whole from each ferret. Spleen were cut up using disposable scissors and placed into gentleMACS C-tubes and dissociated using a gentleMACS Tissue Dissociator (Miltenyi Biotec, Surrey, United Kingdom) with R2 medium. The tissue solution was passed through two cell sieves (100µm then 70µm) and then layered on room temperature Histopaque 1083 (Sigma-Aldrich, Dorset, United Kingdom) in 15ml ACUSPIN™ tubes (Sigma-Aldrich, Dorset, United Kingdom) and a density separation carried out at 800g for 20 minutes. The

buffy coats containing lymphocytes were collected and washed with R2 medium and cells were pelleted by centrifugation at 400g for 10 minutes.

2.4.4 **Isolation of Bronchoalveolar Lavage (BAL) Immune Cells**

Bronchoalveolar lavage washes were performed post overdose, prior to removal of lungs. BAL washes with sufficient R2 medium were layered on room temperature Histopaque 1083 (Sigma-Aldrich, Dorset, United Kingdom) in 15ml ACUSPIN^{TM} tubes (Sigma-Aldrich, Dorset, United Kingdom) and a density separation carried out at 800g for 20 minutes. The buffy coats containing lymphocytes were collected and washed with R2 medium and cells were pelleted by centrifugation at 400g for 10 minutes.

2.4.5 **Isolation of Lung Mononuclear Cells**

Whole lungs were removed from each ferret. The lungs were dissected into small pieces and placed into a 25ml solution of collagenase (715 collagenase units/ml) (Sigma-Aldrich, Dorset, United Kingdom) and DNase (350 DNase units/ml) (Sigma-Aldrich, Dorset, United Kingdom). Lungs were vigorously shaken whilst in a 37±1^{o}C incubator for 1 hour. Partially digested lung tissue was then placed into gentleMACS C-tubes and dissociated using a gentleMACS Tissue Dissociator (Miltenyi Biotec, Surrey, United Kingdom). The tissue solution was passed through two cell sieves (100µm then 70µm) and then layered on room temperature Histopaque 1083 (Sigma- Aldrich, Dorset, United Kingdom). A density separation was carried out at 400g for 30 minutes. The buffy coats containing lymphocytes were collected (**Fig. 2.4.5.1**) and washed with R2 medium by pelleting cells by centrifugation at 400g for 10 minutes.

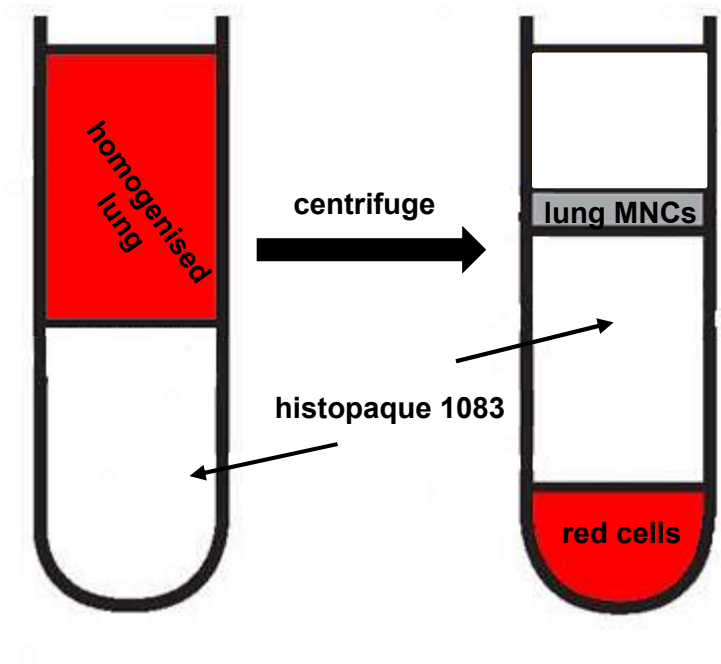

Figure 2.4.5.1 Lung MNC Isolation. The diagram illustrates where the buffy coat forms following centrifugation on the Histopaque 1083 gradient.

2.4.6 **Red Blood Cell Removal Using ACK Lysis Buffer**

Red blood cells were lysed from PBMC, spleen, lung MNC and BAL sample preparations by re-suspending cell pellets in 5ml of ACK Lysing Buffer (Gibco, ThermoFisher Scientific, United Kingdom). The cells were incubated at room temperature with manual gentle agitation for 5 minutes. The ACK Lysing Buffer was inactivated by the addition of an excess of R2 medium. Cells were pelleted by centrifugation at 400g for 10 minutes to remove lysis buffer. If lysis of the red blood cells were incomplete, then the treatment was repeated.

2.4.7 **Immune Cell Counting**

Cell pellets were resuspended with an appropriate volume of R2 medium. Cell counts were carried out using a NucleoCounter® NC-200™ (ChemoMetec, Allerod, Denmark).

2.4.8 **Immune Cell Cryopreservation**

Cells were pelleted by centrifugation at 400g for 5 minutes and resuspend in the appropriate volume of cryomedia (90% FCS + 10% DMSO). DMSO was added as a cryoprotectant to avoid damage to the cells during freezing. Cells were frozen in cryovials (Nunc, Roskilde, Denmark) in 1ml aliquots of concentrations between 3 x 10^6 and 1.3 x10^7 cells per ml. Cyrovials were placed in a Mr Frosty™ Freezing Container and transferred to a -70ºC freezer. The Mr Frosty™ Freezing Container allowed for a rate of cooling of approximately -1ºC/minute allowing for slow freezing of the cells which prevents intracellular ice crystals from forming. After freezing at -70ºC vials were transferred to liquid nitrogen storage.

2.4.9 **Immune Cell Resuscitation**

The appropriate number of vials were removed from liquid nitrogen and placed in a 37°C water bath until visually defrosted. Cells were immediately placed into R10 medium with benzonase. Cells were washed by centrifugation at 400g for 5 minutes and re-suspending in R10 + benzonase twice. Cells were then resuspended and rested for at least 1.5 hours or at most, overnight by incubation at 37±1°C, 5% CO_2 in 50ml sterile centrifuge tubes with loosened lids

to allow gas exchange. Following incubation cells were washed by centrifugation at 400g for 5 minutes and re-suspended in 5ml R10 without benzonase for a viable count.

2.4.10 **Quantification of influenza-specific Interferon-gamma (IFN-γ) production by enzyme linked immunosorbent assay (ELISA)**

The IFN-γ ELISA (**fig 2.4.10.1**) is used to assess the longitudinal influenza-specific IFN-response in circulating peripheral blood of the ferret. High level production of IFN-γ is typically associated with effective host defence against intracellular pathogens. The small volumes of blood (approximately 400µl depending on the number of antigens used for stimulation) required for this assay means samples can be taken from ferrets on a frequent basis.

Heparinised whole blood was diluted 1:10 with serum free RPMI 1640 medium and incubated with A/Perth/16/2009 (H3N2) at a multiplicity of infection (MOI) of 0.8. MOI refers to the number of virions that are added per cell during infection. Phytohemagglutinin PHA-M (PHA) (Sigma-Aldrich, Dorset, United Kingdom) was used as a positive control as it is a potent mitogen used to stimulate cell proliferation in lymphocyte cultures. Egg allantoic fluid was used as a negative control as viruses used were grown in eggs. Blood was stimulated by incubation for 4 days in a 37°±C, 5% CO_2 incubator after which plasma supernatants were collected and cryopreserved at -80 ºC. The Ferret IFN-γ ELISA Development Kit (ALP) (Mab Tech, Nacka. Sweden) was used to determine the quantity of IFN-γ secreted by cells in the blood in response to influenza-specific stimulations. ELISA plates were read using the VersaMax ELISA Microplate Reader (Molecular Devices, Sunnyvale, CA, USA) with SoftMax™ PRO software (Molecular Devices, Sunnyvale, CA, USA). Unknowns were calculated from the standard curve on each plate.

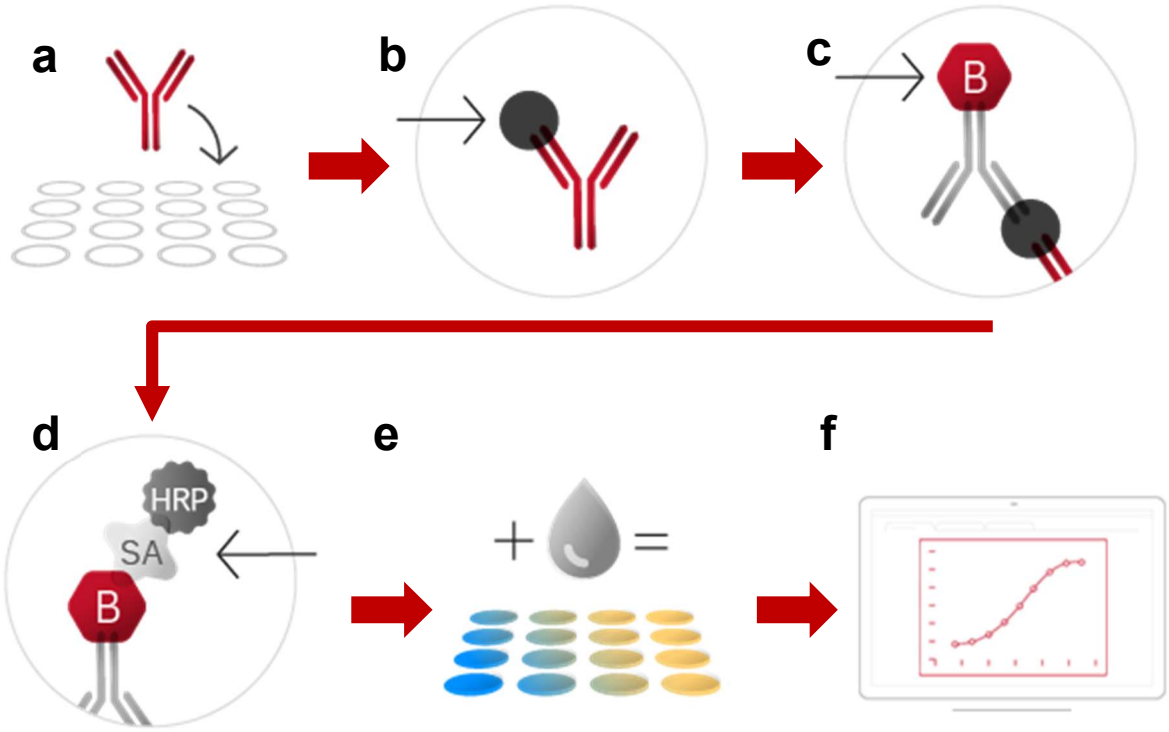

Figure 2.4.10.1 ELISA Overview (Mab Tech, Nacka. Sweden). **a** Antibody Coating: IFN-γ specific monocolonal capture antibody (mAb MTF14) immobilised on high protein binding plates. **b** Protein Capture: Samples and standard dilutions are added to wells and are captured by the bound antibodies **c** Detection Antibody: biotinylated IFN-γ specific detection antibody is added to wells to enable detection of captured IFN-γ **d** Streptavidin-enzyme Conjugate: Streptavidin conjugated with alkaline phosphatase is added to the wells and bind to biotinylated antibody. **e** Colourimetric substrate is added to the wells an forms a coloured solution when catalysed by the enzyme. **f** Absorbance is measured using using the VersaMax ELISA Microplate Reader (Molecular Devices, Sunnyvale, CA, USA) with SoftMax™ PRO software (Molecular Devices, Sunnyvale, CA, USA) and the amount of IFN-γ in samples is detected.

2.4.11 **Interferon-gamma (IFN-γ) Enzyme Linked Immuno-Spot Assay (ELISpot)**

The influenza-specific IFN-γ ELISpot assay was performed with PBMC, spleen, lung MNC and BAL sample. The ELISpot (**fig. 2.4.11.1**) allows determination of the production capacity of influenza-specific T cells in various tissues using a ferret specific IFN-γ kit (Mab Tech, Nacka. Sweden). PBMC, spleen, lung MNC and BAL were resuscitated as described (**Section 2.4.9**). Cells were rested for 2 hours prior to use. PBMC, spleen, lung MNC and BAL were assessed for responses to IAV A/Perth/16/2009 (H3N2). A/Perth/16/2009 was used at multiplicity of infection (MOI) of 0.08. The passage of A/Perth/16/2009 used was egg grown, therefore, egg allantoic fluid was used as a negative control throughout all the ELISpot assays. Phorbol-12-myristate PMA) (100ng/ml; Sigma-Aldrich, Dorset, United Kingdom) and ionomycin (1µg/ml; Merck, Watford, United Kingdom) were combined and used as a positive control. PMA and ionomycin used in combination can stimulate the intracellular production of cytokines. Pre-coated (mAb MTF14) plates (Mab Tech, Nacka. Sweden) were used. A range of cell concentrations were seeded (depending on cell origin) per well in 50µl of R10, with or without antigen, in duplicate and incubated overnight at 37±1ºC. Following culture, plates were washed and incubated for 2 hours with biotinylated anti IFN-γ IgG. Spots were developed by the addition of streptavidin-alkaline phosphatase and 5-bromo-4-chloro-3-indoly phosphate (BCIP)-Nitro Blue tetrazolium (NBT) substrate. Results from duplicate tests were averaged. Data were analysed by subtracting the mean number of spots in the cells and allantoic fluid control wells from the mean counts of spots in wells with cells and antigen. ELISpot plates were scanned on the C.T.L ELISpot Plate Reader using ImmunoSpot 5.0 Analyzer Software and counted using ImmunoSpot 5.1 Counting Software. Plates underwent manual quality control following automatic counting.

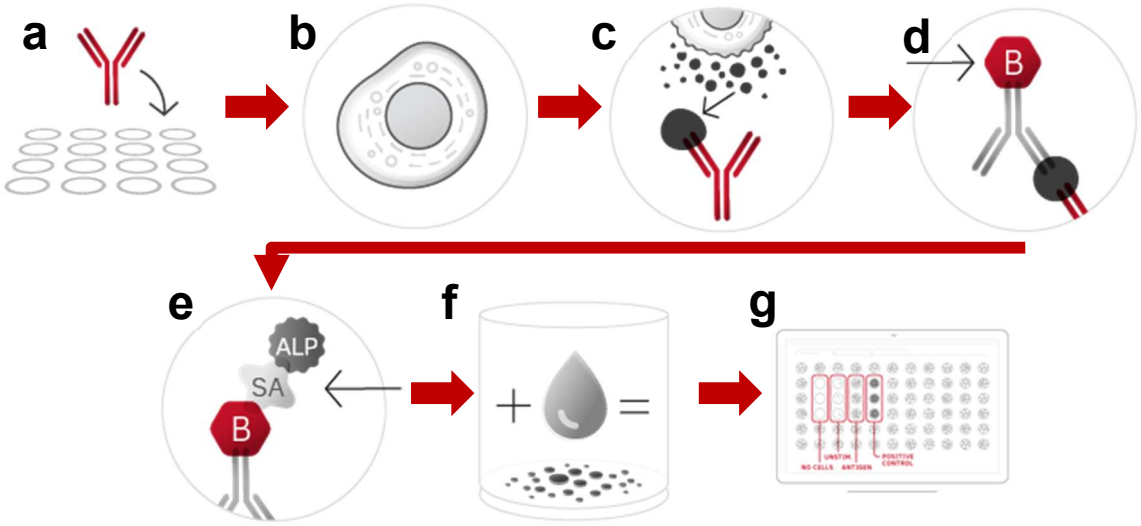

Figure 2.4.11.1 ELISpot Overview (Mab Tech, Nacka. Sweden). **a** Antibody Coating: IFN-γ specific monocolonal capture antibody (mAb MTF14) immobilised on an ethanol-treated PVDF membrane plate. **b** Cell Incubation: Cells are added to the wells in the prescence or absence of stimuli and then incubated to allow IFN-γ secretion. **c** Cytokine Capture: Secreated IFN-γ binds to the capture antibodies on the membrane immediately surrounding the activated cells. **d** Detection Antibody: Following removal of cells and washing of plates, biotinylated IFN-γ specific detection antibody is added to wells. **e** Streptavidin-enzyme Conjugate: To enable the formaton of spots on the membrane, a streptavidin enzyme conjugate is added to wells. **f** Addition of Substrate: Colorimetric substrate is added to the wells and forms an insoluable precipitate when catalysed by the enzyme; this provides a visable representation of IFN-γ release by a single activated cell. **g** Analysis: Spots are counted using a The C.T.L ELISpot Plate Reader and the frequency of secreating cells is calculated.

2.4.12 **Whole Blood Immunophenotyping – Antibody labelling**

Whole Blood Immunophenotyping was used to identify T cell populations in whole circulating blood to determine the number of cells per ml. Two antibodies (**Table 2.4.12.1**), each conjugated with a different fluorochrome, were used in these experiements. The first was a phycoerythrin (PE)-conjugated anti-ferret CD4 (Sino Biological, Bejing, China). This antibody was produced from a hybridoma resulting from the fusion of a mouse myeloma with B cells obtained from a mouse immunized with purified, recombinant Ferret CD4. The second was a Alexa Fluor™ (AF) 700-conjugated anti-human CD8a Clone: OKT8 (eBiosciences, San Diego, USA). This antibody has previously been reported to work well with the ferret model (Reber *et al.*, 2018).

Table 2.4.12.1 Antibodies

Antibody	Manufacturer	Lot number
CD4 PE	Sino Biological	60003-MM02-P-SIB
CD8 AF700	eBiosciences	56-0086-42

The following antibodies were used to determine the compensation setting:

Table 2.4.12.2 Compensation Antibodies

Antibody	Manufacturer	Lot number
IgG PE (anti-human)	eBiosciences	3298651
IgG AF700 (anti-human)	eBiosciences	94762813

Compensation is the process of correcting the spill over from the primary signal in each secondary channel it is measured in. The emission spectra of fluorescent dyes are broad. The peak emission is usually clearly separated for each dye, but there can be considerable overlap between the dyes. Using FITC and PE as examples, **Figure 2.4.12.1** illustrates spectral overlap; where some of the light emitted by the FITC will pass through the filter for PE. This means that some of the cells labelled with the FITC will appear to have PE fluorescence.

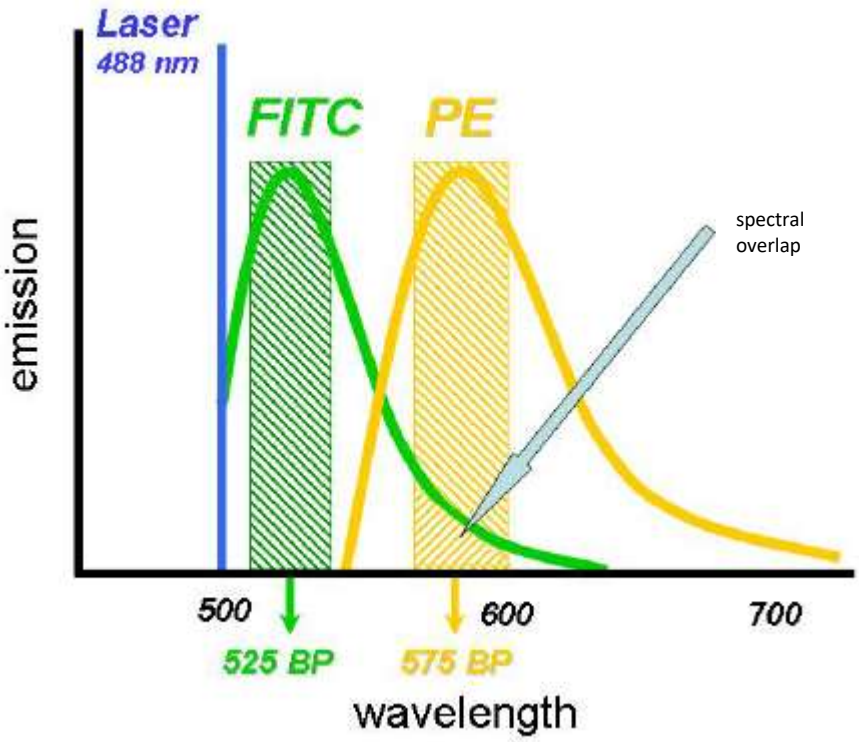

Figure 2.4.12.1 An example of spectral overlap (Omerod, 2008). FITC and PE with two bandpass (BP) filters superimposed. Some of the light from the FITC will pass through the filter used to collect the light from PE.

To obtain a true representation of the data colour compensation needs to be applied. Compensation for spectral overlap can be done by subtracting a fraction of the FITC signal from the PE signal. Compensation has to be applied in both directions to represent the data correctly (Omerod, 2008).

Two tubes were prepared, one for each antibody to be used during compensation. Compensation beads (lot: 3316686) were placed into each tube and treated the same as samples going forward.

All antibodies were added in excess (5µl of each in each tube). Antibodies were only mixed and aliquoted into tubes once blood was available to avoid complexes forming between the antibodies. 50µl of fresh heparinised blood was added to each tube. Samples were vortex mixed for 5-10 seconds and incubated at room temperature for 30 minutes with light excluded. Light was excluded because fluorophore attached the antibody was light sensitive.

Following incubation 50µl of Uti-Lyse™ Reagent A (Dako, Agilent, Stockport, United Kingdom) was added to tubes. Samples were vortexed for 5-10 seconds. Samples were covered and left to incubate at room temperature for 10 minutes. Red blood cells were then lysed by adding 500µl of Uti-Lyse™ (Dako, Agilent, Stockport, United Kingdom) Reagent B to tubes and mixing with a vortex. Samples were left covered for up to 3 hours or until RBC lysis was completed. To fix samples 38µl of 16% methanol free formaldehyde was added to each tube achieving a 1% formaldehyde solution. Samples were left for a minimum of 10 minutes prior to flow cytometric acquisition.

Immediately prior to flow cytometric acquisition, 50µl of Flow Count (Becton Dickinson, New Jersey, United States) beads were added to each tube to enable counts to be carried out.

2.4.13 **Whole Blood Immunophenotyping – Flow Cytometric Acquisition**

All flow cytometric acquisition of whole blood immune-phenotyping was carried out using a BD LSRFortessa™ and BD FACSDiva™ software. Acquisition was stopped after 15,000 lymphocyte events were collected in the lymphocyte region. Flow cytometric analysis was carried out within 24 hours of fixing. Compensation was always performed each time acquisition of the FSC files took place.

BD™CS&T (Cytometer Set-up & tracking) beads (Becton Dickinson, New Jersey, United States) are used on BD flow cytometers to provide a standardised method to perform a quality control of the instruments optics, electronics and fluidics and for adjusting fluorescence compensation. They are a suspension of fluorospheres with uniform and stable size and fluorescence intensity. BD™CS&T (Becton Dickinson, New Jersey, United States) beads were run on each occasion that the Fortessa was used to provide a performance check. The beads were re-suspended by inverting the bottle prior to use. The performance check was run on a medium flow rate. DIVA Software was put into cytometer set up and tracking mode prior to running the BD™CS&T (Becton Dickinson, New Jersey, United States) beads. The administrator will have installed details for the current bead batch prior to use. In a 5ml flow cytometer tube one drop of BD™CS&T (Becton Dickinson, New Jersey, United States) beads were added to 350µl of PBS. The tube of diluted beads was applied to the probe and run. Following acquisition, the flow cytometer was returned to Standby mode. A CS&T report was produced and any out of specification values were highlighted.

Data analysis was carried out using FlowJo (FlowJo LLC, Ashland, Oregon, United States). Granulocyte and lymphocyte populations were identified on pseudo dot plots (FSC vs SSC) and gated as shown in the example below (**Fig. 2.4.13.1**).

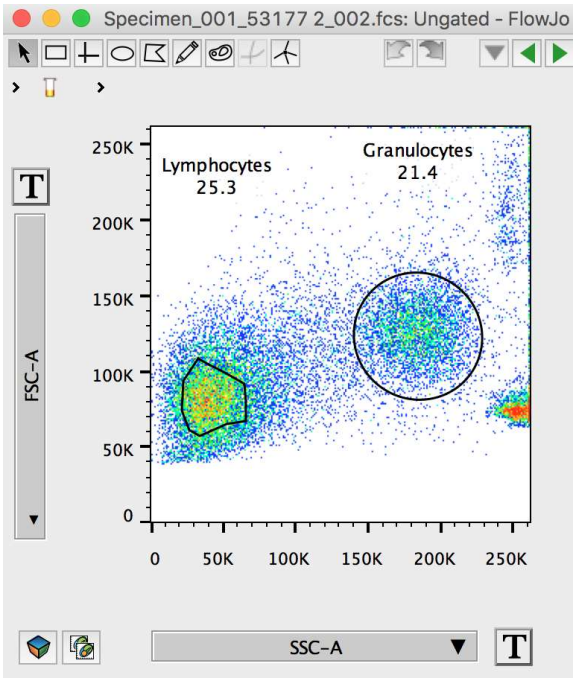

Figure 2.4.13.1 Identification of granulocyte and lymphocyte populations. Gates were drawn around the lymphocyte and granulocyte populations by selecting the polygon shape. These gates were applied to all samples being analysed. Each sample was then QC checked to ensure the gates were in the correct place as populations can appear slightly differently across ferrets.

CD4+ and CD8+ T cell populations were identified by isolating the lymphocyte population on the plot and changing the axis to show the PE (CD4) and AF700 (CD8) detectors. A quad region was drawn as shown below (**Fig. 2.4.13.2**).

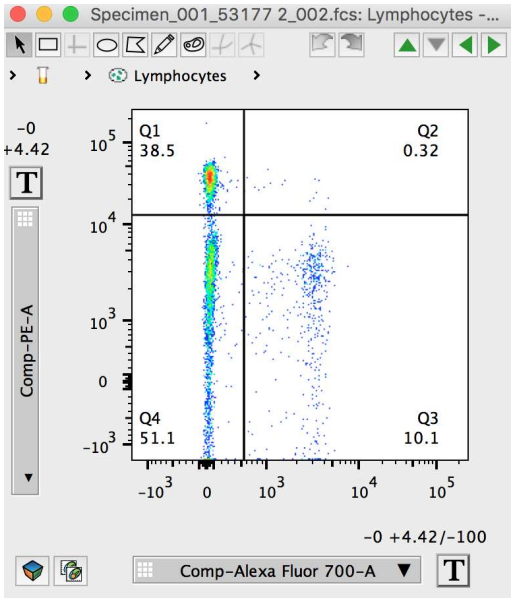

Figure 2.4.13.2 Identification of CD4+ and CD8+ populations. CD4+ and CD8+ T cells within the lymphocyte population were identified using a quad region.

Results were presented as the percentage change in cell per ml from values obtained prior to challenge. This was calculated by dividing the cell per ml of blood after challenge by the mean cells per ml value prior to challenge. The value obtained was multiplied by 100 to calculate the percentage and 100 was subtracted to calculate if the change was positive or negative.

2.5 Statistical Analysis

To compare the amount of virus shed in infected animals the area under the curve (AUC) for each animal was calculated using GraphPad Prism, version 7.0 (GraphPad Software Inc, La Jolla, California, USA). Where animal numbers were sufficient, the AUCs calculated in each test group were compared to those animals in other test groups with a Mann Whitney test using GraphPad Prism, version 7.0 (GraphPad Software Inc, La Jolla, California, USA).

To compare the amount of IFN-γ responses detected by ELISA in circulating blood infected animals the AUC for each animal was calculated using GraphPad Prism, version 7.0 (GraphPad Software Inc, La Jolla, California, USA). The Mann Whitney test was used to determine if there were any differences between influenza-specific IFN-γ responses seen in PBMC and lungs of ferrets inoculated with different strains of influenza. The Spearman correlation test was used to determine the level of correlation between study parameters using GraphPad Prism, version 7.0 (GraphPad Software Inc, La Jolla, California, USA).

3 Characterisation and Development of the Intranasal Low Dose model in Ferrets

3.1 Introduction

The purpose of developing a low dose intranasal model with H3N2 is to provide a baseline comparative model to run alongside the development of two other models: the nose-only aerosol delivery and the respiratory droplet transmission cage model. Intranasal inoculation is the most commonly used method for infection of ferrets with influenza virus inoculation (Belser *et al.*, 2011, Enkirch and von Messling, 2015). The infection of ferrets with seasonal H3N2 influenza via the intra-nasal route causes a characteristically mild to moderate, non-lethal infection resulting in weight loss, brief fever and upper respiratory tract infection. Previous studies have inoculated animals with high doses of influenza to ensure that animals have been infected and induce a clear response. This, however, doesn't provide a true representation of human infection who can be infected with doses as low as 100 $TCID_{50}$ intra-nasally and 0.6-3.0 $TCID_{50}$ via the aerosol route (Nikitin *et al.*, 2014)

Intranasal infection of ferrets with 10^6 plaque forming units (pfu, **Section 2.1.9**) and $TCID_{50}$ of A/California/04/2009 has been widely reported to produce a mild to moderate respiratory response (Maines *et al.*, 2009, Huang *et al.*, 2011, Munster *et al.*, 2009). The PHE Influenza Research Team, however, developed a low dose H1N1 ferret model with A/California/04/2009 and have demonstrated that reducing the challenge dose to 10^2 pfu delays the onset of clinical signs by 1 day and results in a modest reduction in clinical signs and a slowed nasal cavity innate immune response (Marriott *et al.*, 2014). A delay in virus production in the upper respiratory tract (URT) and prolonged virus shedding was also seen. These delayed disease

kinetics are much more similar to the course of influenza disease in humans than those observed with a higher challenge dose (Marriott *et al.*, 2014).

A series of studies were completed evaluating the viral kinetics and pathology in the ferret following intranasal inoculation.

3.2 Chapter Aims

The overall objective of this chapter was to assess the low dose intranasal ferret model for H3N2 A/Perth/16/2009. Specific objectives were to:

- Evaluate and compare the high and low dose intranasal inoculation of ferrets with A/Perth/16/2009
- To confirm that a dose of 10^2 pfu per ferret provides a robust and reproducible model of infection
- To investigate, compare and contrast the cellular immune response seen in ferrets when infected with a high and low dose of A/Perth/16/2009

3.3 Initial Intranasal Dose Pilot Study

The first study designed was a high dose (HD) and low dose (LD) inoculation of ferrets was carried out in study **4965** (see appendix 1)**.** This pilot study was carried out using a stock of A/Perth/16/2009 that was identity confirmed by sequencing of the HA and NA genes. Previously A/Perth/16/2009 had been reported in the literature to cause observable, non-lethal illness in ferrets when delivered intra-nasally at 10^6 PFU/ferret (Maines *et al.*, 2009). Upon commencing this pilot no data was available for lower doses of the virus.

3.3.1 *In vivo* Study Outline

As a first step in developing an H3N2 ferret model for this project, 4 ferrets were used to perform a pilot dose-ranging study. Doses of 10^2 and 10^6 PFU/ferret were tested, as these values spanned the range known to efficiently infect ferrets when using H1N1 (A/California/04/2009) virus (Marriott *et al.*, 2014). Ferrets were monitored for clinical signs and virus shedding, as well as sero-conversion, to inform future studies using an H3N2 challenge.

3.3.2 Ferrets

Ferrets were obtained from Highgate Farm, UK and were 4-6 months at the time of the study. A total of 4 ferrets were used, 2 were allocated to the HD group and 2 to the LD group as shown in **Table 3.3.2.1**. Ferrets were group housed in floor pens designed in accordance with the requirements of the United Kingdom Home Office Code of Practice for the Housing and Care of Animals Used on Scientific Procedures (1989).

Table 3.3.2.1 Ferret Identification Numbers

High Dose (HD) Group	Low Dose (LD) Group
27043 (m), 30654 (f)	47575 (m), 27027(m)

3.3.3 **Prior to Viral Inoculation**

At three days prior to inoculation, ferrets were fully anaesthetised using Ketamine/Xylazine (1ml Ketamine plus 0.4ml Xylazine) given at a dose of 0.25ml/Kg bodyweight. A nasal wash was performed on each ferret to act as a baseline nasal wash count prior to inoculation. Baseline blood samples were taken from the anterior vena-cava vessel of each ferret, 500 µl blood was collected into SST tubes for sera isolation. Sera were tested by HAI (**Section 2.3.8**) for the presence of any pre-existing antibodies to influenza H3N2 A/Perth/16/2009 to ensure ferrets were not previously exposed to this strain of influenza. Sera with an HAI titre equal to or less than 8 was deemed to be seronegative. All baseline sera samples had HAI titres of less than 4 to H3N2 A/Perth/16/2009. It was deemed that these ferrets had no previous exposure to H3N2 and so were suitable for challenge.

3.3.4 **Virus**

Ferrets were inoculated intranasally with H3N2 A/Perth/16/2009 P+2A challenge stock virus diluted in PBS to provide a stock of $1x10^6$ pfu/ferret (HD group) or $10x10^2$ pfu/ferret (LD group). The dose was confirmed on day of administration by back-titration. The challenge materials were given to each animal in a volume of 0.2ml by the intranasal route.

3.3.5 **Sample Collection**

Following virus inoculation, ferret weight was recorded daily, and clinical signs of influenza infection were recorded twice daily. From 1 to 4 dpi and on 7, 9, 11 days post infection (dpi) nasal washes were collected from animals. Nasal washes were counted and frozen to be titred at a later date. At day 14 ferrets were culled. Ferrets were sedated by intramuscular injection of Ketamine/Xylazine (1ml Ketamine plus 0.4ml Xylazine) given at a dose of 0.25ml/Kg bodyweight. Following overdose samples were collected from each ferret; nasal wash and blood in SST for serum. Nasal washes and serum were aliquoted and stored at -70±10ºC for analysis at a later date.

3.3.6 **Results**

3.3.6.1 *Nasal wash cell counts and titres in HD and LD groups*

Nasal wash cell counts were collected for both groups at 1- 4, 7, 9, 11 and 14 days post infection (dpi) (**Fig. 3.3.6.1.1**). Cell counts for the HD group ferrets, 27043 and 30654, both increased at 2 dpi, indicating successful infection. The nasal wash cell count for 30654 then steadily decreased over the sampling period, while ferret 27043 appeared to have a second peak at 7 dpi with a decrease to baseline levels in nasal wash cell counts by 14 dpi. The LD group appeared to have a slower rise in nasal wash cells counts following infection. Ferret 47575 peaked at 3 dpi and a slight second peak at 9 dpi with a decrease to baseline level by 14 dpi. Ferret 27027 had a slower but steady rise in nasal wash cell counts not peaking until around 9 dpi. By 14 dpi nasal wash cell counts were decreasing but not back down to baseline levels.

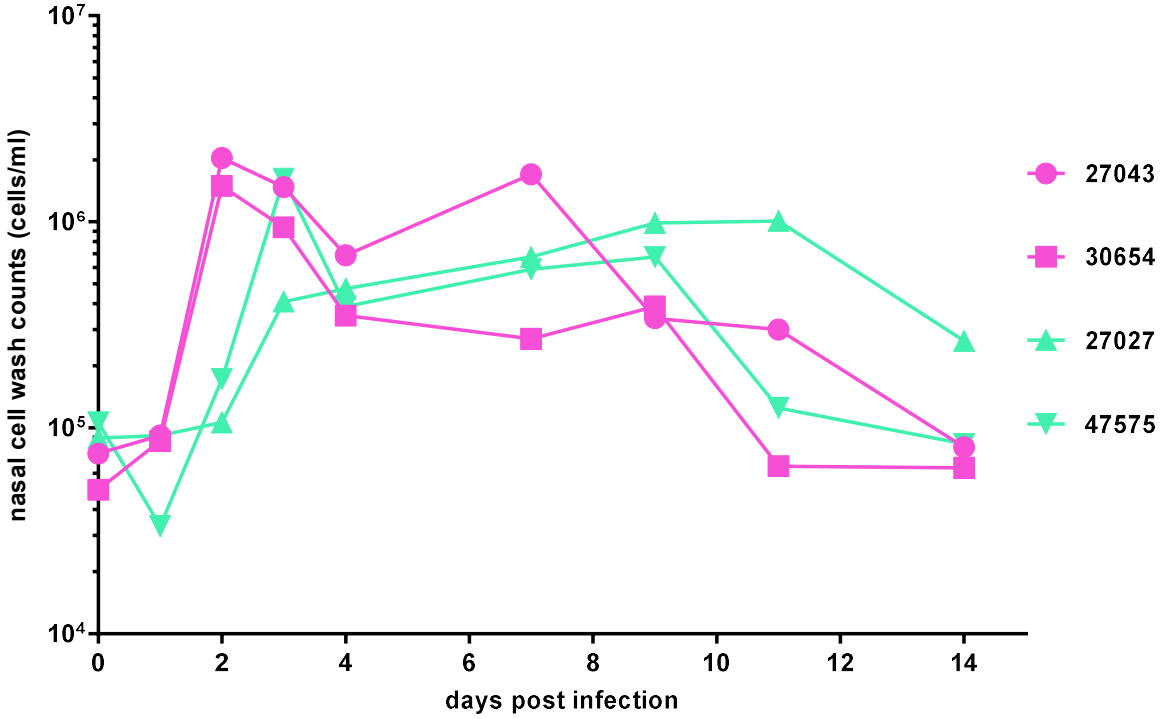

Figure 3.3.6.1.1 Nasal wash cell counts HD Group: 27043, 30654. LD Group: 27027, 47575. Nasal washes were collected at +1 to +4, +7, +9, +11 and +14 dpi. All nasal washes were counted to ascertain the number of cells being shed from each ferret at each timepoint. A rise in nasal wash cells from baseline indicates successful infection. Plots represent individual counts. Single counts were performed on each nasal wash sample from each ferret on each day.

Nasal wash samples were titred to ascertain live viral titres being shed from the ferrets (**Fig. 3.3.6.1.2**). The first peak in the HD group appeared at 1 dpi for both ferrets, 27043 and 30654. This was followed by a fall in titre, with a smaller, lower peak at 4 dpi. Both ferrets stopped shedding virus by 7dpi. The ferrets in the LD group began shedding virus at one (47575) and two (27027) days post infection. Ferrets 47575 and 27027 had peak shedding titres at 3 and 4 dpi, respectively. Ferret 47575 stopped shedding virus by 7 dpi and ferret 27027 stopped shedding virus by 9 dpi. These results are as expected, ferrets successfully infected with influenza virus should start to shed live virus at approximately 1 dpi, but it is expected that these results will differ with inoculation titre.

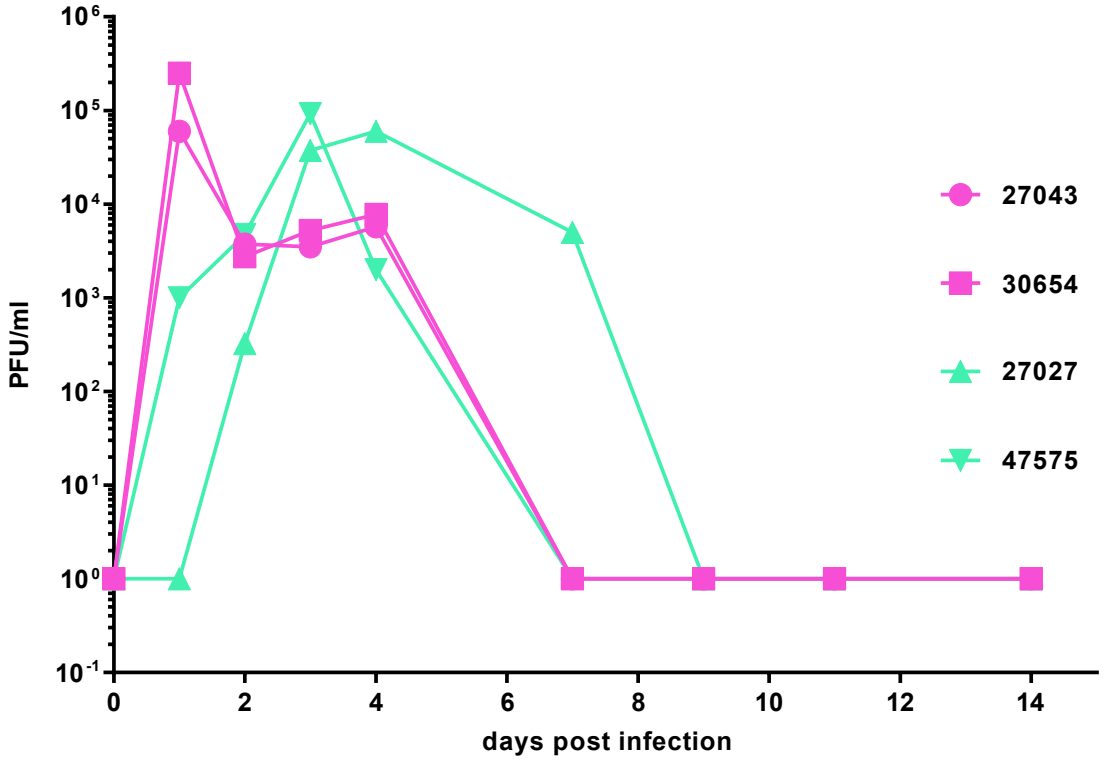

Figure 3.3.6.1.2. Nasal wash titres HD Group: 27043, 30654. LD Group: 27027, 47575. Nasal washes were collected at +1 to +4, +7, +9, +11 and +14 dpi. Nasal washes were plaque assayed to ascertain viral titres shed from ferrets at all timepoints. Plaque forming units (PFU) per millilitre (ml) of nasal wash represent a direct relationship to the amount of live virus in a sample. Plots represent individual assay results. Single plaque assays were performed on each nasal wash sample from each ferret on each

3.3.6.2 *Clinical signs of infection in HD and LD groups*

Weight was monitored once daily throughout the study. Both HD group ferrets initially experienced a drop in percentage weight from baseline following inoculation at 2 dpi. They both recovered by 3dpi and began to put on weight. Ferret 30654 experienced another decrease in percentage weight from baseline at 6 dpi, which appears to coincide with the second peak in nasal wash cell counts identified in **Figure 3.3.1** All four ferrets on the study

gained weight over the course of the study (**Fig. 3.3.3**), showing that the virus had no impact on the ferrets' ability to gain weight overall.

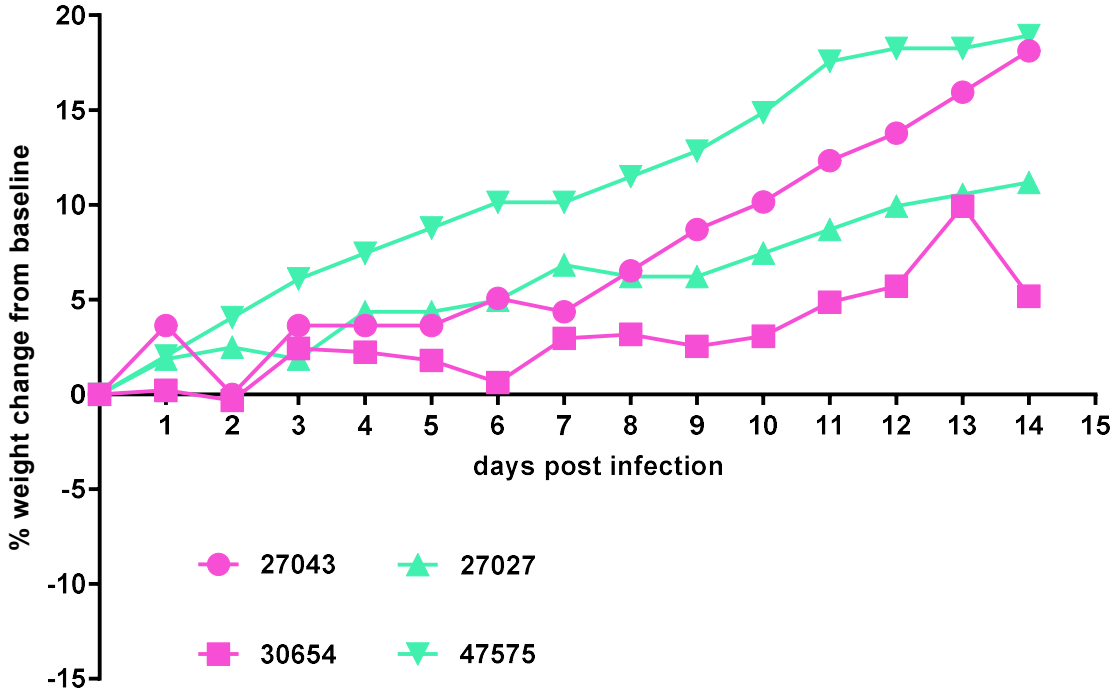

Figure 3.3.6.2.1 Weight percentage change from baseline. HD Group: 27043, 30654. LD Group: 27027, 47575. Percentage weight changes from day of infection for all ferrets (n=4).

Table 3.3.6.2.1. Cumulative incidence of nasal discharge and sneezing

Ferret	Incidence
27043	5
30654	3
47575	2
27027	2

The cumulative incidences for nasal discharge and sneezing, recorded 1-14 dpi, in the HD group were higher when compared to the LD group (**Table 3.3.6.2.1**). Appetite loss was noted for both animals in the HD group, 27043 and 30654, at 7 dpi for two instances. There were

no instances of reduced activity or diarrhoea recorded for any of the animals in either the HD or LD group.

3.3.6.3 *Evidence of seroconversion in HD and LD groups*

The HAI assay confirmed ferrets from both the HD and LD groups seroconverted (**Fig. 3.3.6.3.1**). Seroconversion is the period during which specific antibodies to A/Perth/16/2009 develop to become detectable in the ferret blood. When these antibodies become detectable the ferret blood the ferret is deemed to have seroconverted. Seroconversion is measured by HAI titre. Both the groups show similar HAI titres. It is not expected that the HAI titre would be different depending on titre of virus inoculated with, and therefore between groups. Rather the HAI titre shows that the humoral immune response to influenza infection was successfully elicited. These results confirm, along with the nasal wash titre results, that all the ferrets were successfully infected and produced a robust antibody response.

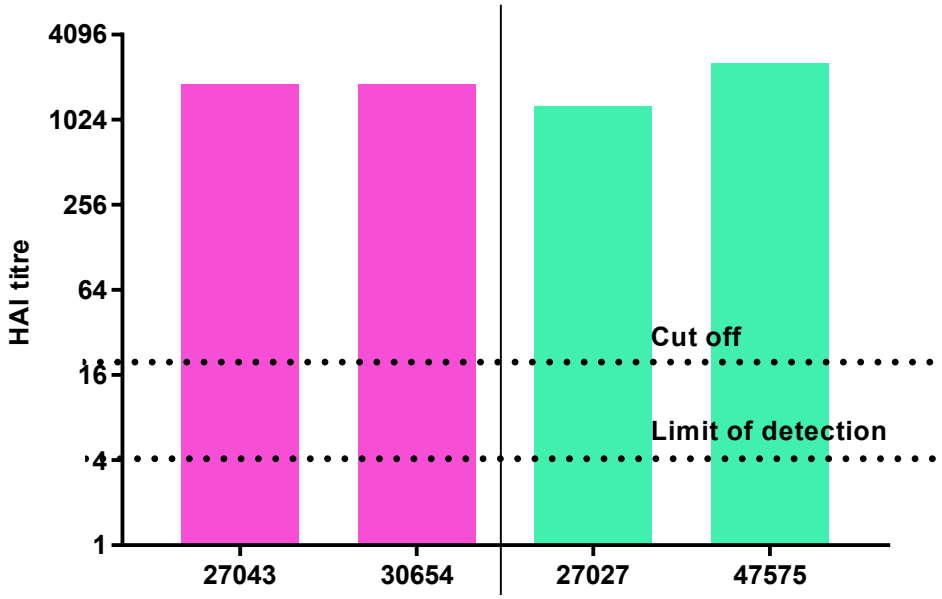

Figure 3.3.6.3.1 Haemagglutination Inhibition (HAI) titres of high and low dose infected ferrets to A/Perth/16/2009. HD Group: 27043, 30654. LD Group: 27027, 47575. All pre-infection titres were

<4. The cut off limit designates the titre under which ferrets are deemed seronegative. Titres above 20 HAI are deemed to show seroconversion.

3.3.7 **Discussion**

This study was designed to be a preliminary investigation into the immunogenicity and viral kinetics of H3N2 A/Perth/16/2009 in ferrets. This study confirmed that ferrets were able to be successfully inoculated with high ($1x10^6$ PFU/ferret) and low ($1x10^2$ PFU/ferret) dose concentrations of A/Perth/16/2009. Nasal wash cell counts indicated that ferrets had been infected, and plaque assays on those nasal wash samples allowed titres of virus being shed by the ferrets to be calculated. Clinical monitoring suggested that infection with H3N2 A/Perth/16/2009 had no significant effect on the weight of animals, all the ferrets gained weight from baseline measurements for the duration of the study. The HAI results show that both titres of virus caused seroconversion in the ferrets. This suggests that the humoral immune response to a low dose of influenza is like that stimulated by a high dose influenza infection. There was a higher incidence of nasal discharge and sneezing in the two ferrets inoculated with the high dose of H3N2 A/Perth/16/2009 when compared to the two ferrets inoculated with the low dose.

3.3.8 **Further Work**

The results from this small-scale study indicate that ferrets were successfully infected with both $1x10^2$ and $1x10^6$ PFU/ferret dose of A/Perth/16/2009. Using a low dose model is preferential as the dose presents a more “true to life” representation of a natural dose. These results show there are some differences between the high and low dose inoculated ferrets but

demonstrates that a low dose causes mild symptoms, viral shedding, increased numbers in nasal cell wash counts and elicits a humoral immune response triggering seroconversion.

Therefore, this study provided the confidence to move forward with a low dose (10^2 pfu/ferret) to look at:

- The presence of virus in the respiratory tract of the ferret
- The reproducibility of the viral shedding in the ferret
- The cellular immune response of ferrets using influenza-specific IFN-γ as a readout

3.4 Serial Cull Study

This section describes a low dose inoculation study, designated study number **5087** (appendix 1)**.** To elucidate the viral kinetics of the H3N2 A/Perth/16/2009 in the ferret model a serial cull study was designed collecting samples which allowed the determination of the kinetics of virus replication and pathogenesis along the length of the respiratory tract. This study was carried out using the same stock of A/Perth/16/2009 used during the initial pilot study, with identity previously confirmed by sequencing of the HA and NA genes. Ferrets were inoculated intranasally with a low dose of 10^2 PFU/ferret. Ferrets were culled from the study 2 at a time at pre-determined time points, with tissues being taken for qRT-PCR. Additionally, they were monitored for clinical signs, virus shedding and sero-conversion as was carried out previously.

3.4.1 *In vivo* Study Outline

Ferrets were inoculated intranasally with $1x10^2$ PFU of A/Perth/16/2009. Ferrets were culled out 2 at a time at 2, 3, 4 and 8 days post infection (**Table 3.4.2**). A total of 8 ferrets were used. These time points were chosen based upon the virus titres shed by low dose inoculated ferrets in the previous study (**Section 3.3**). Both ferrets were shedding live virus by 2 dpi, and peak titres were shed between 3 and 4 dpi. Results from these three timepoints should provide a picture of what is happening in the ferret during the first several days of influenza infection. Based on the previous study day 8 was chosen as the final timepoint because this was around the time of viral clearance.

3.4.2 **Ferrets**

Ferrets were obtained from Highgate Farm, UK and were 9.5-14.5 weeks at the time of the study.

Table 3.4.2.1 Ferret Identification

Day of Cull	Ferrets
2	26166 (f), 27207 (f)
3	18992 (m), 26624 (f)
4	76400 (f), 31048 (m)
8	33920 (f), 86670 (f)

Ferrets were group housed in floor pens designed in accordance with the requirements of the United Kingdom Home Office Code of Practice for the Housing and Care of Animals Used on Scientific Procedures (1989).

3.4.3 **Prior to Viral Inoculation**

At three days prior to inoculation, ferrets were fully anaesthetised using Ketamine/Xylazine (1ml Ketamine plus 0.4ml Xylazine) given at a dose of 0.25ml/Kg bodyweight. Baseline blood samples were taken from the anterior vena-cava vessel of each ferret, 2ml blood collected into SST tubes for sera isolation and a baseline nasal wash was performed. Sera were tested by HAI for the presence of any pre-existing antibodies to influenza H3N2 A/Perth/16/2009. All

baseline sera samples had HAI titres of less than 4 to H3N2 A/Perth/16/2009, and it was deemed that these ferrets had no previous exposure to H3N2 and so were suitable for challenge.

3.4.4 **Virus**

Ferrets were inoculated intranasally with H3N2 A/Perth/16/2009 P+2A challenge stock virus diluted in PBS to provide $1x10^2$ PFU/ferret. The dose was confirmed on day of administration by back-titration. Each animal was inoculated with a volume of 0.2ml by the intranasal route.

3.4.5 **Sample Collection**

Following challenge, weight was recorded daily, and clinical signs recorded twice daily. Nasal washes were collected from 1 to 8 days post infection. Ferrets were culled from the study two at a time (see **table 3.4.1**) on 2, 3, 4 and 8 days post infection. Ferrets were sedated by intramuscular injection of Ketamine/Xylazine (1ml Ketamine plus 0.4ml Xylazine) given at a dose of 0.25ml/Kg bodyweight. Following overdose samples were collected from each ferret; nasal wash, blood in SST for serum. Key tissues from the respiratory tract were collected to assess viral load. Nasal turbinate, trachea and lung were taken and placed into RNALater for RNA extraction. Samples of nasal cavity, trachea and lung were fixed in 10% neutral buffered formalin for pathology analysis.

3.4.6 **Results**

3.4.6.1 *Nasal wash cell counts and titres*

Nasal wash counts were performed on all nasal washes (**Fig. 3.4.6.1.1**). Counts for all animals began to increase at around 2 dpi, indicating successful infection. Counts continued to rise for animals that had not been culled until 5 dpi when they plateaued and then began to slowly decline at around 7dpi, in line with previous results.

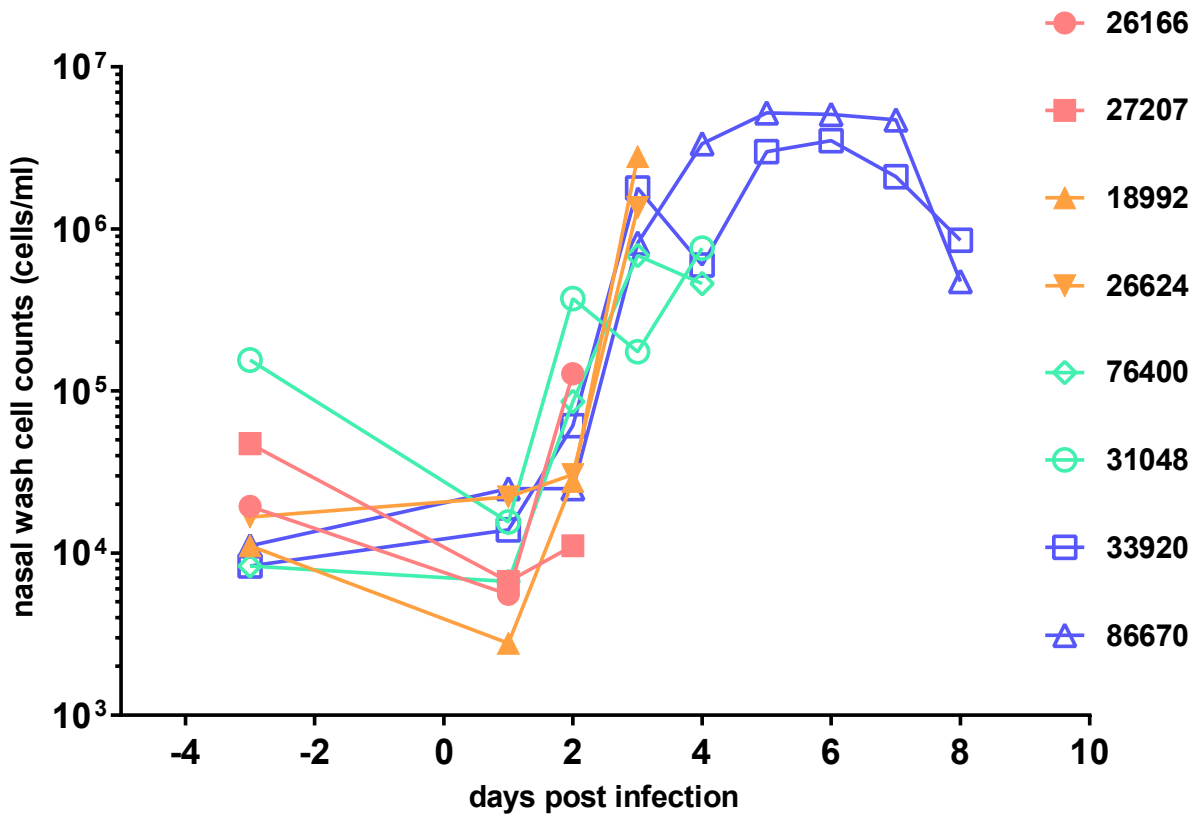

Figure 3.4.6.1.1 Nasal Wash Cell Counts Nasal washes were collected at +1 to +8 dpi. All nasal washes were counted to ascertain the number of cells being shed from each ferret at each timepoint. A rise in nasal wash cells from baseline indicates successful infection. Plots represent individual counts. Single counts were performed on each nasal wash sample from each ferret on each day.

All ferrets began to shed detectable virus titres in their nasal washes at 1 dpi (**Fig. 3.4.6.1.2**). Ferrets 26166 and 27207 were culled at 2 dpi. Ferret 18992 was culled at 3 dpi with ferret 26624. The peak nasal wash viral titre for ferret 18992 was recorded as 3 dpi. Ferrets 76400 and 31048 were culled at 4 dpi. Ferrets 33920 and 86770 had a 'double peak' in in their nasal wash titres, the first peak being at 2 dpi and the second, lower peak being at 6 dpi. These results show the same pattern of shedding as seen in the pilot (**Section 3.3**), however sampling is more frequent in this study.

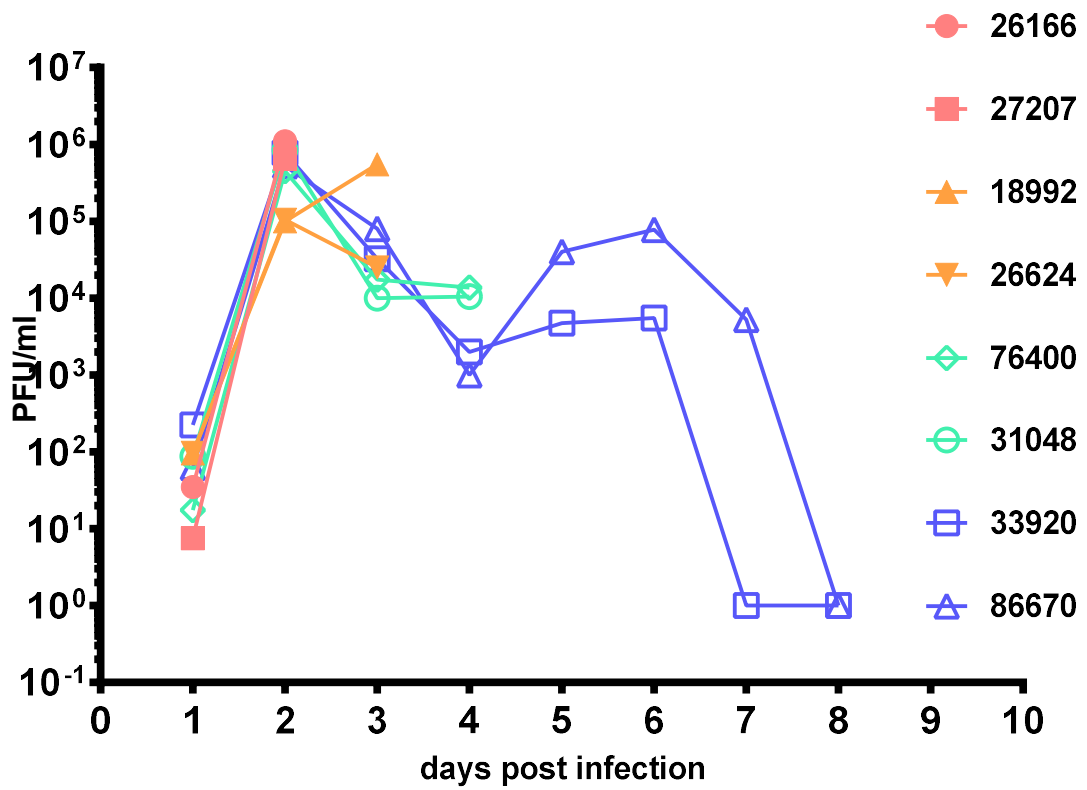

Figure 3.4.6.1.2 Nasal Wash Titres Nasal washes were collected at +1 to +8 dpi. Nasal washes were plaque assayed to ascertain viral titres shed from ferrets at all timepoints. Plaque forming units (PFU) per millilitre (ml) of nasal wash represent a direct relationship to the amount of live virus in a sample. Plots represent individual assay results. Single plaque assays were performed on each nasal wash sample from each ferret on each day.

3.4.6.2 *Clinical signs of infection in ferrets*

It must be noted that the ferrets that were kept alive for the longest (8 dpi) has the higher incidences of sneezing and nasal discharge. The earlier the ferrets were culled, the less incidences of sneezing and nasal discharge that occurred.

Table 3.4.6.2.1 Cumulative incidence of nasal discharge and sneezing

Ferret	Incidence
26166	0
27027	0
18992	1
26624	1
76400	4
31048	2
33920	5
86670	4

3.4.6.3 *Evidence of seroconversion in ferrets*

HAI assays were performed on ferrets culled at 8 dpi; 33920 and 86670. 39920 gave a titre of 64 and 86670 had a titre of 32. These values are above the HAI titre cut of value of 20 suggesting that these ferrets have seroconverted. HAI assays were not performed on the ferrets culled at 2, 3 and 4 dpi as it was highly unlikely that seroconversion would have occurred.

3.4.6.4 *Viral burden detected in ferret tissues*

Viral RNA (vRNA) was extracted from nasal turbinate, trachea and upper and lower right lung lobes to assess viral burden following inoculation with a low dose of A/Perth/16/2009. Tissues had been collected into and stored in RNAlater -20ºC. The H3N2 M gene was used for standard curve and H3N2-specific primers were used as described in **Chapter 2 Materials & Methods**. Upper right and lower right lung lobes were analysed separately and averaged.

The highest viral burden was found in the nasal turbinate tissue, where the highest amount of vRNA was detected. This was consistent for all ferrets across all four cull time points when compared to the viral burden of other tissues (**Fig. 3.4.6.4.1 a, b, c**). The greatest amount of RNA was detected at 2 dpi in ferrets 26166 and 27207. The vRNA copies then declined progressively from day 2 to 8 in the ferrets.

The viral burden in the trachea was variable across the cull days (**Fig. 3.4.6.4.1b**). One ferret culled at 2 dpi (27207) had no vRNA detected in trachea samples. Ferret 31048, culled at 4 dpi, had the highest vRNA detected at 3460 copies per milligram detected. There was a very low amount vRNA detected at 8 dpi for ferrets 33920 and 86670.

Ferret 31048 had the highest amount vRNA present in lung samples with 2381 copies per milligram detected (**Fig. 3.4.6.4.1c**). The remaining ferrets had extremely low vRNA detected in the lung samples of below 50 copies per milligram.

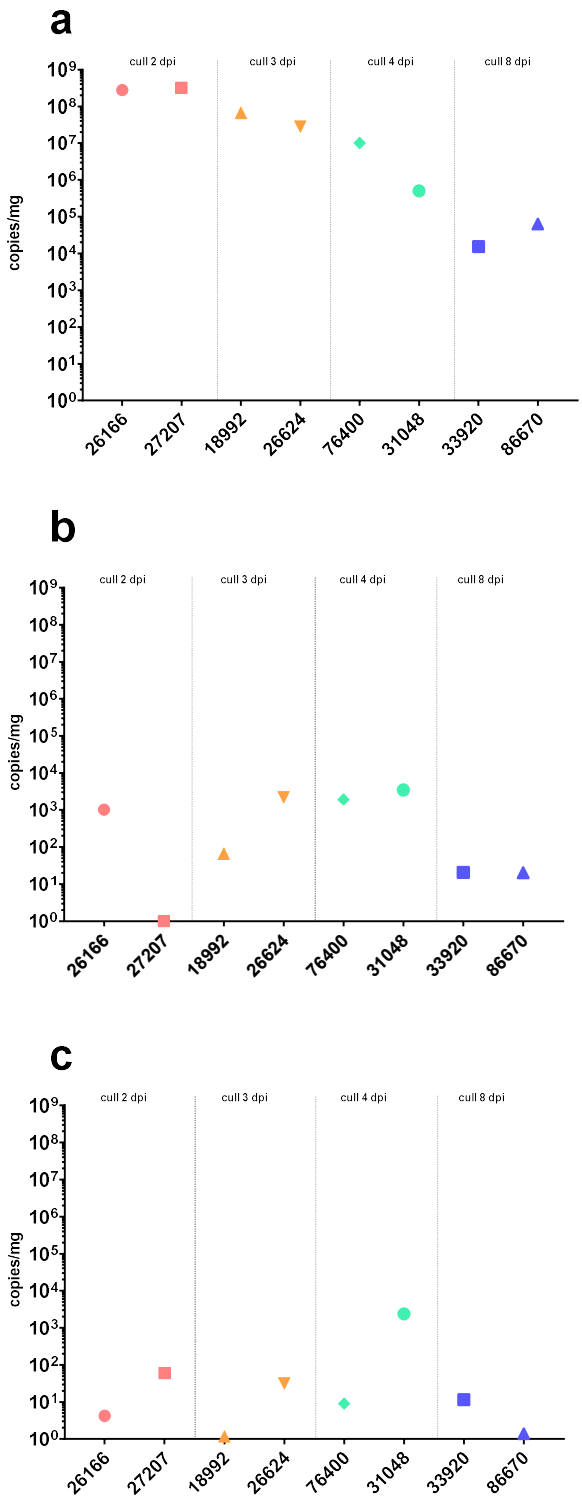

Figure 3.4.6.4.1. Viral burden in ferret tissues. **a** Nasal turbinates, **b** trachea and **c** lung lobes were collected into *RNALater* for each ferret at cull (n=8). Copies per milligram were calculated by using a standard curve as detailed in **Chapter 2 Materials and Methods**. **c** the data points shown above were calculated as the arithmetic mean of the upper right and lower right lobes of lung.

3.4.6.5 *Histopathology of nasal cavity, trachea and lung*

Samples of nasal cavity, trachea and lung were fixed in 10% neutral buffered formalin and sent to the Histology Department at PHE, Porton Down. Fixed tissues were processed to paraffin wax. Sections, approximately 3-5µm thick, were stained with haematoxylin and eosin (HE) for examination. Haematoxylin stains the nucleus of cells blue, and eosin stains the cell cytoplasm pink. HE stain is a gold standard tissue stain used in histology and provides the pathologist with a general overview of the tissue sample's structure. Tissues were examined by light microscopy and evaluated subjectively by the pathologist at PHE Porton Down.

Following infection, the most pronounced histopathological changes were observed in the nasal cavity (**Fig. 3.4.6.5.1**). Changes including inflammatory cell infiltration and occasional oedema of the propria mucosa; epithelial loss, occasional necrosis and prominent attenuation; and suppurative exudation, were detected in the animals. Minimal changes were seen at two days post infection (**Fig. 3.4.6.5.1a**), with severity increasing at three days post infection (**Fig. 3.4.6.5.1b**), with most of moderate changes recorded (**Fig. 3.4.6.5.2**). Marked changes were found to present at 8 dpi (**Fig. 3.4.6.5.1c**).

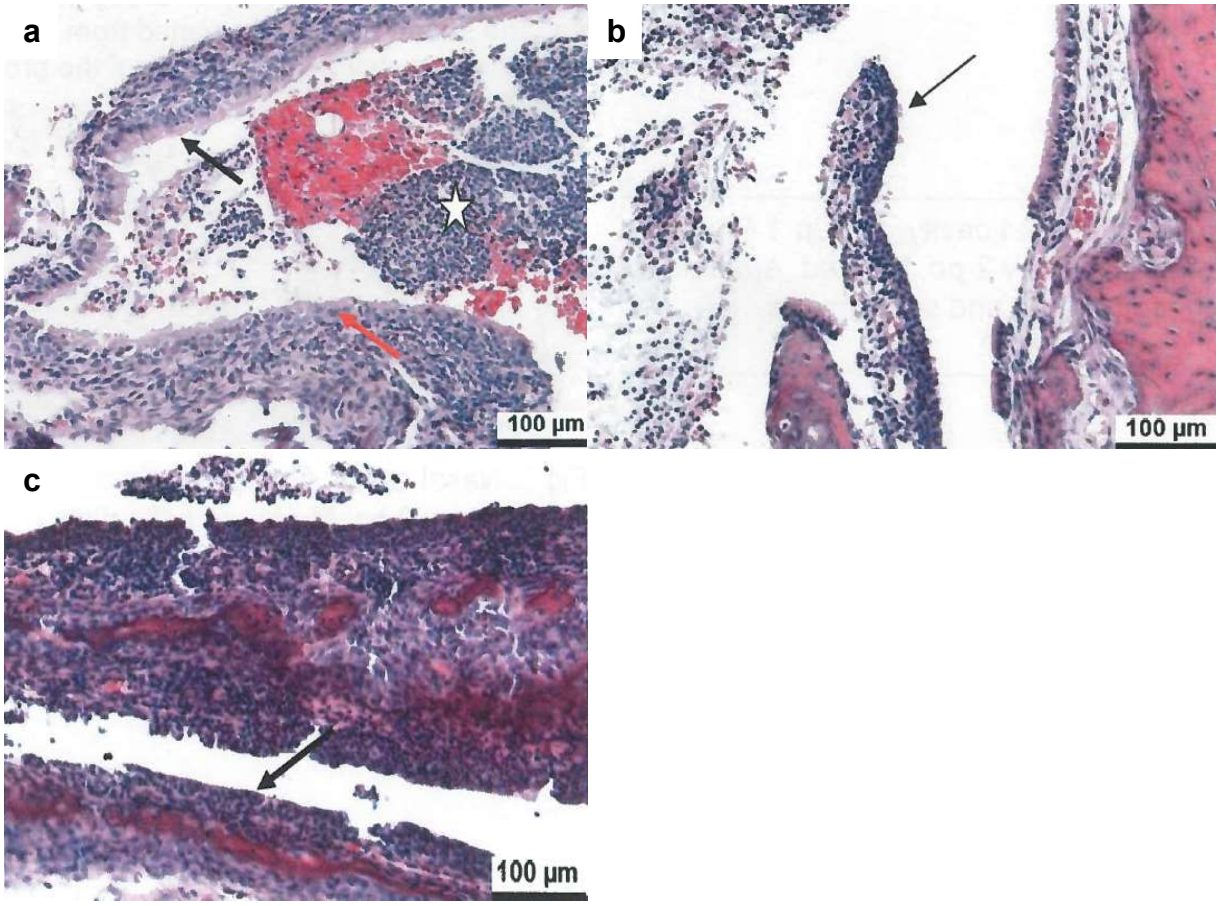

Figure 3.4.6.5.1 HE Staining of the Nasal cavity a Nasal cavity from ferret 26166, culled at 2 dpi. The image shows minimal epithelial attenuation (red arrow) and suppurative exudate (commonly referred to as pus), black arrow shows normal epithelium. **b** Nasal cavity from ferret 26624, culled at 3 dpi. The image shows moderate epithelial attenuation (black arrow) and the normal epithelium remains opposite. **c** Nasal cavity from ferret 33920, culled at 8 dpi. The image shows marked epithelial inflammation, with some attenuation (black arrow). Images provided and analysed by the Histology Department, Public Health England, Porton Down.

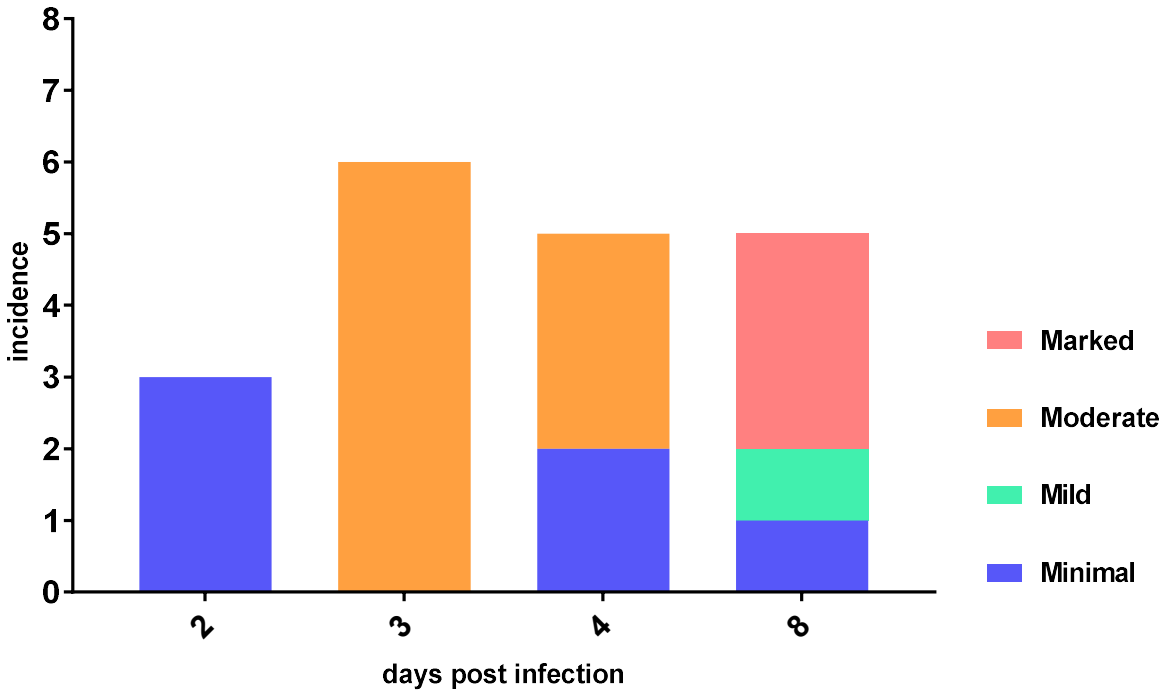

Figure 3.4.6.5.2 Frequency of pathological changes in the nasal cavity Cumulative frequency of pathology seen at each time point (n=2 per time point).

Changes seen in the trachea were sporadic, and minimal for all animals and therefore considered too few to draw any firm conclusions. **Figure 3.4.6.5.3**. shows clear mononuclear inflammatory cell infiltrate (in blue) in both **a** (ferret culled at 2 dpi) and **b** (ferret culled at 8 dpi). The Pathologist interpreting these slides concluded that these images only showed minimal mononuclear inflammatory cell infiltrate. Furthermore, only minimal pathology was observed in the lungs of all ferrets (**Fig 3.4.6.5.4**).This correlates with the low level viral burden present in the lung.

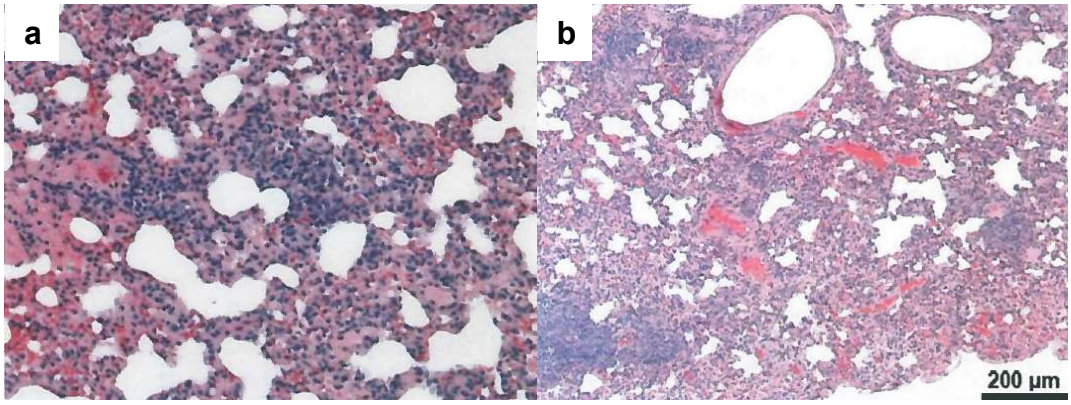

Figure 3.4.6.5.3 HE Staining of Lung Tissue a Lung tissue from ferret 27207, culled at 2dpi. The image shows minimal, parenchymal, mononuclear inflammatory cell infiltrate. **b** Lung tissue from ferret 33920, culled at 8 dpi. The image shows minimal, parenchymal, mononuclear inflammatory cell infiltrate as seen in the sample from 2 dpi. Images provided and analysed by the Histology Department, Public Health England, Porton Down.

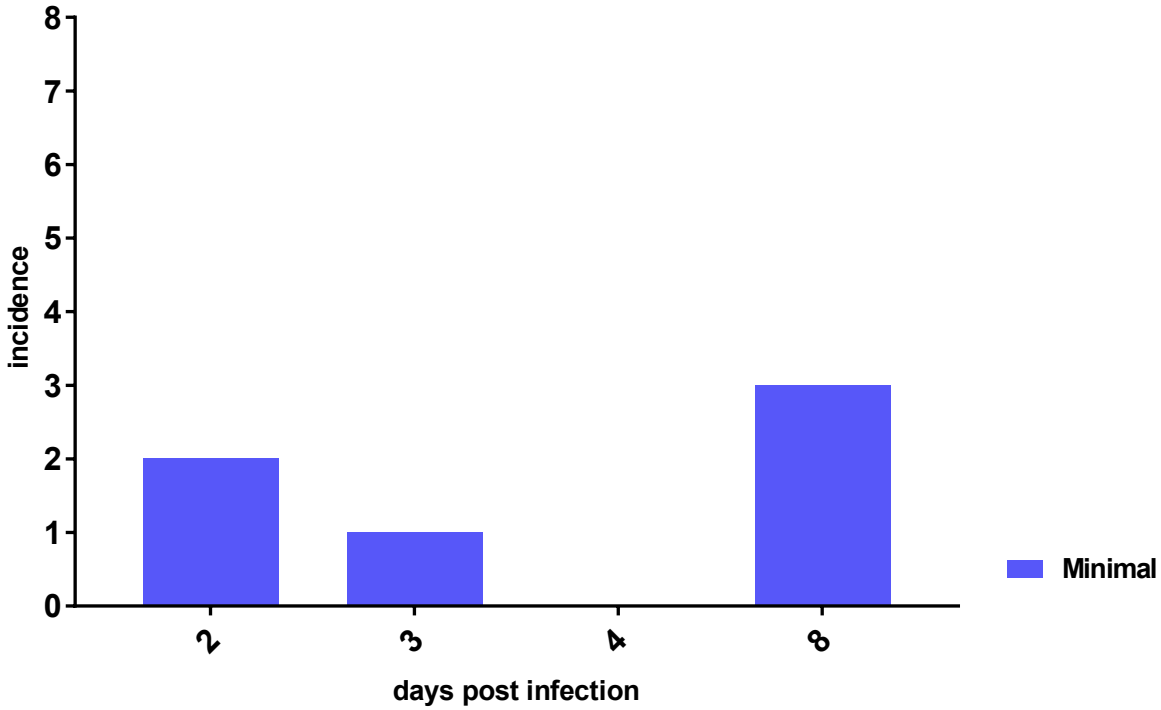

Figure 3.4.6.5.4 Frequency of pathological changes in the lung Cumulative frequency of pathology seen at each time point (n=2 per time point).

3.4.6.6 *Influenza-specific interferon gamma responses detected in the spleen*

Spleens were collected from all ferrets at cull. Splenocytes were isolated from each spleen and the frequency of influenza-specific IFN-γ secreting cells was quantified by ferret specific IFN-γ ELISpot. Responses were seen in all eight ferrets (**Fig. 3.4.6.6.1**). Ferrets culled at 8 dpi showed the highest influenza-specific IFN-γ responses when compared to the ferrets culled at 2, 3 and 4 dpi. Ferrets culled at 4 dpi had the lowest influenza-specific IFN-γ responses. This increase by 8 dpi could be due to the time it takes for the cellular immune response to be triggered. Carrying out in study sampling of circulating peripheral blood and assessing the influenza-specific IFN-γ responses would help to gauge if this result is expected.

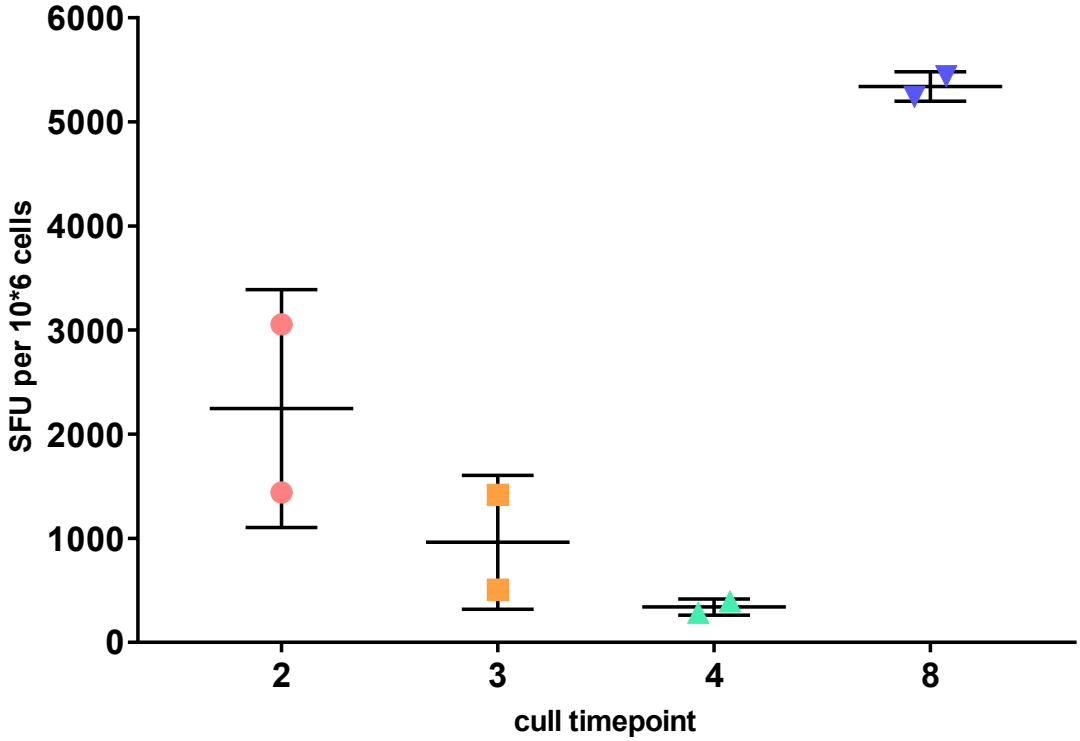

Figure 3.4.6.6.1. Cellular immune response of ferrets infected with A/Perth/16/2009. Spleens were collected from all animals (n=8). Results were normalised by subtracting allantoic fluid control values from virus stimulated samples. Influenza-specific IFN-γ responses were quantified in the spleen samples from all ferrets. The values measured for each ferret are plotted as spot forming units (SFU) per million cells. Bars show standard deviation and mean for each group.

3.4.7 **Discussion**

This study had a total of eight ferrets inoculated intranasally with a low dose ($1x10^2$ PFU/ferret) A/Perth16/2009. All ferrets were successfully infected, as shown by virus shedding and sero-conversion. A serial cull was performed with two ferrets being culled on days two, three, four and eight post infection. The results from two animals per day was not enough to give any statistical significance to the data when comparing animals across timepoints. It did however allow elucidation of the viral kinetics occurring over the first eight days of infection in the ferret model, paired results per day allowed for more robust data.

Seven of eight ferrets had shed peak viral titres at two days post infection. Viral titres for ferret 18992 peaked at three days post infection. The kinetics of viral shedding for ferrets 33920 and 86670 had a distinctive 'double peak' of virus shedding that was not identified in the previous pilot low dose study. However, this could be due to the limited sampling days used in the first study. Ferret 31048 was the only animal to have vRNA present in lung, this correlated with 31048 having the highest amount of vRNA found in the trachea. Strangely no histopathological changes were noted in the lung at four days post infection, the day ferret 31048 was culled out of the study. The low viral RNA copies detected in the lungs of the ferrets (**Fig. 3.4.6.4.1c**) corresponds with the minimal pathology recorded by the Pathologist (**Fig. 3.4.6.5.3**). This suggests that A/Perth/16/2009 may not travel to the lungs as well as the other seasonal circulating IAV, H1N1pdm (Music *et al.*, 2014, Roberts *et al.*, 2012, Carolan *et al.*, 2014, Roberts *et al.*, 2011). These observations are consistent with A/Perth/16/2009 having a tropism for the upper respiratory tract (Ryan *et al.*, 2018).

The high influenza-specific IFN-γ response seen at two days post infection would need to be confirmed with a larger number of animals as it is unlikely that a robust T cell response would present at two days post infection (Ryan *et al.*, 2018). However, the higher influenza-specific IFN-γ responses seen at eight days post infection was in line with similar studies looking at influenza-specific IFN-γ responses to influenza infection in the ferret (Music *et al.*, 2014) and to further studies carried out in this body of work.

3.4.8 **Further Work**

Additional work with more ferrets is required to look at the distinctive 'double peak' of virus shedding identified in the two ferrets culled at day eight. This will be addressed in the next piece of work (**Section 3.5**).

Further work will need to be carried out on the influenza-specific IFN-γ responses that were identified in the spleen during this study. Looking at additional tissues as well as the spleen, for example circulating blood, bronchiolar lavage fluid (BAL) or lung, could help to build a clearer picture of the cellular immune response to influenza infection in the ferret. Development of a method to look at the influenza-specific IFN-γ response of infected ferrets without having to cull animals would be advantageous. This would provide an adequate number of animals for statistical analysis and enable a longitudinal time course of the cellular immune response to influenza infection in the ferret.

3.5 Study to Demonstrate the Reproducibility and Reliability of the Low Dose Intranasal Inoculation

This low dose inoculation study, **5256** (appendix 1), was designed to develop the intranasal delivery ferret model further. This study was intended to confirm the double peak of virus shedding observed in study **5087** (**Section 3.4, Fig. 3.4.6.1.2**).

3.5.1 *In vivo* Study Outline

The study was carried out using the same stock of A/Perth/16/2009 used during previous studies. To clarify the viral kinetics of the H3N2 A/Perth/16/2009 seen previously in the ferret model, six ferrets were infected with a low dose of $1x10^2$ PFU/ferret intranasally (**Table 3.5.2.1**). Ferrets were followed throughout the study until 8 days post infection where they were all culled. This allowed for samples to be collected from all ferrets throughout the study. This meant that vRNA and cellular immune responses were not able to be measured during this study. Ferrets were monitored for clinical signs and virus shedding, as well as sero-conversion as was done previously.

3.5.2 Ferrets

Ferrets (**Table 3.5.2.1**) were obtained from Highgate Farm, UK and were 10+ weeks at the time of the study. A total of 6 ferrets were used. All ferrets were culled at eight days post infection. Ferrets were group housed in floor pens designed in accordance with the

requirements of the United Kingdom Home Office Code of Practice for the Housing and Care of Animals Used on Scientific Procedures (1989).

Table 3.5.2.1 Ferret Identification Numbers

Ferrets	Dose
57277(m), 80693(f), 87677(f), 93202(m), 55702(m), 88448(m)	$1x10^2$ PFU/ferret

3.5.3 **Prior to Inoculation**

At one day prior to inoculation ferrets were fully sedated by an intramuscular injection of Ketamine/Xylazine (1ml Ketamine (100mg/ml) plus 0.4ml Xylazine (20mg/ml) given at a dose of 0.25ml/Kg bodyweight). Baseline blood samples were taken from the anterior vena-cava vessel of each ferret, 2ml blood collected into SST tubes for sera isolation and a baseline nasal wash was performed. Sera were tested by HAI for the presence of any pre-existing antibodies to influenza H3N2 A/Perth/16/2009. All baseline sera samples had HAI titres of less than 4 units to H3N2 A/Perth/16/2009, and it was deemed that these ferrets had no previous exposure to H3N2 and so were suitable for challenge.

3.5.4 **Virus**

Ferrets were fully sedated by an intramuscular injection of Ketamine/Xylazine (1ml Ketamine (100mg/ml) plus 0.4ml Xylazine (20mg/ml) given at a dose of 0.25ml/Kg bodyweight). Ferrets were inoculated intranasally with H3N2 A/Perth/16/2009 P+2A challenge stock virus diluted in

PBS to provide $1x10^2$ PFU/ferret. The dose was confirmed on day of administration by back-titration. Each animal was inoculated with a volume of 0.2ml by the intranasal route.

3.5.5 **Sample Collection**

Post inoculation, weight was recorded daily, and clinical signs recorded twice daily. Nasal washes were collected from 1 to 8 dpi. Ferrets were culled at 8 dpi. Ferrets were sedated by intramuscular injection of Ketamine/Xylazine (1ml Ketamine plus 0.4ml Xylazine) given at a dose of 0.25ml/Kg bodyweight. Following overdose samples were collected from each ferret; nasal wash and blood in SST for serum.

3.5.6 **Results**

3.5.6.1 *Nasal wash cell counts and titres*

Nasal wash cell counts began to increase (**Fig. 3.5.6.1a**) between two and three days post infection indicating that all six ferrets had successfully been infected. Counts remained high for all ferrets until they were culled at eight days post infection. The nasal washes were also assessed for replicating virus by plaque assay (**Fig. 3.5.6.1b**). Virus shedding began in nasal washes at one day post infection for all ferrets. The first peak was recorded at two days post infection for ferrets 80693 and 88448, and at three days post infection for ferrets 57277, 87677, 93202 and 55702. This was followed by a decrease in viral load for all ferrets before a second smaller peak at five days post infection for ferrets 80693 and 57277 and at six days post infection for 88448, 87677, 93202 and 55702. All ferrets had stopped shedding detectable

virus by eight days post infection. The peak shedding titre of the ferrets was found to have a strong positive correlation and significance (R +1.00, P 0.0028) with the total amount of virus shed from each ferret (area under the curve).

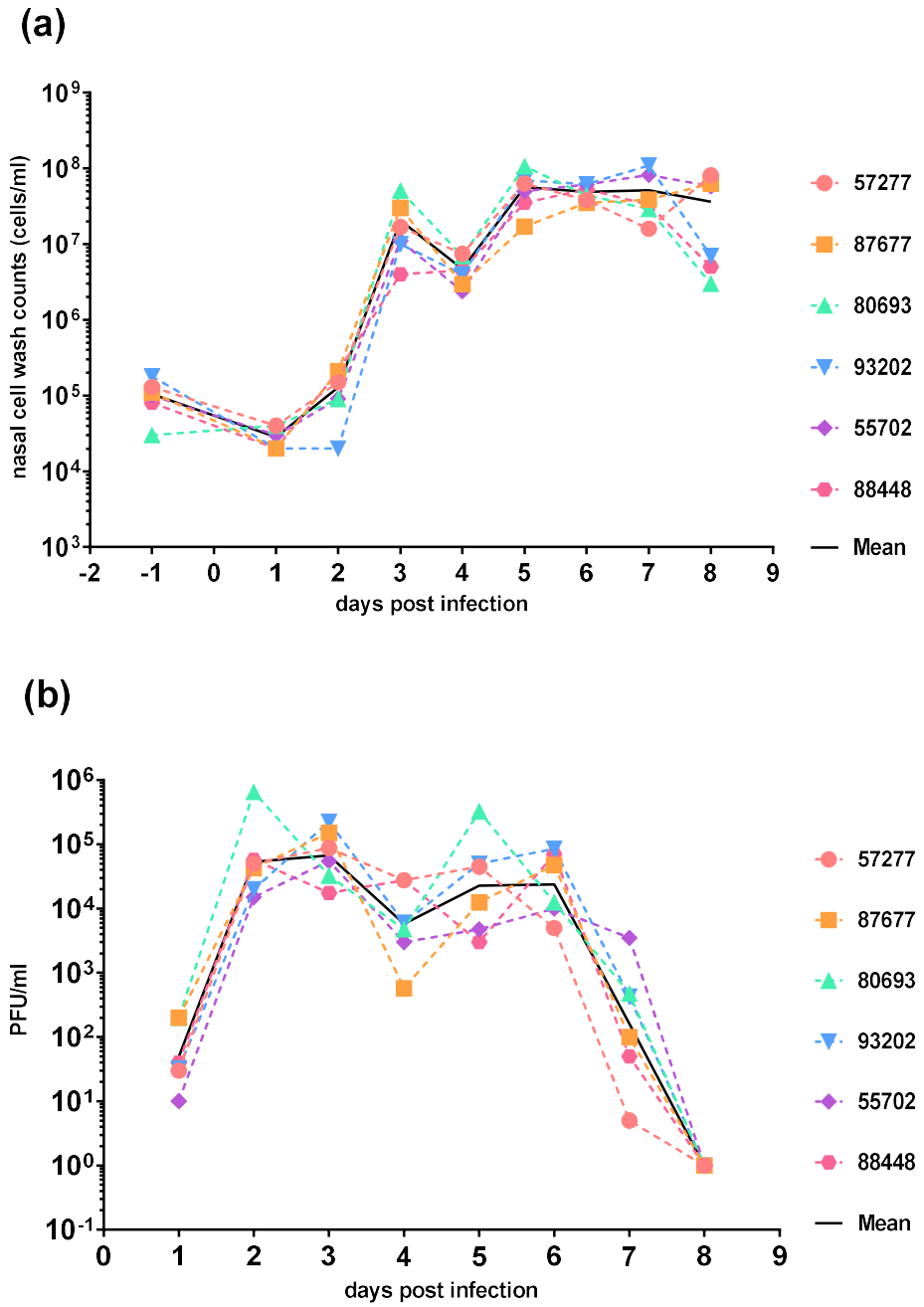

Figure 3.5.6.1 Nasal wash collection. Nasal washes were collected at +1 to +8 dpi. **(a)** All nasal washes were counted to ascertain the number of cells being shed from each individual timepoint (n=6). **(b)** Nasal washes were subsequently plaque assayed to ascertain the titre of virus being shed from each individual ferret (n =6) at these timepoints.

3.5.7 **Clinical signs of infection**

Weight was monitored daily throughout the study. Weight loss from baseline (**Fig 3.5.7.1**) was seen for four of the ferrets; 57277, 87677, 80693 and 93202. These four ferrets dropped below baseline between one and two days post infection, with their highest percentage loss recorded at two days post infection in each case. Following this all ferrets began to gain weight and their weight remained above baseline from four days post infection onwards. Ultimately all six ferrets had gained between 8 and 14% of weight from baseline during the study.

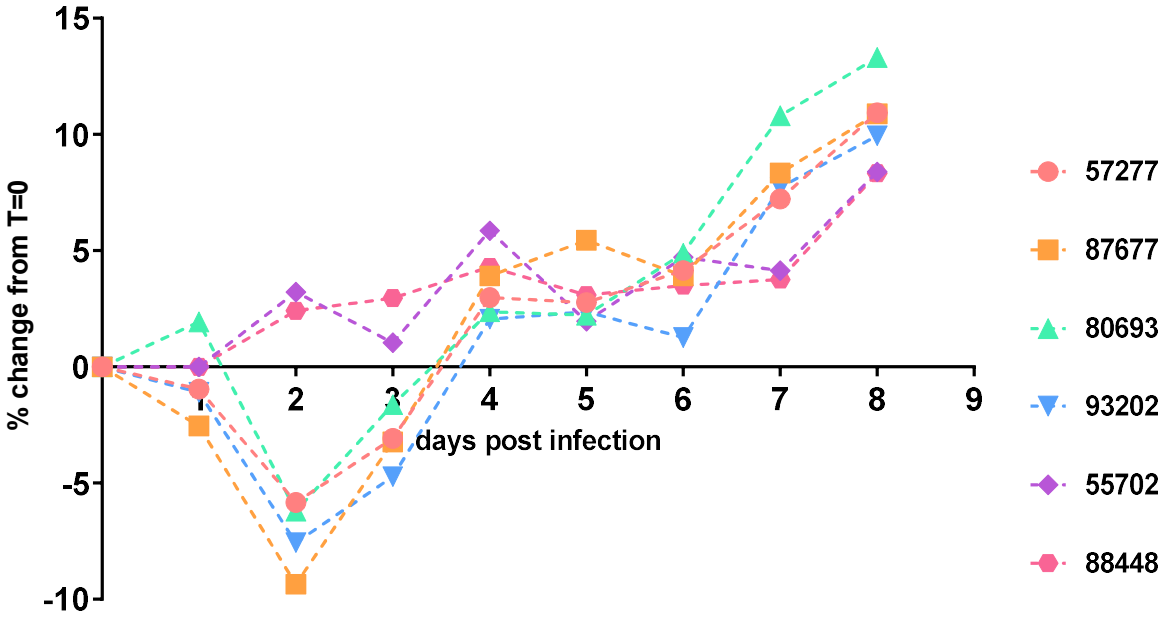

Figure 3.5.7.1 Weight percentage change from baseline. Percentage weight change from day of infection for all ferrets (n=6).

All ferrets were monitored for sneezing, nasal discharge, inactivity, diarrhoea and loss of appetite. The ferrets presented with sneezing and nasal discharge only. The cumulative incidences of sneezing and nasal discharge were recorded during the study (**Table 3.5.7.1**), with the number of incidences varying from 1 to 7. The day of onset also varied widely from day 3 to day 7. This shows that while clinical signs are helpful in determining whether a ferret may be infected, their severity and day of onset for this virus can vary greatly between ferrets and doesn't appears to correlate with virus shedding or nasal wash cell counts.

Table 3.5.7.1 Cumulative incidence of nasal discharge and sneezing.

Ferret	Incidence	Day of Onset
57277	6	4
80693	1	7
87677	4	5
93202	5	3
55702	7	4
88448	2	5

3.5.7.1 *Evidence of seroconversion*

Serum was collected at eight days post infection when the ferrets were culled. All ferrets showed seroconversion when they were assayed against A/Perth/16/2009 (HAI titres greater than 256). These results confirm, along with the nasal wash titres that all ferrets were successfully infected.

3.5.8 **Discussion**

This study was designed to identify the double peak that had been seen during study **5087** in the two ferrets culled at eight days post infection. The double peak was seen in all ferrets in this study. The double peak has been seen previously in this body of work (**Sections 3.3 and 3.4**) and in other published studies (Frise *et al.*, 2016, Dimmock *et al.*, 2012, Marriott *et al.*, 2014, Roberts *et al.*, 2012, Gooch *et al.*, 2019). The double peak could be due to the immune response in the ferrets, with a viral peak followed by an initial clearance of the virus from the nasal cavity by the innate immune response. This could be followed by a second wave of virus production in the nasal cavity ultimately concluding in total viral clearance.

3.6 Low Dose Model to Investigate Cellular Immune Response

This final study combines two groups of ferret studies, **5549** and **5719** (appendix 1), utilising key techniques identified in earlier studies and expanding on the investigation of the cellular immune response seen in the ferret model. A PBS group was included to compare the cellular immune responses seen in infected ferrets with mock ferrets.

3.6.1 *In vivo* Study Outline

Ferrets were inoculated intranasally with low dose of A/Perth/16/2009. Small volume sequential blood samples were taken through the study to assess the longitudinal influenza-specific IFN-γ response in the periphery circulating blood. Whole blood and lung were taken at study termination to assess influenza-specific IFN-γ responses in specific tissues.

3.6.2 Ferrets

Female ferrets (**Table 3.6.2.1**) were obtained from Highgate Farm, UK and were 4-6 months at the time of the study. A total of 12 ferrets were used. All ferrets were culled at 14 days post infection. Ferrets were group housed in floor pens designed in accordance with the requirements of the United Kingdom Home Office Code of Practice for the Housing and Care of Animals Used on Scientific Procedures (1989).

Table 3.6.2.1 Ferret Identification Numbers

H3N2 Low Dose (5719)	Mock (5549)
86654, 86811, 86809, 86659, 86812, 86660	**55432, 45891, 53132, 49686, 52094, 45627**

3.6.3 **Prior to Inoculation**

At seven and three days prior to inoculation ferrets were fully sedated by an intramuscular injection of Ketamine/Xylazine (1ml Ketamine (100mg/ml) plus 0.4ml Xylazine (20mg/ml) given at a dose of 0.25ml/Kg bodyweight). At -7 dpi whole blood samples were collected from all ferrets. At -3 dpi whole blood samples were collected from all ferrets. These two whole blood samples were used to calculated baseline values for the IFN-γ ELISA. Additional baseline blood samples were taken at -3 dpi from the anterior vena-cava vessel of each ferret, 2ml blood collected into SST tubes for sera isolation and a baseline nasal wash was performed. Sera were tested by HAI for the presence of any pre-existing antibodies to influenza H3N2 A/Perth/16/2009. All baseline sera samples had titres of less than 4 HAI units to H3N2 A/Perth/16/2009, and it was deemed that these ferrets had no previous exposure to H3N2 and so were suitable for challenge.

3.6.4 **Virus**

Ferrets were fully sedated by an intramuscular injection of Ketamine/Xylazine (1ml Ketamine (100mg/ml) plus 0.4ml Xylazine (20mg/ml) given at a dose of 0.25ml/Kg bodyweight). Ferrets were inoculated intranasally with H3N2 A/Perth/16/2009 P+2A challenge stock virus diluted in

PBS to provide 100 PFU/ferret. The dose was confirmed on day of administration by back-titration. Each animal was inoculated with a volume of 0.2ml by the intranasal route. Mock ferrets were intranasally inoculated with 0.2ml of PBS.

3.6.5 **Sample Collection**

Post inoculation, weight was recorded daily, and clinical signs recorded twice daily. Temperatures were not recorded. Nasal washes were collected from 1 to 8 days post infection. Whole blood samples were collected from all ferrets at 2, 5, 8 11 and 14 days post infection. Ferrets were sedated by intramuscular injection of Ketamine/Xylazine (1ml Ketamine plus 0.4ml Xylazine) given at a dose of 0.25ml/Kg bodyweight. Following overdose, samples were collected from each ferret; nasal wash, blood in SST for serum and blood into heparin tubes for PBMCs. Lungs were collected into RPMI 1640 media.

3.6.6 **Results**

3.6.6.1 *Nasal wash cell counts and titres*

Nasal wash counts were performed on all nasal washes (**Fig 3.6.6.1.1**). Counts for ferrets infected with A/Perth16/2009 began to increase between two to three days post infection indicating successful infection. Nasal washes from ferrets inoculated with PBS remained at a baseline level throughout the study.

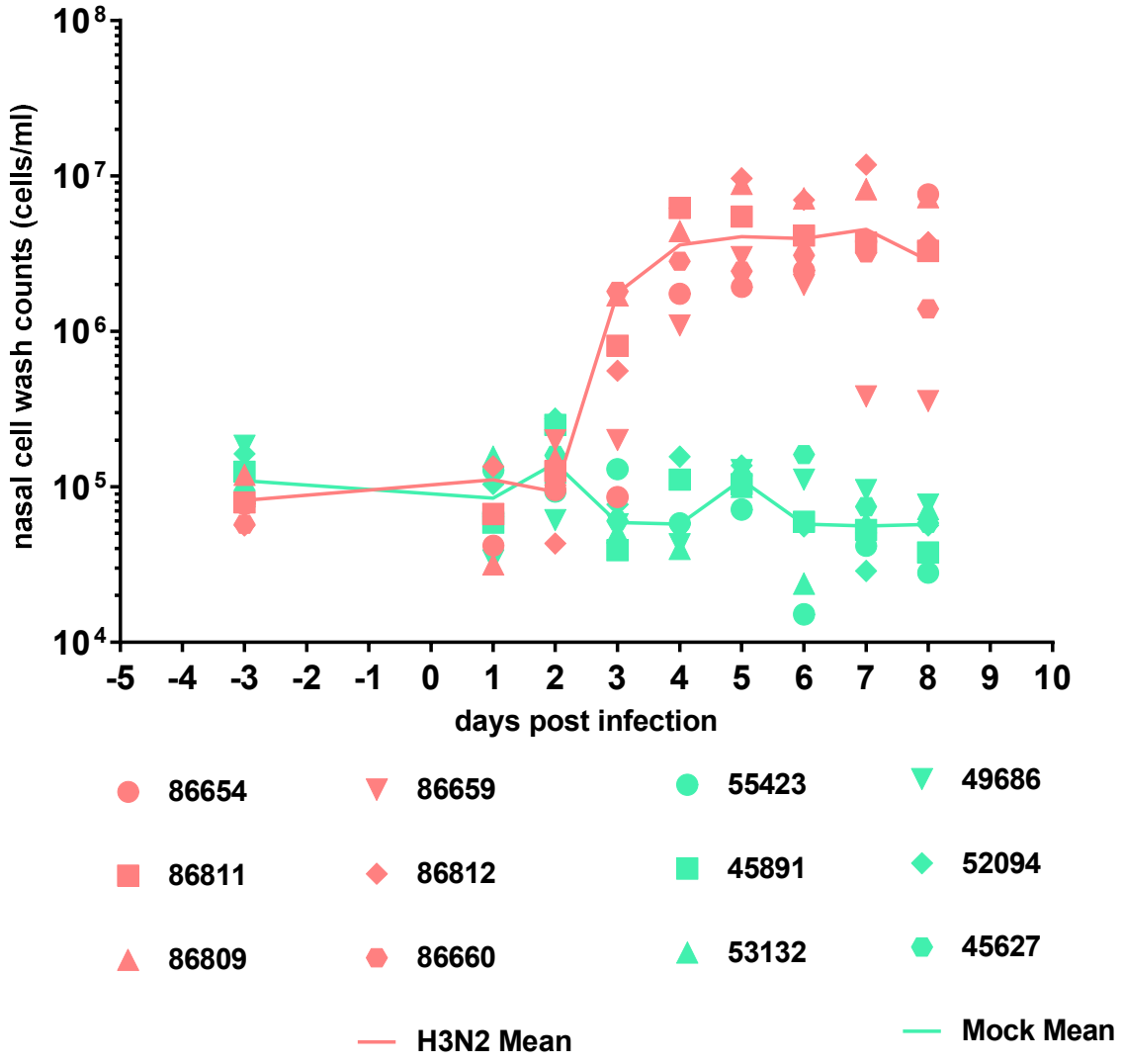

Figure 3.6.6.1.1 Nasal wash cell counts. Nasal washes were collected at +1 to +8 dpi. All nasal washes were counted to ascertain the number of cells being shed from each individual ferret at each time point (n=12). The area under the curve (AUC) was calculated for both the H3N2 (n=6) and mock group (n=6). The area under the curve represents the total amount of virus shed by the ferrets over the timecourse. A Mann-Whitney test was performed and a statistical difference (P=0.022) was found between ferrets intranasally inoculatedwith A/Perth/16/2009 (H3N2 group) and PBS (mock group).

As carried out previously, the nasal washes were tested for the presence of replicating virus by plaque assay (**Fig 3.6.6.1.2**). 4 out of 6 ferrets inoculated with H3N2 began to shed detectable virus at 1 dpi. The remaining two ferrets, 86654 and 86660, began to shed

detectable virus at 2 dpi. Viral shedding peaked at 3 dpi, this was followed by a decrease in virus load and a subsequent smaller, second peak that has been seen previously. The smaller second peak was not found to be statistically significant but this has been noted by others previously (Roberts *et al.*, 2012, Gooch *et al.*, 2019, Marriott *et al.*, 2014, Dimmock *et al.*, 2012). As seen previously the smaller second peak cannot be identified in the nasal wash cell count. Again, as seen previously the peak shedding titre was found to have a strong positive correlation (Spearman) and significance (R +0.9429, P 0.0167) with the total virus shed. Plaque assays for the mock group were carried out. As anticipated no virus was being shed from these animals and therefore the data was not included in **Figure 3.6.6.1.2**.

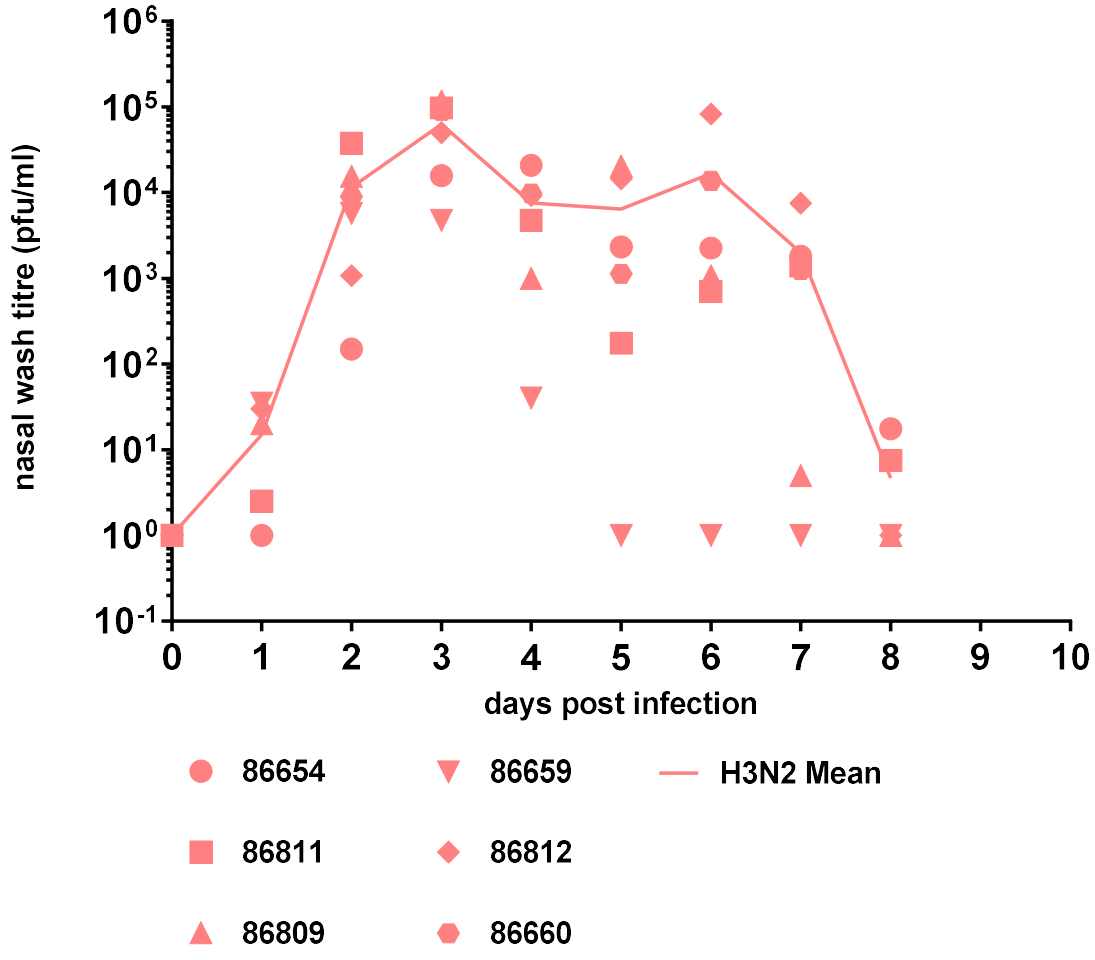

Figure 3.6.6.1.2 Nasal wash titres. Nasal washes were subsequently plaque assayed to ascertain the amount of virus being shed from each individual ferret at all time points collected.

3.6.6.2 *Clinical signs of nasal infection*

Disease progression was monitored up to 14 days post infection (**Table 3.6.6.2.1**). The mock group showed no clinical signs of infection.

Table 3.6.6.2.1 Cumulative incidence of nasal discharge,sneezing and inactivity

Group	Total Nasal Discharge	Total Sneezing	Inactivity
H3N2	0	24	0
Naïve	0	0	0

3.6.6.3 *Evidence of seroconversion in ferrets*

HAI assays were performed on the terminal bleeds of all ferrets. All ferrets inoculated with virus gave titres of ≥512 confirming all ferrets were successfully infected and had seroconverted. Ferrets in the mock group inoculated with PBS had titres <4, confirming they were not infected.

3.6.6.4 *Longitudinal time course of influenza-specific IFN-γ responses in the periphery*

Small volumes of heparinised whole blood were collected at the days shown in **Figure 3.6.6.1.1** to assess the influenza-specific IFN-γ responses in peripheral blood. This was

carried out as described in Materials and Methods (**Section 2.4.10**) using homologous virus. Samples from each ferret were assessed by ELISA and a longitudinal time course was created. Two samples were collected seven and one day's pre-infection. This was to demonstrate that there were low influenza-specific IFN-γ responses in the ferrets prior to infection. If the influenza-specific IFN-γ responses were found to be high the ferrets may have been exposed to influenza previously. All ferrets were found to have responses below 270 pg/ml of IFN-γ in pre-infection samples. These responses were averaged and represent the 0 time point. Following infection with A/Perth/16/2009 low level influenza-specific IFN-γ responses were detected in ferrets from five days post infection and increased at eight to 11 days post infection, peaking between 11 and 14 days post infection. At 14 days post infection some of the responses peak while other begin to decrease, this variation could be due to the outbred nature of ferrets. Ferrets in the mock group inoculated with PBS had responses below 270 pg/ml over the 14 days.

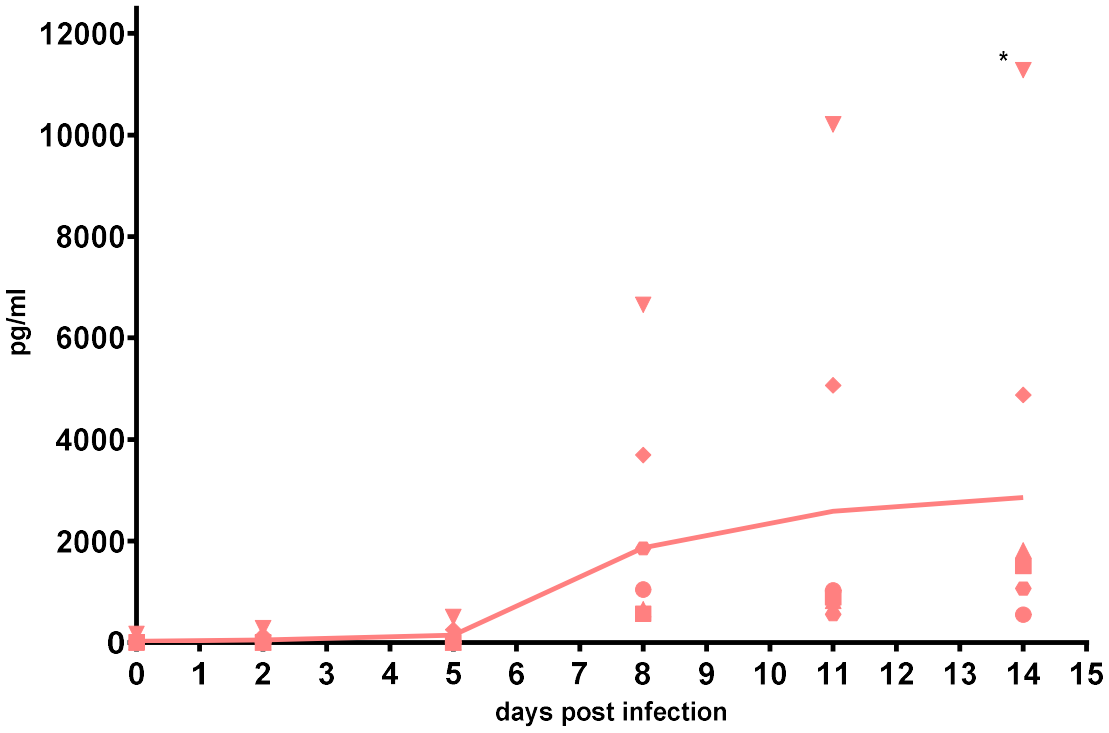

* 12000.00 pg/ml limit of detection for ELISA

Figure 3.6.6.4.1 Quantification of influenza-specific IFN-γ production by ELISA Diluted whole blood samples were collected from all ferrets at -7, -1, 2, 5, 8, 11, and 14 days post infection, stimulated with appropriate antigens (whole virus) and the supernatants harvested. Supernatants were used in the Ferret IFN-γ ELISA Development Kit (ALP). Influenza-specific IFN-γ responses became detectable at 5 days post infection with a peak at 11-14 days post infection for all virus infected animals. No responses were detected in the mock group.

3.6.6.5 *Cellular immune responses measured by ferret specific IFN-γ enzyme linked immunospot assay (ELISpot)*

Animals were culled at 14 days post infection, lymphocytes isolated from whole lung (lung MNCs, **Section 2.4.5**) and whole blood (PBMCs, **Section 2.4.2**) and the frequency of the IFN-γ secreting cells were quantified by ferret-specific IFN-γ ELISpot (**Fig. 3.6.6.5.1**). Virus infected ferrets showed a significant (P 0.0022) increase in the number of influenza-specific IFN-γ secreting PBMCs when compared to mock infected ferrets at 14 days post infection (**Fig. 3.6.6.5.1a**). A very low influenza-specific IFN-γ response was detected in the PBMCs of one of the mock ferrets, none of the remaining PBMCs of the mock ferrets had any detectable influenza-specific IFN-γ responses. No influenza-specific IFN-γ responses were seen in the lung MNCs of mock ferrets or the majority of those infected with virus. Only one ferret, 86659, had a recorded influenza-specific IFN-γ response in lung MNCs. This suggests that the virus did not travel to the lungs of all the ferrets. This is in line with previous observations seen in the serial cull study (**Section 3.4**) where there was a low amount of viral RNA found in the lung suggesting that A/Perth/16/2009 is not lung trophic in the ferret model.

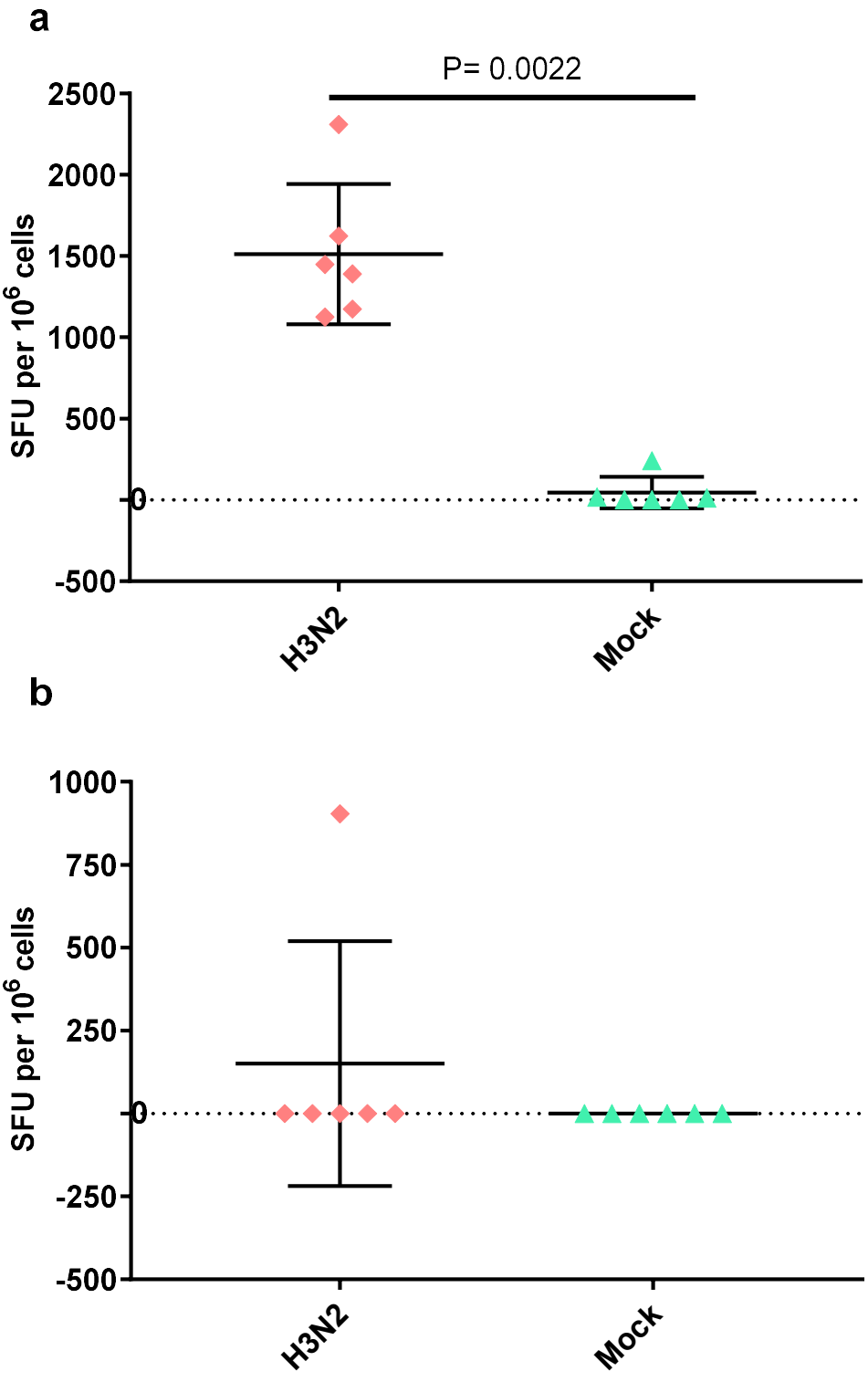

Figure 3.6.6.5.1 Cellular immune responses in ferrets infected with A/Perth/16/2009 PBMCs **(a)** and Lung MNCs **(b)** were collected from all animals (n=12) at 14 dpi. Results were normalised by subtracting the individual sample allantoic fluid control values from virus stimulated sample values

3.6.7 **Discussion**

This study demonstrates it is possible to successfully evaluate cellular immune responses to seasonal influenza infection over a time-course in the ferret. By sequentially taking low volumes of heparinised blood samples from individual animals and detecting influenza-specific IFN-γ as measured by ELISA, a pictureof what occurs in the periphery throughout infection was formed. Furthermore, when the animals were sacrificed, influenza-specific IFN-γ secreting cells in tissues of interest were quantified. Using these complementary techniques, it has been demonstrated that the response to a low dose H3N2 infection in the lung is minimal, and which complements data that was gathered earlier in the chapter with regards to lung pathology and vRNA present in the lower respiratory tract. These results help to enhance the applicability of the ferret model to study acquired immunity and vaccination strategies to influenza.

Ferret 86659 was found to have high influenza-specific IFN-γ response in lung MNCs and in peripheral circulating blood. Although ferrets are outbred and therefore some variation would be expected, these results were particularly unusual when compared to the other five ferrets infected with low dose H3N2.

3.7 Conclusions

These combined studies have shown that a reproducible and reliable low dose intranasal model for H3N2 A/Perth/16/2009 has been successfully set up.

- The high and low dose intranasal inoculations were evaluated and compared in **Section 3.3**. This study highlighted the differences in pathogenesis between the doses, as well as confirming that ferrets could be successfully infected with a low dose of H3N2 A/Perth/16/2009.
- Viral kinetics and pathogenesis seen in ferrets inoculated intranasally with low dose H3N2 A/Perth/16/2009 has been shown to be reproducible across studies conducted at different timepoints. All ferrets were successfully infected.
- The cellular immune response to a low dose intranasal infection was investigated in **Section 3.6**. An understanding of the longitudinal influenza-specific IFN-γ response in the periphery was established. In addition, the influenza-specific IFN-γ responses in two key samples, circulating blood and the lungs, were established.

This low dose intranasal model can now be used to compare to the nose-only aerosol model and droplet transmission cage models which are discussed in the next two chapters.

4 Nose-only Aerosol Infection Model

4.1 Introduction

The intranasal droplet route is the most frequently used route of experimental infection when delivering influenza virus to the ferret model. As previously demonstrated, this allows for a controlled titre of virus to be delivered to the nasal cavity of the animal, ensuring successful infection even at lower titres of virus. It can be argued that this method of infection does not accurately reflect a "natural" influenza virus infection in humans; therefore, it is necessary to explore alternative models of infection. Transmission of influenza between individuals occurs via contact (fomite/direct) and non-contact (droplet) routes:

i. Contact transmission; fomites
ii. Large droplet transmission; particles ≥5μm
iii. Droplet nuclei transmission; particles <5μm (Gustin *et al.*, 2011)

The individual contribution of these modes of transmission to the spread of influenza in the population is dynamic and still not well understood, and although infection via the aerosol route has been shown to cause influenza virus infection in both humans and ferrets, the relative importance of contact and airborne transmission remains unknown in both (Bouvier, 2015). Studies of influenza infected patients found low viral titres in the aerosol generated by sneezing, coughing and breathing (Milton *et al.*, 2013). Similar results have been recorded in ferrets, where animals have been successfully infected with less than 10 PFU (Gustin *et al.*, 2015). Following visits to live bird markets it was shown that even though no direct contact was made with poultry, cases of human H7N9 infection have been recorded. Suggesting that inhalation of aerosols containing the virus was the primary mode of infection in these cases

(Li *et al.*, 2014, Liu *et al.*, 2014). Additionally, detection of H7N9 in the air sampled from live poultry markets (Zhou *et al.*, 2016) suggests that there is a possibility that zoonotic infection can also occur with a low level of aerosolised virus (Creager *et al.*, 2017). Past studies that have used human volunteers have shown a role for aerosols in influenza virus transmission (Milton *et al.*, 2013, Lindsley *et al.*, 2010).

Airborne transmission of influenza can be considered as two types. Droplet spray transmission is when an infected individual coughs or sneezes, expelling respiratory droplets that contain contagious viral particles, impacting directly upon the nasal mucosa of a susceptible person. Aerosol (droplet nuclei) transmission occurs when an infected individual exhales virus laden respiratory droplets, coughs and sneezes (Tellier, 2006a). Aerosols are suspensions in air (or a gas) of liquid or solid particles minute enough that they remain airborne for a period of time due to their low settling velocity (Tellier, 2009), and influenza laden respiratory droplets have been found to remain suspended in air for several hours. Particles of between 5μm and 10μm are able to reach the trachea and particles of ≤5μm have the capability to infiltrate the respiratory tract all the way down to the alveolar region (Tellier, 2006b) causing infection.

In the past, aerosol infection of ferrets has been achieved in two ways; exposure to infected donors (Herfst *et al.*, 2012, van der Vries *et al.*, 2011) and exposure to a nose-only aerosol system (Tuttle *et al.*, 2010a, Lednicky *et al.*, 2010, Gustin *et al.*, 2011) which allows for a calculated and precise dose of virus inoculum to be delivered. It has previously been reported that ferrets exposed to aerosolised H3N2 (A/Panama/2007/99) were infected with approximately 1 $TCID_{50}$ (Gustin *et al.*, 2011). The generation of small particle aerosols with specialised equipment allows the virus to reach the lungs of the animals, whereas intranasal infection, depending on the volume of the dose (Belser *et al.*, 2016) might not enable the virus

to successfully reach the lower respiratory tract. The following *in vitro* and *in vivo* studies provided the opportunity to examine the impact of delivery H3N2 A/Perth/16/2009 to the lungs of ferrets.

4.2 Aims of the Studies

A small number of studies have been published looking at the mechanical aerosolisation of influenza into ferrets (MacInnes *et al.*, 2011, Lednicky *et al.*, 2010, Turgeon *et al.*, 2019, Gustin *et al.*, 2013, Gustin *et al.*, 2011). Thus far no studies have examined and explored the effect of an aerosol H3N2 subtype of IAV infection upon the cellular immune response of the ferret. This study hopes to:

- establish an effective and robust low dose method of nose-only aerosol challenge in ferrets
- evaluate the viral kinetics and the cellular immune responses of ferrets infected via the aerosol route
- successfully deliver H3N2 A/Perth/16/2009 to the lungs of the ferret
- compare and contrast these results to animals infected via the intranasal route as well as a naïve group

4.3 *In vitro* Studies

The nose-only aerosol model was utilised to provide a more accurate experimental representation of natural influenza infection than intranasal inoculation; that could be controlled within defined working constraints, such as exposure time, humidity and presented dose. The nose-only aerosol model acts as a particle delivery system which can deliver droplet nuclei particles to the upper and lower respiratory tract of ferrets. Prior to animal work taking place, an *in vitro* study was carried out to ensure a reproducible spray factor and presented dose could be achieved, identifying the lowest dose that can reliably infect all animals. The spray factor is calculated by dividing the viable aerosol concentration by the inoculum concentration; this is important to help determine the presented dose given to each animal.

The following factors are considered important when considering exposure dose:

- Respiratory function of the ferret at time of exposure
- Aerosol concentration in the test atmosphere
- Duration of exposure
- Deposition and retention of aerosol once inhaled

Inhalation exposures involving biologically active materials, such as influenza virus, pose several specialised considerations on top of this (Hartings and Roy, 2004).

Known concentrations of A/Perth16/2009 P+2A were aerosolised using a mobile form of the Henderson apparatus (**Fig. 4.3.1**) in conjunction with Biaera Technologies Aerosol

Management Platform (Hartings and Roy, 2004). This was carried out to assess the *in vitro* characteristics of A/Perth/16/2009 prior to use in the *in vivo* challenge studies. Aerosol generation and sampling was performed in a flexible film isolator to provide primary containment against operator exposure to the aerosolised virus inoculum.

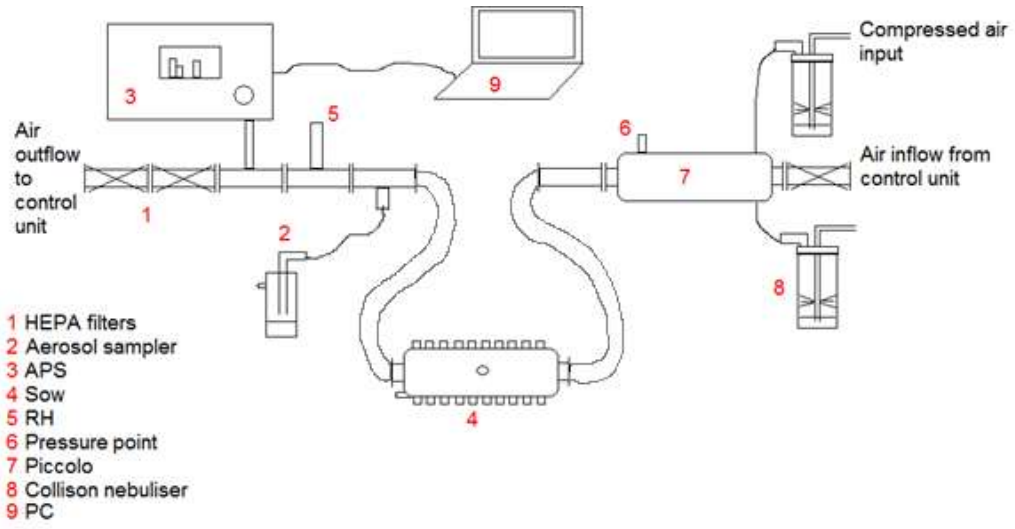

Figure 4.3.1 Mock ferret aerosol exposure system set up Small particle aerosols, which are predominantly <2µm Mass Median Aerodynamic Diameter (MMAD), were produced using a Collison six-jet nebulizer (**8**) (May, 1973) operating at 15L/min for 10 minutes. The MMAD defines the size at which 50% of the particles by mass are larger and 50% of the particles are smaller. The concentration of A/Perth/16/2009 in the aerosol was determined by collecting samples directly from the exposure system (**4**) (post sow) using a glass impinger (**2**) (AGI30 AceGlass Inc.) operating at 6 L/min for 10 minutes and containing 20ml DMEM. MMAD was measured using an aerodynamic particle sizer (**3**) (TSI Instruments). The aerosol stream was conditioned and maintained at room temperature and a relative humidity of 65 ± 5%.

Virus was provided in three 20ml nebuliser aliquots at a titre of $1.1x10^6$ pfu/ml diluted in Dulbecco's Modified Eagle Medium (DMEM). This titre was confirmed by back titration. Each aliquot corresponded to the spray runs as follows:

Nebuliser 1 = Spray 1, 2 & 3

Nebuliser 2 = Spray 4, 5 & 6

Nebuliser 3 = Spray 7, 8, 9 & 10

Following aerosolisation the remaining liquid from each nebuliser sample was collected and plaque assayed for live viral titre. The live viral titres of the nebuliser samples are shown in **Table 4.3.1**. The remainder of each sample was frozen for further analysis if required. There appears to be have been roughly five-fold knock down from the amount of virus put into the nebuliser compared to the amount of virus recovered from the nebuliser. This could be due to the violent nature in which the aerosol is generated. Compressed air is passed through a six-jet nebuliser to aerosolise the virus in DMEM. Influenza is an enveloped virus and is relatively vulnerable to damaging environmental impacts (Arbeitskreis Blut, 2009). Therefore this process could conceivably damage the envelope of the virus, preventing its ability to enter host cells.

During aerosolisation each spray run was collected into 20ml of DMEM in the impinger. Samples from the impingers of the ten aerosol runs were then immediately plaque assayed for live viral titre, the results are shown in **Table 4.3.1**. Impinger samples were plaque assayed immediately to prevent loss of virus titre from the process of freeze thawing. The remainder of each sample was frozen for further analysis if required. A target flow rate of 6 lites per minute was set, however, as is shown in **Table 4.3.1** the flow rate can vary during the spray.

Table 4.3.1 Viral titres in spray samples

Nebuliser	1			2			3			
C_{neb} (pfu/ml)	1.23E+05			2.25E+05			2.75E+05			
Spray	**1**	**2**	**3**	**4**	**5**	**6**	**7**	**8**	**9**	**10**
Impinger Titre (pfu/ml)	2.50E+03	3.25E+03	2.25E+03	3.75E+03	5.25E+03	3.25E+03	3.25E+03	1.33E+03	3.75E+03	4.00E+03
Sample Volume (ml)	20	20	20	20	20	20	20	20	20	20
Sample Flow (L/min)	5.9	5.9	5.7	5.5	5.8	4.8	5.2	5	4.9	4.9
C_{aero} (pfu/ml)	8.5E-01	1.1E+00	7.9E-01	1.4E+00	1.8E+00	1.4E+00	1.3E+00	5.3E-01	1.5E+00	1.6E+00
Spray Factor	6.9E-06	8.9E-06	6.4E-06	6.2E-06	8.0E-06	6.2E-06	4.7E-06	1.9E-06	5.5E-06	5.8E-06
									Mean C_{aero}	**1.2E+00**
									Mean Spray Factor	**6.1E-06**

As well as the live viral titres from the impinger, **Table 4.3.1** lists the aerosol concentration (C_{aero}) and spray factors of each 'spray run'. A mean spray factor of $6.1x10^{-6}$ was calculated.. The spray factor is a measurement of of the efficiency of aerosolising the virus from the starting solution. A figure of 10^{-5} to 10^{-6} is normally expected. The presented dose represents the potential amount of virus inhaled by the ferret, therefore giving an approximate titre of virus with which the ferrets are exposed to.

Presented Dose = (1.2)*(3730) = 4476 PFU

This *in vitro* spray illustrates that A/Perth/16/2009 was able to be aerosolised through the Henderson apparatus successfully. Recovery of live virus from the impingers indicates that when ferrets are introduced into the system they will be successfully inoculated with a reliable dose of virus.

4.4 *In vivo* Study Outline

The results discussed here are from study **5530,** where an aerosol infected group was compared alongside high dose and low dose intranasal infected groups and a mock (intranasal PBS) group. *In vivo* work was carried out on 12 female ferrets aged 4-6 months from Highgate Farm.

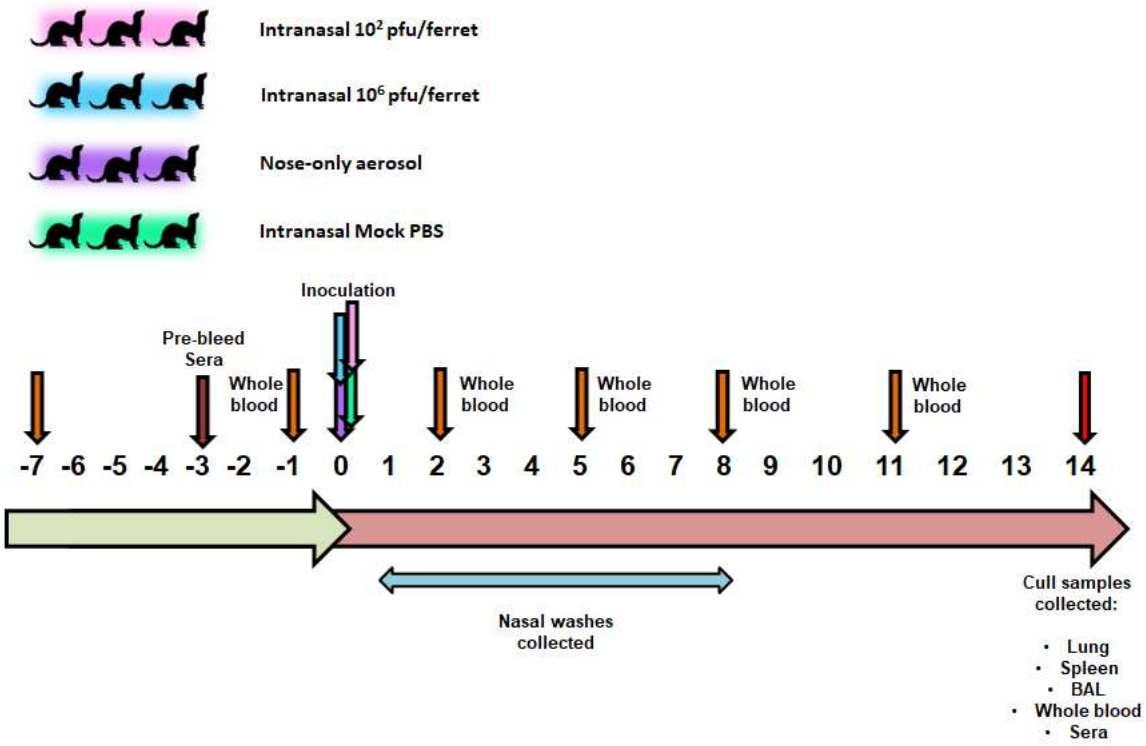

Figure 4.4.2 Study timeline Whole blood for IFNγ ELISA andimmune phenotypingwas taken at -7, -1, +2, +5, +8, +11 and +14 dpi. Baseline bleeds for serum were taken from all ferrets at -3 dpi. At 0 dpi donor ferrets were sedated and challenged via intranasal (I.N) (**4.4.4**) or aerosol (**4.4.3**) and placed into group floor pens. Nasal washes were collected in PBS from +1 dpi to +8 dpi. At cull (+14 dpi) lung,

spleen, bronchiolar lavage (BAL) and whole blood (PBMCs) were taken for the evaluation of the cellular immune response. Blood for serum was also taken to evaluate the humoral immune response.

4.4.1 **Ferrets**

Female ferrets (**Table 4.4.1.1**) were obtained from Highgate Farm, UK and were 4-6 months at the time of the study. A total of 12 ferrets were used. All ferrets were culled at 14 dpi. Ferrets were group housed in floor pens designed in accordance with the requirements of the United Kingdom Home Office Code of Practice for the Housing and Care of Animals Used on Scientific Procedures (1989).

Table 4.4.1.1 Ferret Identification Numbers

Aerosol	Low Dose	High Dose	Mock
40761, 47791, 49800	**53177, 51352, 46171**	**50706, 46313, 46392**	**46476, 48186, 41787**

4.4.2 **Prior to Challenge**

At seven and one days prior to inoculation ferrets were fully sedated by an intramuscular injection of Ketamine/Xylazine (1ml Ketamine (100mg/ml) plus 0.4ml Xylazine (20mg/ml) given at a dose of 0.25ml/Kg bodyweight). Baseline whole blood samples were taken from the anterior vena-cava vessel of each ferret into heparin microtainers using syringes pre-treated with heparin. These whole blood samples were used to ascertain baseline data for whole blood immune phenotyping and IFN-γ ELISA. At three days prior to challenge ferrets were anaesthetised as previously described. The baseline blood samples were taken from the

anterior vena-cava vessel of each ferret, 500 µl blood collected into SST tubes for sera preparation and a baseline nasal wash was performed. Sera were tested by HAI for the presence of any pre-existing antibodies to influenza H3N2 A/Perth/16/2009. All baseline sera samples had HAI titres of less than 4 to H3N2 A/Perth/16/2009, and it was deemed that these ferrets had no previous exposure to H3N2 and so were suitable for challenge.

4.4.3 **Nose-only aerosol infection of ferrets**

On the day of challenge ferrets were fully sedated by an intramuscular injection of Ketamine/Xylazine (1ml Ketamine (100mg/ml) plus 0.4ml Xylazine (20mg/ml) given at a dose of 0.25ml/Kg bodyweight). Ferrets received a presented aerosol dose of H3N2 A/Perth/16/2009 (approximately $3x10^2$ PFU/ferret) using the Collison nebuliser and Henderson apparatus. The stock A/Perth/16/2009 P+2A was provided at a concentration of $1.1x10^7$ pfu/ml diluted to a concentration of $3x10^4$ pfu/ml in serum free DMEM + GlutaMAX™. 10ml of challenge material was aerosolised over a five-minute exposure time. A reduced exposure time of five minutes was implemented for ethical reasons due to the introduction of live animals into the system. Ferrets were removed and placed back into their housing. Ferrets were group housed in floor pens designed in accordance with the requirements of the United Kingdom Home Office Code of Practice for the Housing and Care of Animals Used on Scientific Procedures (1989).

4.4.4 **Intranasal infection of ferrets**

Ferrets were fully sedated by an intramuscular injection of Ketamine/Xylazine (1ml Ketamine (100mg/ml) plus 0.4ml Xylazine (20mg/ml) given at a dose of 0.25ml/Kg bodyweight). Ferrets

were inoculated intranasally with H3N2 A/Perth/16/2009 P+2A challenge stock virus diluted in PBS to provide $1x10^2$ PFU/ferret for the low dose group and $1x10^6$ PFU/ferret for the high dose group. The mock group was also sedated as above and were given sterile PBS. The dose was confirmed on day of administration by back-titration. Each animal was inoculated with a volume of 0.2ml by the intranasal route.

4.4.5 **Sample collection**

Following challenge, weight was recorded daily, and clinical signs recorded twice daily. From one to eight days post challenge nasal washes were collected from animals. At days two, five, eight and eleven whole blood samples were taken from the anterior vena-cava vessel of each ferret into heparin microtainers using syringes pre-treated with heparin. At day 14 ferrets were culled. Ferrets were sedated by intramuscular injection of Ketamine/Xylazine (1ml Ketamine plus 0.4ml Xylazine) given at a dose of 0.25ml/Kg bodyweight. Prior to overdose, 500 µl of whole blood was taken from the anterior vena-cava vessel of each ferret into heparin microtainers using syringes pre-treated with heparin. Following overdose, the following samples were collected from each ferret; nasal wash, blood in SST for serum, remaining whole blood in heparin for PBMC isolation, spleen, BAL and whole lung. Immune cells were immediately isolated from whole blood, spleen, BAL and whole lung.

4.4.6 **Results**

4.4.6.1 *Back titration of aerosol spray*

Virus diluent was prepared on the day of the spray; a stock volume of virus was prepared at a titre of $3x10^4$ PFU/ml which should have given an approximate presented dose of around $3x10^2$ PFU to each ferret. Following preparation, the stock was plaque assayed on the same day and the titre was recorded as $1.74x10^4$ PFU/ml. Therefore, it was anticipated, based on previous calculations, that there would be an presented dose of around 200 PFU. However, the impinger titre was 2.5 PFU/ml, which equates to a presented dose of 0.8 PFU, 250-fold lower than expected.

4.4.7 **Nasal wash cell counts and titres in ferrets following infection**

Nasal wash cell counts for animals in the high and low dose intranasal and aerosol groups increased during the study indicating that all animals had become infected (**Fig. 4.4.7.1a**). The nasal wash cell counts for the mock group remained at baseline levels, as expected. As seen in a previous study (**Section 3.3**) the high dose intranasally infected animals had raised nasal cell wash counts and began to shed virus prior to the low dose intranasally infected group. The nasal wash cell counts for both the aerosol and low dose groups began to increase after 2 dpi rising above the mock group baseline. The nasal wash cell counts (**Fig. 4.4.7.1a**) for the low dose group began to decline at 8 dpi and appeared to plateau just above baseline until 14 dpi. The nasal wash cell counts for the aerosol group remained above baseline until 14 dpi. All ferrets in the low dose group became infected at the same time and this is apparent in the nasal wash cell counts and the amount of virus shed of the course of the study. The low dose results are in line with what has previously been seen in this work and in other published low dose work (Marriott *et al.*, 2014, Ryan *et al.*, 2018, Gooch *et al.*, 2019).

In comparison the aerosol group had an extended high nasal wash cell counts, coupled with a variable amount of virus shed from each ferret within the group. Nasal cell shedding for the aerosol group was anticipated to be in line with the low dose intranasal group, however, as the results were collected it became apparent that two of the animals, 49800 and 40761, were not following the predicted viral kinetics. Animal 47791 nasal wash counts began to increase at 3 dpi with a definite peak seen at 4 dpi. A delay in the increase of cells in 49800 and 40761 in the nasal wash was seen, with counts only increasing at 5 dpi for animal 49800 and at 6 dpi for animal 40761.

All infected ferrets began to shed detectable virus titres in their nasal wash (**Fig. 4.4.7.1a**). Ferrets inoculated intranasally with a high dose began shedding at one day post infection, where they peaked, with a lower, second peak titre at 5 dpi. Viral titres were no longer detected beyond 6 dpi in the high dose group. Peak viral titres were seen in the low dose group at 3 dpi. A delay in virus shedding was seen in the aerosol group when compared to the two intranasal groups. It was expected that the aerosol group ferrets would begin to shed virus at roughly the same time point as ferrets infected intranasally with a low dose of virus. Ferret 47791 began to shed detectable virus at two days post infection, in line with this theory, however ferrets 49800 and 40761 began to shed virus at five and six days post infection respectively.

Unfortunately, it's difficult to compare the aerosol group directly with the low dose group as only ferret 47791 is thought to have been truly infected via the aerosol route. The remaining two ferrets in the aerosol group, 49800 and 40761, most likely became infected by either contact or non—contact transmission from ferret 47791 when it began to shed live virus at 2 dpi. Ferret 47791 had a peak in shedding at 4 dpi while in comparison the low dose ferret peaked at 2 dpi (51352) or 3 dpi (53177, 46171). All the low dose ferrets experienced a

‘second peak’ in nasal wash titre, at 7 dpi (51352) or 6 dpi (53177, 46171), which has been identified in low dose infected ferrets previously. Ferret 47791 also appeared to have a second peak at 8 dpi, however as no nasal washes were taken beyond this point until sacrifice at day 14 this cannot be proven. Generally, it appears as through viral kinetics observed in an aerosol infected animal are like those in a low dose ($1x10^2$ PFU) infected ferret, however there is a time delay from the day of infection, possibly due to the lower presented dose of 3.2 PFU. Ferrets 49800 and 40761 both had delayed viral kinetics compared to the low dose group, however it is difficult to compare the two directly as the route and time point at which these two ferrets became infected is impossible to clarify.

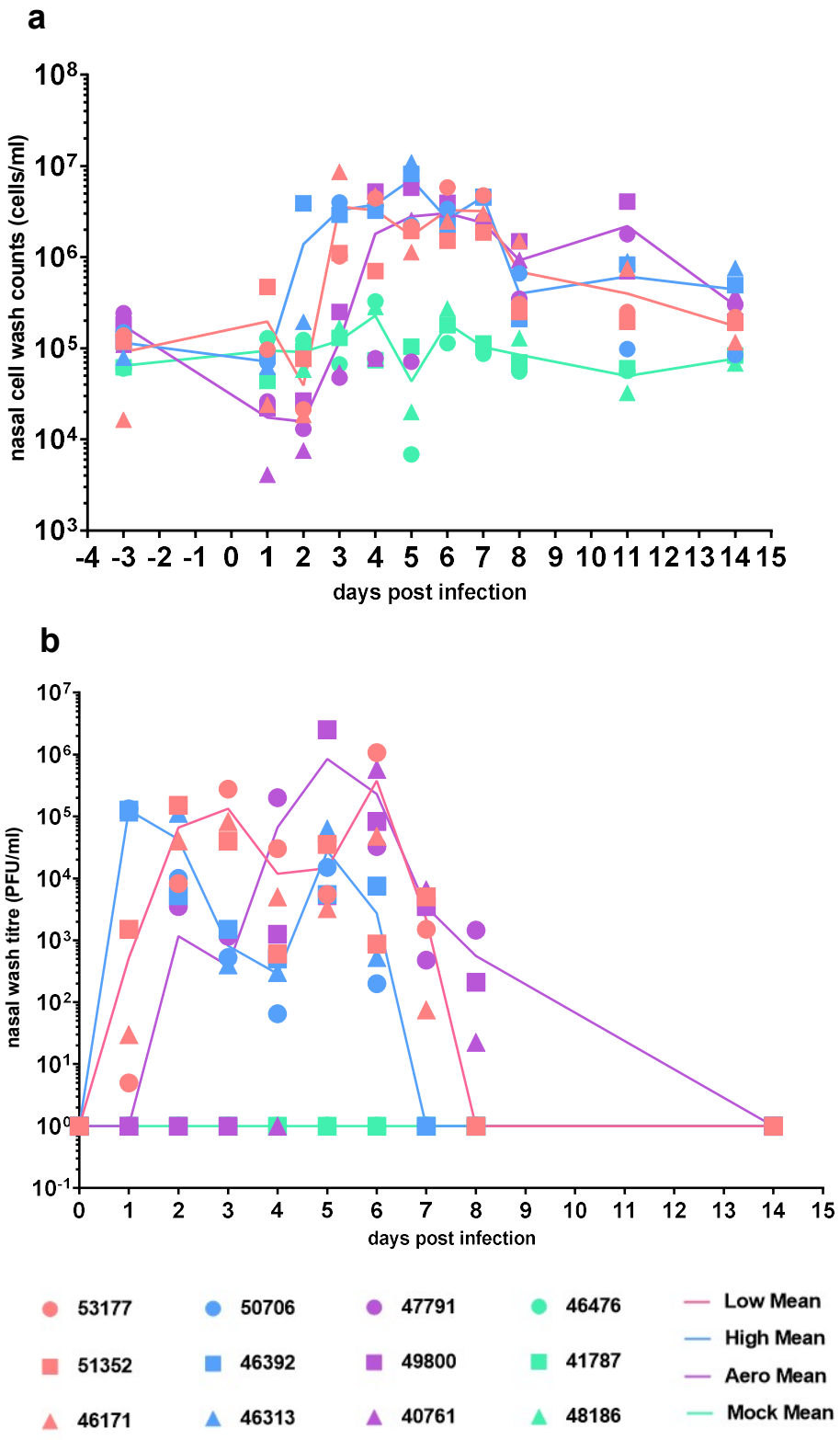

Figure 4.4.7.1 Nasal wash collection. Nasal washes were collected at +1 to +8, +11 and +14 dpi. **(a)** All nasal washes were counted to ascertain the number of cells being shed from each individual ferret at each time point (n=12). **(b)** All nasal washes were subsequently plaque assayed to ascertain the titre of virus being shed from each ferret (n=12).

4.4.8 **Clinical signs of infection found in ferrets**

Weight loss was observed in all groups infected with H3N2, in comparison mock infected ferrets gained weight (**Fig 4.4.8.1**). Of all the infected ferrets the low dose group experienced the greatest mean percentage weight loss and remained below the baseline of percentage change for most of the study.

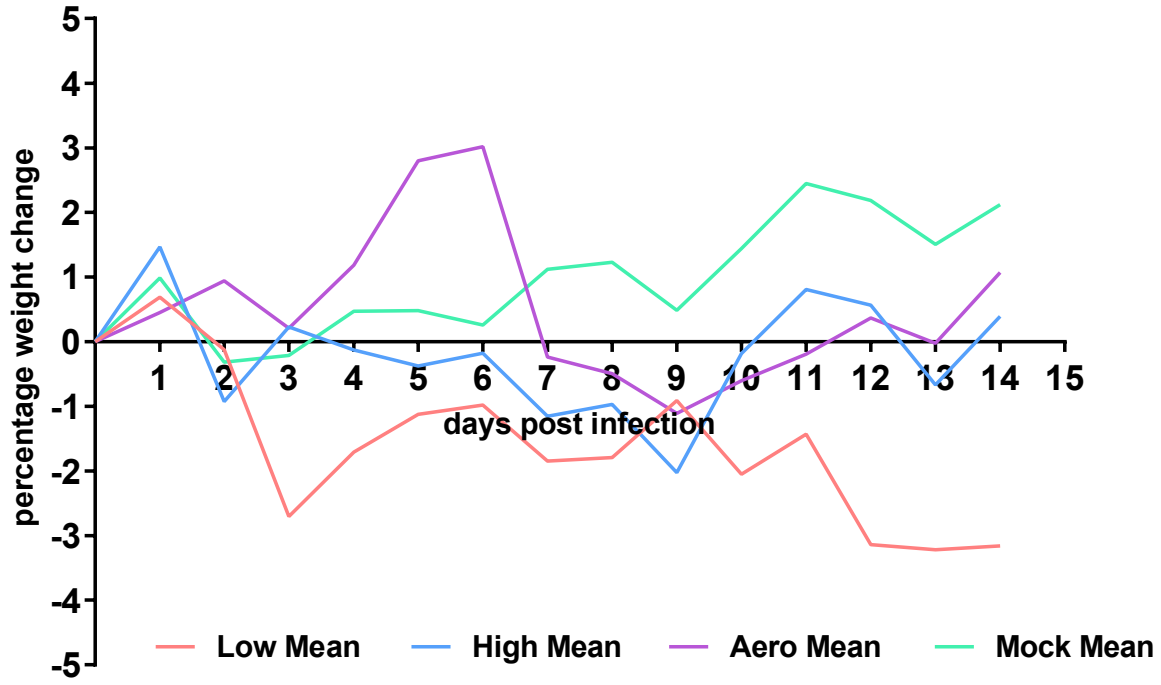

Figure 4.4.8.1 Weight percentage change from baseline. Mean percentage weight change of ferrets infected with H3N2 at high (n=3) and low (n=3) dose intranasally, by nose-only aerosol (n=3) and PBS (n=3).

The high dose group also experienced percentage weight loss below baseline, however the ferrets appeared to gain weight from 9 dpi onward. The aerosol group initially appeared to gain weight. At 7 dpi the percentage weight change dropped below 0 and the ferrets appeared to start to lose weight. This delayed weight loss correlated with the delayed viral shedding

seen in the aerosol group. The mock group of ferrets gained weight over the course of the study. This is expected in ferrets that didn't receive virus.

Table 4.4.8.1 Clinical sign observations.

Group	N	Total Sneezing	Total Nasal Discharge	Total Inactivity	Mean Score per ferret
Low	3	10	3	0	4.3
High	3	15	8	0	7.7
Aero	3	10	3	0	4.3
Mock	3	0	0	0	0

Total instances of clinical observations. N, number of ferrets per group.

Table 4.4.8.1 shows the cumulative incidence of nasal discharge, sneezing and total inactivity recorded over the course of the study for each ferret in all the groups. These results are in line with what was seen in the previous high and low dose intranasal comparison (**Section 3.3**). All ferrets infected with virus experienced either sneezing or nasal discharge over the course of the study. Animals in the high dose group experienced the highest incidence of nasal discharge and sneezing of all the groups with a mean ferret score of 7.7. Ferrets in the low dose and aerosol group had the same mean ferret score of 4.3, with the same incidence of sneezing and nasal discharge recorded across ferrets, with increased sneezing and nasal discharge seen over 2 dpi to 6 dpi. No clinical signs were recorded in the mock group.

4.4.9 **Whole blood immunophenotyping**

Peripheral circulating whole blood was labelled to determine the number and percentage of T cells and T cell subsets in the blood of ferrets and analysed by using two colour flow cytometry. Sampling for whole blood immunophenotyping (**Section 2.4.12**)was carried out post infection on days 2, 5, 8, 11 and 14. Whole blood samples were also taken at -7 and -1 before inoculation to form baseline data. Data was analysed as detailed in the materials and methods.

The granulocyte population (**Fig. 4.4.9.1**) of ferrets in the high dose group showed a general increase for two out of three above baselines in cell numbers over the time course. The granulocyte population for the low dose and mock groups appeared to fluctuate around baseline for the duration of the study. Granulocyte cell numbers for ferrets 47791 and 49800 in the aerosol group peak at 5 dpi, while ferret 40761 remained below 50% change from baseline, in line with the low dose and mock group results. This is consistent with viral shedding results for ferret 40761 which began to shed virus at 6 dpi and therefore was most probably infected last out of the three animals. A decline of cell numbers to baseline for ferrets 47791 and 49800 was seen at 8 dpi.

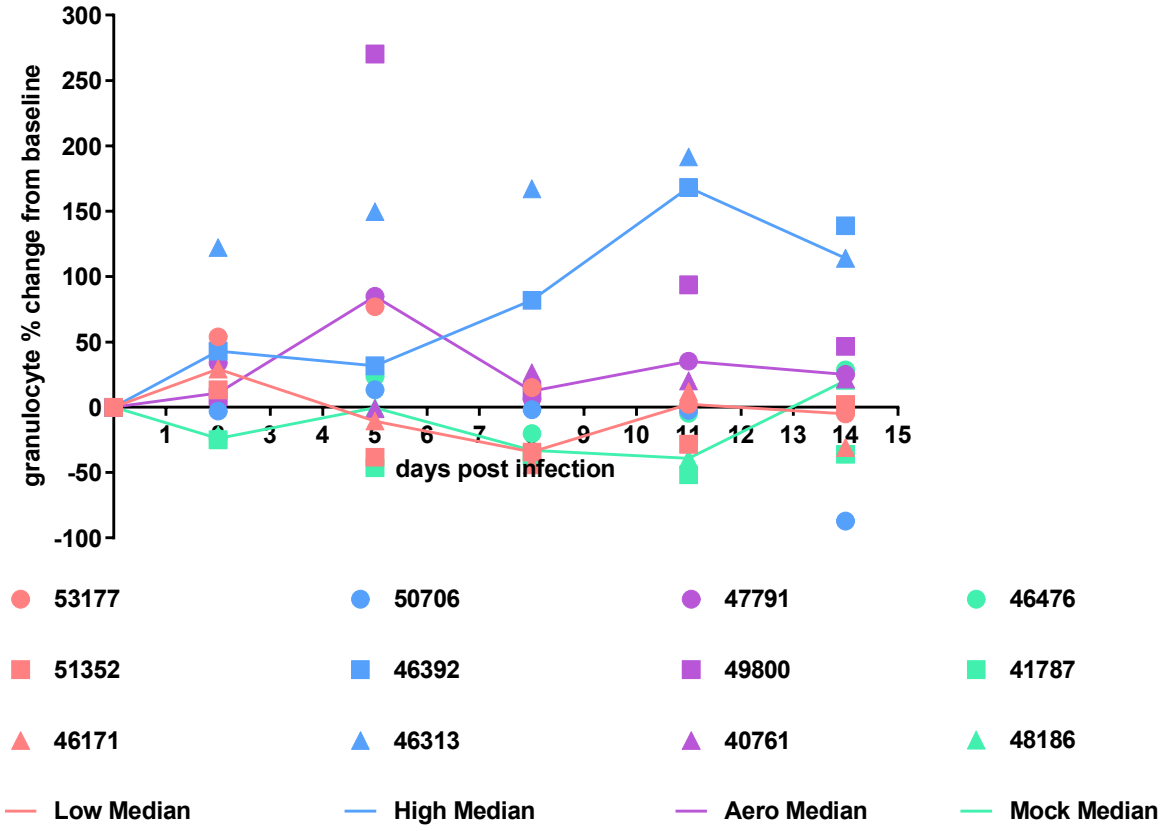

Figure 4.4.9.1 Percentage change from baseline in granulocyte population Percentage change from baseline was calculated using raw granulocyte cell data. Raw cell data was calculated using the following calculation; (A/B) x (C/D) = concentration of samples as cells/µl. Where A = number of cell events, B = number of bead events, C = Assigned bead count of the lot (beads/50 µl) and D = volume of sample (µl).

The high dose group (**Fig. 4.4.9.2**) group showed a steep decline in the lymphocyte population (above 50%) at 2 dpi for all ferrets. This percentage change slowly decreases across the remaining sample days until the population returned to baseline levels at 14 dpi. One ferret, 50706 showed a further decrease percentage change from baseline at 14 dpi. The low dose group had a decline in lymphocyte population following infection, with peak decline at 5 dpi followed by a recovery in numbers. This most likely occur due to cells being sequestered away from the peripheral blood to the site of infection. This early dip is known a lymphopenia, and has been described in influenza-infected patients (Criswell *et al.*, 1979). A decrease in

both T and B cells during experimental inoculation of humans has also been recorded (Dolin *et al.*, 1977). The aerosol group declined from baseline for all three ferrets occurring at 5 dpi, with a peak decline at 8 dpi. Cell numbers appeared to rebound returning to pre-challenge levels or above pre-challenge levels by 11 dpi. These responses are similar, although slightly later, to those observed for the high and low dose group. Ferret 47791 appears to act differently to rest of the aerosol group with a higher percentage change from baseline at 11 and 14 dpi. Ferret 47791 is the individual from the aerosol group that most likely became successfully infected from the aerosol inoculation. It should be noted that two of the three animals in the mock group also have a decline from baseline at 8 dpi.

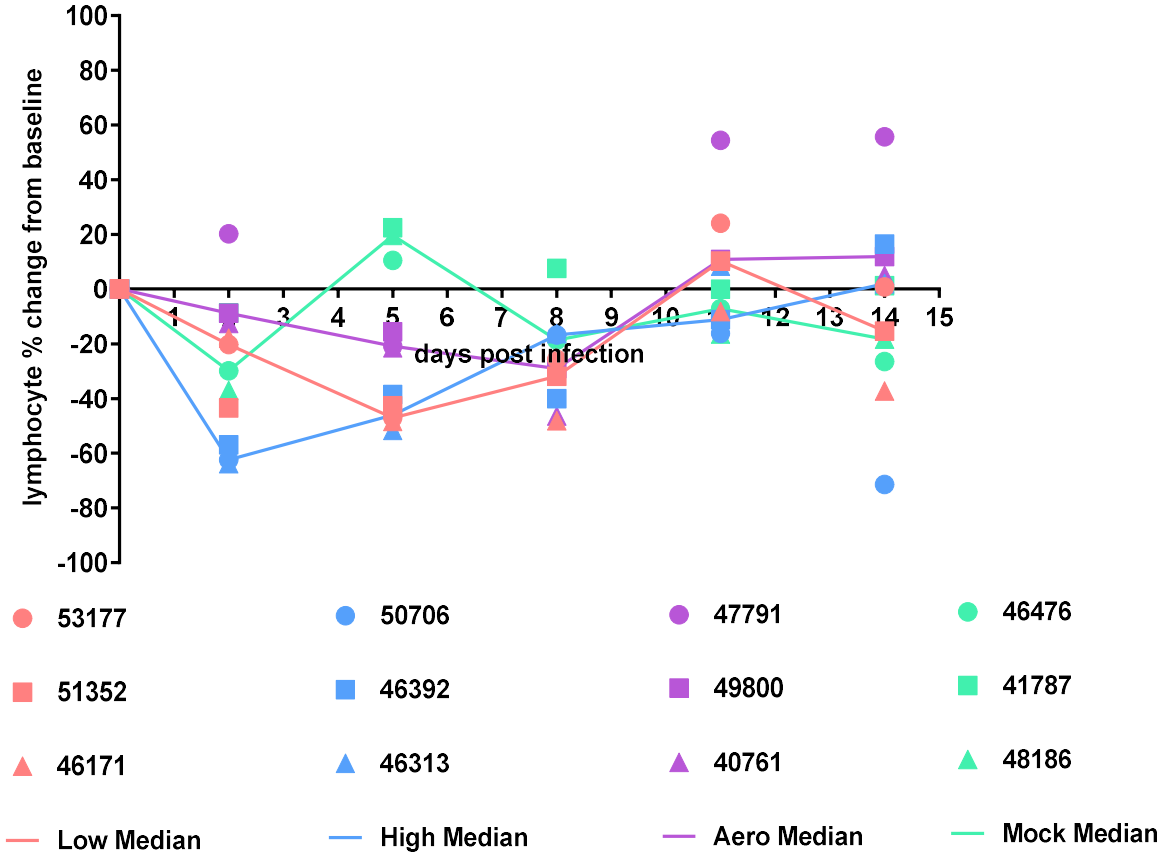

Figure 4.4.9.2 Percentage change from baseline in lymphocyte population Percentage change from baseline was calculated using raw lymphocyte cell data. Raw cell data was calculated as described above in **Fig. 4.4.9.1**.

Results seen in the CD4+ T cell population (**Fig. 4.4.9.3**) were comparable to those seen in the lymphocyte population (**Fig. 4.4.9.2**) with a decline in cell numbers observed at two days post-challenge in the high dose group. The decline in cell numbers occurred later in the low dose group at approximately 5 dpi. Numbers of CD4+ cells of both groups continued to recover to baseline levels for the majority of animals towards the end of the time course. A decline in CD4+ cells also occurred in the aerosol group at 8 dpi, though not as sharply as the high and low dose groups. Numbers returned to baseline by 14 dpi.

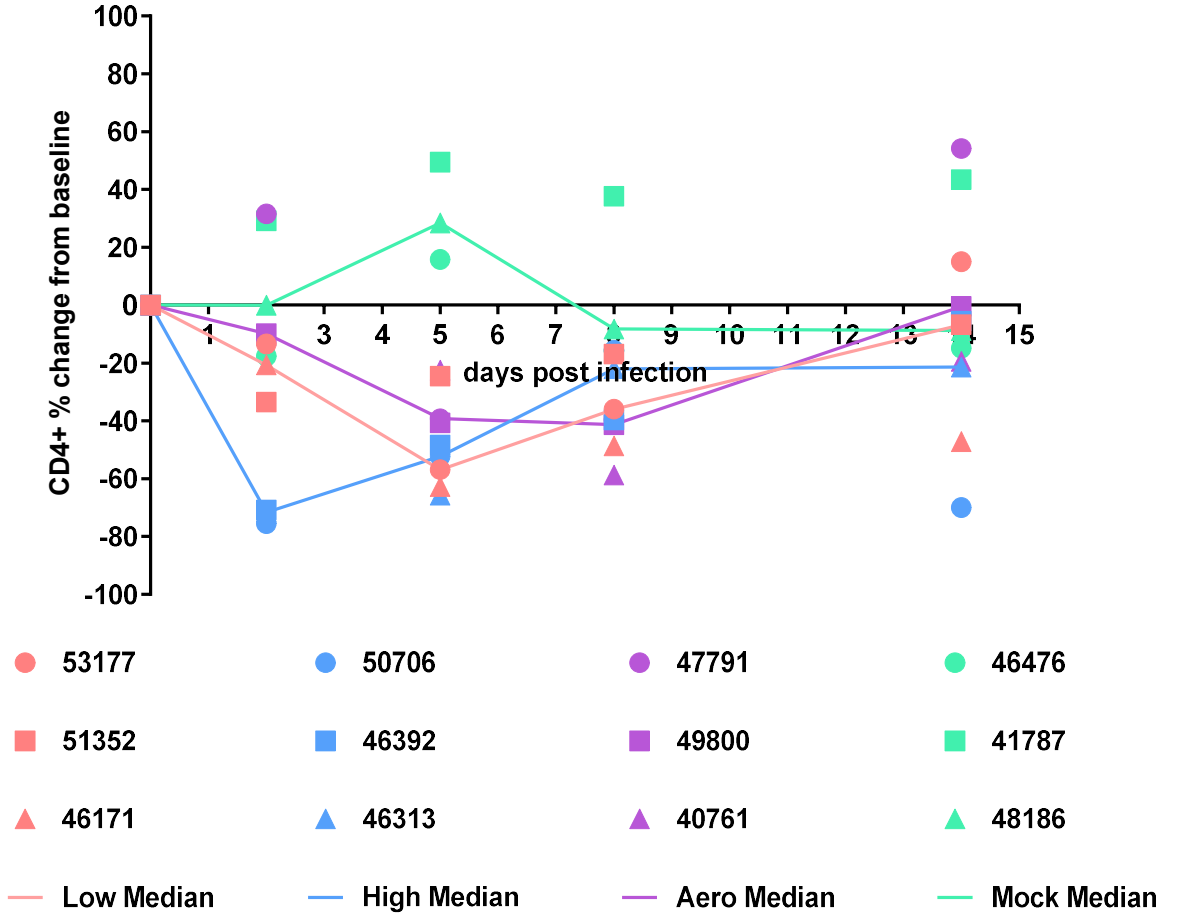

Figure 4.4.7.3 Percentage change from baseline for CD4+ T cells following influenza infection

Percentage change from baseline was calculated using raw CD4+ T cell values. Raw cell data was calculated as described above in **Fig. 4.4.9.1**. Data were not analysed at 11 dpi due to an incorrect batch number of PE CD4+ antibody being used for the whole blood phenotyping; this batch number had been found previously to not work and was used in error; results from 11 dpi were therefore omitted from analysis.

A similar decline was observed in infected groups in the CD8+ T cell population, however it was not as marked as in the lymphocyte (**Fig 4.4.9.2**) or CD4+ T cells (**Fig 4.4.9.3**). An increase in the number of CD8+ T cells was observed at eight days post challenge in the high dose group of animals, a similar increase was also observed in the low dose and aerosol group of animals. There appears to be a decline from baseline in all animals at 11 dpi. Ferret 41787 in the mock group appears to be to be an outlier, as the increase in CD8+ T cells is much higher than expected in the mock group and when compared to other infected ferrets.

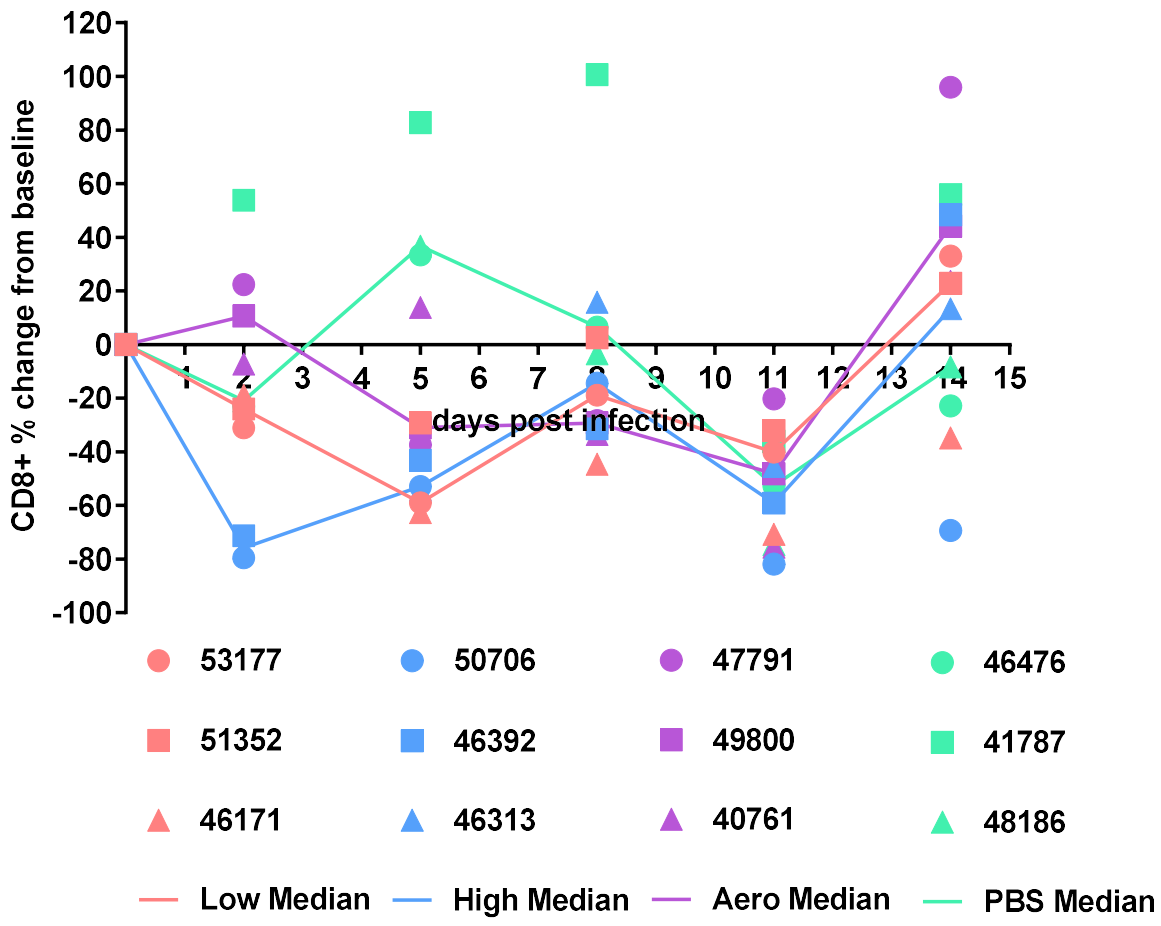

Figure 4.4.7.4 Percentage change from baseline for CD8+ T cells following influenza infection

Percentage change from baseline was calculated using raw CD8+ T cell values. Raw cell data was calculated as described above in **Fig. 4.4.9.1**.

4.4.10 **Comparison of cell types producing influenza-specific IFN-γ response**

All cells used in the assay were isolated at necropsy and assessed for influenza-specific IFN-γ responses (**Fig 4.4.10.1**) in PBMC (**a**), spleen (**b**), Lung MNCs (**c**) and BAL wash (**d**). Results were analysed to look at the number of spot forming units per $1x10^6$ cells, which represents the quantity of cells expressing influenza-specific IFN-γ responses.

The cellular immune response seen in PBMCs (**Fig 4.4.10.1.a**) appears to be the highest for the low dose group, with the high dose and aerosol groups appearing to have comparable influenza-specific IFN-γ response. No response was detected in the mock group. Influenza-specific IFN-γ responses seen in splenocytes (**Fig. 4.4.10.1.b**) were only determined for two out of three ferrets in the low dose group. These results were quite variable, as one ferret had very low spot forming units detected whilst the other had the highest detected of all the ferrets assayed. The high dose and aerosol group ferrets showed similar influenza-specific IFN-γ responses detected with each of their groups in splenocytes. Low responses were detected in the mock group, as expected. Variable influenza-specific IFN-γ responses were detected in the low dose group in lung MNCs (**Fig. 4.4.10.1.c**). The ferret with the high influenza-specific IFN-γ response seen in the lung MNCs for the low dose group was not the same ferret with the high influenza-specific IFN-γ response detected in the splenocytes.

In the aerosol group the highest influenza-specific IFN-γ responses in animal 40761 were found in the PBMCs and in contrast, the lung MNC influenza-specific IFN-γ responses in this ferret were relatively low (**Fig. 4.4.10.1**). Comparatively low influenza-specific IFN-γ responses were seen in the PBMCs of ferrets 47791 and 49800. This corresponds with the sequestering of immune cells to the lung – the primary site of infection. When considering the spot size of

the spot forming units, similar results are seen. Both ferrets 47791 and 49800 have slightly higher influenza-specific IFN-γ responses in lung MNCs than animal 40761 however all of their repsonses are relatively similar.

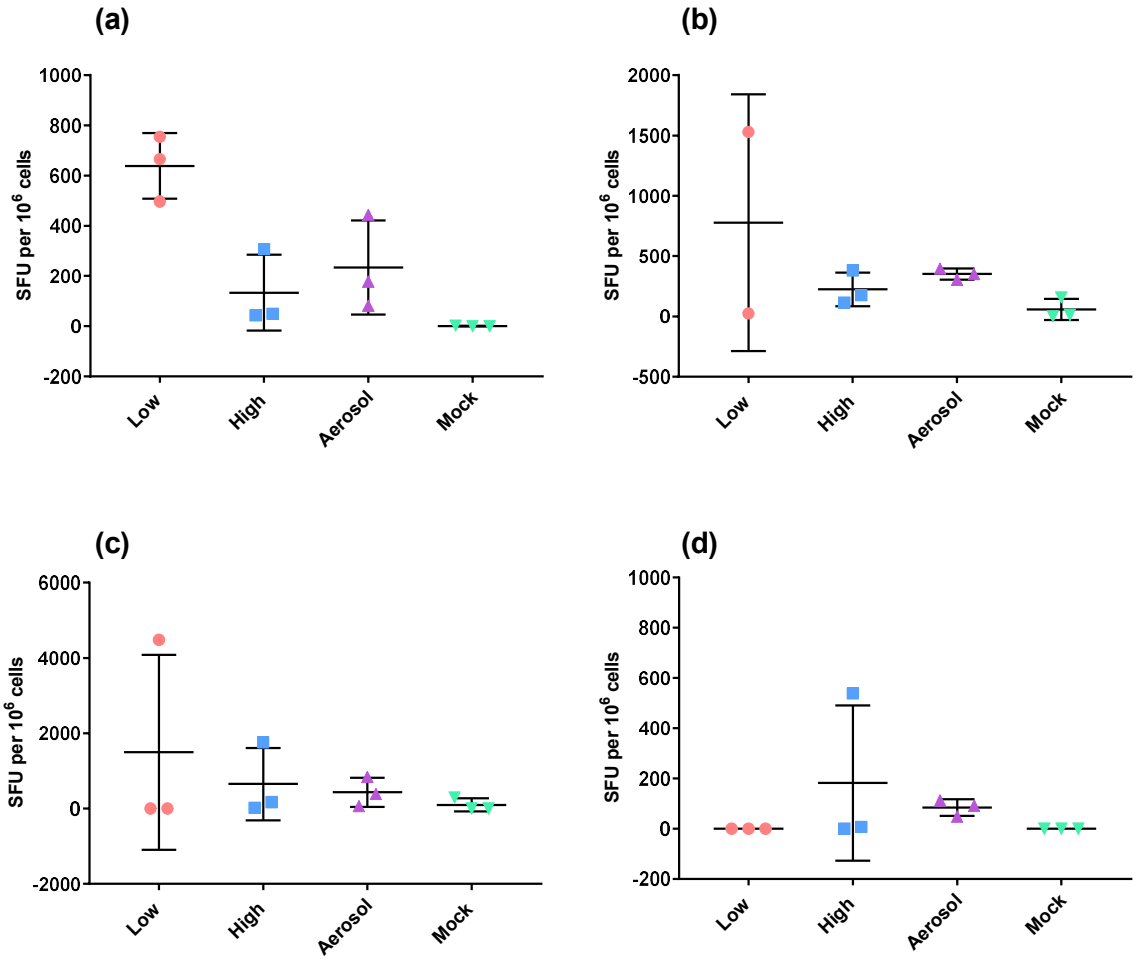

Figure 4.4.10.1 Cellular immune response (a) PBMCs (whole blood), **(b)** splenocytes (spleen), **(c)** lung mononucleocytes (MNCs) and **(d)** bronchiolar lavage (BAL) wash were collected from all animals (n=12, results for splenocytes for ferret 46171 in the low dose group were not able to be reported due to assay failure). Results were normalised by subtracting allantoic fluid control values from virus stimulated samples. Bars show standard deviation and mean for each group.

4.4.11 **A longitudinal time course of circulating IFN-γ in nose-only aerosol challenged ferrets**

Observation of the ongoing cellular immune response to influenza challenge was performed by monitoring influenza-specific IFN-γ responses in circulating blood. Small volumes of heparinised blood were collected at -7, -1, 2, 5, 8, 11 and 14 days post challenge, diluted and stimulated with A/Perth/16/2009. Ferrets in the low dose group acted as previously described in **Chapter 3**, **Section 3.6.6.4** with influenza-specific IFN-γ responses detected as early as 5 dpi (**Fig. 4.4.11.1**). This increased at 8 and 11 dpi, peaking between 11 and 14 dpi. The high dose group had more variable influenza-specific IFN-γ responses. One ferret (46392) didn't produce detectable levels of influenza-specific IFN-γ until 11 dpi. It's not clear why this happened, as the remaining two produced detectable levels of influenza-specific IFN-γ at 5 dpi, as seen previously in low dose infected animals. However, the amount of influenza-specific IFN-γ detected (pg/ml) was, at times, double the amount detected in the low dose group.

The levels of influenza-specific IFN-γ detected in the aerosol group was also variable between ferrets and the delayed detection of responses corresponds with the hypothesis that some of the ferrets were unsuccessfully inoculated via the nose-only aerosol route. Ferret 47791 began to show influenza-specific IFN-γ response on 5 days post challenge, while the remaining two ferrets did not begin to show influenza-specific IFN-γ responses until 11 days post challenge. Ferret 47791 shows a similar longitudinal time course of influenza-specific IFN-γ responses as those seen in ferrets infected intranasally with a low dose of influenza. As proposed previously, it is likely that ferrets 49800 and 40761 were infected through natural transmission after coming into close contact with 47791, this could be the reason for the apparent delayed influenza-specific response observed in these ferrets. As samples were only

collected until 14 days post challenge it is impossible to tell if these responses would continue to rise, however based on the evidence from the low dose inoculated ferrets it could be assumed that this would be the case.

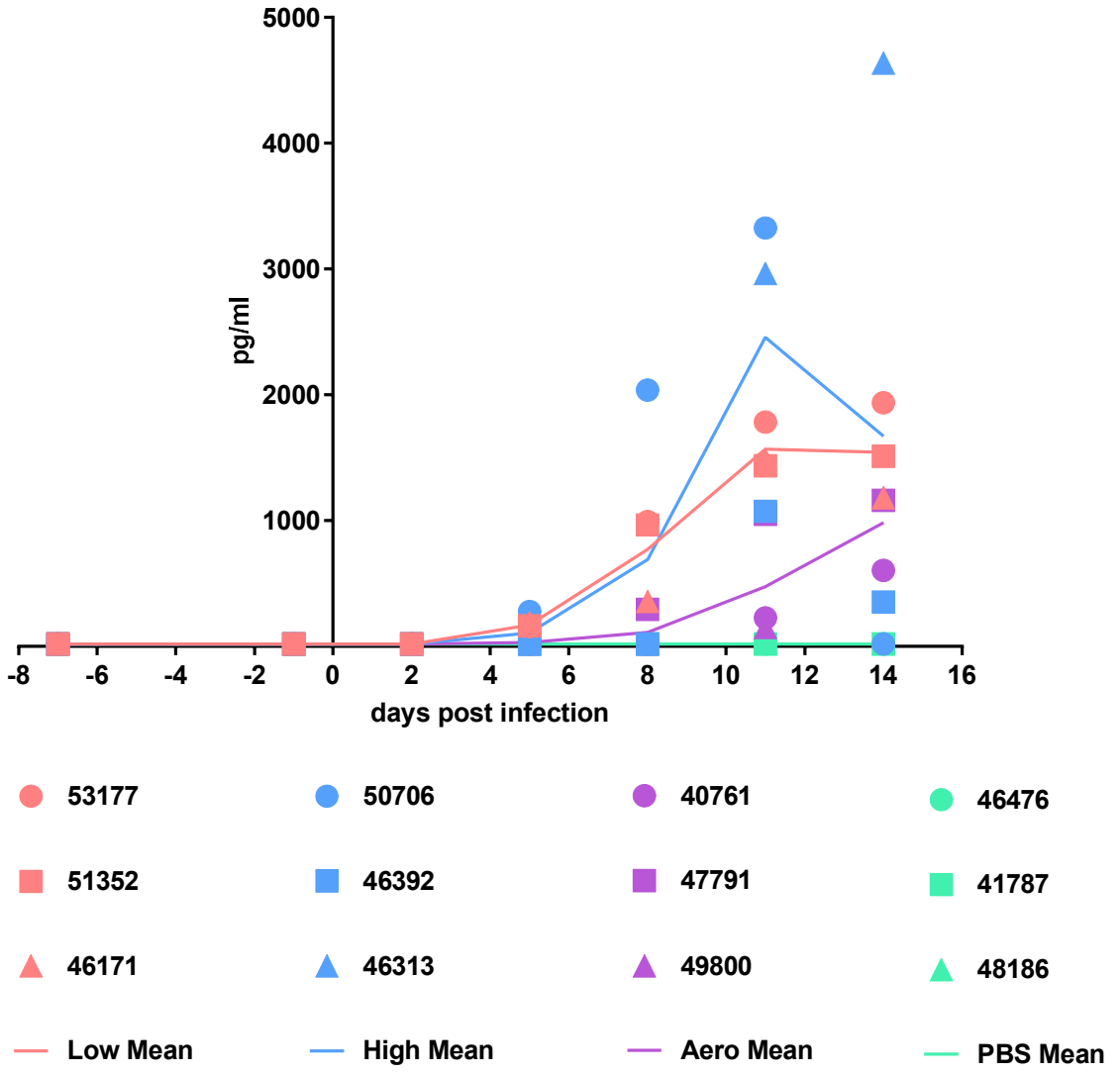

Figure 4.4.11.1. Quantification of influenza-specific IFN-γ production by ELISA Diluted whole blood samples were collected all groups (n = 12) at -7, -1, +2, +5, +8, +11 and +14 dpi, stimulated with appropriate antigens and the supernatants harvested. Supernatants were used in the Ferret IFN-γ ELISA Development Kit (ALP). Influenza-specific IFN-γ responses became detectable at 5 dpi. No responses were detected in PBS ferrets. 12000 pg/ml was the upper limit of detection for the ELISA.

4.5 Discussion

The viral kinetics of the low dose and high dose groups were consistent with those seen in **Chapter 3**. The immunological readouts for the low dose and mock groups were as established previously and provided a good baseline comparison for the high dose and aerosol groups.

The inoculation of the high and low dose groups appeared to be successful. The nose-only aerosol inoculation only appeared to be successful in 1 out of 3 of the ferrets infected via this route. As results were collected from this study it became apparent that two of the three animals that were challenged via the nose-only aerosol route did not respond as anticipated. It is thought that animal 47791 was successfully infected via the nose-only aerosol route; while it appears animals 40761 and 49800 were not. In this study the three ferrets from each group were housed together, therefore it can be concluded that ferret 47791 most probably infected the two other ferrets via a route of natural transmission. From the viral shedding results it can be confirmed that ferrets 40761 and 49800 eventually became infected with A/Perth/16/2009.

This conclusion was initially drawn from the nasal wash counts and viral shedding data due to the differences in the timings of when animals started to shed an excess of nasal wash cells and virus, respectively. Upon further analysis of cellular immune response results it can be seen that there is a delay in the appearance of responses in the longitudinal time course of influenza-specific IFN-γ responses. This seems to confirm that animals 40761 and 49800 were infected later to animal 47791.

ELISpot data suggests that there was a successful infection in the lungs of ferrets 47791 and 49800 as high influenza-specific IFN-γ responses were detected in lung MNCs. Influenza-specific IFN-γ responses seen in the lung MNCs of ferret 40761 were very low compared to ferrets 47791 and 49800 and fell within baseline responses seen in the mock infected, naïve PBS inoculated ferrets. These results suggest that the virus did not successfully reach the lungs of ferret 40761 and therefore it is highly likely that this ferret was not successfully infected via the aerosol route and rather by direct contact transmission. This influenza-specific IFN-γ response seen in lung MNCs was not seen in the majority of ferrets infected intranasally.

4.6 Further Work

The results from this study suggest one of the animals that were challenged via nose-only aerosol became infected. The remaining two animals becoming infected through contact transmission. Analysis of the results identified a range of reasons for why two out of three of the animals may not have been successfully infected during challenge.

1. *Re-evaluation of the <u>in vitro</u> spray factor using the aerosol delivery system to ensure accuracy and reproducibility*

Would the addition of protein, such as bovine serum albumin, make a difference to the survival of influenza particles during the nebulisation process?

Presence of protein is thought to have a protective effect on the virus during aerosolisation (Tuttle *et al.*, 2010b), though many of the studies where this is reported are investigating

aerosol survival rather than aerosol delivery to animals, therefore not taking into account the introduction of a live animal into the aerosol system. A range of studies have been identified using several different diluents including; PBS + 0.5% BSA fraction V (Lednicky *et al.*, 2010) PBS + 0.5% BSA fraction V + molecular-grade antifoam agent B added at 0.25% (v/v) (Tuttle *et al.*, 2010b) and MEM, 0.2% $NaHCO_3$, 20mM HEPES, 1% Antibiotic/Antimycotic, 20mM L-Glutamine, 0.001% BSA, and 100µl of Antifoam A (MacInnes *et al.*, 2011).

The act of nebulising the inoculum is violent and the protein could afford a protective effect on the aerosolised virus particles. A small amount of preliminary *in vitro* aerosol data was generated prior to the start of this body of work with a H1N1 influenza strain comparing the spray factor with and without protein (0.5% BSA). However, there was an insufficient number of replicates, and samples were frozen prior to performing plaque assays. The results from this small study suggested there was little difference between nebulising the inoculum with or without protein (BSA Fraction V), therefore, when designing the set up and testing parameters during *in vitro* testing for A/Perth/16/2009 the addition of protein was not explored. The inclusion of protein needs to be properly evaluated to see if this has an effect upon the survival of influenza once nebulised. This would include running more replicates than were previously carried out during *in vitro* studies as well as carrying out sprays on different days to ensure it was carried out consistently. Beginning with $1x10^6$ PFU of A/Perth/16/2009, aerosols would be generated and collected, and plaque assays will be used to evaluate the amount of virus present in the impinger sample. Virus would be diluted in media (DMEM) with and without protein to identify if BSA Fraction V should be included in the virus diluent in future studies or not. A range of protein concentrations should be included. Following the first experiment, it will be repeated to evaluate if there is any day to day variation in the spray factor using the aerosol delivery system. Three impinger samples will be collected from each Collison run to identify any degradation in the virus suspension.

2. *Ensuring the spray factor is correct when using a range of virus dilutions as a starting point*

Does the spray factor change across a range of starting dilutions or does it remain the same?

A lower concentration of virus was recovered from the impinger than expected during the aerosol challenge of ferrets with A/Perth/16/2009. The spray factor used to calculate the presented dose was based on *in-vitro* spray data when virus was aerosolised at a starting concentration of $1x10^6$ PFU/ml. The starting concentration in the Collison for the H3N2 inoculum was approximately $2x10^4$ PFU/ml and therefore around $1x10^2$ PFU was expected to be recovered from the impinger (based on an expected 2 log drop seen in previous *in vitro* studies). Considerably less was recovered from the impinger and based on that value the calculated presented dose for the study was 0.8 PFU. Therefore, different starting concentrations of virus should be aerosolised to ensure that dropping the initial concentration of virus in the nebuliser does not have influence on the spray factor and therefore the presented dose. This should be repeated to ensure the consistency of the results. The outcome of the experiment should identify if using different dilutions of virus results in different spray factors.

3. Repeating in-vivo work

How does the introduction of animals into the system affect the spray factor and presented dose?

Following the full evaluation of aerosols generated *in-vitro*, assuming the presented dose is robust, reproducible and reliable, *in-vivo* work can begin. In the first instance a series of dose titration studies should be performed with pre-determined target doses; this will ensure the addition of ferrets to the system does not have an effect upon the spray factor and presented dose calculated in prior *in vitro* studies. Ferrets would need to be housed individually to ensure none became infected via the natural transmission route, and potentially confusing the results. The dose to be used in any future ferret studies can then be identified as the lowest dose that reliably infects all ferrets. The starting dose chosen would be dependent upon the outcome of any additional spray factor work carried out. During this study only 1/3 ferrets were successfully infected when the presented dose of $3x10^2$ PFU was used with a spray factor $6.1x10^{-6}$. Therefore, a dose range of $2x10^2$, $4x10^2$ and then $8x10^2$ PFU presented dose would be sensible to evaluate in the ferret model.

Ultimately completing further nose-only aerosol study with the above parameters would provide a much clearer picture for the evaluation of cellular immune responses. However, as animal studies are very expensive and time consuming, as well as considering ethical considerations around using more ferrets, it was not possible to complete within the confines of this project.

4.7 Summary

- Virology and cellular immune readouts work successfully and were observed in all animals
- Assays were able to identify differences between groups of animals
- Responses appeared similar to those seen in the low dose intranasally inoculated animals
- Nose-only aerosol inoculation of ferrets with A/Perth/16/2009 is currently unreliable and requires further optimisation to reliably infect all exposed animals

5 Transmission Cage Model

5.1 Introduction

Human to human transmission of IAV occurs either through contact (direct or indirect) or respiratory droplet (droplet or droplet nuclei) transmission (Bridges *et al.*, 2003). As stated previously, dissociating these transmission routes is complicated, and it is difficult to determine the exact contribution of each of these modes of transmission to infection. However, the transmission of respiratory droplets when an infected individual coughs or sneezes is likely to be a major mode of sustained virus spread in the community setting during seasonal epidemics and occasional pandemics (Maines *et al.*, 2006).

Detection of infectious airborne IAV in clinical settings is limited and lacks sensitivity (Blachere *et al.*, 2011). There are several challenges that are encountered when culturing airborne IAV; low concentrations of virus, damage to virus during sampling and interference by environmental contaminants (bacteria, mould, dust) (Turgeon *et al.*, 2019).

In the laboratory setting several animal models have been used to investigate IAV transmission via respiratory droplets (Lowen *et al.*, 2006, Maines *et al.*, 2009, Maines *et al.*, 2006), including ferrets (Maines *et al.*, 2006, Munster *et al.*, 2009). Ferrets have already been shown to be an ideal candidate to investigate human IAV transmissibility and shed a light on the pandemic potential of emerging zoonotic viruses. Ferret transmission studies provide an important insight into host, viral and environmental factors affecting the transmission of IAV

(Nishiura *et al.*, 2013), with basic analysis in typical ferret experiments being the presence or absence of transmission from an infected ferret to a susceptible ferret.

Transmission of respiratory droplets of IAV from infected donor ferrets to naïve recipients is an effective method of evaluating the ability of the virus to transmit via 'naturally' generated aerosols. Unlike the aerosol exposure system where the presented dose can be calculated, the presented aerosol dose to the naïve recipient would be difficult to calculate. Air sampling in and around transmission cages could help to establish insight into how the virus is shed and at what stages, post infection, the virus is transmitted. Previous investigations showed that influenza transmission amongst ferrets via the air was positively associated with the number of infectious particles exhaled by the infected donor (Lakdawala *et al.*, 2011). However, another investigation with pre-2009 seasonal H1N1 and pandemic H1N1 showed that high viral RNA levels in the air surrounding animals in transmission cages did not predict efficiency of transmissibility of individual virus strains (Koster *et al.*, 2012). This study also showed that as time passed following the initial infection of the donor ferret the less efficient the transmission of virus became between it and its recipient pair despite viral RNA levels staying similar throughout the initial time period of the investigation (Koster *et al.*, 2012). It has been suggested that this may be due to a robust inflammatory response that reduced the viability of the virus, but does not affect the level of viral RNA exhaled (Thangavel and Bouvier, 2014). In any case, robust methods of collecting virus containing particles from exhaled breath for reliable analysis remains an unmet challenge (Milton *et al.*, 2013).

The respiratory droplet transmission model has been well characterised (Herlocher *et al.*, 2001, Maines *et al.*, 2006). The purpose of this type of model is to allow the separation of ferrets; permitting airflow exchange between pairs, while eliminating other sources of direct and indirect contact. This allows for the evaluation of the virus transmissibility, as some

viruses which demonstrate transmissibility through direct contact conditions are unable to be transmitted by the respiratory or aerosol droplet route. A limitation of this model is the difficulty in discriminating between large respiratory droplets and droplet nuclei.

5.2 Aims

Study **5283** (appendix 1) was designed to establish a model of indirect transmission between ferrets infected with the H3N2 strain A/Perth/16/2009 and to explore the influenza transmission kinetics between intranasally challenged ferrets and indirect contact ferrets. This allows airflow exchange between the two ferrets while eliminating all other sources of direct and indirect contact. This study acted as a pilot respiratory transmission cage model which ultimately intended to encompass all three recognised modes of transmission: contact, large droplet and droplet nuclei, however as animal studies are very expensive and time consuming, as well as taking into account ethical considerations around using more ferrets, it was not possible to complete within the confines of this project. Details of how the work would have evolved will be detailed in the further work section of this chapter (**5.6**).

The aim of this model was to represent a more natural route of transmission compared with forced exposure of single ferrets to aerosol exposure apparatus. Successful transmission between donor and recipient was assessed by the detection of infectious virus in nasal wash and/or seroconversion of the recipient. Previous studies have demonstrated that seroconversion in the absence of virus detection is not uncommon.

5.3 *In vivo* Study Outline

5.3.1 Cage Design

The modified ferret cages were designed at PHE, Porton Down by the Biosafety Group. The original standard cages were manufactured by Arrowmight (Arrowmight, Hereford, UK) and were extensively modified by the Biosafety Department to carry out influenza transmission work. New side panels and doors were manufactured by Prosheet (Prosheet Engineering Limited, Crayford, UK) to specification to allow modification of pairs of cages to the transmission system. The ventilation fan units and filter boxes (PFI, Milton Keynes, UK) for use on flexible film isolators were suitably modified. **Figure 5.3.1.1** shows how the cages were set up.

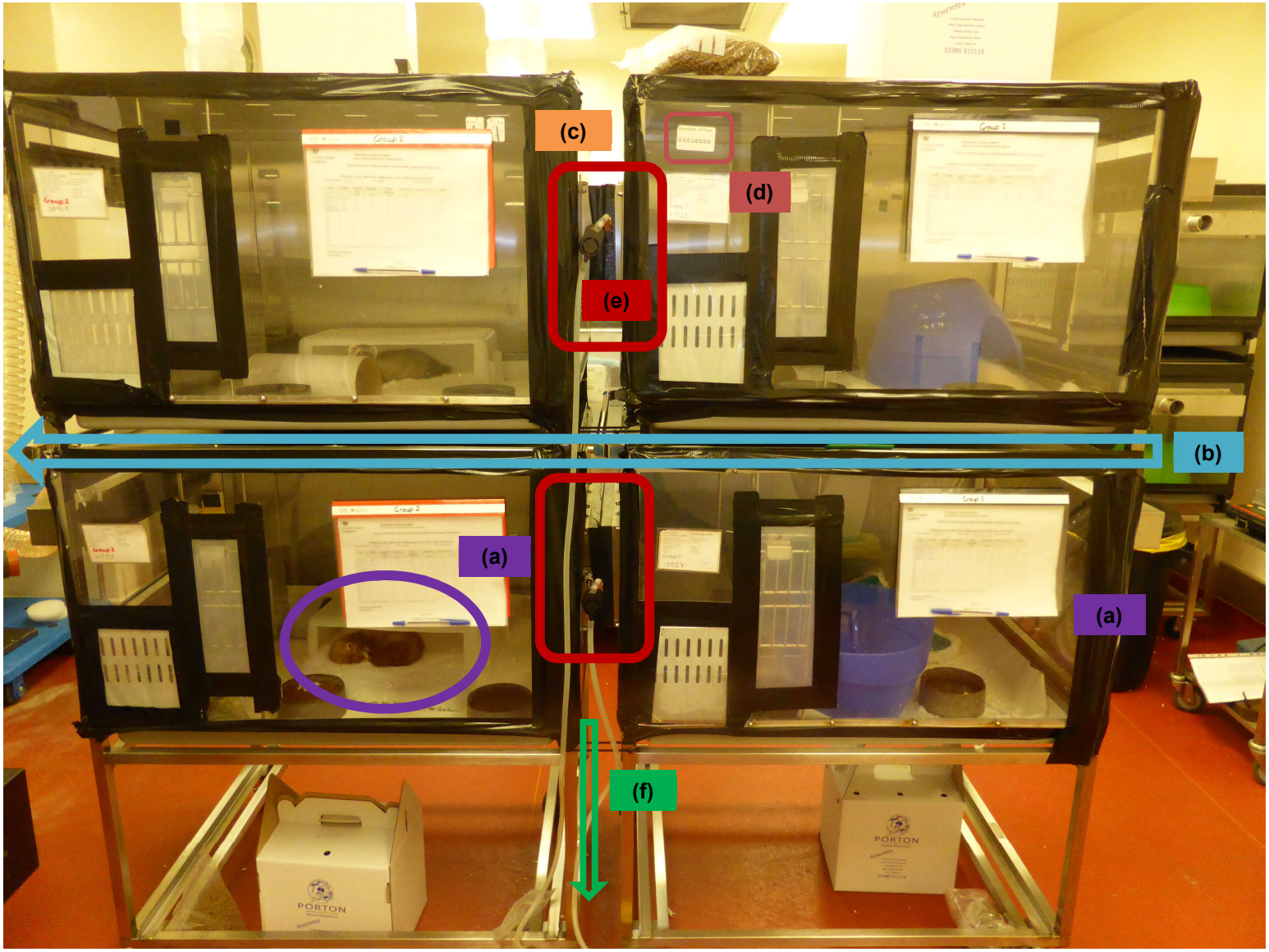

Figure 5.3.1.1 Transmission Cage Design. Cages were sealed using a combination of rubber seals and sufficient tape. **(a)** Ferrets were singly housed in separate individual cages and each donor ferret was paired with a singly housed recipient ferret.

(b) Air was drawn from the laboratory into the first cage via a high-level vent and then on through into the second sealed cage via a connecting tunnel **(c)**. The aperture of the tunnel was covered with a perforated metal mesh on each end. The mesh was covered in 4.8mm holes giving a 50% open surface area and the tunnel was 10cm deep. Having reached the second cage air was drawn back out into the laboratory via a H14 HEPA filter (PFI, Milton Keynes, UK) to prevent any exposure or cross contamination. The system was set up to give 20 air exchanges per hour inside each cage, equating to a face velocity of 0.02msec^{-1} through the connecting tunnel. **(d)** Cages were clearly marked with the direction of airflow to separate procedures carried out on the donor and recipient animals. This was to prevent operator cross-contamination. **(e)** To aid the assessment of the viral kinetics and to see if it was possible to sample air between cages, a personal air sampling system was used during this investigation. **(f)** Air samplers were set up between cages: 1. 41822-38968, 2. 15557-40513 and 3. 18704-40487 (ferret ID pairs).

Six transmission cages were set up as shown (**Fig. 5.3.1.1**). Three of the six paired cages were fitted with personal air samplers (**Fig 5.3.1.2**) to sample the air flowing from the infected donor cage to the recipient cage, sampling for 8 hours.

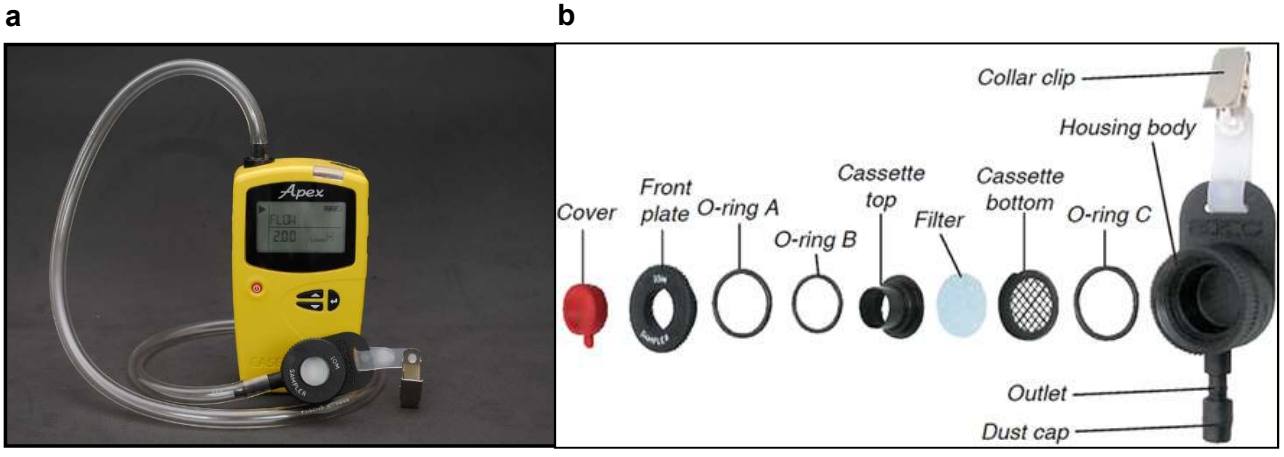

Figure 5.3.1.2 Personal Air Sampler The personal air sampler (Casella UK, Bedford, United Kingdom) **(a)** sampled cage air a total of 4L/min, with sampling taking place each day for approximately 8 hours. **(b)** Each air sampler had a clean gelatine filter fitted every morning on to which the virus was collected.

The individual gelatine filters were then dissolved in 1mL warm (37°C) PBS, aliquoted into two labelled cryovials and stored at -80°C. Air sampling was carried out from +1 to +8 dpi. At a later date, the air sampling aliquots were defrosted, and the RNA was extracted using the QIAgen RNeasy Mini Kit and samples analysed by qRT-PCR (**Chapter 2 Materials & Methods**).

5.3.2 **Study Design**

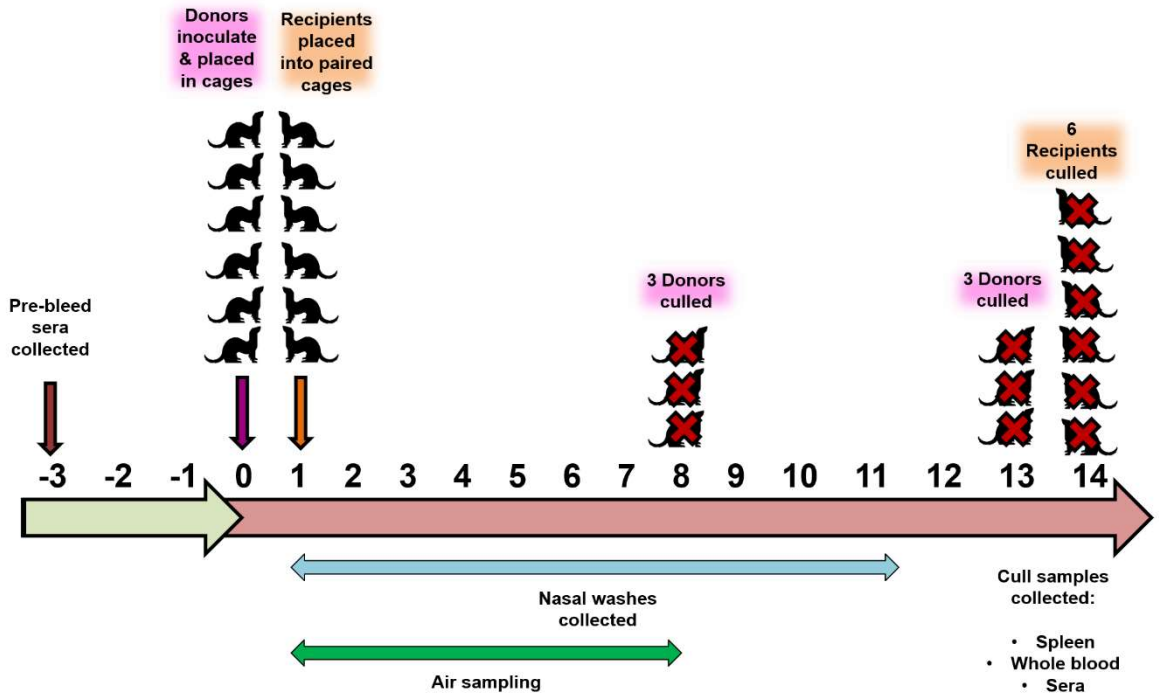

Figure 5.3.2.1 Study timeline. Baseline bleeds were taken from all ferret at -3dpi. At 0 dpi donor ferrets were sedated and inoculated via the intranasal route with $1x10^5$ PFU/ferret of A/Perth/16/2009 and placed singly into individual cages. Recipient ferrets were placed singly into donor-paired cages at 1dpi of donor ferrets. Nasal washes were collected in PBS from 1 dpi to 11 dpi. Air sampling of cages was carried out from 1 dpi to 8 dpi on three of the six paired cages. Three donors were culled 8 dpi and the remaining were culled at 13 dpi. All recipients were culled at 14 dpi. At cull spleen and whole blood were taken for the evaluation of the cellular immune response. Blood for sera, was also taken to evaluate the humoral immune response.

5.3.3 **Ferrets**

A mixture of ferrets were obtained from Highgate Farm, UK, and Simonsen Laboratories, GA, USA, and were 12-16 weeks of age at the time of the study. A total of 12 ferrets were used, with 6 donor animals and 6 matched recipient animals, randomly assigned, as shown in **Table 5.3.3.1**. All baseline sera samples had HAI titres of less than 4 to H3N2 A/Perth/16/2009, and it was deemed that these ferrets had no previous exposure to H3N2 and so were suitable for challenge.

Table 5.3.3.1 Ferret Identification Numbers

Donor Group			Matched Recipient Group		
Number	**Origin**	**Starting Weight (g)**	**Number**	**Origin**	**Starting Weight (g)**
40434 (m)	Simonsen	1110	**95099 (f)**	Simonsen	750
40400 (m)	Simonsen	1262	**11981 (m)**	Highgate	593
40418 (m)	Simonsen	1203	**12950 (f)**	Highgate	1106
41822 (f)	Simonsen	760	**38968 (m)**	Highgate	613
15557 (f)	Highgate	724	**40513 (m)**	Simonsen	543
18704 (f)	Highgate	533	**40487 (f)**	Simonsen	692

5.3.4 **Virus**

Donor ferrets were inoculated intranasally with H3N2 A/Perth/16/2009 P+2A challenge stock virus diluted in PBS to provide a challenge dose of $1x10^5$ pfu/ferret. Donors were inoculated intranasally on day zero. The challenge dose of $1x10^5$ pfu/ferret was chosen to ensure the donor ferrets were successfully infected and was based on a previous H1N1 study using similar transmission cages at PHE Porton (Otte *et al.*, 2016). The dose was confirmed on day

of administration by back-titration using plaque assay. The challenge material was given to each animal in a volume of 0.2 ml via the intranasal route. Infected ferrets were then transferred into the donor halves of the transmission cages. Recipients were placed into the other half of the transmission cages on T=1. From this stage until the end of the study the recipient ferrets were always handled before the donor ferrets to avoid potential cross contamination between uninfected recipients and infected donors.

5.3.5 **Sample collection**

Nasal washes were obtained, and cell counts were performed prior to the nasal washes being frozen down for plaque assay at a later date. Nasal wash samples were taken from all ferrets prior to study start on -1 dpi and then at 1 dpi to 11 dpi or until culled. Three ferrets from the donor group were culled at 8 dpi. The remaining 3 ferrets from the donor group were euthanised at 13 dpi. All ferrets from the recipient group were terminated at 14 dpi. At cull terminal blood samples were taken for serum and for PBMC isolation. Spleens were collected into RPMI media for harvesting splenocytes. Nasal washes were also collected at cull. Termination timepoints of donor ferrets were determined by availability of staff to carry out culls and necropsy. The recipient ferrets were culled on 14 dpi to allow for seroconversion to occur.

5.4 Results

5.4.1 Nasal wash cell counts and titres in donor and recipient ferrets

Nasal wash cell counts (**Fig. 5.4.1.1**) from the first four days of nasal wash collection indicated that not all recipients became infected simultaneously. As the study progressed it became apparent that 2 out of 6 of the recipient ferrets had a productive H3N2 infection. Recipient ferrets 11981 and 12950 showed a rise in nasal wash cells similar to those seen in the donor ferret group. All nasal washes were analysed by plaque assay on study completion to determine if virus had been shed from animals despite a lack of substantially increased nasal wash cell count from some of the recipients. The most effective way to view the data produced was to examine the nasal wash virus titres as individual pairs.

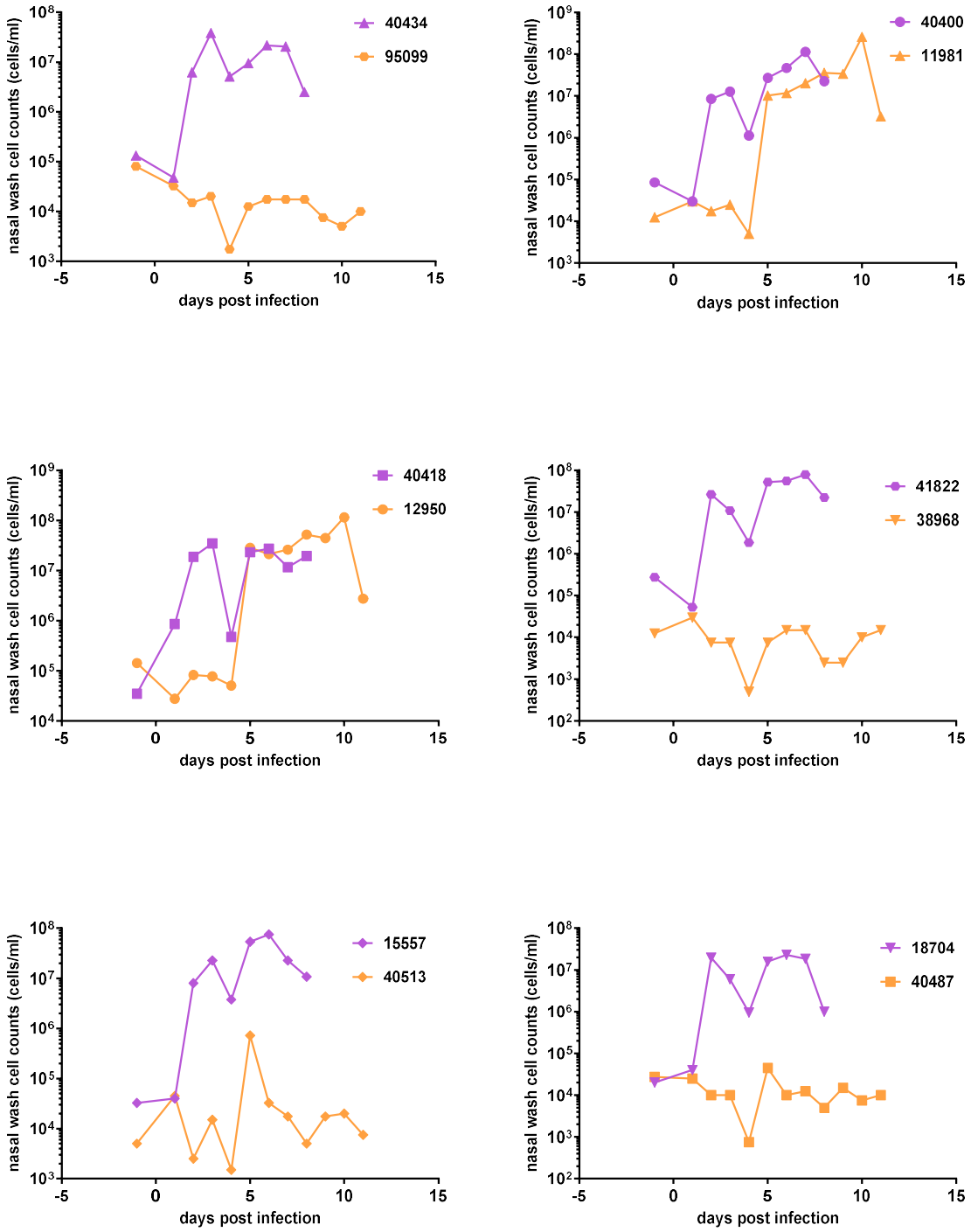

Figure 5.4.1.1 Nasal wash cell counts Nasal washes were collected at 1 to 8/11 dpi. All nasal washes were counted to ascertain the number of cells being shed from each animal at each timepoint. Donor = purple. Recipient = orange.

Figure 5.4.1.2 shows the viral titres determined for each donor and recipient pair. The previously observed double peak of virus production was seen in all of the donor animals at 6 dpi. This second peak has been observed in the previous intranasal infection studies (**Chapter 3**). The first peak in all donor animals occurred at 2 days post infection with a mean viral shedding titre of $2.3x10^5$ pfu/mL. The area under the curve calculation for the two recipients that did shed virus (11981 and 12950) shows that the total amount of virus produced was found to be less than the total amount of virus produced by the donor ferrets. This could be due to the possible low titre of virus received by recipients and due to the route of transmission, aerosol instead of intranasal. Interestingly both 11981 and 12950 appear to have a triple peak of viral shedding at 4, 6 and 8 dpi. This has not been seen previously in any of the low dose intranasally inoculated animals.

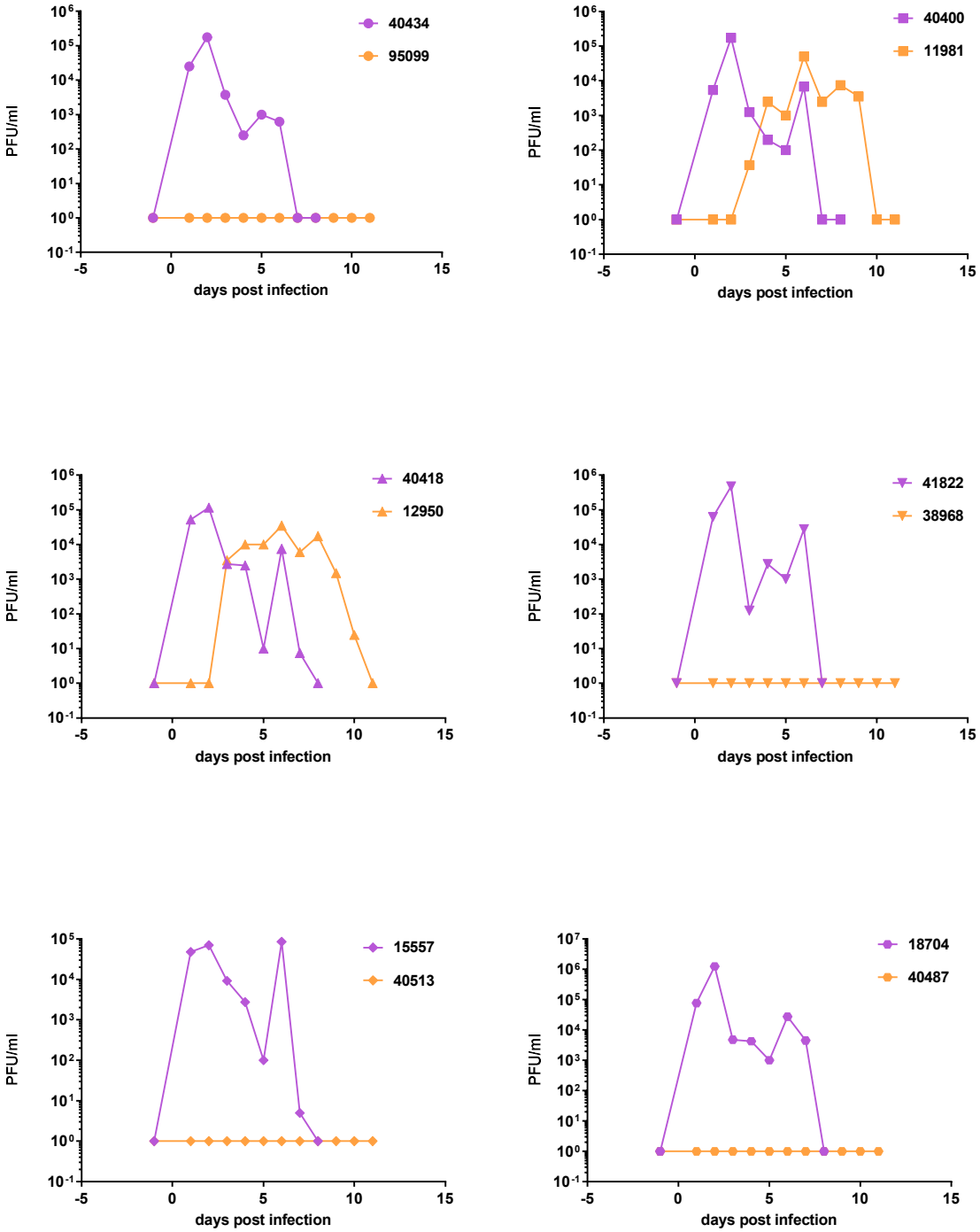

Figure 5.4.1.2 Nasal wash titres Nasal washes were plaque assayed to ascertain viral titres shed from recipient and donor ferrets at all timepoints. Four out of six of the recipient ferrets had no viral titre in their nasal wash. Donor = purple. Recipient = orange.

5.4.2 **Clinical signs of infection in donor and recipient ferrets**

Weight was monitored daily throughout the study. The means for the donor and recipient groups show each group gained weight over the course of the study.

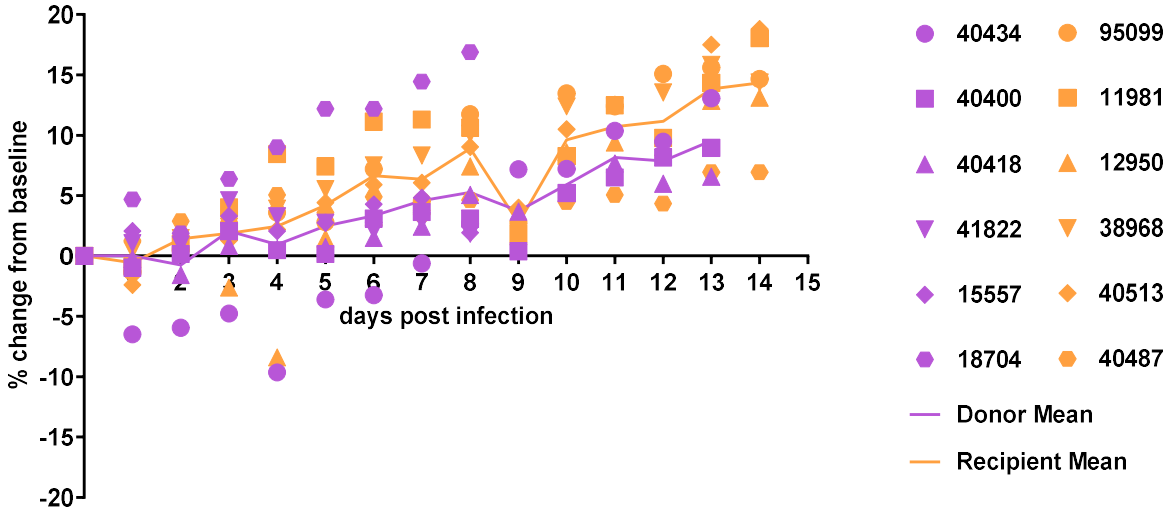

Figure 5.4.2.1 Weight percentage change from baseline. Percentage weight changes for all ferrets from day of infection of donor ferrets.

Weight loss below baseline was observed in three out of six of the donor ferrets; 40434, 40400 and 40418. Ferrets 40400 and 40418 experienced a small negative percentage change in weight from baseline over 1 and 2 dpi but then proceeded to stay at a weight above baseline for the remainder of the study. The weight of the three remaining donors, 41822, 15557 and 18704, all stayed above baseline for the duration of the study.

Percentage weight loss below baseline was observed for four out of six ferrets in the recipient group at 1 dpi (of the donor group); 95099, 11981, 12950 and 40513. The recipient ferrets

were placed within their new paired cages at 1 dpi and the weight loss could be attributed to the change in environment as it would be too soon for the weight loss to be due to infection with IAV based on the results from low dose IAV studies.

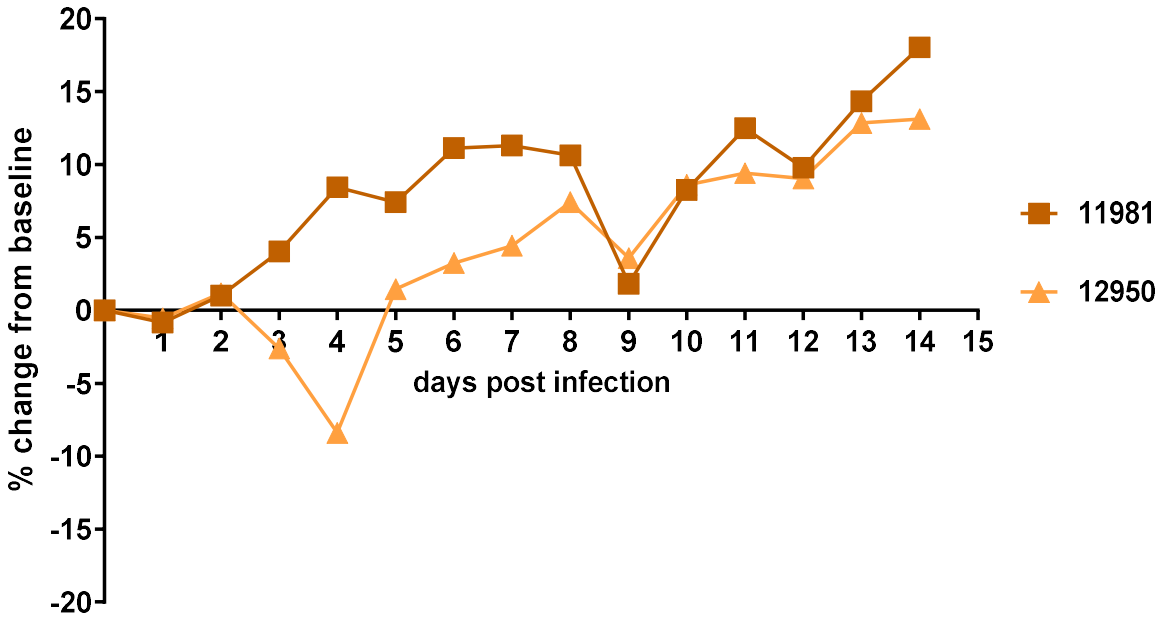

Figure 5.4.2.2 Weight percentage change from baseline. Percentage weight changes for recipient ferrets that shed detectable live virus titre; 12950 and 11981.

Following 1 dpi all ferrets maintained their weight above baseline apart from ferret 12950 which had lost 8.4% of its baseline weight by 3 dpi. Ferret 12950 is one of the two recipient ferrets that became infected (**Fig 5.4.2.2**). The other recipient ferret that became infected, 11981, did not lose any weight below baseline during the study. The recipient ferret group all appeared to lose weight at 9 dpi, with weight gain continuing at 10 dpi. Incidentally the two heaviest donors were the ferrets that successfully infected their paired recipients.

All ferrets in both the donor and recipient groups had normal activity levels throughout the study with no appetite loss or incidence of diarrhoea.

Table 5.4.2.1: Cumulative incidence of nasal discharge and sneezing

Donor	Incidence	Paired Recipient	Incidence
40434	3	95099	0
40400	1	11981	1
40418	7	12950	3
41822	1	38968	0
15557	0	40513	0
18704	1	40487	0

Table 5.4.2.1 shows the cumulative incidence of nasal discharge and sneezing recorded over the course of the study for each ferret. The donor group had several animals with increased sneezing and nasal discharge over 2 dpi to 6 dpi, with ferret 40418 having both the highest incidence of sneezing and nasal discharge. This ferret was paired with one of the successfully infected recipients; 12950. Nasal discharge and sneezing was not recorded in any of the recipient ferrets that were not shedding virus. Recipient ferrets 12950 and 11981 were both recorded to have nasal discharge and sneezing was recorded for 12950 at one time point. This incidence numbers are similar to the rest of the donor group excluding ferret 40418.

5.4.3 **Evidence of seroconversion in donor and recipient ferrets**

The HAI assay (**Fig 5.4.3.1**) confirmed that all donor ferrets seroconverted following infection. Ferrets 15557 and 18704 had slightly lower HAI titres (128 HA units vs >512 HA units) as they were culled and bled at 8 dpi. Had they been allowed to survive to 13 dpi it is probable that their titres would have continued to rise above 128 HA units to >512 HA units. (The dilution point of 1 in 512 was the end point of this HAI assay). The remaining donor ferrets all had HAI titres exceeding 512 HA units. Of the recipients, only ferrets 11981 and 12950 seroconverted.

These results confirm, along with the nasal wash titre results, that these ferrets are the only two recipients to become infected successfully with IAV. The remaining recipient ferrets failed to seroconvert and gave titres expected of naive animals.

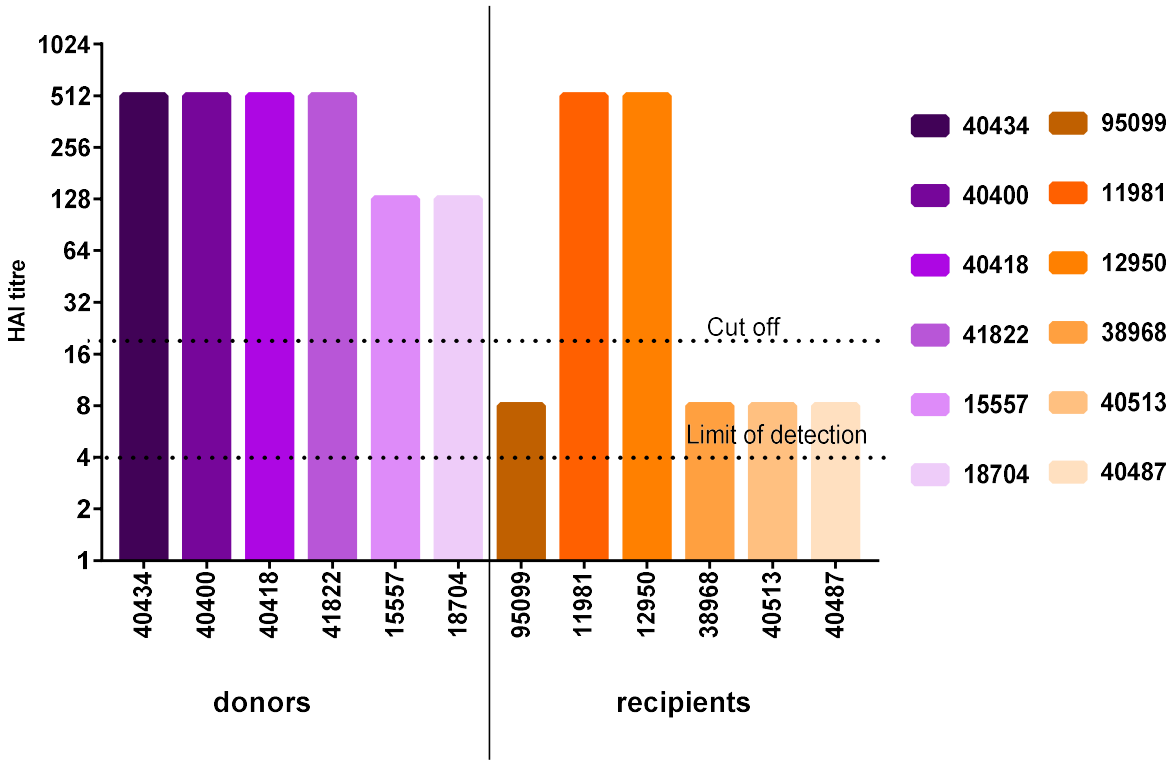

Figure 5.4.3.1 HAI Titres Serum was taken from ferrets at cull. All sera were treated with receptor destroying enzyme (RDE) and HAI assayed against A/Perth/16/2009. Titres of <20 are considered to be seronegative.

5.4.4 Influenza-specific interferon gamma responses present found in the spleen and peripheral circulating blood of donor and recipient ferrets

Splenocytes and PBMCs were isolated as described in the materials and methods, **Section 2.4**. The samples from this study were used to optimise the ELISpot Kit for use with

A/California/04/2009 and A/Perth16/2009 infected ferret tissues and whole blood. Therefore, only a limited number of samples were available for the analysis described. The PBMCs of two recipient ferrets, 12950 and 40513, were tested for influenza-specific IFN-γ responses. Ferret 12950 had shown a productive infection with confirmed seroconversion, while ferret 40513 had shown no signs of successful infection and remained seronegative. In line with these results ferret 12950 (882 SFU) showed significant influenza-specific IFN-γ responses in PBMCs while 40513 (0 SFU) had no detectable influenza-specific IFN-γ responses.

Splenocytes were analysed for donor ferrets 40434, 40418 and recipient ferrets 95099, 38968 and 40487 (**Fig 5.4.4.1**). The three recipient ferrets analysed had no viral titre detected in their nasal wash and remained seronegative when the study concluded. Donor ferrets 40434 and 40418 had influenza-specific IFN-γ responses in the splenocytes. Unexpectedly, the three recipient ferrets, 95099, 38968 and 40487 all had influenza-specific IFN-γ responses (above 850 SFU) suggesting that although the ferrets didn't become infected or seroconvert that they were exposed to the virus enough to trigger a T cell response. For reference naive ferrets inoculated with PBS have low values for influenza-specific IFN-γ responses in the spleen (less than 160 SFU).

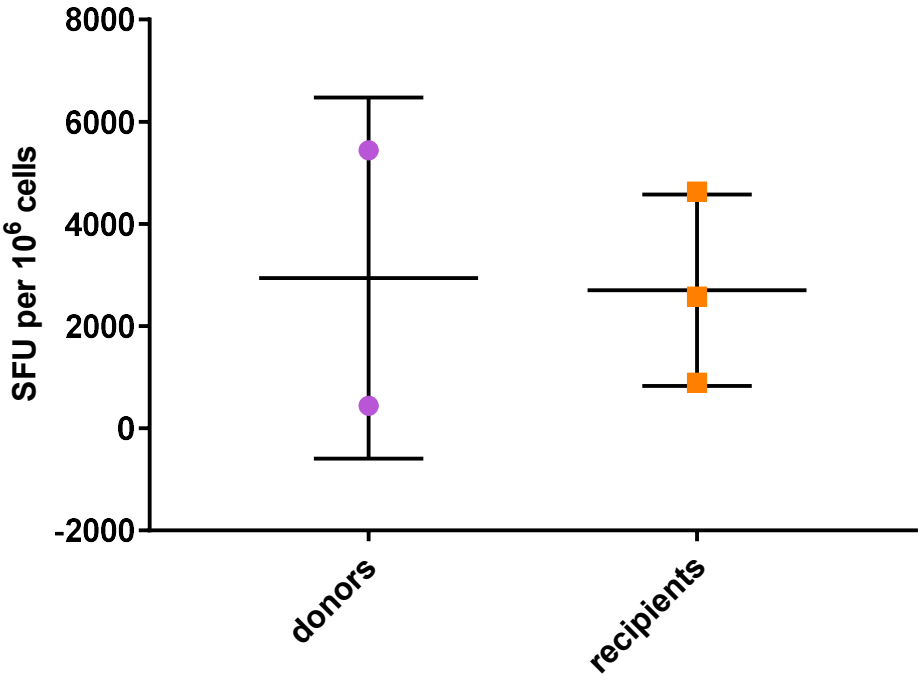

Figure 5.4.4.1 Cellular immune responses seen in the spleen of selected donor and recipient animals Splenocytes were isolated from ferret spleens on the day of cull. Results were normalised by subtracting individual sample allantoic fluid control values from virus stimulated samples. Influenza-specific IFN-γ responses were seen in all ferrets assayed.

5.4.5 **Air Sampling of the Cages**

Air sampling was carried out on 3 of the 6 paired cages due to the availability of air samplers. Cages were randomly selected. These cages were designated at random. The air sampling was carried out on paired cages 1. 41822-38968, 2. 15557-40513 and 3. 18704-40487. None of these recipient ferrets became infected. All filters were processed, and RNA extracted (Qiagen) for analysis using qRT PCR. Interestingly, greater than baseline viral RNA copies were picked up on the filter samples (**Fig. 5.4.5.1**) for all paired cages tested. This suggests that influenza virus was aerosolised by the donor ferret and passed through the transmission cage. The amount of RNA detected at each timepoint varied across the cages and there

appears to be no discernible pattern between each pair. However, each pair does appear to have a 'double peak' in RNA detected. Despite detectable virus in the samplers none of the paired recipient ferrets became infected. This could be because the virus was dispersed into such a low concentration that it failed to successfully infect the recipient ferrets. The detection of viral RNA also indicates the presence of viral copies, it cannot determine if the virus is infectious. Successful infection of ferrets would be defined as recipient ferrets shedding detectable live virus from their nasal washes.

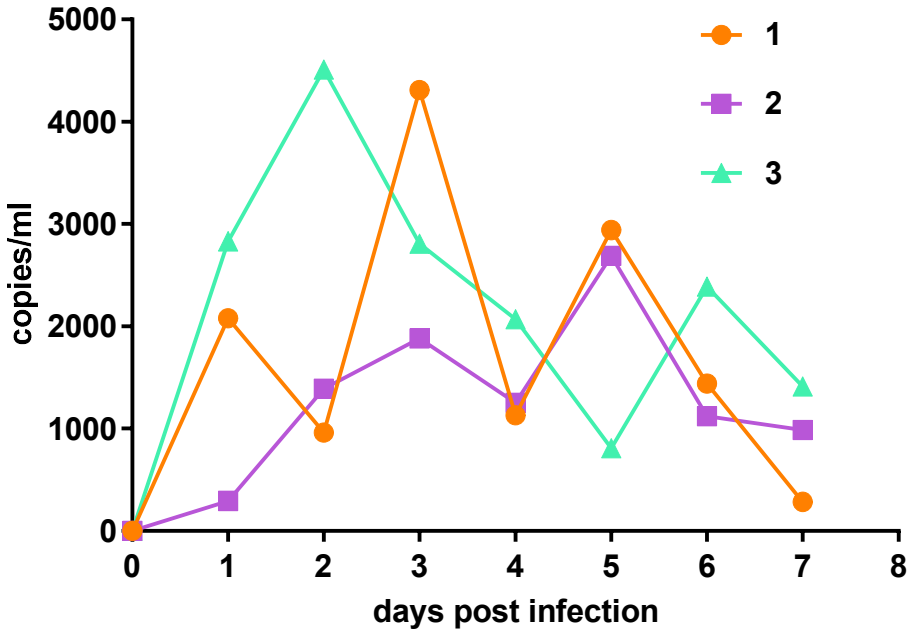

Figure 5.4.5.1 Viral load of air samplers. 1. 41822-38968, 2. 15557-40513 and 3. 18704-40487. Filters were melted in 1ml of PBS when removed from the air samplers following the 8-hr sampling period. Copies per milligram were calculated by using a standard curve as detailed in **Chapter 2 Materials and Methods**.

5.5 Discussion

When this study was designed, it was intended to be a preliminary investigation into the aerosol transmissibility of A/Perth/16/2009. At the time it wasn't deemed critical that the ferrets be of a weight, sex or from a particular origin (**Table 5.3.3.1**). However, this may have influenced the outcome. For example, larger ferrets, with a greater tidal volume would be able to produce a larger volume of aerosol over the infection period. Both the recipient ferrets that became infected were paired with the two largest ferrets 40400 and 40418 respectively.

A relatively high dose of $1x10^5$ pfu of virus per animal was used to inoculate ferrets to ensure that donor ferrets would become infected, start shedding virus and therefore be able to transmit the virus to recipients. However, considering the results obtained in **Chapter 3**, a lower dose of $1x10^2$ pfu of virus per animal would have been a robust inoculation dose and may have led to more virus shedding in total than the $1x10^5$ pfu dose (Marriott *et al.*, 2014). Transmission only partly corresponded with the amount of sneezing and nasal discharge in donors, and the successful transmission donors did not have significantly higher peak titres in nasal wash.

Comparing the two infected recipients to the four uninfected recipients, nasal wash counts, and sneezing and nasal discharge were clear clinical markers for infection, whereas weight loss was of no value in determining infection. The observation of influenza-specific IFN-γ responses in HAI negative ferrets raises the possibility that the IFN-γ ELISpot is more sensitive to sub-infectious influenza dose than antibody response but is only based on a single observation from three ferrets assayed.

It was noted that the viral titres of the two infected recipients reached roughly the same peak titres ($1x10^5$ to $1x10^6$ pfu/ml) seen in ferrets inoculated with a low dose H3N2. There appeared to be a triple peak seen in the two recipients, this contrasts with the distinctive double peak seen in the viral kinetics of ferrets infected intranasally with a low dose.

Crude cage sampling was carried out between 3 out of 6 of the paired cages. Viral RNA was detected passing between the cages but none of the recipient ferrets became infect. It would have been advantageous if all paired cages were included in the air sampling to allow comparison of results between successfully infected recipients and recipients that did not become infected. Subsequent studies have shown that live virus can be plaque assayed from air sample filters (Bekking *et al.*, 2019), therefore it would have been advantageous if samples had been taken for quantification of live virus. This would have allowed a picture of how much live virus was present in the air samples.

5.6 Further Work

This study was designed with the intention that all recipient ferrets would be infected successfully. There could be numerous reasons why only 2 out of 6 ferrets became infected. There are no published transmission studies using the A/Perth/16/2009 strain and other studies that do use H3N2 strains have very small group sizes (Gustin *et al.*, 2011, Herlocher *et al.*, 2001) and use different cage set ups and airflows (MacInnes *et al.*, 2011).

A transmission study using a bioluminescent H1N1 A/California/04/2009 that encoded a luciferase provided a snapshot of influenza infection and transmission by *in vivo* imaging (Karlsson *et al.*, 2015). This studydemonstrated that IAV was able to successfully enter the

respiratory tract of the ferrets, however a successful infection was not established as identified by virus in nasal washes or seroconversion. This suggests that the infection could be sub clinical. The ferret antibody responses were assessed using microneutralisation (MN) assays and a humoral immune response was confirmed despite no virus being shed. The MN assay has been shown to give a similar result to HAI assays. In the study discussed in this chapter recipient ferrets that did not shed live virus also did not have an HAI titre, therefore it can be assumed that these ferrets did not become infected with virus.

Going forward using a low ($1x10^2$ pfu/ferret) donor inoculum would allow for extended shedding of virus which would mean a longer period of exposure for recipient ferrets. This longer window of exposure could help boost the chances of recipient ferrets becoming infected. Additionally, using an alternative H3N2 isolate which is found to transmit better than A/Perth/16/2009, could be an option if attempting to successfully infect all recipient ferrets. Using a larger sample size could also be an improvement, potentially allowing for statistics to be performed; however, there are ethical considerations to consider when using a large number of ferrets for subsequent studies.

Recently a study evaluation of bioaerosol samplers was published (Bekking *et al.*, 2019) using H1N1 and H3N2 strains. It assessed the differences between a polytetrafluoroethylene filter (PTFE filter), a 2-stage National Institute of Occupational Safety and Health cyclone sampler (NIOSH cyclone sampler) and the 6-stage viable Andersen impactor (Andersen impactor). They showed that the PTFE and NIOSH samplers were both useful for influenza virus RNA collection for clinical and environmental samples (Bekking *et al.*, 2019). This is encouraging as the PFTE sampler used in this published study is similar to the sampler used in this transmission cage study. If further transmission cage studies were to take place samplers would need to be placed in between each paired cage. This would allow a comparison of the

amount of viral RNA passing between the cages of infected and non-infected recipients. It would answer whether the amount of viral RNA collected from the air passing through the cages has an effect on the ability of the recipient ferret to become infected, or if there is another factor involved in the ability of the virus to infect.

A clear improvement on this transmission work would be to carry out more extensive and complete cellular immune response analysis on recipient ferrets. This would include collecting spleen, whole blood and lung samples at study termination for analysis of influenza-specific IFN-γ responses using ELISpot. It would also be useful to take sequential small volume whole blood samples to build a time course of influenza-specific IFN-γ responses circulating in the periphery using ELISA. These results would confirm how reproducible the influenza-specific IFN-γ response seen in otherwise virus negative animals is.

5.7 Conclusions

It is evident from these results that evaluation of transmission using transmission cages and paired recipient and donors is complex. The aim of this model was to represent a more natural route of transmission compared with the nose-only aerosol route evaluated previously. Successful transmission between donors and recipients occurred between two out of six paired ferrets. This could be due to a several variables that were present in the study e.g. weight. However, the study did show that A/Perth/16/2009 is able to be transmitted between ferrets without contact, although the transmission rate may be less than 100%.

6 Comparison of H3N2 and H1N1 Subtypes in the Intranasal Ferret Model

The two circulating seasonal subtypes of IAV in humans are currently H3N2 and H1N1. The H1N1 virus originated from the 2009 influenza pandemic caused by a triple reassortment of human, swine and bird type A influenza (Neumann *et al.*, 2009), while the current seasonal H3N2 strain originated from the 1968 Hong Kong pandemic when genomic exchange of RNA occurred between human and avian viruses (Wendel *et al.*, 2015). While this work was being undertaken several studies using a seasonal H1N1 strain, A/California/04/2009, took place. Comparing these two clinically relevant strains allows for assessment of the intranasal model further.

6.1 Aims

The aims of this chapter are to compare and contrast the H3N2 and the H1N1 intranasal infection models:

- to ascertain if there are any similarities or differences between the ability of the two seasonal influenza strains to establish an infection.
- to establish if the viral kinetics of both viruses is similar in the low dose intranasal ferret model.
- to investigate if the cellular immune response elicited in the ferret by each virus is the same.

6.2 Intranasal Comparison Outline

The data from **Chapter 3, Section 3.6** is used here for comparison against a low dose H1N1 intranasal model arm of **Study 5549** (appendix 1). Results for the H1N1 infected ferrets were generated and analysed separately from this project but are being used here to examine the similarities and differences between the two main seasonal subtypes of currently circulating IAVs; H3N2 and H1N1. This data contributes to the publication attached to this thesis (Ryan, Slack *et al*. 2018).

6.2.1 **Ferrets**

Table 6.2.1 Ferret Identification Numbers

H3N2 Low Dose (5719)	H1N1 Low Dose (5549)	Mock (5549)
86654, 86811, 86809, 86659, 86812, 86660	**46707,50573, 52238, 47025, 48889, 46915**	**55432, 45891, 53132, 49686, 52094, 45627**

Ferrets were intranasally infected with previously characterised low dose of influenza ($1x10^2$ plaque forming units (PFU) per ferret) of either A/California/04/2009 (H1N1) (Marriott *et al.*, 2014) or A/Perth/16/2009 (H3N2) (**Chapter 3**).

Female ferrets were obtained from Highgate Farm, UK and were 4-6 months at the time of the study. A total of 18 ferrets were used. All ferrets were culled at 14 days post infection. Ferrets were group housed in floor pens designed in accordance with the requirements of the United

Kingdom Home Office Code of Practice for the Housing and Care of Animals Used on Scientific Procedures (1989).

6.2.2 **Prior to Inoculation**

At seven and three days prior to inoculation ferrets were fully sedated by an intramuscular injection of Ketamine/Xylazine (1ml Ketamine (100mg/ml) plus 0.4ml Xylazine (20mg/ml) given at a dose of 0.25ml/Kg bodyweight). At -7 dpi whole blood samples were collected from all ferrets. At -3 dpi whole blood samples were collected from all ferrets. These two whole blood samples were used to calculated baseline values for the IFN-γ ELISA. Additional baseline blood samples were taken at -3 dpi from the anterior vena-cava vessel of each ferret, 2ml blood collected into SST tubes for sera isolation and a baseline nasal wash was performed. Sera were tested by HAI for the presence of any pre-existing antibodies to influenza H3N2 A/Perth/16/2009. All baseline sera samples had titres of less than 4 HAI units to H3N2 A/Perth/16/2009, and it was deemed that these ferrets had no previous exposure to H3N2 and so were suitable for challenge.

6.2.3 **Virus**

Ferrets were fully sedated by an intramuscular injection of Ketamine/Xylazine (1ml Ketamine (100mg/ml) plus 0.4ml Xylazine (20mg/ml) given at a dose of 0.25ml/Kg bodyweight). Ferrets were inoculated intranasally with either H3N2 A/Perth/16/2009 P+2A or H1N1 A/California/04/2009 P+3H challenge stock virus diluted in PBS to provide $1x10^2$ PFU/ferret. The dose was confirmed on day of administration by back-titration. Each animal was inoculated with a volume of 0.2ml by the intranasal route.

6.2.4 **Sample Collection**

Following inoculation, weight was recorded daily, and clinical signs recorded twice daily. Temperatures were not recorded. Nasal washes were collected from 1 to 8 days post infection. Whole blood samples were collected from all ferrets at 2, 5, 8 11 and 14 days post infection. Ferrets were sedated by intramuscular injection of Ketamine/Xylazine (1ml Ketamine plus 0.4ml Xylazine) given at a dose of 0.25ml/Kg bodyweight. Following overdose samples were collected from each ferret; nasal wash, blood in SST for serum and blood into heparin tubes for PBMCs. Lungs were collected into RPMI 1640 media.

6.3 Results

6.3.1 **Nasal wash cell counts and titres**

Nasal wash cell counts from all influenza infected ferrets began to increase between 2 and 4 dpi whilst mock infected ferrets did not increase over the 8 days of monitoring (**Fig 6.3.1.1**). As anticipated, there was a significant difference found between the virus infected groups and the mock groups (P 0.022). No significant difference was found between the total amounts of cells shed between the groups infected with H1N1 and H3N2 (P 0.7104)

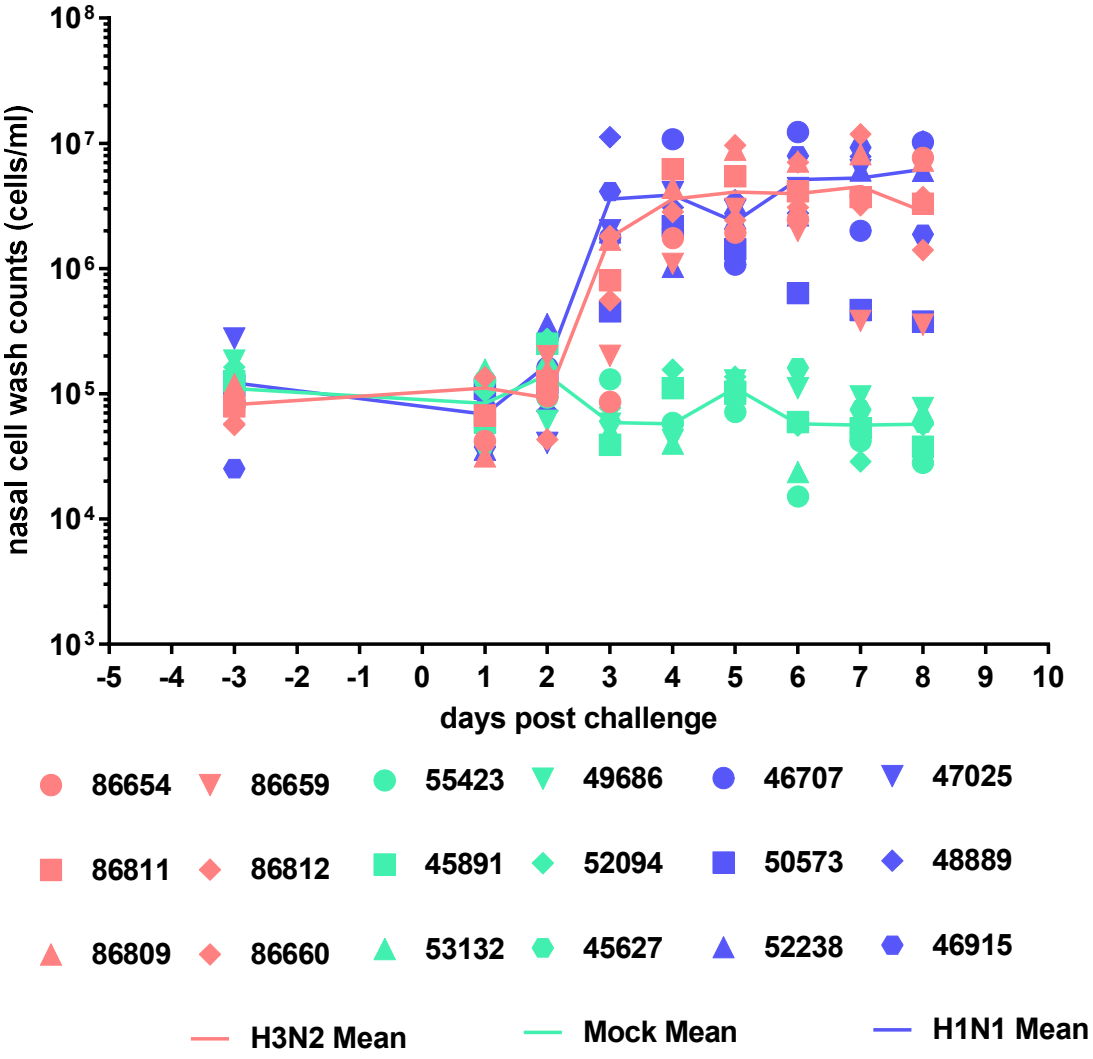

Figure 6.3.1.1 Nasal wash cell counts. Nasal washes were collected at 1 to 8 dpi. All nasal washes were counted to ascertain the number of cells being shed from each individual ferret at each time point (n=18). The area under the curve was calculated for the H3N2 (n=6), H1N1 (n=6) and mock (n=6) groups. A Mann-Whitney test was performed and a statistical difference (P 0.022) was found between ferrets intranasally infected with both A/Perth/16/2009 (H3N2 group), and A/California/04/2009 (H1N1) and the PBS (mock group). There was no significant difference (P 0.7104) found between the ferrets intranasally infected with A/Perth/16/2009 (H3N2 group) and A/California/04/2009 (H1N1 group).

Nasal washes were tested for the presence of replicating virus (**Fig 6.3.1.2**). As mentioned previously, 4 out of 6 ferrets infected with H3N2 began to shed detectable virus at 1 dpi. The

remaining two ferrets, 86654 and 86660, began to shed detectable virus at 2 dpi. All ferrets infected with H1N1 began to shed virus at 1 dpi. Viral shedding for ferrets infected with H3N2 peaked at 3 dpi, compared to ferrets infected with H1N1 which peaked at 2 dpi. The peaks were followed by a decrease in virus load and a subsequent smaller, second peak at 5 dpi (H1N1 group) and one at 6 dpi (H3N2 group) that has been seen previously.

The peak shedding titre was found to have a strong positive correlation and significance (R +0.986, P <0.0001) with the total virus shed from the H3N2 and H1N1 groups. Consequently, as seen previously, the more virus shed by an animal the higher the peak titre of virus found in nasal wash.

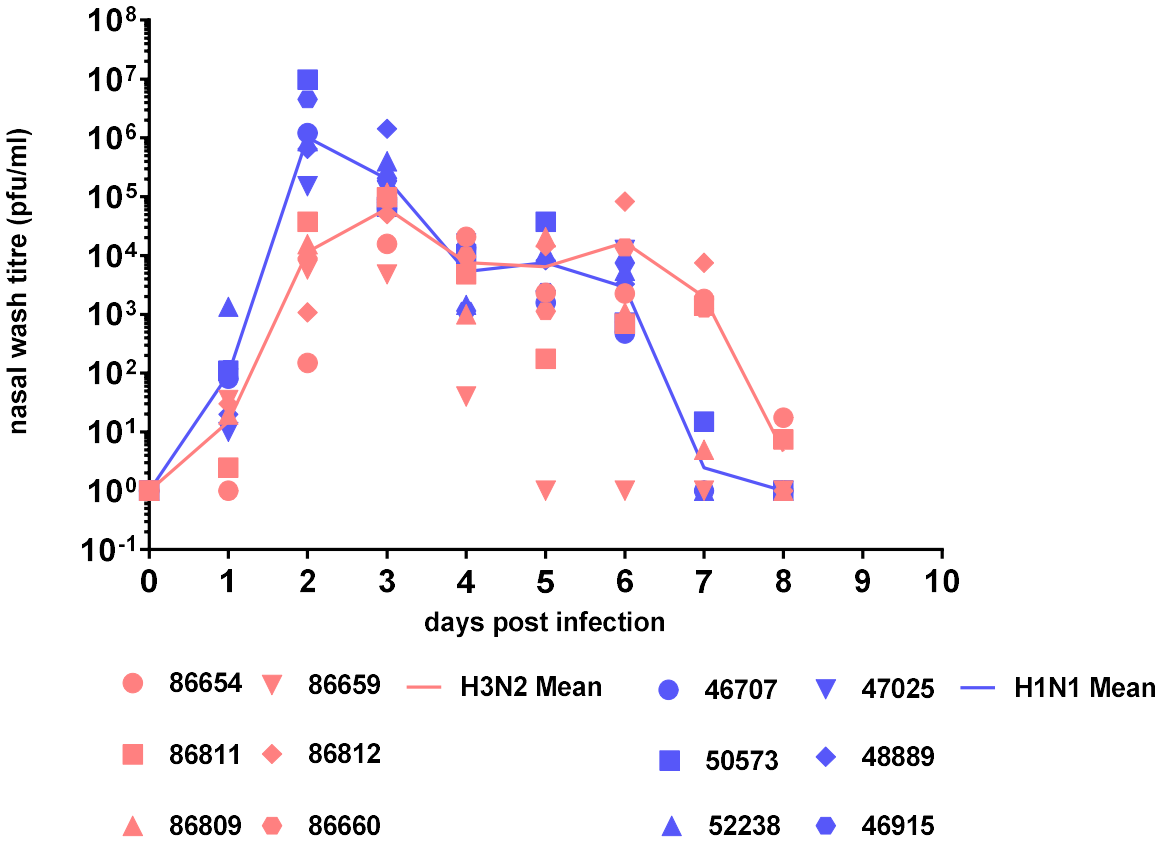

Figure 6.3.1.2 Nasal wash titres. Nasal washes were subsequently plaque assayed to ascertain the amount of virus being shed from each individual ferret at all time points collected. The area under the

curve was calculated for the H3N2 (n=6) and H1N1 (n=6) groups to ascertain the amount of virus shed. A Mann-Whitney test was performed and a statistical difference (P 0.022) was found between the amount of virus shed by ferrets intranasally infected with A/Perth/16/2009 (H3N2 group) and A/California/04/2009 (H1N1 group), with the H1N1 group shedding the most. Ferrets were monitiored up to day 14. No virus was shed after day 14.

6.3.2 **Clinical signs of infection**

All ferrets were monitored twice daily for sneezing, nasal discharge, inactivity, diarrhoea and loss of appetite. As per **Section 2.3.4**, activity level was scored as **0** for normal, **1** for reduced activity and **2** for inactive. Animals infected with H1N1 showed more severe clinical signs compared to ferrets infected with H3N2. In particular, the H1N1 infected ferrets presented with sneezing, nasal discharge and inactivity. By contrast, the H3N2 infected ferrets presented with sneezing only, suggesting that this H3N2 virus produces a much milder disease in ferrets that the H1N1 A/California/04/2009.

Table 6.3.2.1 Cumulative incidence of nasal discharge, sneezing and inactivity.

Group	Total Nasal Discharge	Total Sneezing	Total Inactivity
H3N2	0	24	0
H1N1	10	27	48*
Mock	0	0	0

*This score is the sum of 48 recorded incidences of reduced activity. A score of 1= reduced activity, a score of 2= inactive.

Weight was monitored daily for each ferret. Overall, weight loss from baseline **(Fig 6.3.2.1)** was seen in both the H3N2 and H1N1 groups. The mock group of ferrets gained weight over

the course of monitoring. The weight loss recorded in the H1N1 infected animals was more severe than that recorded in the H3N2 animals, with a mean peak of -5% weight loss from baseline for the H1N1 compared to a peak of -2.5% weight loss from baseline for H3N2 infected animals. This combined with the clinical observations suggests that seasonal H1N1 produces a more severe clinical infection in ferrets when compared to a seasonal H3N2 strain.

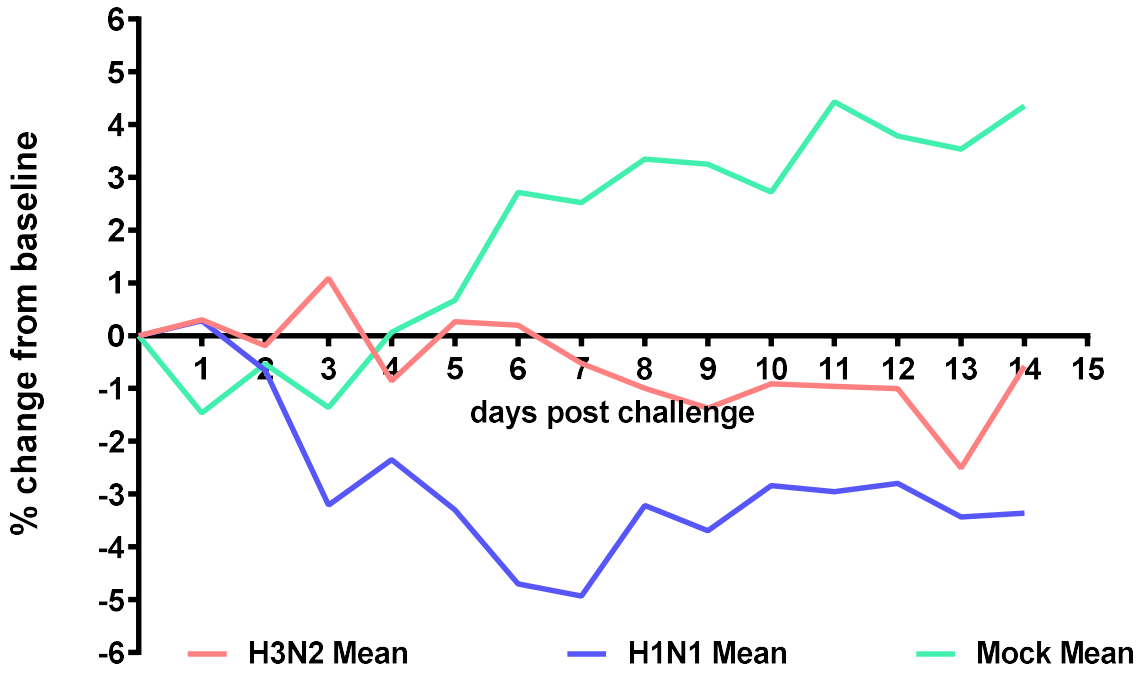

Figure 6.3.2.1 Weight percentage change from baseline. Mean percentage weight change of ferrets infected with H3N2 (n=6), H1N1 (n=6) and PBS (n=6).

6.3.3 **Evidence of seroconversion in ferrets**

HAIs were performed on sera of all ferrets. As previously reported in **Section 3.6**, all ferrets inoculated with H3N2 gave HAI titres of ≥512 to A/Perth/16/2009. Ferrets in the mock group inoculated with PBS had HAI titres of <4 to the corresponding viruses confirming they were not infected. All ferrets inoculated with H1N1 also gave HAI titres of ≥512 to A/California/04/2009. These results confirm that both groups of ferrets inoculated with H3N2

and H1N1 were successfully infected with virus and gave a robust humoral immune response to the corresponding strain of inoculation.

6.3.4 **Longitudinal time course of influenza-specific IFN-γ responses in the periphery**

Small volumes of heparinised whole blood were collected from all ferrets at -7, -1, 2, 5, 8, 11, and 14 dpi to assess the influenza-specific IFN-γ responses in peripheral blood. Samples from each ferret were assessed by ELISA and a longitudinal time course of influenza-specific IFN-γ responses was produced (**Fig. 6.3.4.1**). Two samples were collected prior to infection to demonstrate that there were limited influenza-specific IFN-γ responses in the ferrets prior to infection. All ferrets were found to have responses below 270 pg/ml of IFN-γ in pre-infection samples. These responses were averaged for each animal and represented by the 0 dpi time point (**Fig. 6.3.4.1**). Following infection with either H1N1 or H3N2, low level influenza-specific IFN-γ responses were detectable in ferrets at 5 dpi and increased at 8 and 11 dpi with responses peaking at 11 to 14 dpi. At 14 dpi, responses in the majority of ferrets appear to decrease while some others continue to increase. This variation could be due to the outbred nature of the ferrets. There was no significant difference (P 0.3939) found between the total influenza-specific IFN-γ produced by whole blood from ferrets infected with the H1N1 and H3N2 subtypes. Ferrets in the mock group inoculated with PBS had responses below 270 pg/ml over the 14 days.

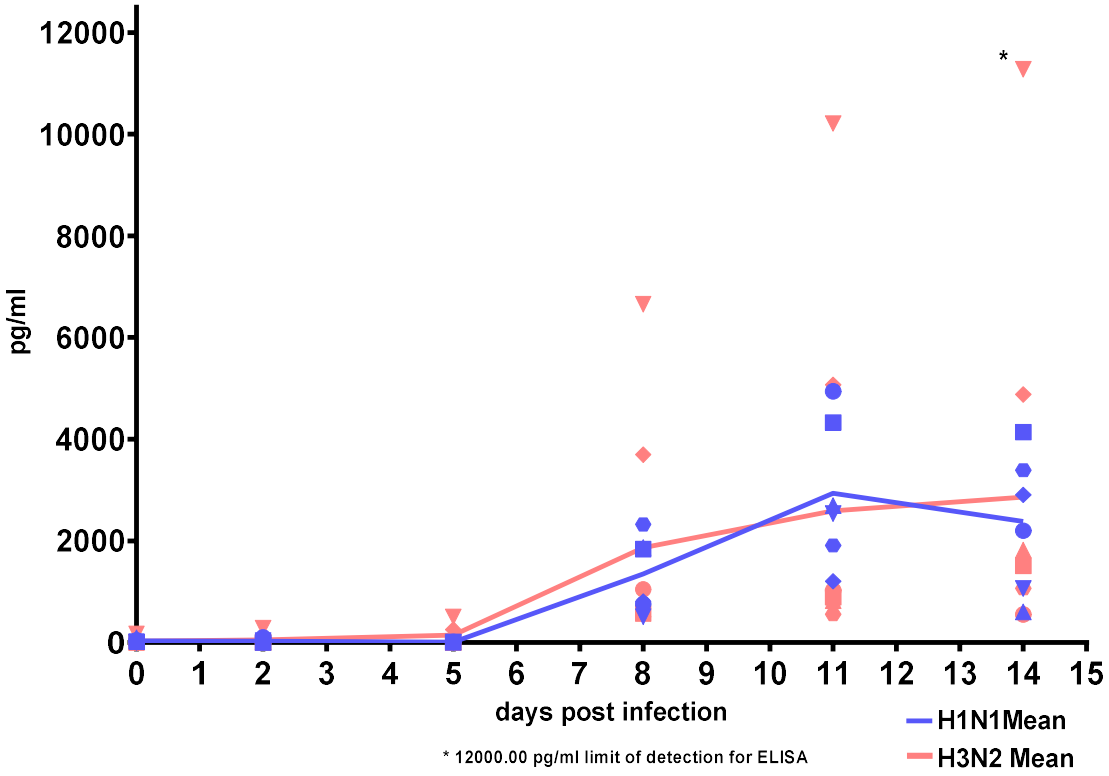

Figure 6.3.4.1 Quantification of influenza-specific IFN-γ production by ELISA. Diluted whole blood samples were collected from all ferrets at -7, -1, 2, 5, 8, 11, and 14 days post infection, stimulated with appropriate antigens and the supernatants harvested. Supernatants were used in the Ferret IFN-γ ELISA Development Kit (ALP). Influenza-specific IFN-γ responses became detectable at 5 days post infection with a peak at 11-14 days post infection for all virus infected animals. No responses were detected in the mock group. A Mann-Whitney test was performed and no statistical difference (P 0.3939) was found in the total influenza-specific IFN-γ detected between ferrets intranasally infected with A/Perth/16/2009 (H3N2 group) and A/California/04/2009 (H1N1 group).

6.3.5 **Cellular immune responses measured by ferret specific IFN-γ enzyme linked immunospot assay (ELISpot)**

Animals were culled at 14 dpi. Lymphocytes were isolated from whole lung (lung MNCs) (**Fig 6.3.5.1b**) and whole blood (PBMCs) (**Fig 6.3.5.1a**) and the number of IFN-γ secreting cells was quantified by ferret-specific INF-γ ELISpot. A significant difference was found in the number of cells producing influenza-specific IFN-γ responses in H1N1 infected animals compared to H3N2 infected animals (P 0.0043) (**Fig 6.3.5.1b**). Additionally, it found a significant difference in the responses between the mock group and H1N1 group (P 0.0022). Comparison of lung MNCs in influenza and mock infected group showed no significant difference in the influenza-specific IFN-γ responses for mock group and H3N2 group. As mentioned previously in **Section 3.6**, only one of the H3N2 infected ferrets was found to have influenza-specific IFN-γ responses in lung MNCs, no responses were detected in remaining ferrets. A moderate positive correlation for all virus groups were found between the peak virus titre shed and the number of lung MNCs secreting influenza-specific IFN-γ (R -0.6767, P 0.0043). A positive correlation was found between the total amount of virus shed by ferrets and the number of lung MNCs secreting influenza-specific IFN-γ (R +0.7396, P 0.0088).

Both virus infected groups showed a significant increase in the number of influenza-specific INF-γ secreting PBMCs when compared to the mock group 14 dpi (H1N1 P 0.0022, H3N2 P 0.0022). No significant difference (P 0.1797) was observed between the number of PBMCs producing influenza-specific IFN-γ responses in the H1N1 and H3N2 groups (**Fig. 6.3.5.1a**).

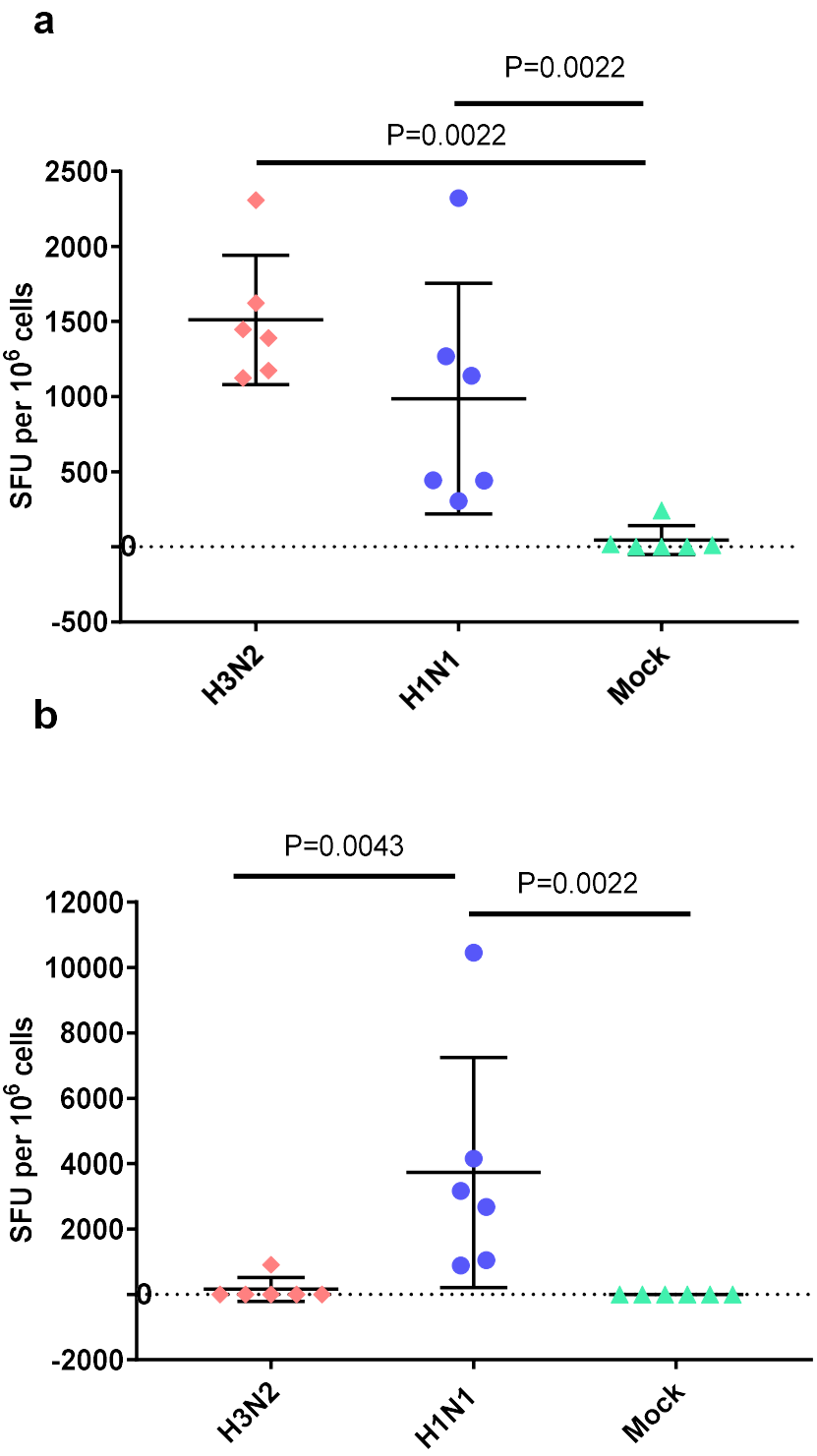

Figure 6.2.5.1. Cellular immune responses in ferrets infected with A/Perth/16/2009 and A/California/04/2009 PBMCs **(a)** and Lung MNCs **(b)** were collected form all animals (n=18) at 14 dpi. Results were normalised by subtracting the individual sample allantoic fluid control values from virus stimulated sample values. **(a)** Influenza-specific IFN-γ responses in PBMCs were seen in all ferrets

inoculated with virus. **(b)** Influenza-specific IFN-γ responses in lung MNCs. The values measured for each ferret are plotted as spot forming units (SFU) per million cells. Bars show mean and standard deviation for each group.

6.3.6 **Discussion**

It has previously been demonstrated, using the H1N1 A/California/04/2009 virus, that there is an approximately 100-fold increase in the inflammatory immune cell count in the nasal wash when infecting animals at a dose of $1x10^2$ PFU, with a delay in peak cell count compared to infection with a high dose ($1x10^6$ PFU). This suggests a delay in the activation of inflammatory immune cell response found in the nasal wash which comprises of mostly neutrophils and monocytes/macrophages (Chen *et al.*, 1995). During this thesis this increase did not occur in ferrets infected with a $1x10^2$ PFU of the H3N2 A/Perth/16/2009 virus compared to $1x10^6$ PFU, where nasal cell wash counts were approximately the same for both amounts of virus.

However, it has also been shown during this thesis that a lower challenge dose of H3N2 does not lead to reduced virus shedding, but instead leads to increased shedding both in terms of total virus shed over the course of the infection, and peak titre of shed virus. This has also been reported for H1N1 A/California/04/2009 (Marriott *et al.*, 2014). This comparison has demonstrated that ferrets infected with a low dose of H1N1 virus shed significantly more virus over an 8 day period compared to ferrets infected with an equivalent dose of H3N2 virus. This also correlates strongly with the peak shedding titre seen in the ferrets, with H1N1 infected ferrets having a higher peak shedding titre than animals infected with H3N2 virus. This comparison has also highlighted that a low dose of H1N1 produces a more severe clinical disease in ferrets when contrasted with the milder H3N2 low dose infection. It has been shown that the H1N1 subtype that emerged during the 2009 pandemic has distinct clinical features.

For example, in several animal models it has been show to cause severe inflammation in the lungs leading to respiratory failure and in some cases, death (Itoh *et al.*, 2009, Fraser *et al.*, 2009). This contrasts with the milder seasonal H1N1 that was circulating endemically in the human population pre-2009.

Comparison of the H1N1 and H3N2 influenza-specific IFN-γ time course in peripheral blood shows a similar pattern of responses in ferrets infected with either subtype. These results, combined with the PBMC ELISpot results, obtained at 14 dpi, suggest that the influenza-specific IFN-γ response seen in ferrets infected with H1N1 and H3N2 is not differentiated by subtype and is instead comparable across both strains in the periphery. It has been established previously that the increase in the number of IFN-γ producing lymphocytes following challenge suggests an expansion of the numbers of influenza-specific T cells as a consequence of progressive viral infection (Martel *et al.*, 2011). Similar kinetics of influenza-specific IFN-γ responses in PBMCs have been reported in pigs infected with a swine influenza (H1N2) virus (Talker *et al.*, 2016). This suggests that the influenza-specific IFN-γ responses seen in the periphery do not vary significantly between seasonal strains or perhaps even host; however, it is possible that the responses seen in a more clinically severe strain, such as H5N1 or H7N9, may be different. Although the responses observed in the periphery are not direct representations of the responses at the site of infection it is valuable to monitor the cellular immune response across a time course, especially in a model where only small volumes of blood can be collected.

The key significant difference seen between the groups of infected ferrets was the number of influenza-specific IFN-γ producing cells seen in lung MNCs of ferrets infected with H1N1 compared to H3N2 infected ferrets and the mock group. It has previously been shown that A/California/04/2009 can be detected in the lung following low dose intranasal infection

(Marriott *et al.*, 2014). These results are in line with the viral burden and pathology seen in the lungs of ferrets infected with H3N2 A/Perth/16/2009 in this thesis (**Section 3.4**), and with ferrets infected with H1N1 A/California/07/2009 in published (Marriott *et al.*, 2014), and unpublished data generated by the Influenza Group at Porton Down. qRT-PCR data in **Section 3.4** showed that vRNA copies were not readily detected in the lungs of ferrets infected with H3N2 A/Perth/16/2009. Only one ferret out of eight tested has vRNA present in the lungs at 4 dpi. However, all ferrets were successfully infected, producing live virus in their nasal washes. This is in comparison to ferrets infected with H1N1 A/California/04/2009 in published data (Marriott *et al.*, 2014) that shows vRNA present in the lungs of ferrets at 1, 2, 4 and 5 dpi, and unpublished data that shows vRNA in the lungs of ferrets at 2, 3, 4 and 8 dpi.

Data in **Section 3.4** shows that there is minimal pathology found in the lungs of ferrets infected with a low dose of H3N2 A/Perth/16/2009. In comparison published data (Marriott *et al.*, 2014) shows that at 4 and 5 dpi the lung pathology of low dose H1N1 A/California/04/2009 ferrets ranges from minimal to marked, exhibiting a much higher frequency and severity of pathological observations compared to the H3N2 virus. These results correlate with evidence showing that the H1N1 subtype that emerged in 2009 has a lung tropism, predominately replicating in alveolar pneumocytes of the lung and possibly infecting lung dendritic cells (Bhatnagar *et al.*, 2013). Evidence also shows that H1N1 replicates efficiently in the lungs of mice (Belser *et al.*, 2010) and ferrets (Maines *et al.*, 2009). In contrast, it has been reported that seasonal H3N2 infrequently go to the lungs of ferrets (Music *et al.*, 2014, Carolan *et al.*, 2014, Gustin *et al.*, 2011, Roberts *et al.*, 2012, van den Brand *et al.*, 2012, Roberts *et al.*, 2011). This suggests that the influenza-specific IFN-γ responses seen in lung MNCs of ferrets infected with H1N1 was due to virus causing infection in the lungs. In comparison the lungs of ferrets infected with H3N2 have either no or very low influenza-specific IFN-γ responses.

This comparison also demonstrates that it is possible to successfully evaluate cellular immune responses to seasonal influenza infection over a time-course in the ferret and reveals that there are differences in the immune signatures induced by different influenza strains. Using these complementary techniques, it has been illustrated that the responses to H1N1 and H3N2 infections in the lung were markedly different and correlated well with known tropisms of the virus strains used.

7 General Discussion

7.1 Chapter Summary

Viral respiratory tract infections are a leading cause of morbidity and mortality worldwide. Influenza A virus is a major contributor to to this, however there are several other key contibuters; measles virus (MV), respiratory syncytial virus (RSV), rhinovirus, adenovirus and coronavirus. All of these viruses can be transmited via the routes discussed previously; contact (direct or indirect), droplet and aerosol. Transmission in humans via each of these routes is complex and depends upon many variables including; environmental factors (e.g. humidity, temperature) and social factors (e.g. occupation, over-crowding) as well as host factors (e.g. receptor distribution). Each of these variables can affect the different transmission routes of these respiratory viruses in a dissimilar way resulting in difficulties investigating them experimentally both in humans and in animal models (Kutter *et al.*, 2018).

This piece of work has contributed to the further understanding of the influenza ferret model and to the ferret model as a whole. For example, based on findings here, when the ferret model is being used for the investigation of a new emerging respiratory pathogens the intranasal route of infection should be selected over the nose only aerosol and transmission cage models. This, and other published work demonstrates that the intranasal route is easlily reproducible and would allow for less variability infection rates if the new pathogen could successfully replicate the ferrets. Ideally when infecting the ferret for the first time intransally a dose ranging study would be conducted to ensure that the correct concentration of pathogen was delivered. However, despite a dose of 10^2 pfu working well for an influenza infection in the ferret, this does not mean that it would work well for other respiratory viruses. Potentially higher doses would need to be considered. Volume of inoculum would also need to be taken into account when developing a new model of infection in the ferret. For instance, if a disease

of the lower respiratory tract was required then a volume of 1ml would be used preferentially over the volume of 0.2ml used in this work based upon published data (Belser *et al.*, 2016).

Influenza virus infections cause seasonal, yearly epidemics which are the source of a significant public health burden worldwide. The ferret model for human IAV is widely used and has several advantages over other animal models such as comparable symptomology, similar receptor distribution in the respiratory tract to humans and the ability to be infected with human isolates without the need for adaptation. Ferrets are a reliable model for influenza infection as shown by the reproducibility of the low dose intranasal infection. However, a major disadvantage of the model has been a lack of reagents for the evaluation of the cellular immune response. Investigation of T cell mediated immunity in ferrets is crucial to vaccine development and efficacy studies.

Studies investigating the H3N2 circulating seasonal strain of influenza have not been as numerous as those looking at the H1N1 strain. This is especially the case following the 2009 H1N1 pandemic. The seasonal H3N2 strain is equally as significant to public health as the H1N1 strain, and often predominates Flu seasons as was the case for 2018/2019. This set of studies sought to address the gap in the knowledge surrounding the H3N2 subtype of influenza A virus and how it behaved in the ferret model. This is important for ongoing vaccine and therapeutic studies using the ferret model.

Characterisation of influenza in the ferret occurs in one outbred species, *Mustela putorius*. There is a large amount of variability that is introduced into the experimental design of animal studies prior to the inoculation of animals. Thus far there is no universal standard established for ferret studies to evaluate the relative risk of influenza virus. Ferret gender, age and source

can vary between studies and laboratories. Young adult ferrets (4-12 months) are frequently used, but this can differ depending on the question being posed, for example looking at young or aged ferrets (Huang *et al.*, 2012, Paquette *et al.*, 2014). During the studies carried out as part of this thesis a variety of ferret ages were used. This was due to the availability of ferrets to work with for this project. When designing future projects using all female ferrets aged 4-6 months would be advantageous as much of the cellular immunology that was carried out in the project was performed on female ferrets of that age range. This would allow for consistency between and provide additional uniformity in studies.

Genetically modified ferrets are not yet readily available for research in the same way the mouse is. However, ferrets have been previously been cloned to produced animals without a CFTR gene, the gene that provides instruction for producing a protein called the cystic fibrosis transmembrane conductance regulator, in an attempt to create a ferret model of cystic fibrosis (Sun *et al.*, 2008). CFTR-knockout ferrets have been shown to develop a multi organ disease of the lung, pancreas, gall bladder and liver, unlike the CFTR-knockout mouse wich failed to present with any related symptoms of CF disease. Pancreatic disease in CF patients often leads to diabetes. This means that this genetically modified ferret provides a model in which to research disease of the lungs and pancreas where the mouse model is unable to.

Additonally, genetic information provided by the completion of the ferret genome enabled a transgenic ferret model where targeted knock-in ferrets using CRISPR technology were engineered (Yu *et al.*, 2019). Although no work has been published with transgenic ferrets and influenza, these developments in the ferret model will no doubt aid future influenza research. For example, a transgenic ferret in the future could allow investigation of influenza infection and it's impact in combination with cystic fibrosis.

7.2 The study hypothesis

The following hypotheses were investigated:

1. **That the pathogenesis of disease following different infection delivery models is similar despite the route of delivery and that pathogenesis is a property of the virus receptor rather than delivery route.**

2. **That influenza infection results from a combination of both droplet (fomite) and aerosol particles and that both particle types contribute to transfer.**

This collection of studies sought to address whether disease following different infection delivery models is similar despite the route of delivery. This was achieved by setting up three different experimental models of infection; low dose intranasal, nose-only aerosol and transmission cage (non-contact droplet) models. Within each of these models a variety of techniques were used to interrogate the viral kinetics and the immune response in the ferrets to establish the pathogenesis of the seasonal influenza H3N2 (A/Perth/16/2009).

From the results collected it's been shown that the pathogenesis of disease following different infection delivery models is similar despite the route of delivery differing. Regardless of the delivery route, animals infected with a low dose of H3N2 were shown to have mild clinical symptoms throughout these studies. Weight loss was not a marker of disease, and some ferrets infected with H3N2 appeared to gain weight despite infection. In studies where lung tissues were assessed the evidence for the presence of virus was very low despite varying inoculation routes.

Many studies using the intranasal infection route to inoculate the ferret use a high titre of virus (approximately $1x10^6$ PFU) (Maines *et al.*, 2009, Govorkova *et al.*, 2011, Kim *et al.*, 2013), this causes an early peak in viral shedding titre, coupled with an overall lower amount of virus shed compared to ferrets inoculated with a lower dose. While inoculation with a high titre of virus can guarantee infection, it has been shown that the titre of virus used to inoculate ferrets does not correlate with disease severity (Marriott *et al.*, 2014, Oh *et al.*, 2015). Lower dose models offer more clinically relevant viral shedding kinetics that gradually rise, peak and then resolve. Often a double peak can be identified in the pattern of shedding. From the studies completed as part of this thesis and other published studies, ferrets infected with H3N2 appear to shed virus in a biphasic manner (Roberts *et al.*, 2012, Roberts *et al.*, 2011) with a peak occurring 1-3 days following inoculation, a decline in virus load detected, before a second peak around days 5-7 followed by virus clearance. This pattern of shedding has also been observed in H1N1 infected ferrets (Dimmock *et al.*, 2012). It appears to be essential that sampling take place at least daily otherwise the peak can be missed, as was most likely the case for the low dose infected group in **Section 3.3**.

It has been demonstrated previously that ferrets are reliably infected with a low dose ($1x10^2$ PFU) influenza virus (H1N1 A/California/04/2009) (Marriott *et al.*, 2014, Dimmock *et al.*, 2012). This collection of studies demonstrates that ferrets can be reliably infected with the same low dose ($1x10^2$ PFU) of H3N2 A/Perth/16/2009 via the intranasal route, showing sero-conversion, virus shedding and clinical signs of disease. Comparison of the low dose intranasal models for H3N2 and H1N1 demonstrated that despite the viruses being inoculated using the same method and the same titre, the pathogenesis of each virus was different. The clinical observations of ferrets infected with H1N1 were more severe than those seen in ferrets infected with H3N2. Comparatively, H1N1 infected ferrets shed more virus than H3N2 infected ferrets and they also had higher peak titres of virus than ferrets infected with H3N2. Additionally, the presence of a cellular immune response in the lungs of ferrets infected with

H1N1 suggested that this virus travelled more readily to the ferret lung than H3N2, despite being administered to ferrets via the exact same method. This correlates with published tropisms of each subtype. Ultimately, from these results, it can be concluded that the pathogenesis of the virus is a property of the virus rather than the delivery route.

Additionally, this piece of work was carried out to address if influenza infection with H3N2 A/Perth/16/2009 can result from a range of infection routes with direct intranasal, contact, non-contact droplet and aerosol routes all successfully infecting ferrets. The robustness and reproducibility of these routes of infection have been shown to vary, with the intranasal low dose inoculation of ferrets being the most reliable and reproducible of the models. This route was the most straightforward to characterise and interpret and allowed for comparison of seasonal viruses.

The infection of ferrets using the transmission cage model replicates one of the most natural routes of infection presented in this piece of work. While this is a more clinically relevant route of infection, there are additional requirements for more animals and complex caging systems to be used to form a robust study. It would be useful for viruses used in this non-contact transmission cage model to be efficiently transmitted via aerosol, so they could provide full, or close to 100% donor to recipient infection. An alternative H3N2 strain could be sourced. It has been demonstrated that with this cage set up that two different strains of the same H1N1 subtype can have different infection rates in recipients (Otte *et al.*, 2016). This study examined two H1N1 strains; one from the early 2009 pandemic phase and one from the late 2009 pandemic phase. Donor and recipient ferrets were housed in pairs. The late phase pandemic H1N1 strain was shown to readily infect ferrets via the non-contact aerosol transmission route with 5 out of 6 recipients becoming infected via this route, with the 6th recipient becoming infected via contact with its cage mate. The early phase pandemic H1N1 strain only caused

infection of half of the recipient ferrets, with the remaining half of the recipeints becoming infected by their cage mates. This study determined that H1N1 strains isolated later in the pandemic had mutations in their viral genome that conferred viral fitness and aided pandemic spread. Alternatively, using a larger number of animals would help increase the number of successfully infected ferrets by viruses that are less efficient at being transmitted naturally via the non-contact route. However, this would be considerably more expensive due to cage adjustments and ethical considerations would need to be considered due to numbers of ferrets being used.

The nose only aerosol model allows aerosol infection to occur directly without the need for a donor ferret. In this study we have shown that a low dose of aerosolised H3N2 has exhibited similar viral shedding kinetics to a low dose intranasal infection. The nose-only aerosol model also allows ferrets to be infected with poorly transmissible strains that wouldn't readily infect recipient ferrets when placed into the non-contact transmission cage model. In theory, the nose-only aerosol model should allow for a more standardised delivery of a known titre of virus via a more natural transmission route. However, as has been shown, only one ferret became infected via the aerosol route, therefore the method of delivery demonstrated in this piece of work is not yet reproducible and reliable. Other published work using nose ony aerosol has shown varying success in infecting all ferrets with IAV. In comparison, measles, a highly contagious negative sense RNA virus transmitted via the respiratory route, has been shown to successfully infect all NHPs challenged (the model for the measles virus) via the aerosol route (Ludlow *et al.*, 2013, de Vries *et al.*, 2012). Demonstrating that successful aerosol challenge may well be down to the fitness of the virus to be transmitted via the aerosol route as opposed to a technical component introduced by the use of different equipment. It also demonstrates that the transmission of influenza between hosts is very much via a mixture of routes; fomite, large aerosol droplets and aerosol nuclei.

In the studies reported above, the initial transmission cage and nose-only aerosol models resulted in a similar percentage of animals being successful infected. Upon reflection, there was an unrealistic assumption that both these models would have a more successful infection rate, much like that of the low dose intranasal infection route. Based on these finidings, the persuit of aiborne transmission, via natural transmission and nose-only aerosol, may not be worthwhile, and would depend on the question that was being asked of the animal model. The practical difficulties and variability associated with both the transmission and nose only aerosol models means that the low dose intranasal model is a far more technically sound method of infection. The low dose intranasal model would provide a much more robust and reliable means of evaluating vaccine and therapeutics even though it doesn't mimic 'real life' infection as closely as natural transmission and nose-only aerosol might do. Ultimately their use would depend purpose of the research taking place, and if a new respiratory pathogen was being investigated in the ferret model the intranasal method of infection would be the most dependable route to attempt.

7.3 Future Work

Future work to develop each model has already been discussed in depth at the end of each results chapter. In addition to what has been discussed, the contributory role of fomites to H3N2 infection would be interesting to investigate. There is limited data on the pathogenesis of disease in the ferret model following infection via fomites. Ideally ferrets would be intranasally inoculated with a low dose of H3N2 and place into individual cage for 48 - 36 hours. Ferrets would then be removed from the cage and a naïve ferret would be placed individually into each cage. It would be important not to change bedding, water bottle, food bowls or enrichment during this period of change. This would allow infection of ferrets via

contaminated fomites to take place. Nasal wash samples and whole blood would then be collected from these ferrets during the study as per previous chapters for viral kinetic and cellular immune response analysis. Whole blood and lungs would be taken on study termination for assessment of the humoral and cellular immune response. Alternatively, to reduce the number of ferrets used, cages could be “spiked” with known quantities of influenza diluted in PBS, ferrets placed in cages and monitored as described.

However, this work is outside the scope and funding of this project. In addition, ethical considerations would need to be considered when using further animals to investigate this route of infection and evaluating the benefit of this model.

7.4 Conclusions

To date mice, rats, ferrets, hamsters, guinea pigs and NHPs have been extensively used for modelling human respiratory virus infection. The availability of immune reagents and ease of genetic manipulation means that the mouse is the most commonly used model. Despite this, the ferret remains the preferred animal model for assessing influenza infection. However, there are many challenges when setting up model of infection. The simplest is the low dose intranasal infection model, providing reproducibility and reliability. This is in line with the vast majority of of models for respiratory viruses which use intranasal inoculation to deliver virus. For this ferret model, both the nose-only aerosol and transmission cage models require a great deal more work to get them to the same reproducibility of the low dose intranasal model. Unfortunately, the time constraints and scope of this PhD meant that these models were unable to be progressed further beyond the work presented in this thesis.

Part of the work in this thesis has been successfully published and highlights the differences in the cellular immune response between seasonal H3N2 and H1N1 (Ryan *et al.*, 2018). The evaluation of cellular immune responses in the ferret model is important for use of the model in future influenzas vaccine development. Current inactivated vaccines are poor inducers of T-cell responses. It's known that cross-reactive T-cell responses are important in the protective response to novel vaccines, especially those based on internal virus antigens (Berthoud *et al.*, 2011). Therefore, the ability to measure these responses in the ferret model of influenza is becoming increasingly valuable. In the future both humoral and cellular responses will need to be measured in animal models as new vaccines are likely to require induction of both.

Ultimately this work enhances and improves the versatility of the ferret model for studying the pathogenesis of influenza and, in the long run can provide information, support and guidance for the public health response to influenza in humans.

8 Appendix 1

Study Index

Study Numbers	4965	5087	5256	5283	5530	5549	5719
Study description	Intranasal Dose Pilot Study	Serial Cull Study	Study to Demonstrate the Reproducibility & Reliability of the Low Dose Intranasal Inoculation	Transmission Cage Model	Nose-only Aerosol Infection Model	Low Dose Model to Investigate Cellular Immune Responses/ H1N1 Comparison	Low Dose Model to Investigate Cellular Immune Responses/ H1N1 Comparison
Number of ferrets	4	8	6	12	12	12	6
Age	4-6 months	9.5-14.5 weeks	10+ weeks	12-16 weeks	4-6 months	4-6 months	4-6 months
ID Numbers	27043 (m) 47575 (m) 30654 (f) 27027 (m)	26166 (f) 27207 (f) 18992 (m) 26624 (f) 76400 (f) 31048 (m) 33920 (f) 86670 (f)	57277(m) 80693(f) 87677(f) 93202(m) 55702(m) 88448(m)	40434 (m) 40400 (m) 40418 (m) 41822 (f) 15557 (f) 18704 (f) 95099 (f) 11981(m) 12950 (f) 38968 (m) 40513 (m) 40487 (f)	40761 (f) 47791 (f) 49800 (f) 53177 (f) 51352 (f) 46171 (f) 50706 (f) 46313 (f) 46392 (f) 46476 (f) 48186 (f) 41787 (f)	55432 (f) 45891 (f) 53132 (f) 49686 (f) 52094 (f) 45627 (f) 46707 (f) 50573 (f) 52238 (f) 47025 (f) 48889 (f) 46915 (f)	86654 (f) 86811 (f) 86809 (f) 86659 (f) 86812 (f) 86660 (f)
Timepoint culled	14 dpi	2, 3, 4 & 8 dpi	8 dpi	8, 13 and 14 dpi	14 dpi	14 dpi	14 dpi
Samples collected	Clinical Obs, weight, NW, sera	Clinical Obs, weight, NW, sera	Clinical Obs, weight, NW, sera	Clinical Obs, weight, NW, sera, whole blood, spleen	Clinical Obs, weight, NW, sera, whole blood, spleen, BAL, lung	Clinical Obs, weight, NW, sera, whole blood, lung	Clinical Obs, weight, NW, sera, whole blood, lung

9 References

AIR, G. M. 2015. Influenza virus antigenicity and broadly neutralizing epitopes. *Current opinion in virology,* 11**,** 113-121.

ALLEN, J. D. & ROSS, T. M. 2018. H3N2 influenza viruses in humans: Viral mechanisms, evolution, and evaluation. *Human vaccines & immunotherapeutics,* 14**,** 1840-1847.

ALTENBURG, A. F., RIMMELZWAAN, G. F. & DE VRIES, R. D. 2015. Virus-specific T cells as correlate of (cross-)protective immunity against influenza. *Vaccine,* 33**,** 500-506.

ALYMOVA, I. V., YORK, I. A., AIR, G. M., CIPOLLO, J. F., GULATI, S., BARANOVICH, T., KUMAR, A., ZENG, H., GANSEBOM, S. & MCCULLERS, J. A. 2016. Glycosylation changes in the globular head of H3N2 influenza hemagglutinin modulate receptor binding without affecting virus virulence. *Scientific Reports,* 6**,** 36216.

ANDERSON, C. S., ORTEGA, S., CHAVES, F. A., CLARK, A. M., YANG, H., TOPHAM, D. J. & DEDIEGO, M. L. 2017. Natural and directed antigenic drift of the H1 influenza virus hemagglutinin stalk domain. *Scientific Reports,* 7**,** 14614.

ARBEITSKREIS BLUT, U. B. B. K. 2009. Influenza Virus. *Transfusion medicine and hemotherapy : offizielles Organ der Deutschen Gesellschaft fur Transfusionsmedizin und Immunhamatologie,* 36**,** 32-39.

ARNON, T., LEV, M., KATZ, G., CHERNOBROV, Y., PORGADOR, A. & MANDELBOIM, O. 2001. Recognition of viral hemagglutinins by NKp44 but not by NKp30. *European journal of immunology,* 31**,** 2680-2689.

BARRÉ-SINOUSSI, F. & MONTAGUTELLI, X. 2015. Animal models are essential to biological research: issues and perspectives. *Future science OA,* 1**,** FSO63-FSO63.

BEKKING, C., YIP, L., GROULX, N., DOGGETT, N., FINN, M. & MUBAREKA, S. 2019. Evaluation of bioaerosol samplers for the detection and quantification of influenza virus from artificial aerosols and influenza virus–infected ferrets. *Influenza and Other Respiratory Viruses,* 0.

BELISLE, S. E., TISONCIK, J. R., KORTH, M. J., CARTER, V. S., PROLL, S. C., SWAYNE, D. E., PANTIN-JACKWOOD, M., TUMPEY, T. M. & KATZE, M. G. 2010. Genomic profiling of tumor necrosis factor alpha (TNF-alpha) receptor and interleukin-1 receptor knockout mice reveals a link between TNF-alpha signaling and increased severity of 1918 pandemic influenza virus infection. *Journal of virology,* 84**,** 12576-12588.

BELSER, J. A., ECKERT, A. M., TUMPEY, T. M. & MAINES, T. R. 2016. Complexities in Ferret Influenza Virus Pathogenesis and Transmission Models. *Microbiology and molecular biology reviews : MMBR,* 80**,** 733-744.

BELSER, J. A., GUSTIN, K. M., MAINES, T. R., PANTIN-JACKWOOD, M. J., KATZ, J. M. & TUMPEY, T. M. 2012. Influenza Virus Respiratory Infection and Transmission Following Ocular Inoculation in Ferrets. *PLoS Pathog,* 8**,** e1002569.

BELSER, J. A., KATZ, J. M. & TUMPEY, T. M. 2011. The ferret as a model organism to study influenza A virus infection. *Disease Models & Mechanisms,* 4**,** 575-579.

BELSER, J. A., WADFORD, D. A., PAPPAS, C., GUSTIN, K. M., MAINES, T. R., PEARCE, M. B., ZENG, H., SWAYNE, D. E., PANTIN-JACKWOOD, M., KATZ, J. M. & TUMPEY, T. M. 2010. Pathogenesis of pandemic influenza A (H1N1) and triple-

reassortant swine influenza A (H1) viruses in mice. *Journal of virology,* 84**,** 4194-4203.

BERTHOUD, T. K., HAMILL, M., LILLIE, P. J., HWENDA, L., COLLINS, K. A., EWER, K. J., MILICIC, A., POYNTZ, H. C., LAMBE, T., FLETCHER, H. A., HILL, A. V. S. & GILBERT, S. C. 2011. Potent CD8+ T-Cell Immunogenicity in Humans of a Novel Heterosubtypic Influenza A Vaccine, MVA−NP+M1. *Clinical Infectious Diseases,* 52**,** 1-7.

BERTRAM, S., GLOWACKA, I., STEFFEN, I., KÜHL, A. & PÖHLMANN, S. 2010. Novel insights into proteolytic cleavage of influenza virus hemagglutinin. *Reviews in Medical Virology,* 20**,** 298-310.

BETTELLI, E., KORN, T., OUKKA, M. & KUCHROO, V. K. 2008. Induction and effector functions of T(H)17 cells. *Nature,* 453**,** 1051-1057.

BHATNAGAR, J., JONES, T., BLAU, D. M., SHIEH, W.-J., PADDOCK, C. D., DREW, C., DENISON, A. M., ROLLIN, D. C., PATEL, M. & ZAKI, S. R. 2013. Localization of pandemic 2009 H1N1 influenza A virus RNA in lung and lymph nodes of fatal influenza cases by in situ hybridization: New insights on virus replication and pathogenesis. *Journal of Clinical Virology,* 56**,** 316-321.

BLACHERE, F. M., CAO, G., LINDSLEY, W. G., NOTI, J. D. & BEEZHOLD, D. H. 2011. Enhanced detection of infectious airborne influenza virus. *Journal of Virological Methods,* 176**,** 120-124.

BODEWES, R., KREIJTZ, J. H. C. M., GEELHOED-MIERAS, M. M., VAN AMERONGEN, G., VERBURGH, R. J., VAN TRIERUM, S. E., KUIKEN, T., FOUCHIER, R. A. M., OSTERHAUS, A. D. M. E. & RIMMELZWAAN, G. F. 2011. Vaccination against

seasonal influenza A/H3N2 virus reduces the induction of heterosubtypic immunity against influenza A/H5N1 virus infection in ferrets. *Journal of virology,* 85**,** 2695-2702.

BODEWES, R., RIMMELZWAAN, G. F. & OSTERHAUS, A. D. M. E. 2010. Animal models for the preclinical evaluation of candidate influenza vaccines. *Expert Review of Vaccines,* 9**,** 59-72.

BONILLA, F. A. & OETTGEN, H. C. 2010. Adaptive immunity. *Journal of Allergy and Clinical Immunology,* 125**,** S33-S40.

BOTTA, D., FULLER, M. J., MARQUEZ-LAGO, T. T., BACHUS, H., BRADLEY, J. E., WEINMANN, A. S., ZAJAC, A. J., RANDALL, T. D., LUND, F. E., LEÓN, B. & BALLESTEROS-TATO, A. 2017. Dynamic regulation of T follicular regulatory cell responses by interleukin 2 during influenza infection. *Nature Immunology,* 18**,** 1249.

BOUVIER, N. M. 2015. Animal models for influenza virus transmission studies: a historical perspective. *Current Opinion in Virology,* 13**,** 101-108.

BOUVIER, N. M. & LOWEN, A. C. 2010. Animal Models for Influenza Virus Pathogenesis and Transmission. *Viruses,* 2**,** 1530.

BRIDGES, C. B., KUEHNERT, M. J. & HALL, C. B. 2003. Transmission of influenza: implications for control in health care settings. *Clin Infect Dis,* 37.

BUEHLER, J., NAVI, D., LORUSSO, A., VINCENT, A., LAGER, K. & MILLER, C. L. 2013. Influenza A Virus PB1-F2 Protein Expression Is Regulated in a Strain-Specific Manner by Sequences Located Downstream of the PB1-F2 Initiation Codon. *Journal of Virology,* 87**,** 10687.

BURNET, F. M. 1936. Influenza Virus on the Developing Egg: I. Changes Associated with the Development of an Egg-passage Strain of Virus. *British Journal of Experimental Pathology,* 17**,** 282-293.

CAROLAN, L. A., BUTLER, J., ROCKMAN, S., GUARNACCIA, T., HURT, A. C., READING, P., KELSO, A., BARR, I. & LAURIE, K. L. 2014. TaqMan real time RT-PCR assays for detecting ferret innate and adaptive immune responses. *Journal of Virological Methods,* 205**,** 38-52.

CARRAGHER, D. M., KAMINSKI, D. A., MOQUIN, A., HARTSON, L. & RANDALL, T. D. 2008. A Novel Role for Non-Neutralizing Antibodies against Nucleoprotein in Facilitating Resistance to Influenza Virus. *The Journal of Immunology,* 181**,** 4168-4176.

CDC. 2009. *Swine Influenza A (H1N1) Infection in Two Children --- Southern California, March--April 2009*

[Online]. Available: https://www.cdc.gov/mmwr/preview/mmwrhtml/mm5815a5.htm [Accessed 09NOV17 2017].

CDC. 2017. *About Flu: Antigenic Characterization* [Online]. Available: https://www.cdc.gov/flu/about/professionals/antigenic.htm [Accessed 26SEP 2019].

CDC. 2018. *How Flu Spreads* [Online]. Available: https://www.cdc.gov/flu/about/disease/spread.htm [Accessed 16 Sep 2019].

CHEN, K. S., BHARAJ, S. S. & KING, E. C. 1995. Induction and relief of nasal congestion in ferrets infected with influenza virus. *International Journal of Experimental Pathology,* 76**,** 55-64.

CHEN, W., CALVO, P. A., MALIDE, D., GIBBS, J., SCHUBERT, U., BACIK, I., BASTA, S., O'NEILL, R., SCHICKLI, J., PALESE, P., HENKLEIN, P., BENNINK, J. R. & YEWDELL, J. W. 2001. A novel influenza A virus mitochondrial protein that induces cell death. *Nature Medicine,* 7**,** 1306.

CHEN, X., LIU, S., GORAYA, M. U., MAAROUF, M., HUANG, S. & CHEN, J.-L. 2018. Host Immune Response to Influenza A Virus Infection. *Frontiers in immunology,* 9**,** 320-320.

CHOWELL, G., SIMONSEN, L., TOWERS, S., MILLER, M. A. & VIBOUD, C. 2013. Transmission potential of influenza A/H7N9, February to May 2013, China. *BMC Medicine,* 11**,** 214.

COELINGH, K. L., LUKE, C. J., JIN, H. & TALAAT, K. R. 2014. Development of live attenuated influenza vaccines against pandemic influenza strains. *Expert Review of Vaccines,* 13**,** 855-871.

COHEN, M., ZHANG, X.-Q., SENAATI, H. P., CHEN, H.-W., VARKI, N. M., SCHOOLEY, R. T. & GAGNEUX, P. 2013. Influenza A penetrates host mucus by cleaving sialic acids with neuraminidase. *Virology Journal,* 10**,** 321.

COMPANS, R. W., CONTENT, J. & DUESBERG, P. H. 1972. Structure of the ribonucleoprotein of influenza virus. *Journal of virology,* 10**,** 795-800.

COUCH, R. B., ATMAR, R. L., FRANCO, L. M., QUARLES, J. M., WELLS, J., ARDEN, N., NIÑO, D. & BELMONT, J. W. 2013. Antibody correlates and predictors of immunity to naturally occurring influenza in humans and the importance of antibody to the neuraminidase. *The Journal of infectious diseases,* 207**,** 974-981.

CREAGER, H. M., ZENG, H., PULIT-PENALOZA, J. A., MAINES, T. R., TUMPEY, T. M. & BELSER, J. A. 2017. In vitro exposure system for study of aerosolized influenza virus. *Virology,* 500**,** 62-70.

CRISWELL, B. S., COUCH, R. B., GREENBERG, S. B. & KIMZEY, S. L. 1979. The Lymphocyte Response to Influenza in Humans. 120**,** 700-704.

DAVIS, A. S., TAUBENBERGER, J. K. & BRAY, M. 2015. The use of nonhuman primates in research on seasonal, pandemic and avian influenza, 1893–2014. *Antiviral Research,* 117**,** 75-98.

DE CONTO, F., COVAN, S., ARCANGELETTI, M. C., ORLANDINI, G., GATTI, R., DETTORI, G. & CHEZZI, C. 2011. Differential infectious entry of human influenza A/NWS/33 virus (H1N1) in mammalian kidney cells. *Virus Research,* 155**,** 221-230.

DE GRAAF, M. & FOUCHIER, R. A. M. 2014. Role of receptor binding specificity in influenza A virus transmission and pathogenesis. *The EMBO Journal,* 33**,** 823-841.

DE JONG, J. C., BEYER, W. E. P., PALACHE, A. M., RIMMELZWAAN, G. F. & OSTERHAUS, A. D. M. E. 2000. Mismatch between the 1997/1998 influenza vaccine and the major epidemic A(H3N2) virus strain as the cause of an inadequate vaccine-induced antibody response to this strain in the elderly. *Journal of Medical Virology,* 61**,** 94-99.

DE JONG, M. D., SIMMONS, C. P., THANH, T. T., HIEN, V. M., SMITH, G. J. D., CHAU, T. N. B., HOANG, D. M., VAN VINH CHAU, N., KHANH, T. H., DONG, V. C., QUI, P. T., VAN CAM, B., HA, D. Q., GUAN, Y., PEIRIS, J. S. M., CHINH, N. T., HIEN, T. T. & FARRAR, J. 2006. Fatal outcome of human influenza A (H5N1) is associated with high viral load and hypercytokinemia. *Nature Medicine,* 12**,** 1203-1207.

DE VRIES, E., TSCHERNE, D. M., WIENHOLTS, M. J., COBOS-JIMÉNEZ, V., SCHOLTE, F., GARCÍA-SASTRE, A., ROTTIER, P. J. M. & DE HAAN, C. A. M. 2011. Dissection of the Influenza A Virus Endocytic Routes Reveals Macropinocytosis as an Alternative Entry Pathway. *PLOS Pathogens,* 7**,** e1001329.

DE VRIES, R. D., MCQUAID, S., VAN AMERONGEN, G., YÜKSEL, S., VERBURGH, R. J., OSTERHAUS, A. D. M. E., DUPREX, W. P. & DE SWART, R. L. 2012. Measles Immune Suppression: Lessons from the Macaque Model. *PLOS Pathogens,* 8**,** e1002885.

DENG, Y.-M., SPIRASON, N., IANNELLO, P., JELLEY, L., LAU, H. & BARR, I. G. 2015. A simplified Sanger sequencing method for full genome sequencing of multiple subtypes of human influenza A viruses. *Journal of Clinical Virology,* 68**,** 43-48.

DIMMOCK, N. J., DOVE, B. K., MENG, B., SCOTT, P. D., TAYLOR, I., CHEUNG, L., HALLIS, B., MARRIOTT, A. C., CARROLL, M. W. & EASTON, A. J. 2012. Comparison of the protection of ferrets against pandemic 2009 influenza A virus (H1N1) by 244 DI influenza virus and oseltamivir. *Antiviral research,* 96**,** 376-385.

DOHERTY, P. C. & CHRISTENSEN, J. P. 2000. Accessing Complexity: The Dynamics of Virus-Specific T Cell Responses. *Annual Review of Immunology,* 18**,** 561-592.

DOLIN, R., RICHMAN, D. D., MURPHY, B. R. & FAUCI, A. S. 1977. Cell-Mediated Immune Responses in Humans after Induced Infection with Influenza A Virus. *The Journal of Infectious Diseases,* 135**,** 714-719.

DOU, D., REVOL, R., ÖSTBYE, H., WANG, H. & DANIELS, R. 2018. Influenza A Virus Cell Entry, Replication, Virion Assembly and Movement. *Frontiers in Immunology,* 9**,** 1581.

DUBOIS, R. M., SLAVISH, P. J., BAUGHMAN, B. M., YUN, M.-K., BAO, J., WEBBY, R. J., WEBB, T. R. & WHITE, S. W. 2012. Structural and Biochemical Basis for Development of Influenza Virus Inhibitors Targeting the PA Endonuclease. *PLOS Pathogens,* 8**,** e1002830.

EICHELBERGER, M. C. & GREEN, M. D. 2011. Animal models to assess the toxicity, immunogenicity and effectiveness of candidate influenza vaccines. *Expert Opinion on Drug Metabolism & Toxicology,* 7**,** 1117-1127.

EISFELD, A. J., NEUMANN, G. & KAWAOKA, Y. 2015. At the centre: influenza A virus ribonucleoproteins. *Nature reviews. Microbiology,* 13**,** 28-41.

ENKIRCH, T. & VON MESSLING, V. 2015. Ferret models of viral pathogenesis. *Virology,* 479–480**,** 259-270.

EUROPEANCOMMISION. 2015. *Statement supporting European Directive 2010/63/EU ("Directive") on the protection of animals used for*

scientific purposes [Online]. Available: https://acmedsci.ac.uk/file-download/36950-57ff32f8b11f0.pdf [Accessed 26SEP 2019].

FERGUSON, L., OLIVIER, A. K., GENOVA, S., EPPERSON, W. B., SMITH, D. R., SCHNEIDER, L., BARTON, K., MCCUAN, K., WEBBY, R. J. & WAN, X.-F. 2016. Pathogenesis of Influenza D Virus in Cattle. *Journal of Virology,* 90**,** 5636.

FRANCIS, T. 1940. A NEW TYPE OF VIRUS FROM EPIDEMIC INFLUENZA. *Science,* 92**,** 405.

FRANCIS, T., SALK, J. E., PEARSON, H. E. & BROWN, P. N. 1945. PROTECTIVE EFFECT OF VACCINATION AGAINST INDUCED INFLUENZA A. *Journal of Clinical Investigation,* 24**,** 536-546.

FRASER, C., DONNELLY, C. A., CAUCHEMEZ, S., HANAGE, W. P., VAN KERKHOVE, M. D., HOLLINGSWORTH, T. D., GRIFFIN, J., BAGGALEY, R. F., JENKINS, H. E., LYONS, E. J., JOMBART, T., HINSLEY, W. R., GRASSLY, N. C., BALLOUX, F., GHANI, A. C., FERGUSON, N. M., RAMBAUT, A., PYBUS, O. G., LOPEZ-GATELL, H., ALPUCHE-ARANDA, C. M., CHAPELA, I. B., ZAVALA, E. P., GUEVARA, D. M. E., CHECCHI, F., GARCIA, E., HUGONNET, S., ROTH, C. & COLLABORATION, W. H. O. R. P. A. 2009. Pandemic potential of a strain of influenza A (H1N1): early findings. *Science (New York, N.Y.),* 324**,** 1557-1561.

FRISE, R., BRADLEY, K., VAN DOREMALEN, N., GALIANO, M., ELDERFIELD, R. A., STILWELL, P., ASHCROFT, J. W., FERNANDEZ-ALONSO, M., MIAH, S., LACKENBY, A., ROBERTS, K. L., DONNELLY, C. A. & BARCLAY, W. S. 2016. Contact transmission of influenza virus between ferrets imposes a looser bottleneck than respiratory droplet transmission allowing propagation of antiviral resistance. *Scientific reports,* 6**,** 29793-29793.

FUKAO, K., ANDO, Y., NOSHI, T., KITANO, M., NODA, T., KAWAI, M., YOSHIDA, R., SATO, A., SHISHIDO, T. & NAITO, A. 2019. Baloxavir marboxil, a novel cap-dependent endonuclease inhibitor potently suppresses influenza virus replication and represents therapeutic effects in both immunocompetent and immunocompromised mouse models. *PLOS ONE,* 14**,** e0217307.

GAMBLIN, S. J. & SKEHEL, J. J. 2010. Influenza Hemagglutinin and Neuraminidase Membrane Glycoproteins. *The Journal of Biological Chemistry,* 285**,** 28403-28409.

GARTEN, R. J., DAVIS, C. T., RUSSELL, C. A., SHU, B., LINDSTROM, S., BALISH, A., SESSIONS, W. M., XU, X., SKEPNER, E., DEYDE, V., OKOMO-ADHIAMBO, M., GUBAREVA, L., BARNES, J., SMITH, C. B., EMERY, S. L., HILLMAN, M. J., RIVAILLER, P., SMAGALA, J., DE GRAAF, M., BURKE, D. F., FOUCHIER, R. A. M., PAPPAS, C., ALPUCHE-ARANDA, C. M., LÓPEZ-GATELL, H., OLIVERA, H., LÓPEZ, I., MYERS, C. A., FAIX, D., BLAIR, P. J., YU, C., KEENE, K. M., DOTSON, P. D., BOXRUD, D., SAMBOL, A. R., ABID, S. H., GEORGE, K. S., BANNERMAN, T., MOORE, A. L., STRINGER, D. J., BLEVINS, P., DEMMLER-HARRISON, G. J., GINSBERG, M., KRINER, P., STEVEWATERMAN, SMOLE, S., GUEVARA, H. F., BELONGIA, E. A., CLARK, P. A., BEATRICE, S. T., DONIS, R., KATZ, J., FINELLI, L., BRIDGES, C. B., SHAW, M., JERNIGAN, D. B., UYEKI, T. M., SMITH, D. J., KLIMOV, A. I. & COX, N. J. 2009. Antigenic and Genetic Characteristics of the Early Isolates of Swine-Origin 2009 A(H1N1) Influenza Viruses Circulating in Humans. *Science (New York, N.Y.),* 325**,** 197-201.

GERHARD, W. 2001. *The Role of the Antibody Response in Influenza Virus Infection*.

GERL, M. J., SAMPAIO, J. L., URBAN, S., KALVODOVA, L., VERBAVATZ, J.-M., BINNINGTON, B., LINDEMANN, D., LINGWOOD, C. A., SHEVCHENKO, A., SCHROEDER, C. & SIMONS, K. 2012. Quantitative analysis of the lipidomes of the influenza virus envelope and MDCK cell apical membrane. *The Journal of Cell Biology,* 196**,** 213-221.

GONG, Y.-N., CHEN, G.-W., CHEN, C.-J., KUO, R.-L. & SHIH, S.-R. 2014. Computational Analysis and Mapping of Novel Open Reading Frames in Influenza A Viruses. *PLOS ONE,* 9**,** e115016.

GOOCH, K. E., MARRIOTT, A. C., RYAN, K. A., YEATES, P., SLACK, G. S., BROWN, P. J., FOTHERGILL, R., WHITTAKER, C. J. & CARROLL, M. W. 2019. Heterosubtypic

cross-protection correlates with cross-reactive interferon-gamma-secreting lymphocytes in the ferret model of influenza. *Scientific reports,* 9**,** 2617-2617.

GOVORKOVA, E. A., MARATHE, B. M., PREVOST, A., REHG, J. E. & WEBSTER, R. G. 2011. Assessment of the efficacy of the neuraminidase inhibitor oseltamivir against 2009 pandemic H1N1 influenza virus in ferrets. *Antiviral research,* 91**,** 81-88.

GRAHAM, M. B., DALTON, D. K., GILTINAN, D., BRACIALE, V. L., STEWART, T. A. & BRACIALE, T. J. 1993. Response to influenza infection in mice with a targeted disruption in the interferon gamma gene. *The Journal of experimental medicine,* 178**,** 1725-1732.

GRANT, E. J., QUIÑONES-PARRA, S. M., CLEMENS, E. B. & KEDZIERSKA, K. 2016. Human influenza viruses and CD8+ T cell responses. *Current Opinion in Virology,* 16**,** 132-142.

GREEN, I. J. 1962. Serial Propagation of Influenza B (Lee) Virus in a Transmissible Line of Canine Kidney Cells. 138**,** 42-43.

GROHSKOPF, L. A., OLSEN, S. J., SOKOLOW, L. Z., BRESEE, J. S., COX, N. J., BRODER, K. R., KARRON, R. A., WALTER, E. B., CENTERS FOR DISEASE, C. & PREVENTION 2014. Prevention and control of seasonal influenza with vaccines: recommendations of the Advisory Committee on Immunization Practices (ACIP) -- United States, 2014-15 influenza season. *MMWR. Morbidity and mortality weekly report,* 63**,** 691-697.

GUSTIN, K. M., BELSER, J. A., VEGUILLA, V., ZENG, H., KATZ, J. M., TUMPEY, T. M. & MAINES, T. R. 2015. Environmental Conditions Affect Exhalation of H3N2 Seasonal

and Variant Influenza Viruses and Respiratory Droplet Transmission in Ferrets. *PLoS ONE,* 10**,** e0125874.

GUSTIN, K. M., BELSER, J. A., WADFORD, D. A., PEARCE, M. B., KATZ, J. M., TUMPEY, T. M. & MAINES, T. R. 2011. Influenza virus aerosol exposure and analytical system for ferrets. *Proceedings of the National Academy of Sciences,* 108**,** 8432-8437.

GUSTIN, K. M., KATZ, J. M., TUMPEY, T. M. & MAINES, T. R. 2013. Comparison of the levels of infectious virus in respirable aerosols exhaled by ferrets infected with influenza viruses exhibiting diverse transmissibility phenotypes. *Journal of virology,* 87**,** 7864-7873.

HALLER, O. & KOCHS, G. 2002. Interferon-Induced Mx Proteins: Dynamin-Like GTPases with Antiviral Activity. *Traffic,* 3**,** 710-717.

HAMILTON, B. S., WHITTAKER, G. R. & DANIEL, S. 2012. Influenza Virus-Mediated Membrane Fusion: Determinants of Hemagglutinin Fusogenic Activity and Experimental Approaches for Assessing Virus Fusion. *Viruses,* 4**,** 1144-1168.

HARTINGS, J. M. & ROY, C. J. 2004. The automated bioaerosol exposure system: Preclinical platform development and a respiratory dosimetry application with nonhuman primates. *Journal of Pharmacological and Toxicological Methods,* 49**,** 39-55.

HASHEM, A. M. 2015. Prospects of HA-based universal influenza vaccine. *BioMed research international,* 2015**,** 414637-414637.

HAUSE, B. M., DUCATEZ, M., COLLIN, E. A., RAN, Z., LIU, R., SHENG, Z., ARMIEN, A., KAPLAN, B., CHAKRAVARTY, S., HOPPE, A. D., WEBBY, R. J., SIMONSON, R. R. & LI, F. 2013. Isolation of a Novel Swine Influenza Virus from Oklahoma in 2011

Which Is Distantly Related to Human Influenza C Viruses. *PLOS Pathogens,* 9**,** e1003176.

HAYASHI, T., CHAIMAYO, C., MCGUINNESS, J. & TAKIMOTO, T. 2016. Critical Role of the PA-X C-Terminal Domain of Influenza A Virus in Its Subcellular Localization and Shutoff Activity. *Journal of Virology,* 90**,** 7131.

HERFST, S., SCHRAUWEN, E. J. A., LINSTER, M., CHUTINIMITKUL, S., DE WIT, E., MUNSTER, V. J., SORRELL, E. M., BESTEBROER, T. M., BURKE, D. F., SMITH, D. J., RIMMELZWAAN, G. F., OSTERHAUS, A. D. M. E. & FOUCHIER, R. A. M. 2012. Airborne Transmission of Influenza A/H5N1 Virus Between Ferrets. *Science,* 336**,** 1534-1541.

HERLOCHER, M., ELIAS, S., TRUSCON, R., HARRISON, S., MINDELL, D., SIMON, C. & MONTO, A. 2001. Ferrets as a transmission model for influenza: sequence changes in HA1 of type A (H3N2) virus. *J Infect Dis,* 184**,** 542 - 546.

HINTZEN, G., OHL, L., DEL RIO, M.-L., RODRIGUEZ-BARBOSA, J.-I., PABST, O., KOCKS, J. R., KREGE, J., HARDTKE, S. & FÖRSTER, R. 2006. Induction of Tolerance to Innocuous Inhaled Antigen Relies on a CCR7-Dependent Dendritic Cell-Mediated Antigen Transport to the Bronchial Lymph Node. *The Journal of Immunology,* 177**,** 7346.

HIRST, G. K. 1942. THE QUANTITATIVE DETERMINATION OF INFLUENZA VIRUS AND ANTIBODIES BY MEANS OF RED CELL AGGLUTINATION. *The Journal of Experimental Medicine,* 75**,** 49-64.

HO, A. W. S., PRABHU, N., BETTS, R. J., GE, M. Q., DAI, X., HUTCHINSON, P. E., LEW, F. C., WONG, K. L., HANSON, B. J., MACARY, P. A. & KEMENY, D. M. 2011. Lung

CD103+ Dendritic Cells Efficiently Transport Influenza Virus to the Lymph Node and Load Viral Antigen onto MHC Class I for Presentation to CD8 T Cells. *The Journal of Immunology,* 187**,** 6011.

HORMAN, W. S. J., NGUYEN, T. H. O., KEDZIERSKA, K., BEAN, A. G. D. & LAYTON, D. S. 2018. The Drivers of Pathology in Zoonotic Avian Influenza: The Interplay Between Host and Pathogen. *Frontiers in immunology,* 9**,** 1812-1812.

HUANG, S. S., BANNER, D., FANG, Y., NG, D. C., KANAGASABAI, T., KELVIN, D. J. & KELVIN, A. A. 2011. Comparative analyses of pandemic H1N1 and seasonal H1N1, H3N2, and influenza B infections depict distinct clinical pictures in ferrets. *PLoS One,* 6**,** e27512.

HUANG, S. S. H., BANNER, D., DEGOUSEE, N., LEON, A. J., XU, L., PAQUETTE, S. G., KANAGASABAI, T., FANG, Y., RUBINO, S., RUBIN, B., KELVIN, D. J. & KELVIN, A. A. 2012. Differential pathological and immune responses in newly weaned ferrets are associated with a mild clinical outcome of pandemic 2009 H1N1 infection. *Journal of virology,* 86**,** 13187-13201.

HUFFORD, M. M., KIM, T. S., SUN, J. & BRACIALE, T. J. 2011. Antiviral CD8+ T cell effector activities in situ are regulated by target cell type. *The Journal of experimental medicine,* 208**,** 167-180.

HUSE, M., LILLEMEIER, B. F., KUHNS, M. S., CHEN, D. S. & DAVIS, M. M. 2006. T cells use two directionally distinct pathways for cytokine secretion. *Nature Immunology,* 7**,** 247-255.

HUTCHINSON, E. C. 2018. Influenza Virus. *Trends in Microbiology,* 26**,** 809-810.

ITOH, Y., SHINYA, K., KISO, M., WATANABE, T., SAKODA, Y., HATTA, M., MURAMOTO, Y., TAMURA, D., SAKAI-TAGAWA, Y., NODA, T., SAKABE, S., IMAI, M., HATTA, Y., WATANABE, S., LI, C., YAMADA, S., FUJII, K., MURAKAMI, S., IMAI, H., KAKUGAWA, S., ITO, M., TAKANO, R., IWATSUKI-HORIMOTO, K., SHIMOJIMA, M., HORIMOTO, T., GOTO, H., TAKAHASHI, K., MAKINO, A., ISHIGAKI, H., NAKAYAMA, M., OKAMATSU, M., TAKAHASHI, K., WARSHAUER, D., SHULT, P. A., SAITO, R., SUZUKI, H., FURUTA, Y., YAMASHITA, M., MITAMURA, K., NAKANO, K., NAKAMURA, M., BROCKMAN-SCHNEIDER, R., MITAMURA, H., YAMAZAKI, M., SUGAYA, N., SURESH, M., OZAWA, M., NEUMANN, G., GERN, J., KIDA, H., OGASAWARA, K. & KAWAOKA, Y. 2009. In vitro and in vivo characterization of new swine-origin H1N1 influenza viruses. *Nature,* 460**,** 1021-1025.

JAYARAMAN, A., CHANDRASEKARAN, A., VISWANATHAN, K., RAMAN, R., FOX, J. G. & SASISEKHARAN, R. 2012. Decoding the distribution of glycan receptors for human-adapted influenza A viruses in ferret respiratory tract. *PloS one,* 7**,** e27517-e27517.

JAYASEKERA, J. P., MOSEMAN, E. A. & CARROLL, M. C. 2007. Natural Antibody and Complement Mediate Neutralization of Influenza Virus in the Absence of Prior Immunity. *Journal of Virology,* 81**,** 3487-3494.

JAYASEKERA, J. P., VINUESA, C. G., KARUPIAH, G. & KING, N. J. C. 2006. Enhanced antiviral antibody secretion and attenuated immunopathology during influenza virus infection in nitric oxide synthase-2-deficient mice. *Journal of General Virology,* 87**,** 3361-3371.

JEGASKANDA, S., CO, M. D. T., CRUZ, J., SUBBARAO, K., ENNIS, F. A. & TERAJIMA, M. 2016. Induction of H7N9-Cross-Reactive Antibody-Dependent Cellular Cytotoxicity

Antibodies by Human Seasonal Influenza A Viruses that are Directed Toward the Nucleoprotein. *The Journal of Infectious Diseases,* 215**,** 818-823.

JERNIGAN, D. B. & COX, N. J. 2013. Human influenza: One health, one world. *Textbook of Influenza.* John Wiley & Sons, Ltd.

KARLSSON, E. A., MELIOPOULOS, V. A., SAVAGE, C., LIVINGSTON, B., MEHLE, A. & SCHULTZ-CHERRY, S. 2015. Visualizing real-time influenza virus infection, transmission and protection in ferrets. *Nat Commun,* 6**,** 6378.

KE, C., MOK, C. K. P., ZHU, W., ZHOU, H., HE, J., GUAN, W., WU, J., SONG, W., WANG, D., LIU, J., LIN, Q., CHU, D. K. W., YANG, L., ZHONG, N., YANG, Z., SHU, Y. & PEIRIS, J. S. M. 2017. Human Infection with Highly Pathogenic Avian Influenza A(H7N9) Virus, China. *Emerging Infectious Diseases,* 23**,** 1332-1340.

KESHAVARZ, M., MIRZAEI, H., SALEMI, M., MOMENI, F., MOUSAVI, M. J., SADEGHALVAD, M., ARJEINI, Y., SOLAYMANI-MOHAMMADI, F., SADRI NAHAND, J., NAMDARI, H., MOKHTARI-AZAD, T. & REZAEI, F. 2019. Influenza vaccine: Where are we and where do we go? 29**,** e2014.

KILLINGLEY, B., GREATOREX, J., CAUCHEMEZ, S., ENSTONE, J. E., CURRAN, M., READ, R. C., LIM, W. S., HAYWARD, A., NICHOLSON, K. G. & NGUYEN-VAN-TAM, J. S. 2010. Virus shedding and environmental deposition of novel A (H1N1) pandemic influenza virus: Interim findings. *Health Technology Assessment,* 14**,** 237-354.

KILLINGLEY, B. & NGUYEN-VAN-TAM, J. 2013. Routes of influenza transmission. *Influenza and other respiratory viruses,* 7 Suppl 2**,** 42-51.

KIM, H. M., KANG, Y. M., KU, K. B., PARK, E. H., YUM, J., KIM, J. C., JIN, S. Y., LEE, J. S., KIM, H. S. & SEO, S. H. 2013. The severe pathogenicity of alveolar macrophage-depleted ferrets infected with 2009 pandemic H1N1 influenza virus. *Virology,* 444**,** 394-403.

KIM, H. M., LEE, Y.-W., LEE, K.-J., KIM, H. S., CHO, S. W., VAN ROOIJEN, N., GUAN, Y. & SEO, S. H. 2008. Alveolar Macrophages Are Indispensable for Controlling Influenza Viruses in Lungs of Pigs. *Journal of Virology,* 82**,** 4265-4274.

KIRKEBY, S., MARTEL, C. J. M. & AASTED, B. 2009. Infection with human H1N1 influenza virus affects the expression of sialic acids of metaplastic mucous cells in the ferret airways. *Virus Research,* 144**,** 225-232.

KLENK, H.-D., WAGNER, R., HEUER, D. & WOLFF, T. 2001. Importance of hemagglutinin glycosylation for the biological functions of influenza virus. *Virus Research,* 82**,** 73-75.

KOSTER, F., GOUVEIA, K., ZHOU, Y., LOWERY, K., RUSSELL, R., MACINNES, H., POLLOCK, Z., LAYTON, R. C., CROMWELL, J., TOLENO, D., PYLE, J., ZUBELEWICZ, M., HARROD, K., SAMPATH, R., HOFSTADLER, S., GAO, P., LIU, Y. & CHENG, Y. S. 2012. Exhaled aerosol transmission of pandemic and seasonal H1N1 influenza viruses in the ferret. *PLoS One,* 7**,** e33118.

KRAMMER, F., HAI, R., YONDOLA, M., TAN, G. S., LEYVA-GRADO, V. H., RYDER, A. B., MILLER, M. S., ROSE, J. K., PALESE, P., GARCÍA-SASTRE, A. & ALBRECHT, R. A. 2014. Assessment of Influenza Virus Hemagglutinin Stalk-Based Immunity in Ferrets. *Journal of Virology,* 88**,** 3432-3442.

KREIJTZ, J. H. C. M., DE MUTSERT, G., VAN BAALEN, C. A., FOUCHIER, R. A. M., OSTERHAUS, A. D. M. E. & RIMMELZWAAN, G. F. 2008. Cross-recognition of avian H5N1 influenza virus by human cytotoxic T-lymphocyte populations directed to human influenza A virus. *Journal of virology,* 82**,** 5161-5166.

KREIJTZ, J. H. C. M., FOUCHIER, R. A. M. & RIMMELZWAAN, G. F. 2011. Immune responses to influenza virus infection. *Virus Research,* 162**,** 19-30.

KREIJTZ, J. H. C. M., KROEZE, E. J. B. V., STITTELAAR, K. J., DE WAAL, L., VAN AMERONGEN, G., VAN TRIERUM, S., VAN RUN, P., BESTEBROER, T., T.KUIKEN, FOUCHIER, R. A. M., RIMMELZWAAN, G. F. & OSTERHAUS, A. D. M. E. 2013. Low pathogenic avian influenza A(H7N9) virus causes high mortality in ferrets upon intratracheal challenge: A model to study intervention strategies. *Vaccine,* 31**,** 4995-4999.

KUTTER, J. S., SPRONKEN, M. I., FRAAIJ, P. L., FOUCHIER, R. A. M. & HERFST, S. 2018. Transmission routes of respiratory viruses among humans. *Current Opinion in Virology,* 28**,** 142-151.

KWON, Y. K., LIPATOV, A. S. & SWAYNE, D. E. 2009. Bronchointerstitial Pneumonia in Guinea Pigs Following Inoculation with H5N1 High Pathogenicity Avian Influenza Virus. *Veterinary Pathology Online,* 46**,** 138-141.

LAKADAMYALI, M., RUST, M. J. & ZHUANG, X. 2004. Endocytosis of influenza viruses. *Microbes and infection / Institut Pasteur,* 6**,** 929-936.

LAKDAWALA, S. S., LAMIRANDE, E. W., SUGUITAN, A. L., JR., WANG, W., SANTOS, C. P., VOGEL, L., MATSUOKA, Y., LINDSLEY, W. G., JIN, H. & SUBBARAO, K. 2011. Eurasian-Origin Gene Segments Contribute to the Transmissibility, Aerosol Release,

and Morphology of the 2009 Pandemic H1N1 Influenza Virus. *PLoS Pathog,* 7**,** e1002443.

LEDNICKY, J., HAMILTON, S., TUTTLE, R., SOSNA, W., DANIELS, D. & SWAYNE, D. 2010. Ferrets develop fatal influenza after inhaling small particle aerosols of highly pathogenic avian influenza virus A/Vietnam/1203/2004 (H5N1). *Virology Journal,* 7**,** 231.

LEE, D.-H., KIM, J.-I., LEE, J.-W., CHUNG, W.-H., PARK, J.-K., LEE, Y.-N., HAN, J. S., KIM, H.-Y., LEE, S.-W. & SONG, C.-S. 2014. Quantitative measurement of influenza virus replication using consecutive bronchoalveolar lavage in the lower respiratory tract of a ferret model. *Journal of veterinary science,* 15**,** 439-442.

LEE, L. Y. H., HA, D. L. A., SIMMONS, C., DE JONG, M. D., CHAU, N. V. V., SCHUMACHER, R., YAN, C. P., MCMICHAEL, A. J., FARRAR, J. J., SMITH, G. L., TOWNSEND, A. R. M., ASKONAS, B. A., ROWLAND-JONES, S. & DONG, T. 2008. Memory T cells established by seasonal human influenza A infection cross-react with avian influenza A (H5N1) in healthy individuals. *Journal of Clinical Investigation,* 118**,** 3478-3490.

LEUNG, G. M. & NICOLL, A. 2010. Reflections on Pandemic (H1N1) 2009 and the International Response. *PLOS Medicine,* 7**,** e1000346.

LI, C. T., CHAN, C. M. & LEE, N. 2015. Clinical Implications of Antiviral Resistance in Influenza. *Viruses,* 7.

LI, J., CHEN, J., YANG, G., ZHENG, Y. X., MAO, S. H., ZHU, W. P., YU, X. L., GAO, Y., PAN, Q. C. & YUAN, Z. A. 2014. Case-control study of risk factors for human

infection with avian influenza A(H7N9) virus in Shanghai, China, 2013. *Epidemiology and Infection,* 143**,** 1826-1832.

LIN, K. L., SUZUKI, Y., NAKANO, H., RAMSBURG, E. & GUNN, M. D. 2008. CCR2⁺ Monocyte-Derived Dendritic Cells and Exudate Macrophages Produce Influenza-Induced Pulmonary Immune Pathology and Mortality. *The Journal of Immunology,* 180**,** 2562.

LINDSLEY, W. G., BLACHERE, F. M., THEWLIS, R. E., VISHNU, A., DAVIS, K. A., CAO, G., PALMER, J. E., CLARK, K. E., FISHER, M. A., KHAKOO, R. & BEEZHOLD, D. H. 2010. Measurements of Airborne Influenza Virus in Aerosol Particles from Human Coughs. *PLoS ONE,* 5**,** e15100.

LINDSLEY, W. G., PEARCE, T. A., HUDNALL, J. B., DAVIS, K. A., DAVIS, S. M., FISHER, M. A., KHAKOO, R., PALMER, J. E., CLARK, K. E., CELIK, I., COFFEY, C. C., BLACHERE, F. M. & BEEZHOLD, D. H. 2012. Quantity and Size Distribution of Cough-Generated Aerosol Particles Produced by Influenza Patients During and After Illness. *Journal of occupational and environmental hygiene,* 9**,** 443-449.

LINGWOOD, D. & SIMONS, K. 2010. Lipid Rafts As a Membrane-Organizing Principle. *Science,* 327**,** 46.

LIU, B., HAVERS, F., CHEN, E., YUAN, Z., YUAN, H., OU, J., SHANG, M., KANG, K., LIAO, K., LIU, F., LI, D., DING, H., ZHOU, L., ZHU, W., DING, F., ZHANG, P., WANG, X., YAO, J., XIANG, N., ZHOU, S., LIU, X., SONG, Y., SU, H., WANG, R., CAI, J., CAO, Y., WANG, X., BAI, T., WANG, J., FENG, Z., ZHANG, Y., WIDDOWSON, M.-A. & LI, Q. 2014. Risk Factors for Influenza A(H7N9) Disease—China, 2013. *Clinical Infectious Diseases,* 59**,** 787-794.

LIU, S.-Y., SANCHEZ, D. J., ALIYARI, R., LU, S. & CHENG, G. 2012. Systematic identification of type I and type II interferon-induced antiviral factors. *Proceedings of the National Academy of Sciences of the United States of America,* 109**,** 4239-4244.

LONG, J. S., MISTRY, B., HASLAM, S. M. & BARCLAY, W. S. 2019. Host and viral determinants of influenza A virus species specificity. *Nature Reviews Microbiology,* 17**,** 67-81.

LOWEN, A. C., MUBAREKA, S., STEEL, J. & PALESE, P. 2007. Influenza virus transmission is dependent on relative humidity and temperature. *PLoS Pathog,* 3**,** 1470-6.

LOWEN, A. C., MUBAREKA, S., TUMPEY, T. M., GARCÍA-SASTRE, A. & PALESE, P. 2006. The guinea pig as a transmission model for human influenza viruses. *Proceedings of the National Academy of Sciences,* 103**,** 9988-9992.

LOWEN, A. C., STEEL, J., MUBAREKA, S. & PALESE, P. 2008. High Temperature (30°C) Blocks Aerosol but Not Contact Transmission of Influenza Virus. *Journal of Virology,* 82**,** 5650-5652.

LUDLOW, M., DE VRIES, R. D., LEMON, K., MCQUAID, S., MILLAR, E., VAN AMERONGEN, G., YÜKSEL, S., VERBURGH, R. J., OSTERHAUS, A. D. M. E., DE SWART, R. L. & DUPREX, W. P. 2013. Infection of lymphoid tissues in the macaque upper respiratory tract contributes to the emergence of transmissible measles virus. 94**,** 1933-1944.

MACINNES, H., ZHOU, Y., GOUVEIA, K., CROMWELL, J., LOWERY, K., LAYTON, R. C., ZUBELEWICZ, M., SAMPATH, R., HOFSTADLER, S., LIU, Y., CHENG, Y.-S. &

KOSTER, F. 2011. Transmission of Aerosolized Seasonal H1N1 Influenza A to Ferrets. *PLoS ONE,* 6**,** e24448.

MAHER, J. & DESTEFANO, J. 2004. The ferret: an animal model to study influenza virus. *Lab Anim (NY),* 33**,** 50 - 53.

MAINES, T. R., CHEN, L.-M., MATSUOKA, Y., CHEN, H., ROWE, T., ORTIN, J., FALCÓN, A., HIEN, N. T., MAI, L. Q., SEDYANINGSIH, E. R., HARUN, S., TUMPEY, T. M., DONIS, R. O., COX, N. J., SUBBARAO, K. & KATZ, J. M. 2006. Lack of transmission of H5N1 avian-human reassortant influenza viruses in a ferret model. *Proc Natl Acad Sci USA,* 103.

MAINES, T. R., JAYARAMAN, A., BELSER, J. A., WADFORD, D. A., PAPPAS, C., ZENG, H., GUSTIN, K. M., PEARCE, M. B., VISWANATHAN, K., SHRIVER, Z. H., RAMAN, R., COX, N. J., SASISEKHARAN, R., KATZ, J. M. & TUMPEY, T. M. 2009. Transmission and Pathogenesis of Swine-Origin 2009 A(H1N1) Influenza Viruses in Ferrets and Mice. *Science,* 325**,** 484-487.

MANCINI, N., SOLFOROSI, L., CLEMENTI, N., DE MARCO, D., CLEMENTI, M. & BURIONI, R. 2011. A potential role for monoclonal antibodies in prophylactic and therapeutic treatment of influenza. *Antiviral Research,* 92**,** 15-26.

MANDELBOIM, O., LIEBERMAN, N., LEV, M., PAUL, L., ARNON, T. I., BUSHKIN, Y., DAVIS, D. M., STROMINGER, J. L., YEWDELL, J. W. & PORGADOR, A. 2001. Recognition of haemagglutinins on virus-infected cells by NKp46 activates lysis by human NK cells. *Nature,* 409**,** 1055.

MARGINE, I. & KRAMMER, F. 2014. Animal Models for Influenza Viruses: Implications for Universal Vaccine Development. *Pathogens,* 3**,** 845.

MARRIOTT, A. C., DOVE, B. K., WHITTAKER, C. J., BRUCE, C., RYAN, K. A., BEAN, T. J., RAYNER, E., PEARSON, G., TAYLOR, I., DOWALL, S., PLANK, J., NEWMAN, E., BARCLAY, W. S., DIMMOCK, N. J., EASTON, A. J., HALLIS, B., SILMAN, N. J. & CARROLL, M. W. 2014. Low Dose Influenza Virus Challenge in the Ferret Leads to Increased Virus Shedding and Greater Sensitivity to Oseltamivir. *PLoS ONE,* 9**,** e94090.

MARTEL, C. J.-M., AGGER, E. M., POULSEN, J. J., HAMMER JENSEN, T., ANDRESEN, L., CHRISTENSEN, D., NIELSEN, L. P., BLIXENKRONE-MØLLER, M., ANDERSEN, P. & AASTED, B. 2011. CAF01 Potentiates Immune Responses and Efficacy of an Inactivated Influenza Vaccine in Ferrets. *PLOS ONE,* 6**,** e22891.

MATROSOVICH, M. & KLENK, H. D. 2003. Natural and synthetic sialic acid-containing inhibitors of influenza virus receptor binding. *Rev Med Virol,* 13.

MATSUOKA, Y., MATSUMAE, H., KATOH, M., EISFELD, A. J., NEUMANN, G., HASE, T., GHOSH, S., SHOEMAKER, J. E., LOPES, T. J. S., WATANABE, T., WATANABE, S., FUKUYAMA, S., KITANO, H. & KAWAOKA, Y. 2013. A comprehensive map of the influenza A virus replication cycle. *BMC systems biology,* 7**,** 97-97.

MAY, K. R. 1973. The collison nebulizer: Description, performance and application. *Journal of Aerosol Science,* 4**,** 235-243.

MAZANEC, M. B., COUDRET, C. L. & FLETCHER, D. R. 1995. Intracellular neutralization of influenza virus by immunoglobulin A anti-hemagglutinin monoclonal antibodies. *Journal of Virology,* 69**,** 1339-1343.

MEDINA, R. A. & GARCÍA-SASTRE, A. 2011. Influenza A viruses: new research developments. *Nature Reviews Microbiology,* 9**,** 590.

MEMOLI, M. J., SHAW, P. A., HAN, A., CZAJKOWSKI, L., REED, S., ATHOTA, R., BRISTOL, T., FARGIS, S., RISOS, K., POWERS, J. H., DAVEY, R. T. & TAUBENBERGER, J. K. 2016. Evaluation of Antihemagglutinin and Antineuraminidase Antibodies as Correlates of Protection in an Influenza A/H1N1 Virus Healthy Human Challenge Model. *mBio,* 7**,** e00417-16.

MENTEN, P., WUYTS, A. & VAN DAMME, J. 2002. Macrophage inflammatory protein-1. *Cytokine & Growth Factor Reviews,* 13**,** 455-481.

MILTON, D. K., FABIAN, M. P., COWLING, B. J., GRANTHAM, M. L. & MCDEVITT, J. J. 2013. Influenza Virus Aerosols in Human Exhaled Breath: Particle Size, Culturability, and Effect of Surgical Masks. *PLoS Pathog,* 9**,** e1003205.

MITCHELL, C. A., GUERIN, L. F. & ROBILLARD, J. 1968. Decay of influenza A viruses of human and avian origin. *Canadian journal of comparative medicine : Revue canadienne de medecine comparee,* 32**,** 544-546.

MONCLA, L. H., ROSS, T. M., DINIS, J. M., WEINFURTER, J. T., MORTIMER, T. D., SCHULTZ-DARKEN, N., BRUNNER, K., CAPUANO, S. V., III, BOETTCHER, C., POST, J., JOHNSON, M., BLOOM, C. E., WEILER, A. M. & FRIEDRICH, T. C. 2013. A Novel Nonhuman Primate Model for Influenza Transmission. *PLoS ONE,* 8**,** e78750.

MOOIJ, P., KOOPMAN, G., MORTIER, D., VAN HETEREN, M., OOSTERMEIJER, H., FAGROUCH, Z., DE LAAT, R., KOBINGER, G., LI, Y., REMARQUE, E. J., KONDOVA, I., VERSCHOOR, E. J. & BOGERS, W. M. J. M. 2015. Pandemic Swine-Origin H1N1 Influenza Virus Replicates to Higher Levels and Induces More Fever and Acute Inflammatory Cytokines in Cynomolgus versus Rhesus Monkeys and Can Replicate in Common Marmosets. *PLoS ONE,* 10**,** e0126132.

MOORE, I. N., LAMIRANDE, E. W., PASKEL, M., DONAHUE, D., KENNEY, H., QIN, J. & SUBBARAO, K. 2014. Severity of clinical disease and pathology in ferrets experimentally infected with influenza viruses is influenced by inoculum volume. *Journal of virology,* 88**,** 13879-13891.

MOZDZANOWSKA, K., MAIESE, K., FURCHNER, M. & GERHARD, W. 1999. Treatment of Influenza Virus-Infected SCID Mice with Nonneutralizing Antibodies Specific for the Transmembrane Proteins Matrix 2 and Neuraminidase Reduces the Pulmonary Virus Titer but Fails to Clear the Infection. *Virology,* 254**,** 138-146.

MUKHERJEE, S., LINDELL, D. M., BERLIN, A. A., MORRIS, S. B., SHANLEY, T. P., HERSHENSON, M. B. & LUKACS, N. W. 2011. IL-17-induced pulmonary pathogenesis during respiratory viral infection and exacerbation of allergic disease. *The American journal of pathology,* 179**,** 248-258.

MUNSTER, V. J., DE WIT, E., VAN DEN BRAND, J. M., HERFST, S., SCHRAUWEN, E. J., BESTEBROER, T. M., VAN DE VIJVER, D., BOUCHER, C. A., KOOPMANS, M., RIMMELZWAAN, G. F., KUIKEN, T., OSTERHAUS, A. D. & FOUCHIER, R. A. 2009. Pathogenesis and transmission of swine-origin 2009 A(H1N1) influenza virus in ferrets. *Science,* 325**,** 481-3.

MURPHY, B. R., KASEL, J. A. & CHANOCK, R. M. 1972. Association of Serum Anti-Neuraminidase Antibody with Resistance to Influenza in Man. *New England Journal of Medicine,* 286**,** 1329-1332.

MURPHY, B. R., NELSON, D. L., WRIGHT, P. F., TIERNEY, E. L., PHELAN, M. A. & CHANOCK, R. M. 1982. Secretory and systemic immunological response in children infected with live attenuated influenza A virus vaccines. *Infection and Immunity,* 36**,** 1102-1108.

MUSIC, N., REBER, A. J., LIPATOV, A. S., KAMAL, R. P., BLANCHFIELD, K., WILSON, J. R., DONIS, R. O., KATZ, J. M. & YORK, I. A. 2014. Influenza Vaccination Accelerates Recovery of Ferrets from Lymphopenia. *PLOS ONE,* 9**,** e100926.

NEUMANN, G., NODA, T. & KAWAOKA, Y. 2009. Emergence and pandemic potential of swine-origin H1N1 influenza virus. *Nature,* 459**,** 931-939.

NICHOLLS, J. M., BOURNE, A. J., CHEN, H., GUAN, Y. & PEIRIS, J. S. M. 2007. Sialic acid receptor detection in the human respiratory tract: evidence for widespread distribution of potential binding sites for human and avian influenza viruses. *Respiratory research,* 8**,** 73-73.

NIKITIN, N., PETROVA, E., TRIFONOVA, E. & KARPOVA, O. 2014. Influenza virus aerosols in the air and their infectiousness. *Advances in virology,* 2014**,** 859090-859090.

NISHIURA, H., YEN, H.-L. & COWLING, B. J. 2013. Sample Size Considerations for One-to-One Animal Transmission Studies of the Influenza A Viruses. *PLOS ONE,* 8**,** e55358.

NÜSSING, S., SANT, S., KOUTSAKOS, M., SUBBARAO, K., NGUYEN, T. H. O. & KEDZIERSKA, K. 2018. Innate and adaptive T cells in influenza disease. *Frontiers of Medicine,* 12**,** 34-47.

OH, D. Y., BARR, I. G. & HURT, A. C. 2015. A Novel Video Tracking Method to Evaluate the Effect of Influenza Infection and Antiviral Treatment on Ferret Activity. *PLOS ONE,* 10**,** e0118780.

OH, D. Y. & HURT, A. C. 2016. Using the Ferret as an Animal Model for Investigating Influenza Antiviral Effectiveness. *Frontiers in microbiology,* 7**,** 80-80.

OMEROD, M. G. 2008. *Flow Cytometry: A basic introduction*.

OTTE, A., MARRIOTT, A. C., DREIER, C., DOVE, B., MOOREN, K., KLINGEN, T. R., SAUTER, M., THOMPSON, K.-A., BENNETT, A., KLINGEL, K., VAN RIEL, D., MCHARDY, A. C., CARROLL, M. W. & GABRIEL, G. 2016. Evolution of 2009 H1N1 influenza viruses during the pandemic correlates with increased viral pathogenicity and transmissibility in the ferret model. *Scientific reports,* 6**,** 28583-28583.

PALESE, P., TOBITA, K., UEDA, M. & COMPANS, R. W. 1974. Characterization of temperature sensitive influenza virus mutants defective in neuraminidase. *Virology,* 61**,** 397-410.

PANG, I. K. & IWASAKI, A. 2011. Inflammasomes as mediators of immunity against influenza virus. *Trends in Immunology,* 32**,** 34-41.

PAQUETTE, S. G., HUANG, S. S. H., BANNER, D., XU, L., LEʹON, A., KELVIN, A. A. & KELVIN, D. J. 2014. Impaired heterologous immunity in aged ferrets during sequential influenza A H1N1 infection. *Virology,* 464–465**,** 177-183.

PARAMESWARAN, N. & PATIAL, S. 2010. Tumor necrosis factor-α signaling in macrophages. *Critical reviews in eukaryotic gene expression,* 20**,** 87-103.

PAULES, C. & SUBBARAO, K. 2017. Influenza. *The Lancet,* 390**,** 697-708.

PEIRIS, J. S. M., HUI, K. P. Y. & YEN, H.-L. 2010. Host response to influenza virus: protection versus immunopathology. *Current Opinion in Immunology,* 22**,** 475-481.

PENG, X., ALFOLDI, J., GORI, K., EISFELD, A. J., TYLER, S. R., TISONCIK-GO, J., BRAWAND, D., LAW, G. L., SKUNCA, N., HATTA, M., GASPER, D. J., KELLY, S. M., CHANG, J., THOMAS, M. J., JOHNSON, J., BERLIN, A. M., LARA, M.,

RUSSELL, P., SWOFFORD, R., TURNER-MAIER, J., YOUNG, S., HOURLIER, T., AKEN, B., SEARLE, S., SUN, X., YI, Y., SURESH, M., TUMPEY, T. M., SIEPEL, A., WISELY, S. M., DESSIMOZ, C., KAWAOKA, Y., BIRREN, B. W., LINDBLAD-TOH, K., DI PALMA, F., ENGELHARDT, J. F., PALERMO, R. E. & KATZE, M. G. 2014. The draft genome sequence of the ferret (Mustela putorius furo) facilitates study of human respiratory disease. *Nat Biotechnol,* 32**,** 1250-5.

PETROVA, V. N. & RUSSELL, C. A. 2017. The evolution of seasonal influenza viruses. *Nature Reviews Microbiology,* 16**,** 47.

PFLUG, A., LUKARSKA, M., RESA-INFANTE, P., REICH, S. & CUSACK, S. 2017. Structural insights into RNA synthesis by the influenza virus transcription-replication machine. *Virus Research,* 234**,** 103-117.

PHE. 2019. *Risk assessment of avian influenza A(H7N9) – seventh update* [Online]. Available: https://www.gov.uk/government/publications/avian-influenza-a-h7n9-public-health-england-risk-assessment/risk-assessment-of-avian-influenza-ah7n9-sixth-update [Accessed 16 Sep 2019].

QUAST, M., SREENIVASAN, C., SEXTON, G., NEDLAND, H., SINGREY, A., FAWCETT, L., MILLER, G., LAUER, D., VOSS, S., POLLOCK, S., CUNHA, C. W., CHRISTOPHER-HENNINGS, J., NELSON, E. & LI, F. 2015. Serological evidence for the presence of influenza D virus in small ruminants. *Veterinary Microbiology,* 180**,** 281-285.

QUIÑONES-PARRA, S., GRANT, E., LOH, L., NGUYEN, T. H. O., CAMPBELL, K.-A., TONG, S. Y. C., MILLER, A., DOHERTY, P. C., VIJAYKRISHNA, D., ROSSJOHN, J., GRAS, S. & KEDZIERSKA, K. 2014. Preexisting CD8+ T-cell immunity to the

H7N9 influenza A virus varies across ethnicities. *Proceedings of the National Academy of Sciences of the United States of America,* 111**,** 1049-1054.

REBER, A. J., MUSIC, N., KIM, J. H., GANSEBOM, S., CHEN, J. & YORK, I. 2018. Extensive T cell cross-reactivity between diverse seasonal influenza strains in the ferret model. *Scientific Reports,* 8**,** 6112.

RICHARD, M. & FOUCHIER, R. A. M. 2016. Influenza A virus transmission via respiratory aerosols or droplets as it relates to pandemic potential. *FEMS microbiology reviews,* 40**,** 68-85.

ROBERTS, K. L., SHELTON, H., SCULL, M., PICKLES, R. & BARCLAY, W. S. 2011. Lack of transmission of a human influenza virus with avian receptor specificity between ferrets is not due to decreased virus shedding but rather a lower infectivity in vivo. *Journal of General Virology,* 92**,** 1822-1831.

ROBERTS, K. L., SHELTON, H., STILWELL, P. & BARCLAY, W. S. 2012. Transmission of a 2009 H1N1 Pandemic Influenza Virus Occurs before Fever Is Detected, in the Ferret Model. *PLoS ONE,* 7**,** e43303.

ROSSMAN, J. S., JING, X., LESER, G. P. & LAMB, R. A. 2010. Influenza virus M2 protein mediates ESCRT-independent membrane scission. *Cell,* 142**,** 902-913.

ROTA, P. A., WALLIS, T. R., HARMON, M. W., ROTA, J. S., KENDAL, A. P. & NEROME, K. 1990. Cocirculation of two distinct evolutionary lineages of influenza type B virus since 1983. *Virology,* 175**,** 59-68.

ROTHBARTH, P. H., GROEN, J., BOHNEN, A. M., DE GROOT, R. & OSTERHAUS, A. D. M. E. 1999. Influenza virus serology—a comparative study. *Journal of Virological Methods,* 78**,** 163-169.

RYAN, K. A., SLACK, G. S., MARRIOTT, A. C., KANE, J. A., WHITTAKER, C. J., SILMAN, N. J., CARROLL, M. W. & GOOCH, K. E. 2018. Cellular immune response to human influenza viruses differs between H1N1 and H3N2 subtypes in the ferret lung. *PloS one,* 13**,** e0202675-e0202675.

SAMSON, M., PIZZORNO, A., ABED, Y. & BOIVIN, G. 2013. Influenza virus resistance to neuraminidase inhibitors. *Antiviral Research,* 98**,** 174-185.

SAUNDERS-HASTINGS, P. R. & KREWSKI, D. 2016. Reviewing the History of Pandemic Influenza: Understanding Patterns of Emergence and Transmission. *Pathogens,* 5**,** 66.

SCHNEIDER, J. & WOLFF, T. 2009. Nuclear functions of the influenza A and B viruses NS1 proteins: Do they play a role in viral mRNA export? *Vaccine,* 27**,** 6312-6316.

SEITZ, C., FRENSING, T., HÖPER, D., KOCHS, G. & REICHL, U. 2010. High yields of influenza A virus in Madin–Darby canine kidney cells are promoted by an insufficient interferon-induced antiviral state. 91**,** 1754-1763.

SKEHEL, J. J. & WILEY, D. C. 2000. Receptor Binding and Membrane Fusion in Virus Entry: The Influenza Hemagglutinin. *Annual Review of Biochemistry,* 69**,** 531-569.

SMITH, G. J. D., VIJAYKRISHNA, D., BAHL, J., LYCETT, S. J., WOROBEY, M., PYBUS, O. G., MA, S. K., CHEUNG, C. L., RAGHWANI, J., BHATT, S., PEIRIS, J. S. M., GUAN, Y. & RAMBAUT, A. 2009. Origins and evolutionary genomics of the 2009 swine-origin H1N1 influenza A epidemic. *Nature,* 459**,** 1122-1125.

SMITH, W., ANDREWES, C. H. & LAIDLAW, P. P. 1933. A VIRUS OBTAINED FROM INFLUENZA PATIENTS. *The Lancet,* 222**,** 66-68.

SPACKMAN, E. 2008. A Brief Introduction to the Avian Influenza Virus. *In:* SPACKMAN, E. (ed.) *Avian Influenza Virus.* Totowa, NJ: Humana Press.

SRIDHAR, S., BEGOM, S., BERMINGHAM, A., HOSCHLER, K., ADAMSON, W., CARMAN, W., BEAN, T., BARCLAY, W., DEEKS, J. J. & LALVANI, A. 2013. Cellular immune correlates of protection against symptomatic pandemic influenza. *Nature Medicine,* 19**,** 1305-1312.

STRUTT, T. M., MCKINSTRY, K. K., DIBBLE, J. P., WINCHELL, C., KUANG, Y., CURTIS, J. D., HUSTON, G., DUTTON, R. W. & SWAIN, S. L. 2010. Memory CD4+ T cells induce innate responses independently of pathogen. *Nature medicine,* 16**,** 558-564.

SU, S., FU, X., LI, G., KERLIN, F. & VEIT, M. 2017. Novel Influenza D virus: Epidemiology, pathology, evolution and biological characteristics. *Virulence,* 8**,** 1580-1591.

SUN, J., MADAN, R., KARP, C. L. & BRACIALE, T. J. 2009. Effector T cells control lung inflammation during acute influenza virus infection by producing IL-10. *Nature Medicine,* 15**,** 277.

SUN, K. & METZGER, D. W. 2008. Inhibition of pulmonary antibacterial defense by interferon-γ during recovery from influenza infection. *Nature Medicine,* 14**,** 558.

SUN, X., YAN, Z., YI, Y., LI, Z., LEI, D., ROGERS, C. S., CHEN, J., ZHANG, Y., WELSH, M. J., LENO, G. H. & ENGELHARDT, J. F. 2008. Adeno-associated virus-targeted disruption of the CFTR gene in cloned ferrets. *The Journal of clinical investigation,* 118**,** 1578-1583.

TALKER, S. C., STADLER, M., KOINIG, H. C., MAIR, K. H., RODRÍGUEZ-GÓMEZ, I. M., GRAAGE, R., ZELL, R., DÜRRWALD, R., STARICK, E., HARDER, T., WEISSENBÖCK, H., LAMP, B., HAMMER, S. E., LADINIG, A., SAALMÜLLER, A. &

GERNER, W. 2016. Influenza A Virus Infection in Pigs Attracts Multifunctional and Cross-Reactive T Cells to the Lung. *Journal of Virology,* 90**,** 9364-9382.

TAO, Y. J. & ZHENG, W. 2012. Visualizing the Influenza Genome. *Science,* 338**,** 1545.

TAUBENBERGER J K, R. A. H., JANCZEWSKI T A, AND FANNING T G 2001. Integrating historical, clinical and molecular genetic data in order to explain the origin and virulence of the 1918 Spanish influenza virus. *Philosophical Transactions of the Royal Society of London. Series B: Biological Sciences,* 356**,** 1829.

TEAM, N. S.-O. I. A. V. I. 2009. Emergence of a Novel Swine-Origin Influenza A (H1N1) Virus in Humans. *New England Journal of Medicine,* 360**,** 2605-2615.

TELLIER, R. 2006a. Review of aerosol transmission of influenza A virus. *Emerg Infect Dis,* 12.

TELLIER, R. 2006b. Review of aerosol transmission of influenza A virus. *Emerg Infect Dis,* 12**,** 1657 - 1660.

TELLIER, R. 2009. Aerosol transmission of influenza A virus: a review of new studies. *Journal of The Royal Society Interface,* 6**,** S783-S790.

THANGAVEL, R. R. & BOUVIER, N. M. 2014. Animal models for influenza virus pathogenesis, transmission, and immunology. *Journal of Immunological Methods,* 410**,** 60-79.

THOMPSON, K. A. & BENNETT, A. M. 2017. Persistence of influenza on surfaces. *Journal of Hospital Infection,* 95**,** 194-199.

THORLUND, K., AWAD, T., BOIVIN, G. & THABANE, L. 2011. Systematic review of influenza resistance to the neuraminidase inhibitors. *BMC infectious diseases,* 11**,** 134-134.

TONG, S., LI, Y., RIVAILLER, P., CONRARDY, C., CASTILLO, D. A. A., CHEN, L.-M., RECUENCO, S., ELLISON, J. A., DAVIS, C. T., YORK, I. A., TURMELLE, A. S., MORAN, D., ROGERS, S., SHI, M., TAO, Y., WEIL, M. R., TANG, K., ROWE, L. A., SAMMONS, S., XU, X., FRACE, M., LINDBLADE, K. A., COX, N. J., ANDERSON, L. J., RUPPRECHT, C. E. & DONIS, R. O. 2012. A distinct lineage of influenza A virus from bats. *Proceedings of the National Academy of Sciences of the United States of America,* 109**,** 4269-4274.

TONG, S., ZHU, X., LI, Y., SHI, M., ZHANG, J., BOURGEOIS, M., YANG, H., CHEN, X., RECUENCO, S., GOMEZ, J., CHEN, L.-M., JOHNSON, A., TAO, Y., DREYFUS, C., YU, W., MCBRIDE, R., CARNEY, P. J., GILBERT, A. T., CHANG, J., GUO, Z., DAVIS, C. T., PAULSON, J. C., STEVENS, J., RUPPRECHT, C. E., HOLMES, E. C., WILSON, I. A. & DONIS, R. O. 2013. New World Bats Harbor Diverse Influenza A Viruses. *PLOS Pathogens,* 9**,** e1003657.

TREANOR, J. J. 2015. 167 - Influenza (Including Avian Influenza and Swine Influenza) A2 - Bennett, John E. *In:* DOLIN, R. & BLASER, M. J. (eds.) *Mandell, Douglas, and Bennett's Principles and Practice of Infectious Diseases (Eighth Edition).* Philadelphia: Content Repository Only!

TUMPEY, T. M., GARCÍA-SASTRE, A., TAUBENBERGER, J. K., PALESE, P., SWAYNE, D. E., PANTIN-JACKWOOD, M. J., SCHULTZ-CHERRY, S., SOLÓRZANO, A., VAN ROOIJEN, N., KATZ, J. M. & BASLER, C. F. 2005. Pathogenicity of Influenza Viruses with Genes from the 1918 Pandemic Virus: Functional Roles of Alveolar

Macrophages and Neutrophils in Limiting Virus Replication and Mortality in Mice. *Journal of Virology,* 79**,** 14933-14944.

TURGEON, N., HAMELIN, M.-È., VERREAULT, D., LÉVESQUE, A., RHÉAUME, C., CARBONNEAU, J., CHECKMAHOMED, L., GIRARD, M., BOIVIN, G. & DUCHAINE, C. 2019. Design and Validation with Influenza A Virus of an Aerosol Transmission Chamber for Ferrets. *International journal of environmental research and public health,* 16**,** 609.

TUTTLE, R., SOSNA, W., DANIELS, D., HAMILTON, S. & LEDNICKY, J. 2010a. Design, assembly, and validation of a nose-only inhalation exposure system for studies of aerosolized viable influenza H5N1 virus in ferrets. *Virol J,* 7**,** e135.

TUTTLE, R. S., SOSNA, W. A., DANIELS, D. E., HAMILTON, S. B. & LEDNICKY, J. A. 2010b. Design, assembly, and validation of a nose-only inhalation exposure system for studies of aerosolized viable influenza H5N1 virus in ferrets. *Virology Journal,* 7**,** 1-12.

VAN DE SANDT, C. E., DOU, Y., VOGELZANG-VAN TRIERUM, S. E., WESTGEEST, K. B., PRONK, M. R., OSTERHAUS, A. D. M. E., FOUCHIER, R. A. M., RIMMELZWAAN, G. F. & HILLAIRE, M. L. B. 2015a. Influenza B virus-specific CD8+ T-lymphocytes strongly cross-react with viruses of the opposing influenza B lineage. *The Journal of general virology,* 96**,** 2061-2073.

VAN DE SANDT, C. E., HILLAIRE, M. L. B., GEELHOED-MIERAS, M. M., OSTERHAUS, A. D. M. E., FOUCHIER, R. A. M. & RIMMELZWAAN, G. F. 2015b. Human Influenza A Virus-Specific CD8+ T-Cell Response Is Long-lived. *The Journal of infectious diseases,* 212**,** 81-85.

VAN DE SANDT, C. E., KREIJTZ, J. H. C. M., DE MUTSERT, G., GEELHOED-MIERAS, M. M., HILLAIRE, M. L. B., VOGELZANG-VAN TRIERUM, S. E., OSTERHAUS, A. D. M. E., FOUCHIER, R. A. M. & RIMMELZWAAN, G. F. 2014. Human cytotoxic T lymphocytes directed to seasonal influenza A viruses cross-react with the newly emerging H7N9 virus. *Journal of virology,* 88**,** 1684-1693.

VAN DEN BRAND, J. M. A., STITTELAAR, K. J., VAN AMERONGEN, G., REPERANT, L., DE WAAL, L., OSTERHAUS, A. D. M. E. & KUIKEN, T. 2012. Comparison of Temporal and Spatial Dynamics of Seasonal H3N2, Pandemic H1N1 and Highly Pathogenic Avian Influenza H5N1 Virus Infections in Ferrets. *PLOS ONE,* 7**,** e42343.

VAN DER VRIES, E., VELDHUIS KROEZE, E. J., STITTELAAR, K. J., LINSTER, M., VAN DER LINDEN, A., SCHRAUWEN, E. J. A., LEIJTEN, L. M., VAN AMERONGEN, G., SCHUTTEN, M., KUIKEN, T., OSTERHAUS, A. D. M. E., FOUCHIER, R. A. M., BOUCHER, C. A. B. & HERFST, S. 2011. Multidrug Resistant 2009 A/H1N1 Influenza Clinical Isolate with a Neuraminidase I223R Mutation Retains Its Virulence and Transmissibility in Ferrets. *PLOS Pathogens,* 7**,** e1002276.

VIRALZONE. 2014. *Orthomyxoviridae* [Online]. Available: https://viralzone.expasy.org/223?outline=all_by_protein [Accessed 26SEP 2019].

VON HOLLE, T. A. & MOODY, M. A. 2019. Influenza and Antibody-Dependent Cellular Cytotoxicity. *Frontiers in immunology,* 10**,** 1457-1457.

WANG, Z., WAN, Y., QIU, C., QUIÑONES-PARRA, S., ZHU, Z., LOH, L., TIAN, D., REN, Y., HU, Y., ZHANG, X., THOMAS, P. G., INOUYE, M., DOHERTY, P. C., KEDZIERSKA, K. & XU, J. 2015. Recovery from severe H7N9 disease is associated with diverse response mechanisms dominated by CD8+ T cells. *Nature Communications,* 6**,** 6833.

WATANABE, T. & KAWAOKA, Y. 2011. Pathogenesis of the 1918 Pandemic Influenza Virus. *PLOS Pathogens,* 7**,** e1001218.

WENDEL, I., RUBBENSTROTH, D., DOEDT, J., KOCHS, G., WILHELM, J., STAEHELI, P., KLENK, H.-D. & MATROSOVICH, M. 2015. The Avian-Origin PB1 Gene Segment Facilitated Replication and Transmissibility of the H3N2/1968 Pandemic Influenza Virus. *Journal of Virology,* 89**,** 4170-4179.

WESTGEEST, K. B., RUSSELL, C. A., LIN, X., SPRONKEN, M. I. J., BESTEBROER, T. M., BAHL, J., VAN BEEK, R., SKEPNER, E., HALPIN, R. A., DE JONG, J. C., RIMMELZWAAN, G. F., OSTERHAUS, A. D. M. E., SMITH, D. J., WENTWORTH, D. E., FOUCHIER, R. A. M. & DE GRAAF, M. 2014. Genomewide analysis of reassortment and evolution of human influenza A(H3N2) viruses circulating between 1968 and 2011. *Journal of virology,* 88**,** 2844-2857.

WHO. 2014. *H5N1 highly pathogenic avian influenza: Timeline of major events* [Online]. WHO. Available: http://www.who.int/influenza/human_animal_interface/h5n1_avian_influenza_update20140714.pdf?ua=1&ua=1 [Accessed 09NOV17 2017].

WHO. 2017a. *Global Influenza Surveillance and Response System (GISRS)* [Online]. Available: http://www.who.int/influenza/gisrs_laboratory/en/ [Accessed 10NOV17 2017].

WHO. 2017b. *Influenza at the human-animal interface. Summary and assessment, 25 July 2017 to 27 September 2017* [Online]. WHO Available: http://www.who.int/influenza/human_animal_interface/Influenza_Summary_IRA_HA_interface_09_27_2017.pdf?ua=1 [Accessed 09NOV17 2017].

WHO. 2018. *Fact Sheet: Influenza (Seasonal)* [Online]. Available: https://www.who.int/en/news-room/fact-sheets/detail/influenza-(seasonal) [Accessed 19/06/19 2019].

WHO. 2019a. *Avian Influenza Weekly Update Number 704* [Online]. Available: https://www.who.int/docs/default-source/wpro---documents/emergency/surveillance/avian-influenza/ai-20190830.pdf?sfvrsn=30d65594_34 [Accessed 16 Sep 2019].

WHO. 2019b. *Influenza* [Online]. Available: https://www.who.int/mediacentre/infographic/influenza/en/ [Accessed 20/06/19].

WILEY, J. A., CERWENKA, A., HARKEMA, J. R., DUTTON, R. W. & HARMSEN, A. G. 2001. Production of interferon-gamma by influenza hemagglutinin-specific CD8 effector T cells influences the development of pulmonary immunopathology. *The American journal of pathology,* 158**,** 119-130.

WISE, H. M., BARBEZANGE, C., JAGGER, B. W., DALTON, R. M., GOG, J. R., CURRAN, M. D., TAUBENBERGER, J. K., ANDERSON, E. C. & DIGARD, P. 2011. Overlapping signals for translational regulation and packaging of influenza A virus segment 2. *Nucleic acids research,* 39**,** 7775-7790.

YAMAYOSHI, S., WATANABE, M., GOTO, H. & KAWAOKA, Y. 2016. Identification of a Novel Viral Protein Expressed from the PB2 Segment of Influenza A Virus. *Journal of Virology,* 90**,** 444.

YEN, H.-L., LIPATOV, A. S., ILYUSHINA, N. A., GOVORKOVA, E. A., FRANKS, J., YILMAZ, N., DOUGLAS, A., HAY, A., KRAUSS, S., REHG, J. E., HOFFMANN, E. &

WEBSTER, R. G. 2001. Inefficient Transmission of H5N1 Influenza Viruses in a Ferret Contact Model. *J Virol,* 81.

YOO, E. 2014. Conformation and Linkage Studies of Specific Oligosaccharides Related to H1N1, H5N1, and Human Flu for Developing the Second Tamiflu. *Biomolecules & therapeutics,* 22**,** 93-99.

YU, M., SUN, X., TYLER, S. R., LIANG, B., SWATEK, A. M., LYNCH, T. J., HE, N., YUAN, F., FENG, Z., ROTTI, P. G., CHOI, S. H., SHAHIN, W., LIU, X., YAN, Z. & ENGELHARDT, J. F. 2019. Highly Efficient Transgenesis in Ferrets Using CRISPR/Cas9-Mediated Homology-Independent Insertion at the ROSA26 Locus. *Scientific reports,* 9**,** 1971-1971.

ZHOU, J., WU, J., ZENG, X., HUANG, G., ZOU, L., SONG, Y., GOPINATH, D., ZHANG, X., KANG, M., LIN, J., COWLING, B. J., LINDSLEY, W. G., KE, C., PEIRIS, J. S. M. & YEN, H. 2016. Isolation of H5N6, H7N9 and H9N2 avian influenza A viruses from air sampled at live poultry markets in China, 2014 and 2015. *Euro surveillance : bulletin Europeen sur les maladies transmissibles = European communicable disease bulletin,* 21**,** 10.2807/1560-7917.ES.2016.21.35.30331.

ZHU, J., YAMANE, H. & PAUL, W. E. 2010. Differentiation of effector CD4 T cell populations (*). *Annual review of immunology,* 28**,** 445-489.

10 Publication

PLOS ONE

RESEARCH ARTICLE

Cellular immune response to human influenza viruses differs between H1N1 and H3N2 subtypes in the ferret lung

Kathryn A. Ryan, Gillian S. Slack, Anthony C. Marriott, Jennifer A. Kane, Catherine J. Whittaker, Nigel J. Silman, Miles W. Carroll, Karen E. Gooch*

National Infection Service, Public Health England, Porton Down, Wiltshire, United Kingdom

* karen.gooch@phe.gov.uk

OPEN ACCESS

Citation: Ryan KA, Slack GS, Marriott AC, Kane JA, Whittaker CJ, Silman NJ, et al. (2018) Cellular immune response to human influenza viruses differs between H1N1 and H3N2 subtypes in the ferret lung. PLoS ONE 13(9): e0202675. https://doi.org/10.1371/journal.pone.0202675

Editor: Balaji Manicassamy, The University of Chicago, UNITED STATES

Received: February 12, 2018

Accepted: July 13, 2018

Published: September 7, 2018

Data Availability Statement: All relevant data are within the paper.

Funding: This work was supported by the Department of Health, grant in aid, (https://www.gov.uk/government/organisations/department-of-health-and-social-care). The funder had no role in study design, data collection and analysis, decision to publish, or preparation of the manuscript.

Competing interests: The authors have declared that no competing interests exist.

Abstract

Seasonal influenza virus infections cause yearly epidemics which are the source of a significant public health burden worldwide. The ferret model for human influenza A virus (IAV) is widely used and has several advantages over other animal models such as comparable symptomology, similar receptor distribution in the respiratory tract to humans and the ability to be infected with human isolates without the need for adaptation. However, a major disadvantage of the model has been a paucity of reagents for the evaluation of the cellular immune response. Investigation of T-cell mediated immunity in ferrets is crucial to vaccine development and efficacy studies. In this study we have used commercially produced antibodies to ferret interferon gamma (IFN-γ) allowing us to reliably measure influenza-specific IFN-γ as a marker of the cellular immune response using both enzyme-linked immunospot (ELISpot) and enzyme-linked immunosorbent (ELISA) techniques. Here we demonstrate the application of these tools to evaluate cellular immunity in ferrets infected with clinically relevant seasonal H1N1 and H3N2 IAV subtypes at equivalent doses. Using small heparinised blood samples we were able to observe the longitudinal influenza-specific IFN-γ responses of ferrets infected with both seasonal subtypes of IAV and found a notable increase in influenza-specific IFN-γ responses in circulating peripheral blood within 8 days post-infection. Both seasonal strains caused a well-defined pattern of influenza-specific IFN-γ responses in infected ferrets when compared to naïve animals. Additionally, we found that while the influenza specific IFN-γ responses found in peripheral circulating blood were comparable between subtypes, the influenza specific IFN-γ responses found in lung lymphocytes significantly differed. Our results suggest that there is a distinct difference between the ability of the two seasonal influenza strains to establish an infection in the lung of ferrets associated with distinct signatures of acquired immunity.

Introduction

Influenza is a significant global health problem with 5–15% of the population infected each year, leading to approximately 200,000 to 500,000 influenza attributed deaths [1, 2]. Influenza

has an RNA genome and this allows the virus to mutate rapidly leading to antigenic drift and shift. Antigenic drift occurs via the gradual change of viral surface epitopes, leading to yearly epidemics, whilst antigenic shift is caused by the reassortment of genomes between two or more strains of influenza, which can ultimately lead to new and potentially pandemic strains. Influenza A virus (IAV) infects humans and is split into subtypes based on the neuraminidase (NA) and haemagglutinin (HA) surface glycoproteins found on the virus. There are currently two IAV subtypes circulating in the human population; H1N1 and H3N2. The H1N1 virus originated from the 2009 influenza pandemic caused by a reassortment of human, swine and bird type A influenza[3], while the current seasonal H3N2 strain originated from the 1968 Hong Kong pandemic when genomic exchange of RNA occurred between human and avian viruses[4]. Vaccination is the most efficient method to protect the population from influenza; therefore understanding seasonal influenza strains is important since they dictate annual vaccine strategies.

Two types of vaccine are currently used to combat seasonal influenza; the trivalent inactivated vaccines (TIV) which elicit a mainly humoral response and the live attenuated influenza vaccine (LAIV) which elicits a protective mucosal immune response without causing clinical disease[5]. Both need to be reformulated annually due to their strain-specific immune responses. Much current research is directed at developing novel, more universally protective vaccines, and animal models are required to facilitate assessment of novel vaccine immunogenicity and efficacy. An ideal universal vaccine would confer long term protection to influenza viruses with broad immune coverage including antibodies and T-cells In practice this has not been the case for the current inactivated vaccine, especially during seasons where a mismatch between circulating and current strains occur[6], strengthening the need for a universal vaccine.

There are a range of animal models that have been used to study influenza. Ferrets have been used extensively to study influenza pathogenesis [7–10], transmission [7, 11–14], vaccine and antiviral efficacy [15–17] and remain the gold standard animal model for IAV. Ferrets are highly susceptible to both human and avian influenza strains [2], they have comparable clinical signs and disease outcomes to humans when infected with influenza viruses as well as having similar sialic acid receptors in their respiratory tracts when compared to humans. Not unlike humans, ferrets infected with seasonal H1N1 and H3N2 strains produce mild clinical symptoms with widespread infection of the upper respiratory tract due to the viruses high affinity for alpha 2,6- linked sialic acid receptors while tissues in the lower respiratory tract are decreasingly affected [8]. The evaluation of the cell mediated immune response in ferrets is exceptionally important for modelling human disease. It has been shown that T-cells recognise epitopes derived from conserved internal proteins of IAV and crucially, human T-cells do not distinguish between IAV sub-types due to conservation of specific structural proteins[18]. This is significant as it may provide a key to a universal vaccine that could be used to vaccinate against multiple IAV strains over several seasons negating the requirement to formulate a new vaccine each season. Moreover, T-cell mediated immunity has recently been shown to be a significant correlate of protection in humans [18–20] therefore it is important to develop key techniques for the ferret model to provide a well characterised animal model available for study of T-cell mediated protective immunity in order to help us identify new correlates of protection.

Recent ferret studies have established a number of techniques and reagents that enable the identification and quantifications of key cell types and cytokines involved in antigen specific T-cell responses following influenza infection [21–23]. One of these cytokines is the multipotent Interferon gamma (IFN-γ) which plays a key role in the development of innate and adaptive immune response [24–27] and is widely accepted as a marker of the adaptive immune response IFN-γ is produced by CD4+ Th1 cells, most CD8+ cells, and NK cells, is known to be

an important contributor to antiviral immunity to influenza [28] and is able to control viral infection and induce inflammatory damage [29]. Previous ferret studies have identified that IFN-γ T-cell responses allow a more precise assessment of the vaccine induced protection level [27]. Studies have also looked at cell populations of CD4+ and CD8+ T-cells, using influenza-specific IFN-γ responses to characterise leukocyte composition and antigen-specific T-cell responses in key lymphoid tissue following influenza infection in ferrets using an enzyme-linked immunospot (ELISpot) method [21] as well as daily tracking of peripheral blood leukocytes in infected ferrets using a flow cytometric technique [16]. These studies infect ferrets with relatively high doses of influenza virus and fail to provide a comparison of the cellular immune response between strains. In addition they are unable to provide an illustration of the ongoing influenza-specific IFN-γ responses as a marker of the cellular immune response in the ferret during infection.

Despite the numerous advantages of the ferret model, ferrets are a relatively small animal and therefore it is not possible to collect the large volumes of blood required for some cellular immune evaluation methods without termination. This, coupled with the previous lack of available reagents has significantly hampered efforts to study the cellular immune response to influenza in ferrets. To address this, we performed a longitudinal time course assessing influenza- specific IFN-γ responses to two clinically relevant subtypes of seasonal influenza, H1N1 (A/California/04/2009) and H3N2 (A/Perth/16/2009) negating the need to sacrifice the animals. This allowed us to comprehensively look at the influenza-specific IFN-γ response as a marker of the cellular immune response in the periphery, and go on to compare and contrast this to the influenza-specific IFN-γ responses seen in the lung and peripheral blood mononuclear cells (PBMCs) upon study conclusion.

Methods

Virus

Influenza A/California/04/2009 (H1N1) and A/Perth/16/2009 (H3N2) were propagated in Madin-Darby Canine Kidney (MDCK) cells obtained from The European Collection of Authenticated Cell Cultures (ECACC, Porton Down, United Kingdom). The identity of both viruses was confirmed by sequencing the HA and NA genes. Virus titres were determined by plaque assay on MDCK cells under an agar overlay, followed by staining with crystal violet.

Ferrets

Adult (4–6 months) ferrets (*Mustela putorious fura)* from Highgate Farm, UK, confirmed seronegative for influenza A/California/04/2009 (H1N1) and A/Perth/16/2009 (H3N2) by haemagglutination inhibition (HAI) assay, were used for these studies. Ferrets were weighed once daily at approximately the same time. Appetite, sneezing, nasal discharge, diarrhoea and activity level were monitored twice daily and were recorded as present or absent. Activity levels were scored from 0–2 (0 = normal, 1 = reduced activity and 2 = inactive) A score was generated by summing the number of observations of each sign over the 14 days post-challenge. Nasal washes were obtained using 2ml PBS. Ferrets were allocated into five study groups as illustrated in **Table 1**. The animal study described was scrutinized and approved by the Animal Welfare and Ethical review Body of Public Health England (Porton), as required by the UK Home Office Animals (Scientific Procedures) Act, 1986.

Virus infection of ferrets

Influenza stock was diluted in PBS to provide a challenge dose of 10^2 pfu/ferret, confirmed using back titration by plaque assay. Animals were sedated by intramuscular injection using

Table 1. Experimental animal groups.

Group	Challenge Virus	Number of Animals	Nasal Wash Sample Days	Whole Blood Sample Days
1	A/California/04/2009	4	1–2, 5, 8, 11, 14	N/A
2	A/California/04/2009	6	1–8, 11, 14	-7, -1, 2, 5, 8, 11, 14
3	A/Perth/16/2009	3	1–8, 11, 14	-7, -1, 2, 5, 8, 11, 14
4	A/Perth/16/2009	6	1–8, 11, 14	-7, -1, 2, 5, 8, 11, 14
5	PBS	6	1–8, 11, 14	-7, -1, 2, 5, 8, 11, 14

A total of 25 ferrets were distributed across 5 groups. Animals were infected with a low dose (10^2 pfu/ferret) of each virus. A naïve group of 6 animals was given PBS. All inoculations were performed intranasally with 0.2ml of fluid.

https://doi.org/10.1371/journal.pone.0202675.t001

ketamine/xylazine given at a dose of 0.25ml/kg bodyweight prior to intranasal administration of 0.2ml of challenge virus, 0.1ml per nostril. Naïve animals were sedated as described, prior to intranasal administration of 0.2ml of PBS, 0.1ml per nostril.

Isolation of peripheral blood mononuclear cells

Fresh heparin anti-coagulated blood was layered on room temperature Histopaque 1083 (Sigma- Aldrich, Dorset, United Kingdom) in 15ml ACUSPIN™ tubes (Sigma-Aldrich, Dorset, United Kingdom) and a density separation carried out at 800g for 20 minutes. The buffy coats containing lymphocytes were collected and washed with medium (R2) consisting of RPMI 1640 medium (Sigma-Aldrich, Dorset, United kingdom) with the addition of L-glutamine (2mM)(Sigma-Aldrich, Dorset, united Kingdom), 0.05mM 2-mercaptoethanol (Invitrogen, Paisley, United Kingdom), 25mM HEPES buffer (Sigma-Aldrich, Dorset, United Kingdom), and 2% heat inactivated foetal bovine serum (Sigma-Aldrich, Dorset, United Kingdom), cells were pelleted by centrifugation at 400g for 10 minutes.

Isolation of lung mononuclear cells

Whole lungs were removed from each ferret. The lungs were dissected into small pieces and placed into a 25ml solution of collagenase (715 collagenase units/ml) (Sigma-Aldrich, Dorset, United Kingdom) and DNase (350 DNase units/ml)(Sigma-Aldrich, Dorset, United Kingdom). Lungs were vigorously shaken whilst incubating at 37 C for 1 hour. Partially digested lung tissue was then placed into gentleMACS C-tubes and dissociated using a gentleMACS Tissue Dissociator (Miltenyi Biotec, Surrey, United Kingdom). The tissue solution was passed through two cell sieves (100μm then 70μm) and then layered on room temperature Histopaque 1083 (Sigma- Aldrich, Dorset, United Kingdom). A density separation was carried out at 400g for 30 minutes. The buffy coats containing lymphocytes were collected and washed with R2 medium by pelleting cells by centrifugation at 400g for 10 minutes.

Red blood cell removal using ACK lysis buffer

Red blood cells were lysed from PBMC and lung MNC preparations by re-suspending cell pellets in 5ml of ACK Lysing Buffer (Gibco, ThermoFisher Scientific, United Kingdom). The cells were incubated at room temperature with gentle agitation for 5 minutes. The ACK Lysing Buffer was inactivated by the addition of an excess of R2 medium. Cells were pelleted at 400g for 5 minutes to remove lysis buffer. If lysis of the red blood cells was incomplete the treatment was repeated.

Viable cell counts

Viable cells in nasal washes, PBMCs and lung MNCs were counted using a NucleoCounter® NC-200™ (ChemoMetec, Allerod, Denmark).

Cryopreservation of cells

Cells were pelleted by centrifuging at 400g for 5 minutes. Cells were then re-suspended in an appropriate volume of cryomedia (90% FCS + 10% DMSO) allowing the cells to be frozen in liquid nitrogen in 1ml aliquots at a concentration of 3 x10^6 to 1.3 x 10^7 cells/ml.

Interferon-gamma (IFN-γ) ELISpot assay

An IFN-γ ELISpot assay was performed with PBMC and lung MNC to determine the production capacity of influenza-specific T cells in PBMC and Lungs using a Ferret IFN-γ kit (Mab Tech, Nacka. Sweden). PBMC and lung MNC were defrosted into pre-warmed medium (R10) consisting of RPMI 1640 medium (Sigma-Aldrich, Dorset, United kingdom) with the addition of 2mM L-glutamine (Sigma-Aldrich, Dorset, United Kingdom), 0.05mM 2-mercaptoethanol (Invitrogen, Paisley, United Kingdom), 25mM HEPES buffer (Sigma-Aldrich, Dorset, United Kingdom), 10% heat inactivated foetal bovine serum (Sigma-Aldrich, Dorset, United Kingdom), and benzonase (Novogen, Merck, Darmstadt, Germany). Cells were rested for 2 hours prior to use. PBMC and lung MNC were assessed for responses to A/California/07/2009 (H1N1) and A/Perth/16/2009 (H3N2). Both viruses were used at a MOI of 0.08 to re-stimulate the PBMCs and lung MNCs. Viruses were egg grown, therefore, egg allantoic fluid was used as a negative control. Phorbol-12-myristate (100ng/ml; Sigma-Aldrich, Dorset, United Kingdom) and ionomycin (1μg/ml; Merck, Watford, United Kingdom) were combined and used as a positive control. Pre-coated (mAb MTF14) plates (Mab Tech, Nacka. Sweden) were used. 50,000 lung MNCs and 200,000 PBMCs were plated per well in 50μl of R10, with or without antigen, in duplicate and incubated overnight. Following culture, plates were washed and incubated for 2 hours with biotinylated anti IFN-γ IgG. Spots were developed by the addition of streptavidin-alkaline phosphatase and 5-bromo-4-chloro-3-indoly phosphate (BCIP)-Nitro Blue tetrazolium (NBT) substrate. Results from duplicate tests were averaged. Data were analysed by subtracting the mean number of spots in the cells and allantoic fluid control wells from the mean counts of spots in wells with cells and antigen.

Quantification of influenza specific IFN-γ production by enzyme linked immunosorbent assay (ELISA)

Heparinised whole blood was diluted 1:10 with serum free RPMI 1640 medium and incubated with either A/California/07/2009 (H1N1) or A/Perth/16/2009 (H3N2), corresponding with the virus of infection. Phytohemagglutinin PHA-M (PHA) (Sigma-Aldrich, Dorset, United Kingdom) was used as a positive control and egg allantoic fluid was used as a negative control as viruses were egg grown. Blood was stimulated for 4 days at 37˚C, after which plasma supernatants were collected and cryopreserved at -80˚C. The Ferret IFN-γ ELISA Development Kit (ALP) (Mab Tech, Nacka. Sweden) was used to determine the quantity of IFNγ secreted by cells in the blood in responses to influenza-specific stimulations. ELISA plates were read using the VersaMax ELISA Microplate Reader (Molecular Devices, Sunnyvale, CA, USA) with SoftMax™ PRO software (Molecular Devices, Sunnyvale, CA, USA).

Statistical analysis

Statistical analysis was performed with GraphPad Prism 7 (GraphPad Prism, GraphPad Software, La Jolla, CA). The Mann-Whitney Test was used to analyse significant difference between groups. $P < 0.05$ was considered significant.

Results

Clinical signs and virus shedding following low dose challenge with seasonal influenza strains

Ferrets were intranasally infected with a well characterised low dose of influenza (10^2 plaque forming units (PFU) per ferret) of either A/California/04/2009 (H1N1)[17] or A/Perth/16/2009 (H3N2) (Table 1). This low dose intranasal challenge has previously been shown to infect 100% of inoculated ferrets infected with H1N1[17] and was therefore selected as the method of challenge.

Disease progression was monitored up to 14 days post infection (dpi). Ferrets used as a naïve control (group 5) were mock infected intranasally with PBS and also monitored for 14 days. Weight loss from baseline was seen in all ferrets infected with influenza, in comparison mock infected ferrets gained weight (Fig 1).

All ferrets were monitored for sneezing, nasal discharge, inactivity, diarrhoea and loss of appetite. Animals infected with H1N1 showed more severe clinical signs compared to ferrets infected with H3N2. In particular, the H1N1-infected ferrets of groups 1 and 2 presented with sneezing, nasal discharge and inactivity (mean of 6.4, 1.7 and 6.8 observations per ferret,

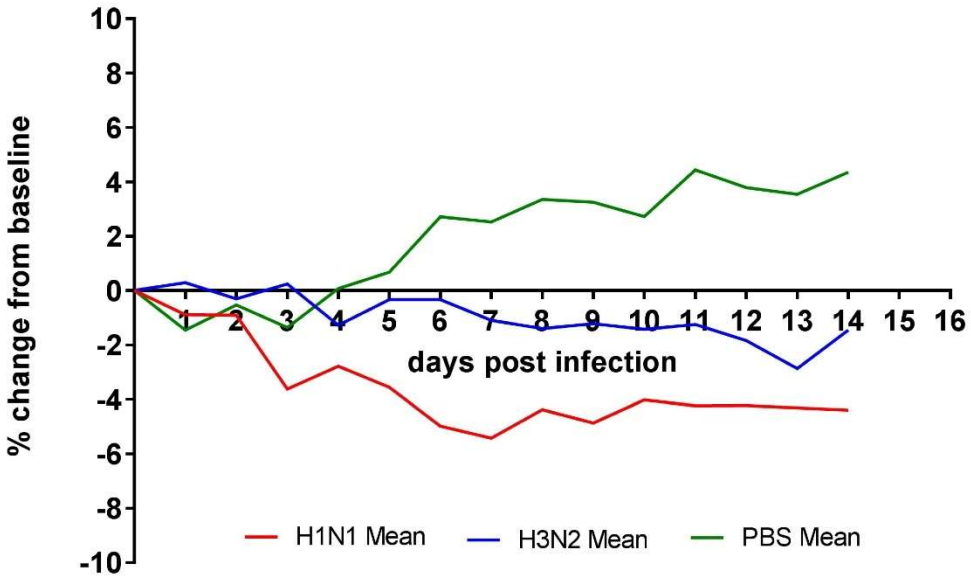

Fig 1. Clinical scoring. (a) Mean percentage weight change of ferrets infected with H1N1 (groups 1 and 2 combined, n = 10), H3N2 (groups 3 and 4 combined n = 9) and PBS (group 5, n = 6).

https://doi.org/10.1371/journal.pone.0202675.g001

Table 2. Clinical sign observations.

Group	N	Total Sneezing	Total Nasal Discharge	Total Inactivity Score	Mean Score per Ferret
1+2	10	64	17	68	14.9
3+4	9	34	3	0	4.1
5	6	0	0	0	0

Total instances of clinical sign observations. N, number of ferrets per group.

https://doi.org/10.1371/journal.pone.0202675.t002

respectively). By contrast, the H3N2-infected ferrets of groups 3 and 4 presented with sneezing and nasal discharge only (mean 3.8 and 0.3 observations per ferret, respectively) (Table 2). An increase in nasal wash cell counts has previously been shown to correlate with successfully infected animals[17, 30] and therefore they were recorded daily from 1 dpi to 8 dpi, 11 dpi and 14 dpi in groups 2–5. Counts were recorded at 1, 2, 5, 8, 11 and 14 dpi for group 1 (Table 1). Nasal wash cell counts from all influenza infected ferrets began to increase between 2 and 4 dpi whilst mock infected ferrets did not increase over the 14 days (Fig 2A). No significant difference was found between the total amounts of cells shed between the groups infected with H1N1 and H3N2.

In addition to cell counts, nasal wash samples were tested for the presence of replicating virus by plaque assay. Virus shedding in nasal washes began by 1 dpi for all 10 ferrets infected with H1N1 and 7 out of 9 ferrets infected with H3N2 (Fig 2B). Viral shedding in ferrets infected with H1N1 (groups 1 and 2) peaked at 2dpi, while viral shedding from ferrets infected with H3N2 (groups 3 and 4) peaked a day later at 3 dpi, followed by a decrease in viral load before a second smaller peak at 5 dpi (H1N1) and 6 dpi (H3N2). This smaller second peak was not found to be statistically significant; however it has been noted by others previously[31]. It is also worth noting that the second peak is not seen the nasal wash cell counts. Viral clearance (absence of live virus found in nasal wash) had occurred in all infected groups by 11 dpi. No virus was detected in the mock infected animals at any time. The peak shedding titre was found to have a strong positive correlation and significance (R +0.9781, P <0.0001) with the total virus shed from groups 1, 2, 3 and 4. Consequently, the more virus shed by an animal the higher the peak titre of virus found in nasal wash. Using area under the curve, which represents the total virus shed by each ferret, it was found that there was significantly (P 0.0028) more virus shed by ferrets infected with H1N1 (group 2) compared to ferrets infected with H3N2 (groups 3 and 4) (Fig 2C).

Longitudinal time course of influenza-specific IFN-γ responses in the periphery/ IFN-γ response to challenge

Small volumes of heparinised whole blood were collected from groups 2, 3, 4 and 5 at days shown in Table 1 to assess the influenza-specific IFN-γ responses in peripheral blood. This was done by stimulating diluted whole blood samples with homologous virus or appropriate controls as detailed in the methods section; secreted IFN-γ was detected by enzyme linked immunosorbant assay (ELISA). Samples from each ferret were assessed by ELISA and a longitudinal time course of influenza-specific IFN-γ responses was produced (Fig 3). Two samples were collected prior to infection (-7 and -1 dpi) to demonstrate that there were low influenza specific IFN-γ responses in the ferrets prior to infection. All ferrets were found to have responses below 270 pg/ml of IFN-γ in pre-infection samples. These responses were averaged for each animal and represented by the 0 dpi time point (Fig 3). Following infection with either H1N1 or H3N2, low level influenza-specific IFN-γ responses were detectable in ferrets at 5 dpi and increased at 8 and 11 dpi with responses peaking at 11 to 14 dpi. At 14 dpi,

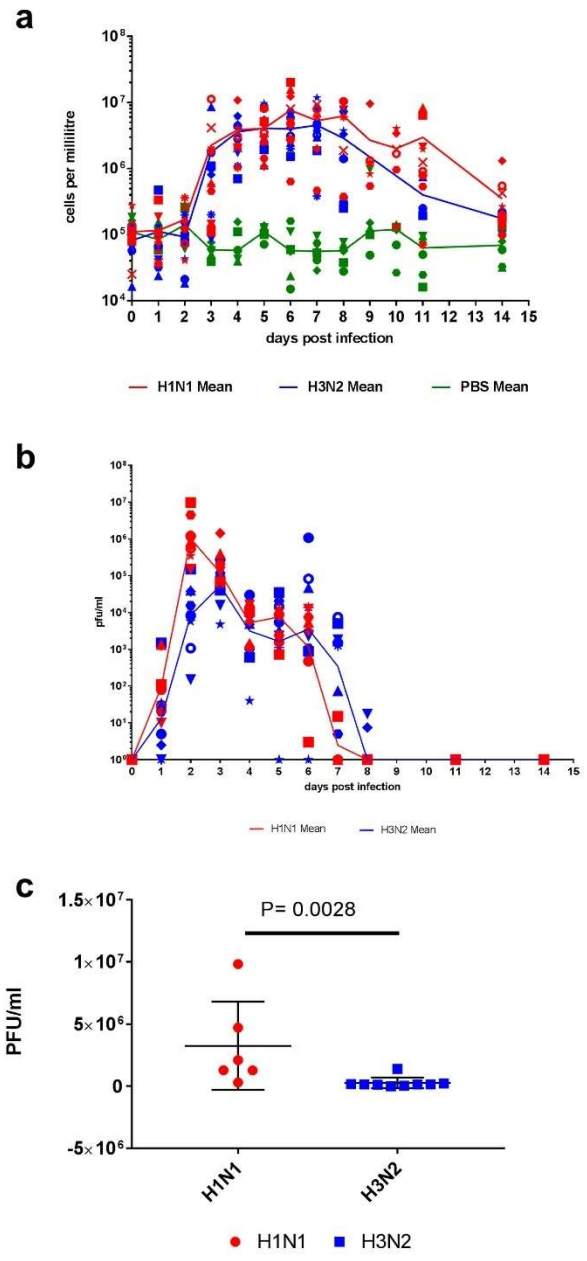
a
cells per millilitre
days post infection
H1N1 Mean
H3N2 Mean
PBS Mean
b
pfu/ml
days post infection
H1N1 Mean
H3N2 Mean
c
PFU/ml
P= 0.0028
H1N1
H3N2
H1N1
H3N2

Fig 2. Nasal wash collection. Nasal washes were collected at +1 to +8 dpi, 11 dpi and 14 dpi for Groups 2–5. Group 1 had nasal washes taken at +1, +2, +5, +8, +11 and +14 dpi. (a) All nasal washes were counted to ascertain the number of cells being shed from each individual ferret at each time point (n = 25). (b) Nasal washes were subsequently plaque assayed to ascertain the titre of virus being shed from each individual ferret (n = 19) at these time points. (c) The area under the curve was calculated for groups 2 (n = 6), and 3 and 4 combined (n = 9). Group 1 was omitted from this statistical analysis as the nasal wash samples were not collected at the same time points as groups 2, 3 and 4. A Mann-Whitney test was performed and a statistically significant difference (P = 0.0028) was found between ferrets infected with H1N1 and H3N2.

https://doi.org/10.1371/journal.pone.0202675.g002

responses in the majority of ferrets appear to decrease while some others continue to increase. This variation could be due to the outbred nature of the ferrets. There was no significant difference found between the total influenza-specific IFN-γ produced in whole blood from ferrets infected with the H1N1 and H3N2 sub-types, nor was there a difference between the subtypes at any time-point.

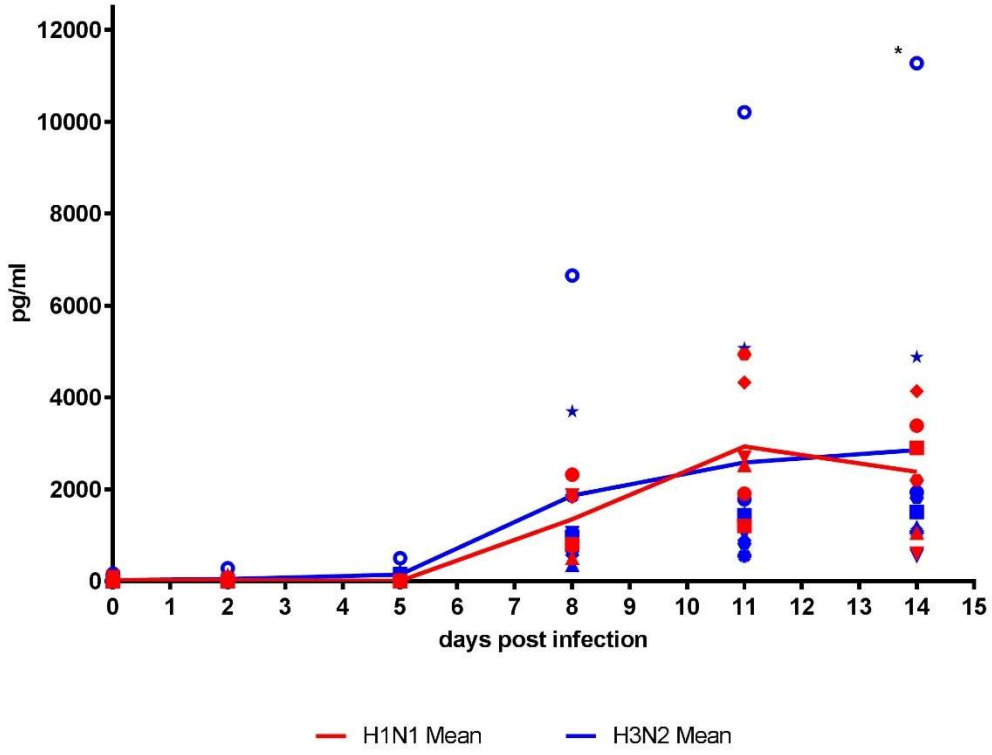

Fig 3. Quantification of influenza specific IFN-γ production by ELISA. Diluted whole blood samples were collected from groups 2 to 5 (n = 21) at -7, -1, +2, +5, +8, +11 and +14 dpi, stimulated with appropriate antigens and the supernatants harvested. Supernatants were used in the Ferret IFN-γ ELISA Development Kit (HRP). Influenza specific IFN-γ responses became detectable at 5 dpi with a peak at 11–14 dpi for all virus infected animals from groups 2 to 4 (n = 15). No responses were detected in mock ferrets (not shown, n = 6). 12000 pg/ml was the upper limit of detection for the ELISA.

https://doi.org/10.1371/journal.pone.0202675.g003

Cellular immune responses measured by ferret specific IFN-γ enzyme-linked immunospot assay (ELISpot)

Animals were culled at 14 dpi. Lymphocytes were isolated from whole lung (lung MNCs) and whole blood (PBMCs) and the frequency of IFN-γ secreting cells was quantified by ferret-specific INF-γ ELISpot. We found a significant difference in the number of cells producing influenza-specific IFN-γ in H1N1 infected animals compared to H3N2 infected animals (P 0.0306) (Fig 4A). The mean values of the H1N1 group was 2305 SFU while the mean value for the H3N2 group was 210 SFU, representing an 11-fold difference between the two groups. Additionally we found a significant difference in the responses between the mock infected ferrets (group 5) and H1N1 infected ferrets (group 1 and 2) (P 0.0017). Comparison of lung MNCs in influenza and mock infected ferrets (group 5) showed no significant difference in the influenza-specific IFN-γ responses for mock (group 5) and H3N2 infected ferrets (group 3 and 4). Only two H3N2 infected ferrets were found to have influenza specific IFN-γ responses in lung MNCs, no responses were detected in remaining ferrets. Moderate positive correlations for all groups were found between the peak virus titre shed and the number of lung MNCs secreting influenza-specific IFN-γ (R +0.5775, P 0.0096), and the total amount of virus shed by ferrets and the number of lung MNCs secreting influenza-specific IFN-γ (R +0.5870, P 0.0082).

All virus infected ferrets (groups 1–4) showed a significant increase in the number of influenza-specific INF-γ secreting PBMCs when compared to the mock infected ferrets (group 5) at 14 dpi (H1N1 P 0.0002, H3N2 P 0.0004). No significant difference was observed between the number of PBMCs producing influenza-specific IFN-γ responses in the H1N1 and H3N2 infected groups (Fig 4B). These PBMC responses support the results seen in the longitudinal time course as measured by ELISA; there are similarities with both the influenza specific IFN-γ responses being produced over the course of the infection and number of cells responsible for producing influenza specific IFN-γ response as a result of infection with the two subtypes of influenza.

Discussion

Influenza A virus infection can result in a spectrum of disease outcomes in humans, ranging from sub-clinical with seasonal strains to lethal with subtypes such as H5N1 and H7N9. The ability of seasonal influenza A viruses to continuously evolve antigenically means individuals can become infected on numerous occasions throughout their lives despite having immunity to previous strains. This antigenic drift also necessitates continuous updating of the trivalent and tetravalent vaccines. In this study our aims were to demonstrate the use of new reliable techniques to compare the kinetics and signatures of acquired immunity in ferrets challenged with low dose infections of seasonal influenza.

A low dose ferret model of infection for IAV can be considered more appropriate when attempting to model influenza infection as it represents a more 'true to life' dose of influenza [17]. We have previously demonstrated, using an H1N1 2009 pandemic virus, that there is an approximately 100-fold increase in the innate immune cell count in the nasal wash when infecting animals at a dose of 100 pfu, with a delay in peak cell count compared to infection with a high dose (10^6 pfu). This suggests a delay in the activation of innate immune cell response found in the nasal wash which comprises of mostly neutrophils and monocytes/macrophages[32]. We have also shown that a lower challenge dose does not lead to reduced virus shedding, but instead leads to increased shedding both in terms of total virus shed over the course of the infection, and peak titre of shed virus[17]. Here we have illustrated that ferrets infected with a low dose (100 pfu) of H1N1 virus shed significantly more virus over a 14 days period compared to ferrets infected with an equivalent dose of H3N2 virus. This also correlates

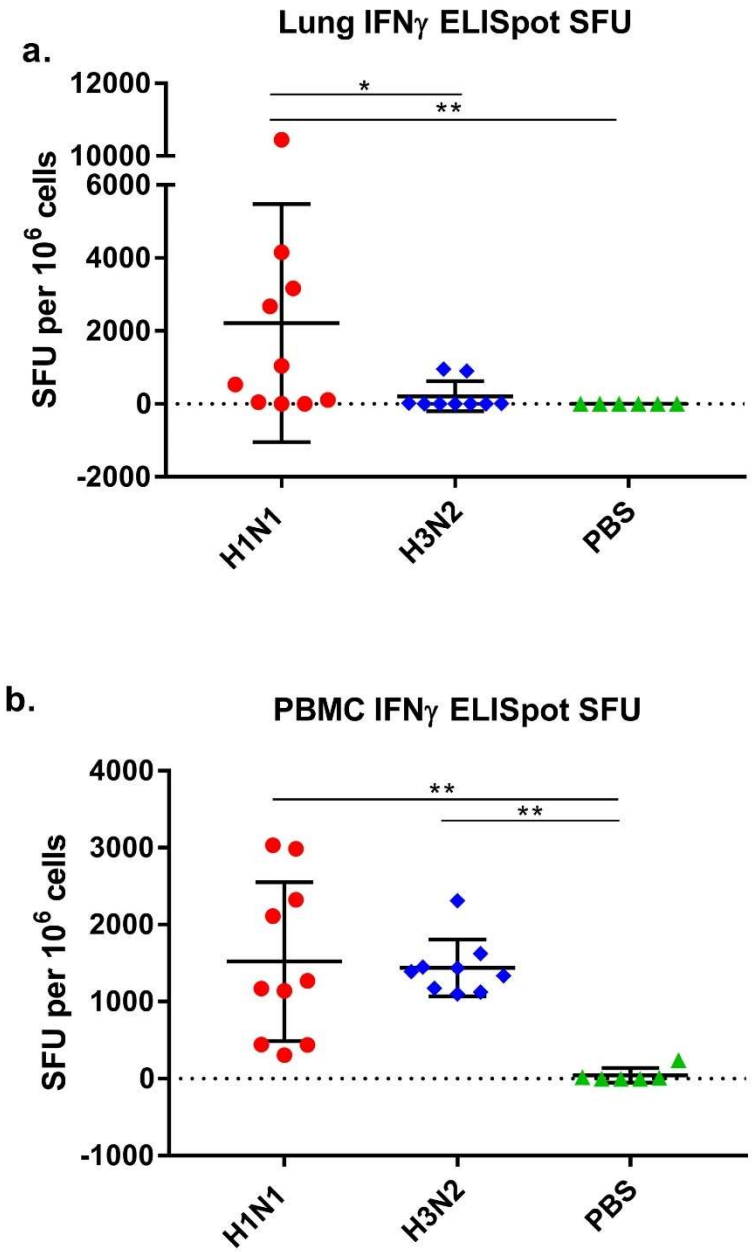
a.
Lung IFNγ ELISpot SFU
SFU per 10^6 cells
12000
10000
6000
4000
2000
0
-2000
*
**
H1N1
H3N2
PBS
b.
PBMC IFNγ ELISpot SFU
SFU per 10^6 cells
4000
3000
2000
1000
0
-1000
**
**
H1N1
H3N2
PBS

Fig 4. Cellular immune responses of ferrets infected with seasonal influenza. Lung MNCs (a) and PBMCs (b) were collected from all animals (n = 25) at 14 dpi. Results were normalised by subtracting the individual sample allantoic fluid control values from virus stimulated sample values. Influenza specific IFN-γ responses were quantified in lung MNC and PBMC samples from all ferrets. (a) Influenza specific IFN-γ responses in lung MNCs to corresponding viruses were seen in eight out of ten H1N1 infected ferrets. Only two of nine H3N2 infected ferrets were found to have influenza specific IFN-γ responses in lung MNCs, no responses were detected in remaining ferrets. (b) Influenza specific IFN-γ responses in PBMCs to corresponding viruses were seen in all virus infected ferrets. A very low influenza specific IFN-γ response was detected in the PBMCs of one ferret (less than those seen in the low H1N1 infected ferrets), none of the remaining PBMCs or lung MNCs of mock ferrets had any detectable influenza specific IFN-γ responses. The values measured for each ferret are plotted as spot forming units (SFU) per million cells. Bars show mean and standard deviation for each group.

https://doi.org/10.1371/journal.pone.0202675.g004

strongly with the peak shedding titre seen in the ferrets, with H1N1-infected ferrets having a higher peak shedding titre than animals infected with H3N2 virus. This is most likely due to a difference in replicative efficiency between the virus strains, as we did not observe a significant difference in the peripheral innate or adaptive immune responses to the viruses.

Comparison of the H1N1 and H3N2 influenza-specific IFN-γ time course in peripheral blood shows a similar pattern of responses in ferrets infected with either subtype. These results, combined with the PBMC ELISpot results, obtained at 14 dpi, suggest that the influenza-specific IFN-γ response as a marker of the cellular immune response seen in ferrets infected with H1N1 and H3N2 is not differentiated by sub-type and is instead comparable across both strains in the periphery. As established previously, the increase in the number of IFN-γ producing lymphocytes following challenge suggests an expansion of the numbers of influenza-specific T-cells as a consequence of progressive viral infection[33]. NK cells play an important role in controlling the virus in the early stages of infection[34]; therefore it is also possible that a fraction of these influenza-specific IFN-γ producing cells may be NK cells. Similar kinetics of influenza specific IFN-γ responses in PBMCs have been reported in pigs infected with a swine influenza (H1N2) virus[35]. This suggests that the influenza specific IFN-γ responses seen in the periphery do not vary significantly between seasonal strains or perhaps even host; however it is possible that the responses seen in a more clinically severe strain, such as H5N1 or H7N9, may be different. Although the responses observed in the periphery are not direct representations of the responses at the site of infection it is valuable to monitor the cellular immune response across a time course, especially in a model where only small volumes of blood can be collected. The key significant difference seen between the groups of infected ferrets was the number of influenza-specific IFN-γ producing cells seen in lung MNCs of ferrets infected with H1N1 compared to H3N2 infected ferrets and the mock-infected control group. It has previously been shown that A/California/04/2009 can be detected in the lung following low-dose intra-nasal infection[17]. This suggests that the influenza specific IFN-γ responses seen in the lungs of ferrets infected with H1N1 was due to virus causing infection in the lungs. In comparison the ferrets infected with H3N2 have either no or low influenza-specific IFN-γ responses. It has previously been reported that seasonal strains of H3N2 infrequently go to the lungs of ferrets[16, 31, 36–39], for example in one study H3N2 virus was delivered mostly by the intra-tracheal route using a high dose inoculum (10^6 $TCID_{50}$); despite this, very little evidence of H3N2 viral replication was seen in the lower respiratory tract[38]. These observations are in line with our findings of the minimal influenza specific IFN-γ responses seen in the lungs of ferrets infected with H3N2 virus.

This study demonstrates that it is possible to successfully evaluate cellular immune responses to seasonal influenza infection over a time-course in the ferret, and reveals that there are differences in the immune signatures induced by different influenza strains. By sequentially taking low volumes of heparinised blood samples from individual animals and

detecting influenza-specific IFN-γ as measured by ELISA, we are able to form a picture of what is occurring in the periphery throughout infection. Furthermore, when the animals were sacrificed, we were able to quantify influenza-specific IFN-γ secreting cells in tissues of interest. While the use of the ELISA and ELISpot techniques is not unique, their use to examine influenza specific IFN-γ responses as a marker of the cellular immune response over a time course in the ferret model is. Using these complementary techniques, we have demonstrated that the responses to H1N1 and H3N2 infections in the lung were markedly different and correlated well with known tropisms of the virus strains used in this study. We believe this study enhances the applicability of the ferret model to study acquired immunity and vaccination strategies to influenza.

The current inactivated vaccines are poor inducers of T-cell responses. Cross-reactive T-cell responses are important in the protective response to novel vaccines, especially those based on internal virus antigens [40] and so the ability to measure these responses in the ferret model of influenza will become increasingly valuable. In the future we need to be able to measure both humoral and cellular responses in animal models as new vaccines are likely to require induction of both.

Acknowledgments

The authors would like to thank the staff of the Biological Investigations Group at PHE Porton for their technical expertise in conducting the animal experiments, animal husbandry and clinical observations. The views expressed in this publication are those of the author(s) and not necessarily those of the Public Health England.

Author Contributions

Conceptualization: Kathryn A. Ryan, Gillian S. Slack, Nigel J. Silman, Miles W. Carroll, Karen E. Gooch.

Data curation: Kathryn A. Ryan, Gillian S. Slack, Karen E. Gooch.

Formal analysis: Kathryn A. Ryan, Karen E. Gooch.

Investigation: Kathryn A. Ryan, Gillian S. Slack, Jennifer A. Kane, Karen E. Gooch.

Methodology: Kathryn A. Ryan, Gillian S. Slack, Karen E. Gooch.

Project administration: Kathryn A. Ryan, Karen E. Gooch.

Supervision: Karen E. Gooch.

Validation: Karen E. Gooch.

Writing – original draft: Kathryn A. Ryan.

Writing – review & editing: Gillian S. Slack, Anthony C. Marriott, Catherine J. Whittaker, Miles W. Carroll, Karen E. Gooch.

References

1. Stohr K. Influenza—WHO cares. Lancet Infectious Diseases. 2002; 2(9):517–. https://doi.org/10.1016/s1473-3099(02)00366-3 PubMed PMID: WOS:000177759100016. PMID: 12206966
2. Belser JA, Katz JM, Tumpey TM. The ferret as a model organism to study influenza A virus infection. Disease Models & Mechanisms. 2011; 4(5):575–9. https://doi.org/10.1242/dmm.007823 PMID: 21810904
3. Neumann G, Noda T, Kawaoka Y. Emergence and pandemic potential of swine-origin H1N1 influenza virus. Nature. 2009; 459(7249):931–9. https://doi.org/10.1038/nature08157 PMID: 19525932

4. Wendel I, Rubbenstroth D, Doedt J, Kochs G, Wilhelm J, Staeheli P, et al. The Avian-Origin PB1 Gene Segment Facilitated Replication and Transmissibility of the H3N2/1968 Pandemic Influenza Virus. Journal of Virology. 2015; 89(8):4170–9. https://doi.org/10.1128/JVI.03194-14 PubMed PMID: PMC4442368. PMID: 25631088
5. Fischer WA, Brighton M, Jaspers I. Live Attenuated Influenza Vaccine Strains Elicit a Greater Innate Immune Response than Antigenically-Matched Seasonal Influenza Viruses during Infection of Human Nasal Epithelial Cell Cultures. Vaccine. 2014; 32(15):1761–7. https://doi.org/10.1016/j.vaccine.2013.12.069 PubMed PMID: PMC3979967. PMID: 24486351
6. Hua S, Li X, Liu M, Cheng Y, Peng Y, Huang W, et al. Antigenic variation of the human influenza A (H3N2) virus during the 2014–2015 winter season. Sci China Life Sci. 2015:1–7. https://doi.org/10.1007/s11427-015-4899-z PMID: 26219513
7. Bouvier NM, Lowen AC. Animal Models for Influenza Virus Pathogenesis and Transmission. Viruses. 2010; 2(8):1530. https://doi.org/10.3390/v20801530 PMID: 21442033
8. Enkirch T, von Messling V. Ferret models of viral pathogenesis. Virology. 2015; 479–480(0):259–70. https://doi.org/10.1016/j.virol.2015.03.017 PMID: 25816764
9. Zitzow LA, Rowe T, Morken T, Shieh WJ, Zaki S, Katz JM. Pathogenesis of avian influenza A (H5N1) viruses in ferrets. J Virol. 2002; 76. https://doi.org/10.1128/jvi.76.9.4420–4429.2002
10. Maines TR, Jayaraman A, Belser JA, Wadford DA, Pappas C, Zeng H, et al. Transmission and Pathogenesis of Swine-Origin 2009 A(H1N1) Influenza Viruses in Ferrets and Mice. Science. 2009; 325 (5939):484–7. https://doi.org/10.1126/science.1177238 PMID: 19574347
11. Tellier R. Aerosol transmission of influenza A virus: a review of new studies. Journal of The Royal Society Interface. 2009; 6(Suppl 6):S783–S90.
12. Herfst S, Schrauwen EJA, Linster M, Chutinimitkul S, de Wit E, Munster VJ, et al. Airborne Transmission of Influenza A/H5N1 Virus Between Ferrets. Science. 2012; 336(6088):1534–41. https://doi.org/10.1126/science.1213362 PMID: 22723413
13. Pappas C, Yang H, Carney PJ, Pearce MB, Katz JM, Stevens J, et al. Assessment of transmission, pathogenesis and adaptation of H2 subtype influenza viruses in ferrets. Virology. 2015; 477:61–71. Epub 2015/02/11. https://doi.org/10.1016/j.virol.2015.01.002 PMID: 25659818.
14. Koster F, Gouveia K, Zhou Y, Lowery K, Russell R, MacInnes H, et al. Exhaled aerosol transmission of pandemic and seasonal H1N1 influenza viruses in the ferret. PLoS One. 2012; 7(4):e33118. Epub 2012/04/18. https://doi.org/10.1371/journal.pone.0033118 PMID: 22509254; PubMed Central PMCID: PMCPMC3317934.
15. Margine I, Krammer F. Animal Models for Influenza Viruses: Implications for Universal Vaccine Development. Pathogens. 2014; 3(4):845. https://doi.org/10.3390/pathogens3040845 PMID: 25436508
16. Music N, Reber AJ, Lipatov AS, Kamal RP, Blanchfield K, Wilson JR, et al. Influenza Vaccination Accelerates Recovery of Ferrets from Lymphopenia. PLOS ONE. 2014; 9(6):e100926. https://doi.org/10.1371/journal.pone.0100926 PMID: 24968319
17. Marriott AC, Dove BK, Whittaker CJ, Bruce C, Ryan KA, Bean TJ, et al. Low Dose Influenza Virus Challenge in the Ferret Leads to Increased Virus Shedding and Greater Sensitivity to Oseltamivir. PLoS ONE. 2014; 9(4):e94090. https://doi.org/10.1371/journal.pone.0094090 PMID: 24709834
18. Sridhar S. Heterosubtypic T-Cell Immunity to Influenza in Humans: Challenges for Universal T-Cell Influenza Vaccines. Frontiers in Immunology. 2016; 7(195). https://doi.org/10.3389/fimmu.2016.00195 PMID: 27242800
19. Wilkinson TM, Li CKF, Chui CSC, Huang AKY, Perkins M, Liebner JC, et al. Preexisting influenza-specific CD4+ T cells correlate with disease protection against influenza challenge in humans. Nat Med. 2012; 18(2):274–80. http://www.nature.com/nm/journal/v18/n2/abs/nm.2612.html#supplementary-information. https://doi.org/10.1038/nm.2612 PMID: 22286307
20. Sridhar S, Begom S, Bermingham A, Hoschler K, Adamson W, Carman W, et al. Cellular immune correlates of protection against symptomatic pandemic influenza. Nature Medicine. 2013; 19(10):1305–12. https://doi.org/10.1038/nm.3350 PMID: 24056771
21. DiPiazza A, Richards K, Batarse F, Lockard L, Zeng H, García-Sastre A, et al. Flow Cytometric and Cytokine ELISpot Approaches To Characterize the Cell-Mediated Immune Response in Ferrets following Influenza Virus Infection. Journal of Virology. 2016; 90(17):7991–8004. https://doi.org/10.1128/JVI.01001-16 PubMed PMID: PMC4988159. PMID: 27356897
22. Nakata M, Itou T, Sakai T. Quantitative analysis of inflammatory cytokines expression in peripheral blood mononuclear cells of the ferret (Mustela putorius furo) using real-time PCR. Veterinary Immunology and Immunopathology. 2009; 130(1):88–91. https://doi.org/10.1016/j.vetimm.2008.12.009.

23. Pillet S, Kobasa D, Meunier I, Gray M, Laddy D, Weiner DB, et al. Cellular immune response in the presence of protective antibody levels correlates with protection against 1918 influenza in ferrets. Vaccine. 2011; 29(39):6793–801. https://doi.org/10.1016/j.vaccine.2010.12.059 PMID: 21211587

24. Sridhar S, Begom S, Bermingham A, Ziegler T, Roberts KL, Barclay WS, et al. Predominance of heterosubtypic IFN-γ-only-secreting effector memory T cells in pandemic H1N1 naive adults. European journal of immunology. 2012; 42(11):2913–24. https://doi.org/10.1002/eji.201242504 PubMed PMID: PMC4310933. PMID: 22777887

25. Lalvani A, Brookes R, Hambleton S, Britton WJ, Hill AVS, McMichael AJ. Rapid Effector Function in CD8⁺ Memory T Cells. The Journal of Experimental Medicine. 1997; 186 (6):859. PMID: 9294140

26. Bot A, Bot S, Bona CA. Protective Role of Gamma Interferon during the Recall Response to Influenza Virus. Journal of Virology. 1998; 72(8):6637–45. PubMed PMID: PMC109853. PMID: 9658110

27. Ochi A, Danesh A, Seneviratne C, Banner D, Devries ME, Rowe T, et al. Cloning, expression and immunoassay detection of ferret IFN-γ. Developmental & Comparative Immunology. 2008; 32(8):890–7. http://dx.doi.org/10.1016/j.dci.2007.12.008.

28. Whitmire JK, Tan JT, Whitton JL. Interferon-γ acts directly on CD8(+) T cells to increase their abundance during virus infection. The Journal of Experimental Medicine. 2005; 201(7):1053–9. https://doi.org/10.1084/jem.20041463 PubMed PMID: PMC2213135. PMID: 15809350

29. Muller U, Steinhoff U, Reis LF, Hemmi S, Pavlovic J, Zinkernagel RM, et al. Functional role of type I and type II interferons in antiviral defense. Science. 1994; 264(5167):1918. PMID: 8009221

30. Reuman P, Keely S, Schiff G. Assessment of signs of influenza illness in the ferret model. J Virol Methods. 1989; 24:27–34. https://doi.org/10.1016/0166-0934(89)90004-9 PMID: 2760163

31. Roberts KL, Shelton H, Stilwell P, Barclay WS. Transmission of a 2009 H1N1 Pandemic Influenza Virus Occurs before Fever Is Detected, in the Ferret Model. PLoS ONE. 2012; 7(8):e43303. https://doi.org/10.1371/journal.pone.0043303 PMID: 22952661

32. Chen KS, Bharaj SS, King EC. Induction and relief of nasal congestion in ferrets infected with influenza virus. International Journal of Experimental Pathology. 1995; 76(1):55–64. PubMed PMID: PMC1997137. PMID: 7537523

33. Martel CJ-M, Agger EM, Poulsen JJ, Hammer Jensen T, Andresen L, Christensen D, et al. CAF01 Potentiates Immune Responses and Efficacy of an Inactivated Influenza Vaccine in Ferrets. PLOS ONE. 2011; 6(8):e22891. https://doi.org/10.1371/journal.pone.0022891 PMID: 21850242

34. Schoenborn JR, Wilson CB. Regulation of Interferon-γ During Innate and Adaptive Immune Responses. Advances in Immunology. 96: Academic Press; 2007. p. 41–101. https://doi.org/10.1016/S0065-2776(07)96002-2 PMID: 17981204

35. Talker SC, Stadler M, Koinig HC, Mair KH, Rodríguez-Gómez IM, Graage R, et al. Influenza A Virus Infection in Pigs Attracts Multifunctional and Cross-Reactive T Cells to the Lung. Journal of Virology. 2016; 90(20):9364–82. https://doi.org/10.1128/JVI.01211-16 PubMed PMID: PMC5044846. PMID: 27512056

36. Carolan LA, Butler J, Rockman S, Guarnaccia T, Hurt AC, Reading P, et al. TaqMan real time RT-PCR assays for detecting ferret innate and adaptive immune responses. Journal of Virological Methods. 2014; 205:38–52. https://doi.org/10.1016/j.jviromet.2014.04.014 PMID: 24797460

37. Gustin KM, Belser JA, Wadford DA, Pearce MB, Katz JM, Tumpey TM, et al. Influenza virus aerosol exposure and analytical system for ferrets. Proceedings of the National Academy of Sciences. 2011; 108(20):8432–7. https://doi.org/10.1073/pnas.1100768108 PMID: 21536880

38. van den Brand JMA, Stittelaar KJ, van Amerongen G, Reperant L, de Waal L, Osterhaus ADME, et al. Comparison of Temporal and Spatial Dynamics of Seasonal H3N2, Pandemic H1N1 and Highly Pathogenic Avian Influenza H5N1 Virus Infections in Ferrets. PLOS ONE. 2012; 7(8):e42343. https://doi.org/10.1371/journal.pone.0042343 PMID: 22905124

39. Roberts KL, Shelton H, Scull M, Pickles R, Barclay WS. Lack of transmission of a human influenza virus with avian receptor specificity between ferrets is not due to decreased virus shedding but rather a lower infectivity in vivo. Journal of General Virology. 2011; 92(8):1822–31. https://doi.org/10.1099/vir.0.031203–0

40. Berthoud TK, Hamill M, Lillie PJ, Hwenda L, Collins KA, Ewer KJ, et al. Potent CD8(+) T-Cell Immunogenicity in Humans of a Novel Heterosubtypic Influenza A Vaccine, MVA–NP+M1. Clinical Infectious Diseases: An Official Publication of the Infectious Diseases Society of America. 2011; 52(1):1–7. https://doi.org/10.1093/cid/ciq015 PubMed PMID: PMC3060888. PMID: 21148512